DEPARTMENT OF GEOLOGY
CHULALONGKORN UNIVERSITY

Proceedings of the Second International Symposium on

Geoscience Resources and Environments of Asian Terranes

GREAT2018

19 - 20 November 2018
Chulalongkorn University
Bangkok, Thailand

Special Issue of
Bulletin of Earth Sciences of Thailand (BEST, 2018)

PTTEP

SCG
CEMENT-BUILDING MATERIALS

Organized by
Department of Geology
Faculty of Science,
Chulalongkorn University

GREAT2018

The Second International Symposium on

Geoscience Resources and Environments of Asian Terranes

19-23 November 2018 Bangkok, Thailand

Symposium Organizing Committee

Chairman

Dr. Pitsanupong Kanjanapayont

Organizing Committee

Dr. Punya Charusiri
Dr. Chakkaphan Sutthirat
Dr. Thasinee Charoentitirat
Dr. Akkaneewut Chabangborn
Dr. Piyaphong Chenrai
Dr. Sukonmeth Jitmahantakul
Dr. Thanawat Jarupongsakul
Dr. Thanop Thitimakorn
Dr. Vichai Chutakositkanon
Dr. Santi Pailoplee
Dr. Waruntorn Kanitpanyacharoen
Dr. Kantapon Suraprasit
Dr. Abhisit Salam
Dr. Montri Choowong
Dr. Srilert Chotpantarat
Dr. Sumet Phantuwongraj
Dr. Sakonvan Chawchai

Post-Symposium Excursion Leader

Dr. Thasinee Charoentitirat

To order proceedings

Please contact:
Department of Geology
Faculty of Science
Chulalongkorn University
Bangkok, 10330, Thailand
Tel: 66-2-2185442-3
Fax: 66-2-2185464

ISSN: 1906-280X

PREFACE

In commemoration of the 60th Anniversary of the Department of Geology, Faculty of Science, Chulalongkorn University, the Department has organized the "The Second International Symposium on Geoscience Resources and Environments of Asian Terranes" in the year 2018 or "GREAT 2018" for providing an opportunity for geoscientists and earth scientists to meet and share of exchange their research works and new findings. This symposium is the fifth of its kind following the first conference on "Application of Geology and the National Development" in 1984 for 25th Anniversary, the second conference on "Development Geology for Thailand into the year 2000" in 1992 for 30th Anniversary, the third conference on "Mineral, Energy and Water Resources of Thailand Towards the year 2000" in 1999 for 40th Anniversary, and the forth conference on "Geoscience Resources and Environments of Asian Terranes" in the year 2008 or "GREAT 2008".

The breath and depth of the technical sessions are international in scope and span across multiple geosciences disciplines including not only the sciences of solid Earth but also the hydrospheric and atmospheric sciences of the Asian countries. Therefore, technical themes will cover tectonics and structural geology, stratigraphy and sedimentology, paleontology, environmental geochemistry, energy resources, petrology, mineralogy and mineral deposits, and geohazards.

I would like to gratefully acknowledge the support and cooperation from various organizations. Without their generous supports, neither the Symposium nor this Proceedings would have been possible. I believe that being fully aware of the situation and recognition of the "new normal" of our profession for the benefit of our society, geoscientists and earth scientists will play important role to the direct benefit of our country. Finally, I would like to express my sincere gratitude to the Symposium Organizing Committee and all participants who have contributed their times and efforts to make this Symposium possible.

Pitsanupong Kanjanapayont , Dr.rer.nat.
Chairman of the Organizing Committee

EDITORS' NOTE

This volume of the GREAT 2018 proceedings is a peer-reviewed publication of the works from researchers who join the 60th Anniversary of the Department of Geology, Faculty of Science, Chulalongkorn University. The editorial team has edited all of the abstract, extended abstract and full papers where necessary based on the correction and comments from reviewers and editor. The aim of editing was not only bringing uniformity and consistency to the format, but also to improve the scientific ideas and the quality of all submitted works as scientific standard in equal to international journal. Some typographical and grammatically errors as well as errors in phraseology and spelling have been corrected with the permission from author(s); however, some were left as submitted version with the agreement also from the author(s). It is important to note that during the editorial process, no manuscript was rejected. This indicated the successful of the symposium and the high quality of the works from all participants.

The editorial team would like to thank all author(s) who submitted their works in a good form and all those who have helped in corresponding and correcting their works that greatly improved the quality of the proceedings. Thanks, are also extended to the reviewers and proof-readers for their effort and contributions.

Finally, the editorial team would like to gratefully acknowledge the support and cooperation from Chulalongkorn University and sponsorships. Without their generous supports, neither the symposia nor the proceedings would have been possible. Thanks, are also extended to numerous persons whose names do not appear here for their dedications and contributions.

Editorial team

Professor Dr. Montri Choowong, Ph.D

Associate Professor Dr. Santi Pailoplee, Ph.D

Dr. Akkaneewut Chabangborn, Ph.D

Dr. Piyaphong Chenrai, Ph.D

Dr. Sukonmeth Jitmahantakul, Ph.D

Patrons of the Symposia

PTT Exploration and Production Public Company Limited

SCG Cement Limited

CONTENTS

GREAT2018 Poster Exhibition

GREAT2018 Technical Program

Monday
19
NOVEMBER 2018

Keynote speakers

Chaiporn Siripornpibul
Geological Society of Thailand

Katsumi Ueno
Fukuoka University

Chris Morley
Chiang Mai University

GREAT Sponsors

PTTEP

SCG

9:00-9:30 **Welcome address by Pitsanupong Kanjanapayont**
Head of the Department of Geology, Chulalongkorn University

9:30-10:00 **Chaiporn Siripornpibul** (Keynote speaker)
More than Basic Geological Works in Cave and Kast Study in Thailand

Break

10:20-10:40 **Pitaksit Ditbanjong**, Wittaya Kandharosa & Yupa Thasod
Sedimentology and facies analysis of the Upper Paleozoic shallow marine siliciclastic deposit from Doi Tu Pu, Chiang Rai Province, Northern Thailand : Preliminary note

10:40-11:00 **Thitikan Junratanamanee**, Nitipon Noipow & Anisong Chitnarin
Facies analysis and paleoenvironmental reconstruction of Tha Manao Limestone (Middle Ordovician) in Sri Sawat District, Kanchanaburi Province

11:00-11:20 **Abhisit Salam**, Sebastien Meffre, Supitchaya Paipana, Maysa Wittayanontawet, Takayuki Manaka & Khin Zaw
Characteristics of Granites from Sukhothai Arc and Loei Fold Belt: Application for tectonic setting

11:20-11:40 **Tanad Soisa**, Abhisit Salam, Somboon Khositanont & Takayuki Manaka
Geology and Epithermal Gold-Silver Mineralization of Suwan Prospect, Central Thailand

11:40-12:00 **Sirawit Kaewpaluk**, Abhisit Salam & Takayuki Manaka
Epithermal Gold-Silver Mineralization and Alteration of B prospect, Phichit Province, Central Thailand

Lunch

13:00-13:30 **Katsumi Ueno** (Keynote speaker) Yoshihito Kamata, Koji Uno, Thasinee Charoentitirat, Punya Charusiri, Khamseng Vilaykham & Rossana Martini
The Sukhothai Zone in northern Laos: what can we see with Triassic carbonates?

13:30-13:50 **Hidetoshi Hara**, Tetsuya Tokiwa, Toshiyuki Kurihara & Thasinee Charoentitirat
Detrital zircon U-Pb ages of the Uttaradit Group and the Pha Song metamorphic rocks, northern Thailand: their provenance and tectonic setting

13:50-14:10 **Keisuke Suzuki** & Toshiyuki Kurihara
Unroofing of a Permian-Jurassic magmatic arc in East Asia, based on detrital zircon U-Pb ages and sandstone provenance of the Hida Gaien belt, central Japan

14:10-14:30 **Toshiyuki Kurihara**
Development of the Middle Paleozoic in Japan inferred from radiolarian biostratigraphy, U-Pb zircon ages, and relationships with SE Asia

Break

14:50-15:20 **Chris Morley** (Keynote speaker)
Challenges and progress in understanding the tectonics and structure of the Indosinian Orogeny in Thailand

15:20-15:40 **Michael Ridd** & Michael Crow
Suggested history of the Hukawng Block of Northern Myanmar, and postulated role of the Medial-Myanmar Shear Zone in the origin of the Jade Mines Belt

15:40-16:00 **Thikapong Thata** & Phisit Limtrakun
Structural and Deformation of Metamorphic Rocks in the Doi Phuk Sung Area, Wiang Sa District, Nan Province

16:00-16:20 **Yoshihito Kamata**, Katsumi Ueno, Hidetoshi Hara, Thasinee Charoentitirat & Punya Charusiri
Paleozoic and Mesozoic back-arc basin chert of the Paleo-Tethys in Thailand

16:20-16:40 **Michał Krobicki** & Jan Golonka
Comparison of Alpine-Carpathian (European Western Tethys) and Indochina (SE Asian Eastern Tethys) orogenic systems and events – idea of the new IGCP project

16:40-17:00 **Mongkol Udchachon**, Hathaithip Thassanapak & Clive Burrett
Reworked conodonts from the Lower Permian carbonate turbidites in the Inthanon Terrane, Northern Thailand and their tectonic significance

GREAT2018 Technical Program

Tuesday 20 NOVEMBER 2018

9:00-9:30 **Urs Klötzli** (Keynote speaker) Jürgen Österle, Pitsanupong Kanjanapayont, Bernhard Neugschwentner & Jolanta Burda
Geochronological research in the crystalline basement units of N Thailand: A review

9:30-9:50 **Phattharawadee Wacharapornpinthu** & Phisit Limtrakun
U-Pb Age Dating of Zircons and Petrography of Rocks Along the Contact Zones Between Country Rocks and Intrusive Igneous Rocks from Khao Khi Nok Area, Tambon Pa Khai, Thong Saen Khan District, Uttaradit Province

9:50-10:10 **Tawatchai Chualaowanich**, Maung Maung Naing, Alongkot Fanka, Tanut Watcharamai, Myint Soe, Han Lynn Moe, Phyo Zaw Thwin & Alin Suksawat
Crystallization temperature range of corundum from Yatkansin Taung area, Myanmar

10:10-10:30 **Pornchanit Sawasdee**, Prayath Nanthasin, Christoph Hauzenberger & John Booth
Characteristics of mantle xenoliths enclosed in alkali basalt at Bo Phloi District, Kanchanaburi Province

Break

10:50-11:10 **Bowornlak Amnatmetta**, Prayath Nantasin, Sotaro Baba, Tomokazu Hokada, Atsushi Kamei, Ippei Kitano, Yoichi Motoyoshi, NugrohoSetiawan, Davaa-ochir Dashbaatar & John Booth
Retrograde texture in calc-silicate rocks at Akarui Point, Lützow-Holm Complex, East Antarctica: Implication for metamorphic evolution

11:10-11:30 **Penchan Thaworndumrongsakul**, Prayath Nantasin, Sotaro Baba, Tomokazu Hokada, Atsushi Kamei, Ippei Kitano, Yoichi Motoyoshi, Nugroho Setiawan, Davaa-ochir Dashbaatar & John Booth
Ruby-bearing calc-silicate at West Ongul Island, Lützow-Holm Complex, East Antarctica

11:30-11:50 Srett Santitharangkun & **Burapha Phajuy**
Mineral Chemistry of Cordierite, Plagioclase and Biotite in the Cordierite-Bearing Tonalite in Bokeo Province, Lao PDR

11:50-12:10 **Ladda Tangwattananukul**, Daizo Ishiyama & Punya Charusiri
Characteristics of gold mineralization in Huai Kham On gold deposit in Sukhothai Fold Belt, Northern Thailand

Lunch

13:00-13:30 **Ludvig Löwemark** (Keynote speaker) Akkaneewut Chabangborn, Sakonvan Chawchai, Helmut Duerrast, Mao-Chang Liang, Midhun Madhavan & Chung-Ho Wang
Understanding oxygen isotope records of climate change: Insights from a 5-year, daily resolved $\delta^{18}O$ precipitation record from Krabi, Thailand

13:30-13:50 **Ismail Hossain**, Md. Sazzadur Rahman, Md. Abdur Rahim, Pradip Kumar Biswas, A.S.M. Mehedi Hasan & Md. Ibrahim Adham
Subsurface Late Quaternary ironstones in Northwest Bangladesh: A geochemical review

13:50-14:10 **Thanakorn Jiwarungrueangkul**, Zhifei Liu & Karl Stattegger
Variation in chemical weathering intensity in the Mekong River basin over the past 30,000 years

14:10-14:30 **Ken-ichiro Hisada**
Geologic significance of Iranian Zagros for World Diffusion of Homo sapiens

Break

14:50-15:20 **Montri Choowong** (Keynote speaker) Sumet Phantuwongraj, Parisa Nimnate, Nikhom Chaiwongsaen & Stapana Kongsen
Coastal and Flooding Hazard Research in Thailand : Progress and Challenges

15:20-15:40 **Romyupa Srikraiwest**, Rungroj Arjwech & Mark E. Everett
Understanding Causes and Impacts of Urban Salinity in Khon Kaen Province, northeast Thailand

15:40-16:00 **Rungroj Arjwech**, Thunyatorn Sarntima & Mark E. Everett
Mapping of Shallow Rock Salt Using Seismic Refraction and 2D Electrical Resistivity Topmography Methods at Borabue, Maha Sarakham, Thailand

16:00-16:20 **Benjawan Prajaklertwittaya** & Danupon Tonnayopas
Utilization of pumice aggregate blended with serpentinite and palm oil fuel clinker in lightweight mortar

16:30-17:00 **Post-Conference Fieldtrip Meeting**

Keynote speakers

Urs Klötzli
University of Vienna

Ludvig Löwemark
National Taiwan University

Montri Choowong
Chulalongkorn University

GREAT Sponsors

PTTEP

SCG

Proceedings of the Second International Symposium on Geoscience Resources and Environments of Asian Terranes (GREAT 2018)
19 - 23 November 2018 Bangkok, Thailand

More than basic geological works in cave and karst study in Thailand

Chaiporn Siripornpibul[1]*

1 Department of Mineral Resources, Ministry of Natural Resources and Environment, Thailand.

* Corresponding author email: alekchaiporn@gmail.com

Abstract

Karst resources have played the greatest roles in the creation of important resources such as landforms, soils, water and vegetation which will provide suitable places for plants, animals, and human to live on these available resources. Karst features of both exokarst (surface karst) and endokarst (underground karst or caves) in Thailand are the good examples of the close relationship between nature and people since the ancient time until today. In the past, people have been using caves as the shelters, religious and cultural activities, they also used karst lakes and cave springs as the sources of water for their daily life. Soils in the paleokarst areas are very fertile and suitable for many agricultural activities. Karst features are the outstanding places because of its beauty and astonishing figures. Many people would like to join various types of tourism in karst areas such as eco-tourism, adventure in the caves, cultural learning, sight-seeing in the marine karst areas, even though the geo-tourism, research and education programs. Karst features are very fragile, especially speleothems in caves. The sustainable measures are urgently needed. We must do more scientific research works especially about geology and its applications. Furthermore, in the scientific point of view, there are many subjects that we should do more in research works such as karst biodiversity, paleontology, paleo-climate, carbon sink and neo-tectonic that can be applied in this region.

Proceedings of the Second International Symposium on Geoscience Resources and Environments of Asian Terranes (GREAT 2018)
19 - 23 November 2018 Bangkok, Thailand

The Sukhothai zone in northern Laos: what can we see with Triassic carbonates?

Katsumi Ueno[1]*, Yoshihito Kamata[2], Koji Uno[3], Thasinee Charoentitirat[4], Punya Charusiri[4], Khamseng Vilaykham[5] and Rossana Martini[6]

1 Department of Earth System Science, Fukuoka University, Japan

2 Graduate School of Life and Environmental Sciences, University of Tsukuba, Japan

3 Graduate School of Education, Okayama University, Japan

4 Department of Geology, Chulalongkorn University, Thailand

5 Department of Geology and Minerals, Lao P.D.R.

6 Department of Earth Sciences, University of Geneva, Switzerland

* Corresponding author email: katsumi@fukuoka-u.ac.jp

Abstract

In mainland Southeast Asia, Permian–Triassic subduction of the Paleo-Tethyan oceanic lithosphere formed an island arc system called the Sukhothai Zone along the margin of the Indochina Block. This zone was originally defined in Northern Thailand and is considered to extend northward to the Lincang Massif of southwestern Yunnan, China, but so far lacked concrete evidence from northern Laos between them. In the Oudom Xai area in northern Laos, recent findings of scattered limestone bodies of Late Permian and Triassic ages suggested a close geotectonic relation of that area with the Sukhothai Zone of Northern Thailand. However, information is still insufficient in entire northern Laos.

In the Long area of northwestern Laos, there is an isolated massive carbonate body, which has been considered as Carboniferous—Early Permian. We found Triassic foraminifers from this limestone, which supports the western part of northern Laos to belong to the extension of the Sukhothai Zone. The relevant limestone forms a kilometer-sized massive body, surrounded by Permian clastics and volcanics/volcaniclastics. Cement-rich reefal sediments consisting of Tubiphytes-microbial boundstone and sparse-allochem bioclastic grainstone are commonly observed. They suggest open-marine sedimentation on a shallow carbonate platform. A Carnian (early Late Triassic) age was substantially corroborated based on foraminifers, such as Aulotortus sinuosus, A. tumidus, Ophthalmidium danneri, Diplotremina astrofimbriata, and Palaeolituonella majzoni.

In neighboring Northern Thailand, Carnian limestone with similar lithological and paleontological properties is distributed only in the Doi Long Formation of the Lampang Group in the Sukhothai Zone, which provides a firm basis for the tectonostratigraphic characterization of northwestern Laos. Consequently, our study is not merely important in revising the age of this limestone but also more crucial in giving a clue to clarify the extension in northern Laos of a Permian–Triassic Sukhothai Zone, which is one of major tectonostratigraphic units comprising mainland Southeast Asia.

Key words: foraminifers, northern Laos, Sukhothai Zone, tectonostratigraphy, Triassic limestone

Proceedings of the Second International Symposium on Geoscience Resources and Environments of Asian Terranes (GREAT 2018)
19 - 23 November 2018 Bangkok, Thailand

Challenges and progress in understanding the tectonics and structure of the Indosinian Orogeny in Thailand

Chris K. Morley[1]

1 Department of Geological Sciences, Chiang Mai University Chiang Mai, Thailand

Abstract

The Indosinian Orogeny involved the collision of ribbon continents, which impacted the structural, metamorphic and igneous history of the orogenic belt, as well as the stratigraphic of the continents prior to collision. The narrow width, widespread rifting of ribbon continents influences a variety of factors to make their collisions significantly different from major continental collision zones. Key characteristics of the tectonics of Sibumasu are: 1) a tendency towards basin inversion, and mixed thick-skinned and thin-skinned style deformation. Well-developed fold and thrust belts are very rare. 2) Extensional collapse is an important feature of Sibumasu in northern Thailand (and probably other areas too). 3) Slab delamination and extensional decompression melting were probably important mechanisms for generating granites in addition to crustal thickening. 4) The timing of deformation in Sibumasu (Early Triassic collision vs Middle-Late Triassic collision), and the significance of the Late Permian-Early Triassic unconformity in Malaysia and Sumatra remain disputed. The case for late collision is best made in northern Thailand. Middle Triassic deposition is interpreted as occurring largely in a post-rift setting with some minor extensional fault reactivation (similar to the LHR), while post-collisional extensional collapse is regarded as being largely Norian or later in age. A number of key problems remain, including: 1) the timing and significance of structural, stratigraphic, metamorphic and igneous events for reconstructing the Indosinian collision. 2) The timing and extent of extension within the orogenic belt, and 3) interpretation of the tectonic setting of Carboniferous-Permian deepwater deposits in the Slate Belt of Myanmar and the Peninsular of Thailand, and deepwater Carboniferous-Triassic deposits in the Mae Sariang area. Continuation of dating of sections by fossils, U-Pb dating of zircons and monazite, detrital zircon maximum ages, and less conventional dating techniques (e.g. dating of authigenic illite in fault zones, U-Pb dating of calcite veins) is helping to address 1) above. For 2) above a number of areas both in western, eastern and northern Thailand exhibit Late Triassic or younger extension, the timing, kinematics and magnitude of the extension is not well known, and represents a significantly understudied aspect of the orogeny.

Proceedings of the Second International Symposium on Geoscience Resources and Environments of Asian Terranes (GREAT 2018)
19 - 23 November 2018 Bangkok, Thailand

Geochronological research in the crystalline basement units of N Thailand: a review

Urs Klötzli[1]*, Jürgen Österle[2], Pitsanupong Kanjanapayont[3], Bernhard Neugschwentner[1] and Jolanta Burda[4]

1 Department of Lithospheric Research, University of Vienna, Austria

2 School of Geography, Environment and Earth Sciences, Victoria University of Wellington, New Zealand

3 Basin Analysis and Structural Evolution Special Task Force for Activating Research (BASE STAR), Department of Geology, Chulalongkorn University, Bangkok, Thailand

4 Faculty of Earth Sciences, University of Silesia, Katovice, Poland

* Corresponding author email: urs.kloetzli@univie.ac.at

Extended Abstract

The presentation will give an overview on the geochronological work which has been conducted by different research teams in the last 30 or so years in N Thailand. After a short review of the tectonic evolution of Sundaland the presentation mainly centers on the discussion of zircon and monazite growth/recrystallization ages reflecting high-temperature events during the evolution of Thailand as part of Sundaland. Special emphasis will be put on data obtained from the Lan Sang gneisses.

Tectonic evolution

In Thailand basement rocks are restricted to a north-south trending belt of high-grade metamorphic rocks and granites, the Chiang Mai-Lincang Belt, prominently exposed in NW Thailand and minor exposures within strike-slip systems in the central and southern parts of the country. Traditionally the basement rocks were interpreted as entirely pre-Cambrian in age due to their association with overlying sediments of (presumably) Cambrian age. However, earliest radiometric dating studies already showed that these basement rocks were at least overprinted and partly intruded in the Late Triassic-Early Jurassic.

Starting in the Devonian, Gondwana-derived continental fragments migrated northwards in three successive phases bracketed by the opening and closure of the intervening Tethyan ocean (s). Subduction of the Paleo-Tethys led to the construction of a continental magmatic arc-the Sukhothai Arc-along the southern margin of Indochina in the late Carboniferous-early Permian that was subsequently separated by back-arc spreading and then re-accreted onto Indochina by back-arc collapse in the Triassic. The final closure of the Paleo-Tethys in the Late Triassic led to the collision of Sibumasu and Sukhothai/Indochina and gave rise to

the formation of Sundaland, the continental core of SE Asia. This collision is referred to as the Indosinian orogeny.

The post-collisional development of Sundaland was characterized by tectonic quiescence until the Cretaceous, resulting in shallow marine sedimentation in the west and massive accumulation of continental red beds (Khorat Plateau) in the east of Thailand. During the same time interval from Jurassic to Early Cretaceous, Andean-type convergence with subduction occurred along the western margin of Sundaland, generating voluminous I-type magmatism in the Mogok Metamorphic and Slate belts. It is, however, unclear whether this convergent margin setting had any effect on the Thai basement rocks. After a phase of relative quiescence in mid-Mesozoic times, renewed Neo-Tethys subduction led to mixed I-type and S-type magmatism of the Western Granite Belt and a high-temperature metamorphism of Thai basement rocks, as evidenced by zircon and monazite U-Th-Pb growth and mica Ar-Ar cooling ages.

The Cenozoic evolution of Sundaland was dominated by the collision of India and Eurasia since ~50 Ma resulting in the Himalayan orogeny. While the timing of this collision is still debated, based on our age data we prefer an earlier, Paleocene-Early Eocene age. The collision-initiated strike-slip systems accommodating the strain and relative motion of India with respect to Sundaland and simultaneously leading to the syn-collisional lateral extrusion of Sundaland along these fault zones. Based on experiments and satellite images the 'continental extrusion' model involving the horizontal motion of rigid blocks bounded by left-lateral strike-slip faults, such as the Ailoa Shan-Red River and Mae Ping shear zones, were established. However, various aspects of this model have been recently challenged, such as the timing of fault initiation, the depth of penetration, or the magnitude of geological offset.

In Thailand the four major strike-slip fault systems are the NW-SE trending Mae Ping and the Three Pagodas fault zones and the NE-SW trending Ranong fault zone and the Khlong Marui shear zone. The Klaeng shear zone east of Bangkok may be a continuation of the Mae Ping or the Three Pagodas shear zone. Along these shear zones basement units were exhumed during the Cenozoic. In contrast, basement rocks in the Doi Inthanon and Doi Suthep metamorphic core complexes were likely brought to the surface by low-angle normal faulting.

Geochronological data

The collision of Sibumasu with Indochina resulted in the Indosinian orogeny. The exact timing of continental collision remains poorly constrained, but has been proposed at 215±6 Ma, based on the occurrence of Permian-Triassic detrital zircons in the Loi-an Group of the Sibumasu terrane. Permo-Triassic zircon U-Pb ages, common in the Sukhothai Arc, signal the onset of sediment transport across the suture zone and deposition on the Sibumasu terrane. The Indosinian orogenesis is also manifested in zircon U-Pb ages in basement rocks across Thailand. However, the significance and what events/processes these zircon U-Pb ages actually reflect are ambiguous.

A lower intercept U-Pb age of 197 +2/-3 Ma for a gneiss from the Take to Mae Sot transect was interpreted as the age of amphibolite-facies metamorphism. Quasi-contemporaneous zircon U-Pb lower-intercept ages from the Lan Sang gneiss (190 +5/-6 Ma), the Umphang gneiss (202±3 Ma) and gneiss samples in the vicinity of Mae Sariang (199 +8/-10 Ma) and Ban Tak (212 +6/-7 Ma) were also determined. In addition, εTCHUR(Nd) values of -10.6 to -13.7 for the same samples, classifying them as of (meta-)sedimentary origin and supporting the notion of a high-grade metamorphic event during the Late Triassic-Early Jurassic, were reported.

Significantly younger zircon U-Pb lower-intercept ages from gneisses near Hot (148 +6/-8) and the Khlong Lan National Park (174 +5/-6) were interpreted as geologically meaningless because of inferred Pb loss due to a later metamorphic overprint. In contrast, the corresponding upper-intercepts of above-mentioned gneiss samples are predominately Paleoproterozoic, interpreted to reflect either inherited material or protolith emplacement. In the Doi Inthanon and Doi Suthep area, zircon from two orthogneiss samples yielded Late Triassic-Early Jurassic ages (211±4 Ma, 203±4 Ma) that were interpreted to date the time of crystallization of the granitic protolith. A coeval zircon U-Pb age (205 +3/-4 Ma) from the adjacent Mae Chaem pluton, located to the west of Doi Inthanon, was used in support for the magmatic origin of the gneisses. An alternative interpretation of the Triassic-Early Jurassic zircon U-Pb ages is based on the paucity of textural evidence for polymetamorphism in the amphibolite- to lower granulite-facies rocks exposed in the Three Pagodas shear zone. Thus, the ages are thought to rather reflect detrital ages of metasediments with depositional ages of <200 Ma.

Monazite U-Th-Pb ages in basement rocks of Thailand document renewed metamorphic activity in late Early Cretaceous times. Concordant monazite ages from Khlong Lan (117±3 Ma) and two monazite core

Th-Pb ages from the Lan Sang gneisses (~114 Ma, ~123 Ma) provide some evidence for an Early Cretaceous thermal or metamorphic overprint.

A second event in the Late Cretaceous is recorded in monazite U-Pb ages from orthogneiss of the Doi Inthanon (84±2 Ma, 72±1 Ma, ~83-69 Ma) and a monazite Th-Pb age from a garnet-two-mica granite dike (66±2 Ma) from the Bhumipol Lake area. Additionally, zircon U-Pb ages from a cross-cutting dike in the Lan Sang gneiss (76±1 Ma), mylonitic granites of the Ranong (crystallization age ~71-81 Ma) and the Khlong Marui (~62-70 Ma), as well as a gneiss (67±1 Ma; zircon rim age) and a leucogranite (77±1 Ma) from the Klaeng shear zones all imply an episode of Late Cretaceous magmatism.

The Cenozoic evolution was dominated by the India-Eurasia collision. The Eocene collision resulted in deformation and magmatism in Sundaland as reflected in U-Pb ages in the Doi Inthanon and Doi Suthep area (mylonitic granite: 40.0±0.5 Ma, zircon; 40.0 +1.2/-0.5 Ma, monazite; calc-silicate: 37±7 Ma, zircon; 47±28 Ma, titanite), the Thabsila metamorphic core complex (paragneiss: 51±7 Ma; orthogneiss: 57±1 Ma; zircon), the Klaeng strike-slip shear zone (43±1, monazite; 36±3 Ma, titanite), and the Ranong (48±1 Ma, zircon) and Khlong Marui (orthogneiss: 46±1 Ma; mylonitic granite: ~55-50 Ma; pegmatite: 49±1 Ma; zircon) strike-slip zones.

Following wide-spread deformation in the Eocene, the Oligocene-Early Miocene was characterized by late- and post-kinematic intrusion in the Doi Inthanon area and exhumation and the uplift of metamorphic core complexes.

What remains of the former 'pre-Cambrian' basement? To date, no unambiguous pre-Cambrian magmatic or metamorphic ages have been found in the basement rocks of Thailand. The oldest rock dated so far is the Khan Tao orthogneiss (Hua Hin Group) with a Cambrian zircon U-Pb protolith age (508±8 Ma). Also, worth mentioning is the Khao Dat Fa granite at Khanom with an Ordovician zircon U-Pb protolith age (477±7 Ma).

More on the evolution of the Lan Sang gneisses

The in-situ methodology employed in our study details a complex temporal evolution of the basement rocks in the Lan Sang area not revealed in previous studies. Despite these complexities, two main age populations that are contemporaneous with the Indosinian and Himalayan orogenies dominate the isotopic age determinations. Zircon cores likely related to the original magmatic protolith, from an augen gneiss, yield

Late Triassic crystallization ages with evidence for possible minor zircon modifications and growth throughout the Mesozoic and a major period of metamorphic overgrowth in the Eocene (~44 Ma). The Indosinian age (223 – 210 Ma) for the granitic protolith formation contradicts a recently published Early Cretaceous age (123-114 Ma) interpreted to date protolith emplacement. The pre- or synkinematic intrusion of the magmatic protolith of a biotite gneiss into the Late Triassic augen gneiss in the Late Eocene (~35 Ma) constrains the timing of mylonitic deformation in the Mae ping shear zone and the greenschist-facies overprint of both gneisses. These zircon U-Pb constraints agree with recently published monazite Th-Pb ages that were interpreted to reflect the onset of mylonitic shear zone deformation at ~37 Ma. Ductile shearing of the gneisses likely ceased at ~30-33 Ma based on previously determined biotite $^{40}Ar/^{39}Ar$ ages, although deformation may have continued in the rheologically weaker calc-silicate and marble core of the shear zone. A late undeformed subvolcanic dike that cross-cuts the mylonitic fabric of the calc-silicate and marble core, dated in this study at ~22 Ma, provides a minimum age for the timing of ductile deformation and the metamorphic event that instigated zircon neo-crystallization in the augen gneiss, intrusion of the protolith of the biotite gneiss and monazite recrystallization in both. Our dataset is en par with studies from other major strike-slip shear zones of Thailand and the Mogok Metamorphic Belt in Myanmar showing that subsequent to the Indosinian orogeny the Sibumasu basement experienced a major phase of metamorphism and igneous activity in the Eocene most likely related to tectonics associated with the indentation of India into the Eurasian continent.

Key words: Thailand, dating, basement, geochronology, Lan Sang

Proceedings of the Second International Symposium on Geoscience Resources and Environments of Asian Terranes (GREAT 2018)
19 - 23 November 2018 Bangkok, Thailand

Understanding oxygen isotope records of climate change: Insights from a 5-year, daily resolved $\delta^{18}O$ precipitation record from Krabi, Thailand

Ludvig Löwemark[1]*, Akkaneewut Chabangborn[2], Sakonvan Chawchai[2], Helmut Duerrast[3], Mao-Chang Liang[4], Midhun Madhavan[5] and Chung-Ho Wang[6]

1 Department of Geosciences, National Taiwan University, No 1. Sec. 4 Roosevelt Road, P.O. Box 13-318, 106 Taipei, Taiwan

2 Department of Geology, Faculty of Science, Chulalongkorn University, Phayathai Rd., Bangkok, 10330, Thailand

3 Department of Physics, Faculty of Science, Prince of Songkla University, Kanjanavanich Road 15, HatYai, 90112, Thailand

4 Research Center for Environmental Changes, Academia Sinica, 128, Sec. 2, Academia Road, Nankang, Taipei 11529, Taiwan

5 Department of Atmospheric Sciences, Cochin University of Science and Technology, Kochi, India

6 Institute of Earth Sciences, Academia Sinica, 128, Sec. 2, Academia Road, Nankang, Taipei 11529, Taiwan

* Corresponding author email: ludvig@ntu.edu.tw

Abstract

Variations in oxygen isotopes in speleothems are often interpreted to reflect variations in the amount of precipitation controlled by changes in climate phenomena such as the monsoon or ENSO. However, this amount effect has recently been questioned, favoring other mechanisms such as moisture source(s), rainout history, or the influence of local convection. A more than 5 years long daily resolved precipitation and $\delta^{18}O$ record from Thailand allows the relationship between precipitation patterns and rainwater $\delta^{18}O$ to be examined. Rainfall at the Krabi station was highly irregular with rain events ranging from 0.1 mm to nearly 150 mm per day. Rainwater $\delta^{18}O$ values vary from -17.50 to 8.24 ‰, with a long-term average close to -5 ‰. We demonstrate that while daily and amounted weighted seasonal $\delta^{18}O$ values show no correlation with rain amount, the amount weighted monthly values display a significant correlation with monthly rainfall. Statistical comparison to atmospheric parameters reveals a strong correlation to outgoing longwave radiation, suggesting that local convection rather than precipitation amount control variations in rainwater $\delta^{18}O$ in this region. Comparison to a short cave drip water record suggests that the atmospheric $\delta^{18}O$ signal is recorded with a muted amplitude in the drip water, and with a lag of one to two weeks.

Proceedings of the Second International Symposium on Geoscience Resources and Environments of Asian Terranes (GREAT 2018)
19 - 23 November 2018 Bangkok, Thailand

Coastal and flooding hazard research in Thailand: progress and challenges

Montri Choowong[1]*, Sumet Phantuwongraj[1], Parisa Nimnate[2], Nikhom Chaiwongsaen[1] and Stapana Kongsen[1]

1 Morphology of Earth Surface and Advanced Geohazard in Southeast Asia (MESA) Research Unit, Department of Geology, Chulalongkorn University

2 Division of Geoscience, Mahidol University, Kanchanaburi Campus, Kanchanaburi, Thailand

* Corresponding author email: Montri.c@Chula.ac.th

Abstract

The 2004 Indian Ocean Tsunami devastated large parts of the Andaman coast of Thailand and the countries around Indian Ocean. In late 2011, mega-flooding occurred in Thailand and caused billions of dollars of economic loss especially in the industrial zones of the central plain. In this presentation, we show how these two major disasters form the back drop to progress geo-hazard research in Thailand focusing on coastal hazards and flooding. We also examine some of the remaining challenges. Since 2004, sedimentological studies of the Indian Ocean Tsunami have been carried out by local and foreign geo-scientists. These studies include sedimentological recognition of 2004 tsunami deposit and the search for paleo-tsunami deposits. Some major goals for these workers include documenting evidence for pre-historical tsunami and using paleo-tempestology to distinguish these events from records of storm events. In Thailand, analyses of geological proxies for tsunamis and storm events have been successful in developing a greater understanding of the mechanical processes involved and the frequency of such events. However, there is a need to extend the scope of these studies to the other coastal zones of Southeast Asian mainland, such as Cambodia (the South China Sea) and Vietnam (the Pacific Ocean).

In 2011, mega-flooding occurred throughout Thailand. Its root cause was natural and due to a series of heavy rainfalls. However, there was also undoubtedly a failure to provide sufficient protection for the industrial and economic zones due to both an under-estimation of the volume of water that needed to be considered and insufficient water management. To help address this imbalance, since 2012 we have been undertaking a detailed investigation of the flooding in the Chao Phraya River Basin and the Mun River on the Khorat Basin. In case of Chao Phraya River, we found that parts of all rivers in this area have undergone a rapid decrease of water storage capacity and an increase of sand bar areas in river embayment. The reduction of sediment supply led to non-equilibrium in the deltaic zone of the upper Gulf of Thailand. Our findings highlight the need for continued geomorphological and sedimentological research in Thailand and the need of geological studies to help respond to societal needs to mitigate such natural disasters on local and global scales.

Key words: Coastal hazards, 2011 mega-flooding, 2004 IOT, Paleo-tempestology

Proceedings of the Second International Symposium on Geoscience Resources and Environments of Asian Terranes (GREAT 2018)
19 - 23 November 2018 Bangkok, Thailand

Sedimentology and facies analysis of the Upper Paleozoic shallow marine siliciclastic deposit from Doi Tu Pu, Chiang Rai Province, Northern Thailand: Preliminary note

Pitaksit Ditbanjong[1]*, Wittaya Kandharosa[1], Yupa Thasod[1] and Rattanaporn Fongngern[1]

1 Department of Geological Sciences, Faculty of Science, Chiang Mai University

* Corresponding author email: pitaksit.d@cmu.ac.th

Abstract

An old quarry at Doi Tu Pu, situated about 5 km NW of Chiang Rai city, provides a chance to study sedimentology and stratigraphy of the siliciclastic sedimentary succession with high resolution. According to the previous work, the study area has been mapped as Carboniferous rock unit. Stratigraphic framework shows that the study area overlies a conglomerate rock unit and is capped by Permian limestone. Sedimentary strata are dominantly composed of fine-grained clastic sediment (mudstone/siltstone) interbedded with very thin- to medium-bedded sandstone. In general, the strata are E-W striking and sub-vertical S-dipping (080-100/70-90°S), except for the southern part of the quarry, where the strata become overturned with N-dipping. Several E-W trending faults with sub-vertical fault planes cross cut and separate study area into many blocks. The objective of this work is to study sedimentology, sedimentary process in order to interpret the deposition environment by lithofacies analysis from field observations. Facies analysis is based on three measured stratigraphic sections which can be subdivided into 13 lithofacies such as mudstone dominated, rhythmites sandstone/mudstone, HCS/SCS sandstone facies. They can be interpreted as constituents of intertidal and subtidal, shoreface, and transition zone subenvironments where sedimentary transportation is dominated by tidal, wave and storm influence. In addition, plants debris are commonly found in dark-grey shales. Fossiliferous beds being made up of brachiopod, crinoid, bryozoan, trilobite and gastropod are presented by postmortem transportation. Vertical and sub-horizontal bioturbation are well preserved and common. Detailed study on ichnofacies will be helpful to determine depositional environment in the future works. The sedimentary stack shows repeated cycles of shallowing upward facies with fining upward grain-size trend that appear to be typical of parasequences occurring on a tide-dominated shoreline.

Key words: Shallow marine deposit, tidal rhythmites, intertidal subtidal environments, parasequences, Upper Paleozoic, Doi Tu Pu, Chiang Rai Province, Northern Thailand

Proceedings of the Second International Symposium on Geoscience Resources and Environments of Asian Terranes (GREAT 2018)
19 - 23 November 2018 Bangkok, Thailand

Facies analysis and paleoenvironmental reconstruction of Tha Manao Limestone (Middle Ordovician) in Sri Sawat District, Kanchanaburi Province

Thitikan Junrattanamanee[1]*, Nitipon Noipow[2] and Anisong Chitnarin[1]

1 School of Geotechnology, Suranaree University of Technology, 111 University Avenue, Suranaree subdistrict, Mueang district, Nakhon Ratchasima province, 30000, Thailand

2 Disaster Management and Public Hazard Mitigation Program, Faculty of Science and Technology, Valaya Alongkorn Rajabhat University under the Royal Patronage, Pathum Thani 13180

* Corresponding author email: t_junrattanamanee@hotmail.co.th

Abstract

The Tha Manao Limestone succession exposed on the east side of Srinagarind reservoir in Kanchanaburi province were measured and collected, and aimed to define the stratigraphy and their depositional environments. The succession is medium-to thick-bedded, dark grey – to greenish grey, micritic and fossiliferous. Co-occurring macrofossils such as Actinocerus sp., Endocerus sp., Teiichispira sp., Fisherites sp. indicate Middle Ordovician (Dapingian – Darriwilian) in age. From a total 157-meters thick section, many rock slabs and 127 thin sections were prepared and studied under stereomicroscope and polarized-light microscope. The microfacies (MF) can be divided into 11 types notably (MF1) Algal- intraclast-pelloidal packstone, (MF2) pelloidal calcisiltite, (MF3) coarse packstone with microbially coated grains, (MF4) fine packstone with intraclast, (MF5) bio-intraclast packstone, (MF6) Intraclast-pelloidal wackestone with microbially coated grains, (MF7) rounded clast grainstone, (MF8) abundant shell packstone, (MF9) molluscan-pelloidal packstone, (MF10) molluscan packstone and (MF11) finely pelloidal mudstone. The microfacies contributed in 6 depositional environments from peritidal, lagoon, shoal, open marine, mid ramp and outer ramp. The successions are divided into 3 Sequences from bottom to top accordingly; 1) Lower sequence (0-55 meters), the sequence dominated by intraclast and pelloid-rich pack-grainstone facies which represents the outer ramp to inner ramp environment; 2) Middle sequence (55-110 meters), the sequence represents mid ramp to inner ramp environments, evidenced by larger and mixed grains; 3) Upper sequence (110-157 meters), in this sequence shows abundant shell and mollusk, which were normally deposited in the outer ramp to the inner ramp. From Lithology and macrofossils found in the studied section can be correlated to sequence in Thong Pha Phum area, Western Thailand, Thung Song Group, Southern Thailand and Lower Setul Limestone, Langkawi Island.

Key words: Microfacies, Thung Song Limestone, Sibumasu Terrane

Proceedings of the Second International Symposium on Geoscience Resources and Environments of Asian Terranes (GREAT 2018)
19 - 23 November 2018 Bangkok, Thailand

Characteristics of granites from Sukhothai Arc and Loei Fold Belt: Application for tectonic setting

Abhisit Salam[1,2,3]*, Sebastien Meffre[2], Supitchaya Paipana[2], Maysa Wittayanontawet[1], Takayuki Manaka[3,4] and Khin Zaw[2]

1 Department of Geology, Faculty of Science, Chulalongkorn University, Phayathai, Bangkok 10330, Thailand

2 CODES ARC Centre of Excellence in Ore Deposits, School of Physical Sciences, University of Tasmania, Private Bag 126, Hobart, Tas 7001, Australia

3 CIMER Centre of Indochina Mineral and Environmental Research, Department of Geology, Faculty of Science, Chulalongkorn University, Phayathai, Bangkok 10330, Thailand

4 Survey of Japan, AIST Central 7, 1-1-1, Higashi, Tsukuba, Ibaraki, 305-8567, Japan

* Corresponding author email: Abhisit.A@chula.ac.th

Abstract

Thailand comprises of two tectonic blocks namely, Shan-Thai (Sibumasu) and Indochina, and in between there are Sukhothai Arc (Suhkothai Fold Belt-SFB) in the west and Loei Fold Belt-LFB (western edge of Indochina terrane) in the east. However, the detailed tectonic setting of these belts has not been understood particularly their magmatisms. The geochronological data indicate that there are two distinct age groups in these belts including Late Permian-Early Triassic (260-240 Ma) and Late Triassic-Early Jurassic (210-190 Ma). Comparison of the newly collected ages from eastern Thailand with the data of LFB in Thailand (mainly from central and northeastern Thailand) and Southwest Cambodia indicating that the Late Permian-Early Triassic ages from eastern Thailand are comparable to the early magmatism of the LFB which was associated with subduction event between the Sibumasu and Indochina Terranes. In contrast, the Late Triassic-Early Jurassic ages from eastern Thailand is comparable to the late stage magmatism of LFB which may have formed during post-collisional event of the Sibumasu and Indochina Terranes. However, timing of magmatism at the SFB is constrained to 250-180 Ma at northwestern Thailand and the belt is interpreted to continue into eastern Thailand and thus the ages could represent the magmatism of the SFB as well. It is also known that similar ages of granites were recorded from southwest Cambodia (200-170 Ma). These ages of granites from eastern Thailand and southwest Cambodia could be grouped together. Further geochemical distinction of magmatic rocks from the LFB (mainly Phetchabun-Nakhon Sawan) and SFB (mainly eastern Thailand and

western Cambodia may support some variation in tectonic setting and their associated mineralization in these belts. In terms of genetic link to ore deposits in the LFB, it is likely that both magmatic events are closely associated with Ag-Au and Cu-Au mineralisation in which the Late Permian-Early Triassic volcanic rocks commonly host epithermal-style Ag-Au bearing veins, whereas the Late Triassic-Early Jurassic granites are typically associated with Cu-Mo-Au porphyry/skarn-style mineralisation within the LFB (e.g., French Mine Prospect) and southwest Cambodia (e.g., Phnom Basset Prospect). In the LFB, the Late Permian-Early Triassic volcanic rocks commonly host epithermal-style Au bearing veins (Huai Kham On prospect) whereas, the Late Triassic-Early Jurassic granites are typically associated with Sb-Au veins style mineralisation (e.g., Bo Thong prospect).

Key words: granite, volcanic, gold, copper, mineralization

Proceedings of the Second International Symposium on Geoscience Resources and Environments of Asian Terranes (GREAT 2018)
19 - 23 November 2018 Bangkok, Thailand

Geology and Epithermal Gold-Silver Mineralization of Suwan Prospect, Phitsanulok Province, Central Thailand

Tanad Soisa[1], Abhisit Salam[1,2]*, Somboon Khositanont[3] and Takayuki Manaka[2,4]

1 Department of Geology, Faculty of Science, Chulalongkorn University, Phayathai road, Bangkok 10330, Thailand

2 CIMER Centre of Indochina Mineral and Environmental Research, Department of Geology,

Faculty of Science, Chulalongkorn University, Phayathai road, Bangkok 10330, Thailand

3 Royal Thai Department of Mineral Resources, Rama VI Rd, Bangkok 10400, Thailand

4 Geological Survey of Japan, AIST Central 7, 1-1-1, Higashi, Tsukuba, Ibaraki, 305-8567, Japan

* Corresponding author email: Abhisit.A@chula.ac.th

Abstract

The Suwan prospect is located about 6 km northwest of the Chatree gold mine in Phitsanulok province, central Thailand. Gold-silver mineralization occurs as veins and stockworks hosted in volcaniclastic and volcanogenic-sedimentary rocks of Late Permian-Early Triassic age, an extension of the Chatree volcanic succession. From top to bottom, the hosted volcanic succession can be divided into 3 units, namely 1) Fiamme breccia unit (Unit 1), 2 Volcanogenic-sedimentary unit (Unit 2), and 3) Andesite unit (Unit 3). Unit 1 consists predominantly of crystal-rich fiamme breccia, lithic-rich fiamme breccia and polymictic andesitic breccia. The volcanogenic-sedimentary unit (Unit 2) consists of fine- to coarse-grained sandstone, sandy-matrix polymictic breccia, mudstone and limestone lenses. Unit 3 comprises plagioclase-phyric-basaltic andesite, phyric andesite and monomictic andesitic breccia. At least 3 stages of mineralization have been identified namely, 1) pre-gold stage; quartz-pyrite vein (stage 1), 2) main gold stage; quartz-carbonate-sulfides-electrum vein (stage 2), and 3) post-gold stage; quartz-carbonate vein (stage 3). In the main gold stage (stage 2), pyrite is a major sulfide mineral with minor amount of sphalerite, chalcopyrite and galena. These sulfide minerals are closely associated with quartz and calcite, major gangue minerals of stage 2. Gold mainly occurs as inclusions in pyrite and EPMA analysis confirms that it forms as electrum. On the basis of petrographic observation and X-Ray Diffraction Analyzes (XRD), the hydrothermal alteration at the Suwan prospect can be divided into 3 zones. From proximal to distal to the ore zone, they are 1) Silicic zone (quartz-adularia), 2) Phyllic zone (adularia-quartz-illite-sericite), and 3) Propylitic zone (chlorite-epidote-calcite). Based on geological information such as mineralogy, vein textures, and hydrothermal alteration, the Suwan prospect could be classified as low sulfidation epithermal gold-silver deposit similar to the well-known Chatree deposit.

Key words: volcanic, epithermal, gold, silver, mineralization

Proceedings of the Second International Symposium on Geoscience Resources and Environments of Asian Terranes (GREAT 2018)
19 - 23 November 2018 Bangkok, Thailand

Epithermal Gold-Silver Mineralization and Alteration of B prospect, Phichit Province, central Thailand

Sirawit Kaewpaluk[1], Abhisit Salam[1,2]* and Takayuki Manaka[2,3]

1 Department of Geology, Faculty of Science, Chulalongkorn University, Phyathai Road, Bangkok 10330, Thailand

2 CIMER Center of Indochina Mineral Resources and Environmental Research, Department of Geology, Faculty of Science, Chulalongkorn University, Phyathai Road, Bangkok 10330, Thailand

3 Survey of Japan, AIST Central 7, 1-1-1, Higashi, Tsukuba, Ibaraki, 305-8567, Japan

* Corresponding author email: Abhisit.A@chula.ac.th

Abstract

The B prospect is located about 3 km southeast of the Chatree gold mine along the NNW-SSE trending major structure (fault) that extends more than 10 km. Geology of the B prospect is characterized by Late Permian-Early Triassic volcaniclastic and volcanogenic-sedimentary rocks, an extension of Chatree volcanic succession. The thickness of host volcanic succession at B prospect is at least of 300 meter which can be divided into four main stratigraphic units from top to the bottom of the stratigraphy: polymictic breccia unit (Unit 1), volcanogenic sedimentary unit (Unit 2), fiamme breccia unit (Unit 3) and andesitic breccia unit (Unit 4). Gold-silver mineralization mainly occurs in polymictic breccia and volcanogenic sedimentary units. Most dykes are postdated gold-silver minealization and comprise 3 types namely, 1) Hornblende-plagioclase phyric andesite, 2) Plagioclase phyric andesite and 3) Hornblende phyric andesite. Gold-silver mineralization occurs as quartz ± carbonate – sulfides – electrum veins/veinlets and stock works, and at least three stages of mineralization have been identified namely, 1) Stage 1: Quartz -pyrite veins, 2) Stage 2: Quartz ± carbonate – sulfides – electrum veins and 3) Stage 3: Quartz ± carbonate veins. The main gold stage (Stage 2) is characterized by typical vein textures of low sulfidation epithermal deposit such as crustiform, colloform banding, comb textures and consist mainly of quartz and minor calcite gangue. Pyrite is a major sulfide mineral with minor sphalerite, chalcopyrite and galena. Gold is identified both as inclusion in sulfides particularly pyrite and free grain associated with quartz and calcite. EPMA analysis confirmed that gold occurs as electrum with fineness ranging from 595 to 632. Petrographic and XRD study suggested that the hydrothermal alteration at B prospect can be divided into 3 types: 1) Quartz-adularia, 2) Adularia – sericite – illite – quartz ± calcite and 3) Sericite – illite ± chlorite ± calcite. The mineralization at B prospect can be identified as epithermal low sulfidation style deposit on the basis of mineralogy, vein textural features and associated hydrothermal alterations especially the presence of abundant adularia both in gold bearing veins and altered wall rock.

Key words: Epithermal, volcanic, gold, mineralization, alteration

Proceedings of the Second International Symposium on Geoscience Resources and Environments of Asian Terranes (GREAT 2018)
19 - 23 November 2018 Bangkok, Thailand

Detrital zircon U-Pb ages of the Uttaradit Group and the Pha Song metamorphic rocks, northern Thailand: their provenance and tectonic setting

Hidetoshi Hara[1]*, Tetsuya Tokiwa[2], Toshiyuki Kurihara[3] and Thasinee Charoentitirat[4]

1 Geological Survey of Japan, AIST, 1-1-1 Higashi, Tsukuba, Ibaraki 305-8567, Japan

2 Faculty of Science, Shinshu University, Matsumoto 390-8621, Japan

3 Graduate School of Science and Technology, Niigata University, Niigata 950-2181, Japan

3 Department of Geology, Faculty of Science, Chulalongkorn University, Bangkok 10330, Thailand

* Corresponding author email: hara-hide@aist.go.jp

Abstract

We examined detrital zircon U–Pb ages of the Uttaradit Group and the Pha Song metamorphic rocks in northern Thailand. The Uttaradit Group was newly named for Permian strata which is a part of the Phrae Group (Ueno and Charoentitirat, 2011). This group is mainly composed of sandstone, interbedded sandstone and shale, shale, with subordinate chert and limestone. The Pha Song metamorphic rocks consist of psammitic schist, pelitic schist, and tuffaceous schist, corresponding to a member of the Nan back-arc accompanied with ophiolitic rocks (Singharajwarapan and Berry, 1993). However, depositional age of clastic rocks from these two geological units was not established because of no diagnostic fossils. In this study, we try to estimate the depositional age of both units, and discuss their provenance and tectonic setting, based on detrital zircon U–Pb ages. We collected three sandstone samples from the Uttaradit Group, and two samples of psammitic schist from the Pha Song metamorphic rocks. Distribution patterns of zircon ages are very similar between both units, characterized by a clear Triassic youngest peak, and abundant Paleozoic zircons, with minor Proterozoic zircons. Youngest peak ages of the Uttaradit Group present ranging from 233 to 237 Ma, and those of the Pha Song metamorphic rocks are 234 Ma and 259 Ma. These ages suggest the depositional ages of both units were inferred after Middle Triassic at least, although a sample shows an old peak. Recently, Thassanapak et al. (2017) reported Middle Triassic radiolarians from chert in the Uttaradit Group, and discussed to deposit around forearc region. The depositional ages are correlative between clastic rocks and chert. On the other hand, the Uttaradit Group was assigned as the Permian based on occurrence of Permian limestones (Ueno and Charoentitirat, 2011). Here, the Uttaradit Group is redefined as Middle Triassic clastic succession with minor chert. Permian limestones probably correspond to parts of the Permian Ngao

Group, or Nan back-arc basin deposits as well as limestone occurrence of the Sa Kaeo suture. In addition, distribution patterns of zircon ages from both units are very similar to those of Triassic strata within the western Indochina block reported by Arboit et al. (2916) and our unpublished data. Furthermore, detrital U–Pb ages from forearc deposits are characterized by a clear single youngest peak with very small amount of Paleozoic and Proterozoic zircons by Hara et al. (2017). This suggests that tectonic setting of the Uttaradit Group is related to back-arc basin rather than forearc basin.

Key words: Provenance, U–Pb dating, Sukhothai Arc, Nan Back-arc, Triassic

Proceedings of the Second International Symposium on Geoscience Resources and Environments of Asian Terranes (GREAT 2018)
19 - 23 November 2018 Bangkok, Thailand

Unroofing of a Permian-Jurassic magmatic arc in East Asia, based on detrital zircon U-Pb ages and sandstone provenance of the Hida Gaien belt, central Japan

Keisuke Suzuki[1]* and Toshiyuki Kurihara[1]

1 Gradusate School of Sience and Techonology, Niigata University

* Corresponding author email: f17e065d@mail.cc.niigata-u.ac.jp

Abstract

The unroofing of a Permian-Jurassic magmatic arc in East Asia is directly related to the origin and development of Paleozoic rocks in Japan, such as the Hida Gaien, South Kitakami, Kurosegawa, and Maizuru belts. Recently, the U-Pb dating of detrital zircons has become a very useful tool to estimate the diversity of sandstone provenance and the characteristic of tectonic denudation, which contributes to reconstructing the proto-Japan arc in Paleozoic-Mesozoic (e.g., Nakama et al., 2010; Okawa et al., 2013; Isozaki et al., 2015). However, the tectonic setting of the Hida Gaien belt has been still unknown, because it is composed of various rocks with different origins. To slove this problem, we are now conducting the detrital zircon U-Pb dating and sandstone provenance analyses for Permian-Jurassic sandstones of this belt.

The lithostratigraphy of the Lower Permian to Lower Jurassic strata was studied in the Hongo and Moribu areas of the Hida Gaien belt, located in the northern part of Takayama City, Gifu Prefecture, central Japan. The lithology of the Lower Permian and Upper Triassic strata is characterized by tuffaceous sandstone and mudstone. The upper Middle Permian to Lower Triassic strata is turbidite and mudstone of deep-water facies. The Lower Jurassic strata (Suzuki and Kurihara, 2017) are characterized by alternating sandstone and mudstone. The age distribution of 619 detrital zircon grains from these strata shows the following three youngest model peaks by Isoplot 4.15 (Ludwig, 2012): (1) 261-257 Ma (Middle Permian: lower-middle part of the Moribu Formation), (2) 248 Ma (Early Triassic: upper part of the Moribu Formation), and (3) 186 Ma (Early Jurassic: Lower Jurassic strata). The sandstones also contain Middle Ordovician to Middle Carboniferous grains (465-320 Ma), along with a small amount of Precambrian (1850-1600 Ma) and Late Triassic grains (225 Ma). The sandstone compositions of 18 samples obtained from the upper part of the Moribu Formation (248 Ma) and the Lower Jurassic strata (186 Ma) are mostly plotted on the field of "transitional-dissected arc

provenance" in the discrimination diagram by Dickinson et al. (1983). In particular, The Lower Jurassic sandstones include various rock fragments such as granite, shale, and sandstone.

According to Yoshida and Tazawa (2000) and Yoshida and Machiyama (2004), the sandstones of Middle Permian strata in the Hida Gaien and South Kitakami belts show the characteristics of the transitional provenance from undissected arc to basement uplift by Dickinson et al. (1983). Together with our data for Lower Jurassic sandstones mentioned above, the magmatic arc had gradually matured during Middle Permian to Early Jurassic with the cycle of the active phase of volcanism and denudation. The significant contribution in the sedimentary supply from the magmatic arc to the Permian-Jurassic strata implies that the sedimentary basin of the proto-Japan was arc-related basins, such as a fore-arc basin or a back-arc basin, along the active continental margin of the East Asian continental blocks. In addition, a small amount of Precambrian grains indicates that there were factors (e.g., back-arc opening) preventing the supply of old grains from continental blocks.

Key words: Hida Gaien belt, U–Pb dating, sandstone composition, provenance, magmatic arc, Permian, Jurassic

Proceedings of the Second International Symposium on Geoscience Resources and Environments of Asian Terranes (GREAT 2018)
19 - 23 November 2018 Bangkok, Thailand

Development of the Middle Paleozoic in Japan inferred from radiolarian biostratigraphy, U-Pb zircon ages, and relationships with SE Asia

Toshiyuki Kurihara[1]*

1 Graduate School of Science and Technology, Niigata University

* Corresponding author email: kurihara@geo.sc.niigata-u.ac.jp

Abstract

The Sillurian and Devonian strata of Japan, composed of coherent carbonate and tuffaceous clastic-rock sequences deposited on a shallow-marine shelf and within a deep basin around a volcanic arc, are important in understanding the origin and early tectonic history of 'proto-Japan'. Many workers have accumulated lithostratigraphic and paleontological data from Silurian and Devonian rocks of the Hida-gaien, Kurosegawa, and South Kitakami belts, and discussed their paleobiogeographical provinces. However, a clear faunal similarity to a particular paleobiogeographical province has not been recognized for Japanese Siluro-Devonian fossils, thereby limiting our understanding of the paleogeography of Japan and tectonic relationships with neighboring paleocontinents and orogenic belts of East Asia. Recently, studies of radiolarian biostratigraphy and U-Pb zircon ages of Middle Paleozoic strata in Japan have made significant advances, and most of the sedimentary rocks of this age have been well dated. Here I present a summary of the stratigraphy of, and the radiolarian and U-Pb age-based correlations among, the Middle Paleozoic in Japan. The implications of these findings for the relationship between the Japanese Middle Paleozoic and neighboring orogenic belts of SE Asia are also discussed.

In the Inner Zone of Southwest Japan, the Hida-gaien belt contains Silurian to Devonian shallow-marine carbonates and arc-related felsic tuffaceous sequences that overlie Ordovician tuffaceous rocks and basalts (e.g., Tsukada, 1997; Kurihara, 2004, 2007). The Kurosegawa and South Kitakami belts are characterized by a succession of Silurian volcaniclastic rocks overlying an Ordovician igneous basement, fossiliferous limestone, and Upper Silurian to Lower Devonian radiolarian-bearing tuffaceous turbidites, and Middle-Upper Devonian shallow-marine strata. In total, eight radiolarian assemblages have been recognized in these belts (Kurihara, 2004). U-Pb datings of detratal zircons were performed for sandstones of the Hida-gaien and South Kitakami belts. As a result, the zircons of the Lower-Middle Devonian of the Hida-gaien belt

make a clear peak around 410 Ma with small peaks of 480 Ma and 440 Ma. The zircons of Upper Devonian plant-bearing strata of the South Kitakami belt shows a large youngest age peak of ca. 370 Ma and characteristically include grains ranging in age from 1,500 to 1,000 Ma.

Biostratigraphic correlations clearly show that the Upper Silurian to Lower Devonian strata of deep-water origin in the Hida-gaien belt are similar to those in the Kurosegawa and South Kitakami belts in terms of depositional age and trends in the lithological succession. The Upper Devonian strata of these belt consist of shallow-marine clastic rocks, indicating the shallowing of sedimentary basins throughout the belts. These observations constrain the nature of the link between these belts during the early stages of their geologic history. Prior to the opening of the Sea of Japan, the Japanese Islands were directly connected to the East Asian continent. The age distribution of detrital zircons of the Upper Devonian in the South Kitakami belt is similar to those of the Indochina block and other continents around the northern part of East Gondwana documenting the Grenvillian tectonothermal event (Okawa et al., 2013), not to the North China Block. Therefore, it is necessary to consider that the Japanese Middle Paleozoic strata have a strong relationship to the eastern margin of SE Asia.

Key words: Middle Paleozoic, Japan, radiolarian biostratigraphy, U–Pb age, paleogeography

Suggested history of the Hukawng Block of Northern Myanmar, and postulated role of the Medial-Myanmar Shear Zone in the origin of the Jade Mines Belt

Michael F Ridd and Michael J Crow

Extended Abstract

The Hukawng Valley is the topographic expression of the Hukawng Basin of Cretaceous and Cenozoic sediments. It lies north of, and apparently on trend with, the Cretaceous and Cenozoic system of basins called here the Central Burma Depression that extends south to the Andaman Sea. But that apparent continuity overlooks the fact that the Hukawng Basin and the Central Burma Depression are separated by the Jade Mines Belt, a complex belt of schists and ultrabasic rocks that includes jadeitite formed deep in a subduction zone (Figure 1a).

In plate-tectonic terms, the Central Burma Depression occupies the Irrawaddy Block, and it is suggested that this had a different history from the Hukawng Block that lies to its north. North of about Mandalay the Sagaing Fault divides into a number of splay faults, and some of these bound the Hukawng Block on its eastern side. About 400 km of dextral displacement overall is widely accepted to have occurred on this Neogene-age fault system. A palinspastic reconstruction of the disposition of blocks before that dextral faulting shows that the Hukawng Block lies adjacent to the Tengchong Block, and it is suggested that they were formerly a single entity before being disrupted in the Neogene (Figure 1b).

On that palinspastic reconstruction (Figure 1b) the Irrawaddy Block is seen close to the (now combined) Hukawng-Tengchong Block, with a narrow Jade Mines Belt between them. Analytical studies of zircons by others have given U-Pb Late Jurassic ages for the jadeitite, that are interpreted as the age of the protolith oceanic crustal rocks that were then metasomatised deep in the subduction zone (Fig 1c). We suggest that the eversion and uplift of the Jade Mines Belt was related to dextral movement on the Medial-Myanmar Shear Zone. Although such movement has not been dated in Myanmar, further to the south, in Thailand, two periods of dextral shift have been recognized on the Khlong Marui and Ranong faults: an early pre-Campanian phase followed by a Palaeogene phase. We suggest that the earlier phase closed the gap between the Irrawaddy Block and the Hukawng-Tengchong Block, laterally compressing and everting the intervening

subduction-zone rocks and eroding the upper surface; the Paleogene phase uplifted the Jade Mines Belt and caused the antiform that persists to the present.

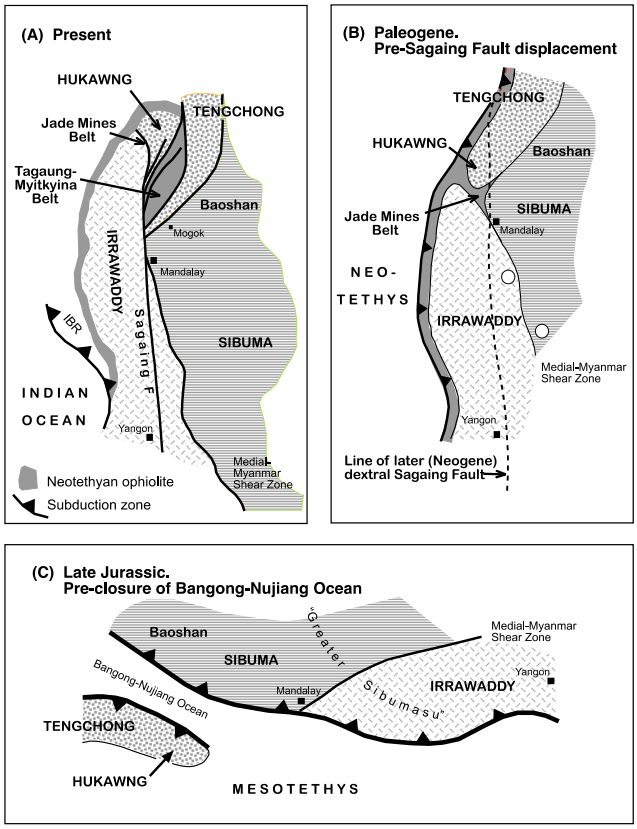

Figure 1. Suggested plate-tectonic history of the component blocks of Myanmar. (a) The present, showing the Hukawng Block separated from the Irrawaddy Block by the Jade Mines Belt. (b) Paleogene, when the Hukawng and Tengchong blocks were continuous, before separation by dextral displacement on the Sagaing Fault. White spots show notional displacement on Medial-Myanmar Shear Zone. (c) Late Jurassic, before closure of the Bangong-Nujiang branch of Mesotethys, and before dextral movement on the Medial-Myanmar Shear Zone closed the gap and everted the subduction-zone rocks between the Irrawaddy and Hukawng-Tengchong blocks.

Footnote: This abstract is based on a paper submitted to the Journal of the Geological Society of London by M.F.Ridd and M.J.Crow, and currently under review: "The Hukawng Block in Northern Myanmar: a possible allochthonous Gondwana-derived terrane, and implications for the origin of the Jade Mines Uplift".

Proceedings of the Second International Symposium on Geoscience Resources and Environments of Asian Terranes (GREAT 2018)
19 - 23 November 2018 Bangkok, Thailand

Structural and Deformation of Metamorphic Rocks in the Doi Phuk Sung Area, Wiang Sa District, Nan Province

Thikapong Thata[1]* and Phisit Limtrakun[1]

1 Department of Geological Sciences, Faculty of Science, Chiang Mai University

* Corresponding author email: thikapong_thata@cmu.ac.th

Abstract

The Nan–Uttaradit suture is the most complex suture in Thailand. It has been interpreted to mark the boundary between the Sibumasu block located in the west of Thailand (Sukhothai Zone) and the Indochina block located in the east of Thailand. The Mafic and Ultramafic and Metamorphic rocks are exhumed along the Nan river and are evidenced by the subduction zone. The amalgamation of these two blocks may have occurred in the Permian–Triassic. The study area is located in the south of Nan province and covers an area of approximately 22 km2. The purpose of this study is to characterize deformation event of metamorphism and define structural geology by using petrography and structural analyses. The geological setting of the study area can be divided into 3 rock units. All rock units are not conformable and bounded with thrust faults. (1) The Limestone unit includes bedded limestone. (2) The Mélange block unit consists of metapelite, metabasite, and pyroclastic rocks. The relationship of rocks is a block in matrix fabrics. The metapelite is stilpnomelane quartz schist and phyllite. The metabasite is metaperidotite and metagabbro block in the serpentine matrix. (3) The Red bed sedimentary rocks unit comprises reddish brown conglomerate, sandstone, siltstone and volcanic rock. Metapelite in the mélange block unit recorded two events of deformation, S1, and S2 events. The S1 is foliation showing in metapelites while the S2 evidence in crenulation and folded of foliation (S1). The controlled tectonic in the study area is the convergent plate boundary. The evidence in this study is a thrust fault and mélange unit. Thrust faults make the older rock unit overlying on the younger rock unit. The mélange unit had two events of deformation including foliation (S1) and folding (S2). The studied schist contains mineral assemblages of stilpnomelane + chlorite + phengite + albite + tremolite + quartz + K-feldspar ± biotite that formed under P-T conditions of 250 – 400 °C, and 2 – 9 kbars. The equilibrated P-T condition is stable in blueschist facies. The studied metabasite contains mineral assemblages of magnesite + quartz that formed under P-T conditions of 220 – 400 °C, and 4-6 kbars. The equilibrated P-T condition is stable in greenschist facies.

Key words: Structural, Deformation, Metamorphism, Nan Suture, Tectonics, Thailand

Proceedings of the Second International Symposium on Geoscience Resources and Environments of Asian Terranes (GREAT 2018)
19 - 23 November 2018 Bangkok, Thailand

Paleozoic and Mesozoic Back-Arc basin chert of the Paleo-Tethys in Thailand

Yoshihito Kamata[1]*, Katsumi Ueno[2], Hidetoshi Hara[3], Thasinee Charoentitirat[4] and Punya Charusiri[4]

1 Graduate School of Life and Environmental Sciences, University of Tsukuba

2 Department of Earth System Science, Fukuoka University

3 Geological Survey of Japan, AIST

4 Department of Geology, Chulalongkorn University

* Corresponding author email: yoshi_kamata@geol.tsukuba.ac.jp

Abstract

Geologically, SE Asia consists of the several continental blocks derived from Gondwana Supercontinent during the Paleozoic to Mesozoic era. Geological history of the formation of SE Asia contains various tectonic settings such as the dispersion of supercontinent, the subduction of oceanic crust, the formation of the Arc, and the collision of continents after the closure of huge main oceans (e.g., Metcalfe, 1999, 2013).

In Thailand, the Nan-Uttaradit Suture Zone and Sa Kaeo Suture Zone, which contain ultramafic, mafic rocks with Permian to Triassic radiolarian chert, have long been considered to represent the closure zone of the main Paleo-Tethyan ocean between the Sibumasu and Indochina continental Blocks (e.g., Bunopas, 1981; Metcalfe, 1999). In the last decade, however, accumulation of geological information has led to the new interpretation of the geotectonic divisions of the mainland Thailand (e.g., Ueno and Hisada, 2001; Ueno and Charoentitirat, 2011), and the new geological significance of these suture zones as a closure zone of back-arc basin situated between the Sukhothai Zone (arc system) and the Indochina continental block has been proposed (e.g., Ueno and Hisada, 1999; Ueno, 2002; Hara et al., 2018).

In Thailand, four geotectonic units can be recognized; from west to east, Shibumasu Block, Inthanon Zone, Sukhothai Zone, and Indochina Block (e.g., Ueno and Hisada, 2001; Metcalfe, 2013; Ueno and Charoentitirat, 2011). Among them, siliceous sediments such as siliceous shale and bedded radiolarian chert including radiolarian tests are mainly distributed in the Sibumasu Block, Inthanon Zone, and a boundary unit between Sukhothai and Indochina Block (the Nan-Uttaradit Suture Zone and Sa Kaeo Suture Zone). The wide distribution of chert indicates that Thailand has high potential on the study of chert sedimentation within several tectonic settings. Discrimination of chert deposited on several tectonic basins such as the huge main ocean and the marginal narrow sea should be important to understand geotectonic amalgamation history of the SE Asia because the history should be included formation and closure of back-arc basin due to formation of volcanic island arcs.

Key words: Radiolarian bedded chert, Paleo-Tethys, Back-arc basin, Nan-Uttaradit Suture Zone, Sa Kaeo Suture Zone.

Proceedings of the Second International Symposium on Geoscience Resources and Environments of Asian Terranes (GREAT 2018)
19 - 23 November 2018 Bangkok, Thailand

Comparison of Alpine-Carpathian (European Western Tethys) and Indochina (SE Asian Eastern Tethys) orogenic systems and events – idea of the new IGCP project

Michał Krobicki[1]* and Jan Golonka[1]

1 AGH University of Science and Technology, Mickiewicza 30, 30-059 Kraków, Poland

* Corresponding author email: krobicki@geol.agh.edu.pl

Abstract

Tethys was originally defined as the Jurassic realm between Atlantic and SE Asia. The western part of this realm in Europe is as the Alpine Tethys, which developed as a system of basins during Jurassic time between Inner Carpathian-Eastern Alpine terrane and North European Platform as a result of the break-up of Pangea. In the western part known as the Penninic realm it contains the ophiolitic sequences indicating the truly oceanic crust. In the eastern part, the ophiolitic sequences are known only as olistholits and pebbles in flysch, the basement of was partly formed by the attenuated crust. In Poland, Slovakia and Ukraine the Alpine Tethys is represented by the Jurassic, Cretaceous, Paleogene and Miocene sedimentary sequences. Some of these sequences are recently located in the suture zone between Inner Carpathians and North European Platform (the Pieniny Klippen Belt (PKB)), other sequences are involved in the allochthonous units covering the North European platform or accreted to the Inner Carpathian terrane. The Czorsztyn submerged ridge (one of the most important part of the PKB structure) was a part of the Alpine Tethys dividing the oceanic basin into two subbasins. The southern subbasin and the ridge traditionally constitute the Pieniny domain and its sequences are involved in the PKB, strongly tectonized structure about 800 km long and 1-20 km wide, which stretches from Vienna (Austria) on the West to the NE Romania on the East.

The parts of Alpine Tethys constitute also important paleogeographic elements of the future Outer Carpathians, which form a great arc of mountains that stretches more than 1 300 km from the Vienna Forest to the Iron Gate on the Danube (Romania). On the west the Carpathians are linked with the eastern Alps and on the east pass into the Balkan chain. Traditionally the Carpathians are subdivided into the West and East Carpathians. The West Carpathians consists of an older range known as the Inner or Central Carpathians and the younger one, known as the Outer or Flysch Carpathians. At the boundary of these two ranges lies the PKB. The Inner Carpathians nappes contact along a Tertiary strike-slip boundary with PKB. The PKB is

composed of several successions (mainly deep and shallow-water limestones), covering a time span from the Early Jurassic to Neogene. The Outer Carpathians are built up of a stack of nappes and thrust-sheets changing along the Carpathians, built mainly of continual flysch sequences up to six kilometers thick representing the time span from the latest Jurassic to the Early Miocene. All the Outer Carpathian nappes are thrust over the southern part of the North European Platform covered by the autochthonous Miocene deposits of the Carpathian Foredeep at a distance of at least 60-100 km. The northern Carpathians nappes became uprooted from the basement during overthrusting movement, and only their basinal parts were preserved. A narrow zone of folded Miocene deposits was developed along the frontal Carpathian thrust.

From the point of view of the plate tectonic evolution of the basins the following major elements could be distinguished in the Outer Carpathians and the adjacent part of the Inner Carpathians:

(i) Inner Carpathian Terrane – continental plate built of the continental crust of Hercynian (Variscan) age and Mesozoic-Cenozoic sedimentary cover. The Inner Carpathians form a prolongation of the Northern Calcareous Alps, and are related to the Apulia plate. The uppermost Paleozoic – Mesozoic continental and shallow marine sedimentary sequences of this plate are folded and thrust into a series of nappes. They are divided into several nappes that are the prolongation of the Austroalpine nappes. The nappes and the Hercynian basement are unconformably covered by mid-Eocene/ Oligocene flysch and Early/Middle Miocene marine and terrestrial (continental) molasses;

(ii) North European Platform – large continental plate amalgamated during Precambrian- Paleozoic time. Proterozoic, Vendian (Cadomian), Early Paleozoic (Caledonian), Late Paleozoic (Hercynian=Variscan) fragments could be distinguished within the folded and metamorphosed basement of this plate. Beneath of the Outer Carpathians the sedimentary cover consists of the autochthonous Upper Paleozoic, Mesozoic and Cenozoic sequences covered by the allochthonous Jurassic–Neogene rocks. The North European Platform history is connected with Baltica (Eastern Europe) evolution which have collided with the Cadomian part of Gondwana during the Vendian time. At the same time rifting occurred along the other Baltica border related perhaps to the opening of the Iapetus Ocean. Laurentia rifted away from Pannotia along future Iapetus Ocean during Vendian time and along the Ouachita Ocean during Cambrian time. One of the possible, speculative reconstructions is linking Central Asian Orogenic Belt terranes with the Cadomian orogeny in Europe. The Caledonian orogeny (during Late Silurian time) and transpressional collision of Gondwana and Laurentia was related to the formation of the enigmatic large supercontinent Oldredia, which existed during Early Devonian

times, and included all major plates. The orogenic events happened also in the Central Asian Orogenic Belt and in Southeast Asia. These events indicate possible connection of Asiatic plates with Oldredia;

(iii) Severin-Moldavidic realm (in Romania known as Outer Dacides and Moldavides), developed within the North European Platform as rift and/or back-arc basin. The sedimentary cover is represented by Jurassic-Lower Miocene sequences of belonging to several tectonic units in Poland and Czech Republic. The Severin part (Severinides) of the basin is represented in Ukraine by Kaminnyi Potik (including the Lower Cretaceous volcano-sedimentary deposits) and Rahiv units;

(iv) the Getic-Marmarosh Ridge (also known as Median Dacides) constitutes a fragment of the North European Platform rifted away during the opening of the Severin-Moldavidic basins. It includes Precambrian, Early Paleozoic (Caledonian) granites and metamorphic rocks, Late Paleozoic (Variscan) metamorphic rocks as well as the late Paleozoic and Mesozoic sedimentary cover. The Polish Carpathians form the northern part of the Carpathians. The Carpathian overthrust forms the northern boundary.

The Mesozoic and Cenozoic paleogeography of the Outer Carpathians reflects the series of continental break-ups, rifts and collisions. The Magura Basin originated as part of the Alpine Tethys created during Mesozoic time between Inner Carpathian terranes and Eurasia. The other Outer Carpathian basins had developed in the process of rifting and fragmentation of the European platform. During the Cretaceous tectonic re-organization the new Outer Carpathian realm was formed. Within this realm in the foreland of the folded Inner Carpathians area, several basins divided by ridges and underwater swells became distinctly separated. The orogenic processes in the Northern Outer Carpathians produced an enormous amount of the clastic material that started to fill the basins. The material was derived from the northern and southern margins as well as from the inner ridges and swells. Each basin had the specific type of clastic deposits, and sedimentation commenced in different time. In Paleogene, the movement of terranes resulted in gradual closing of the flysch basins and development of an accretionary prism. The ridges dividing the flysch basins in Outer Carpathians became more distinguished providing favorable conditions for development of shallow banks with the carbonate platform sedimentation. These platforms have been destroyed during the orogenic process. The platform deposits formed numerous carbonate fragments that have been found in the Outer Carpathians flysch and olistostromes. These fragments were transported with the turbidity currents to the flysch, forming the organodetritic limestones and sandstones. During the final orogenic stage Africa converged with Eurasia. The direct collision of the continents never happened, but their convergence lead to

the collision of intervening terranes leading to the formation of the Alpine-Carpathian orogenic system. Through the Miocene tectonic movements caused final folding of the basins fill and created several imbricate nappes which generally reflect the basin margin configurations after the Cretaceous reorganization and Paleogene development of the Carpathian accretionary prism.

The SE Jurassic Tethyan realm in SE Asia, originated as a result of the Late Triassic collisions, now known as Early Cimmerian and Indosinian orogenies. Blocks of the Cimmerian provenance and Eurasia were involved in these collisions with the southern margin of Eurasia. This series of collisions closed the Paleotethys Ocean and opened Jurassic (Neotethys) Ocean. The closure happened earlier in the Alpine-Carpathian-Mediterranean area (Western Tethys), later in the Eastern Europe-Central Asia and latest in the South-East Asia (Eastern Tethys). Microplates now included in the Alpine-Carpathian systems formed the marginal part of Europe. Subduction developed south of this zone. Late Triassic collisional events occurred in the Moesia-Rhodopes areas. Almost in the same time Alborz and South Caspian Microcontinent collided with the Scythian platform in Eastern Europe, and the other Iranian plates (including the large Lut block), collided with the Turan platform. The relationship between Panthalassa terranes and Cimmerian plates was previously postulated and mapped. The Western Panthalassa reefs from Japan corresponds with those of the Tethys Ocean during the Late Triassic. On the other hand, Indochina SE Asian plates and Qiangtang were sutured to South China and therefore the Paleotethys between Qiangtang and Eurasia was closed during Late Triassic times. The eastern Cimmerian plates were involved in the Indosinian orogeny. This name was derived from Indochina, the region where orogeny was noted one hundred years ago. The major unconformity was observed in Northwest Vietnam. The deformed Lower – lowermost Upper Triassic (up to Carnian) marine metamorphosed rocks arranged into nappes and thrusts are covered by Upper Triassic continental red conglomerates ("terraines rouges"). The main metamorphic event occurred 250-240 Ma. The Late Triassic unconformity and 225-205 Ma postorogenic plutonism also suggested that the geodynamic evolution Jinshajiang and Ailaoshan belts in China correlate with Vietnamese events marking the same Indosinian Orogeny. It was related to the closure of Paleotethys Ocean along Raub-Bentong, Sra Kaeo and Nan-Uttaradit sutures between Sibumasu, Indochina and Ailaoshan terranes and South China. One of the best examples of the Late Triassic orogenic event occurs in Thailand/Myanmar trans-border zone. The Triassic-Jurassic succession in the Mae Sot area (northern Thailand), belongs to the ShanThai terrane. This zone contains rocks of Triassic cherts (radiolarites), carbonates and flysch (turbiditic) facies, which indicate both pelagic condition

and synorogenic deposits. From a paleogeographic point of view, the Shan-Thai block was a remnant of Paleotethys Ocean, which occupied a wide realm between Cimmerian Continent and Eurasian plate during Late Paleozoic-Early Mesozoic times. On the other hand, the Late Triassic Indosinian orogenic event has been connected with docking and amalgamation of Indoburma, Shan-Thai (Sibumasu) and Indochina terranes, which constitute recently the main part of SE Asia, well dated by the so-called "base-conglomerate" of the uppermost Triassic or lowermost Jurassic beds characterized by limestone and chert pebbles-bearing conglomerate, which is significant for the understanding of the tectonic evolution of the Shanthai terrane and determination of the age of the Indosinian (Shanthai = Mae Sariang) orogeny. Such synorogenic turbidites and postorogenic molasses were associated with this Indosinian orogeny. The comparison of main orogenic events in the South East Asia regions and their main pulses indicates diachronic, multi-stages movements of Indosinian Orogeny [for example – Early Triassic and Carnian/Norian transition orogenic time in Vietnam and late Middle Triassic–early Late Triassic (so-called second Indosinian event) and close to Triassic/Jurassic transition in Thailand], firstly terranes docking to Asian plate in the East and later in the West, progressively (in recent coordinates). Additionally, the Late Triassic volcanogenic-sedimentary event in Myanmar correlates presumable with such synorogenic processes, which are represented by the Upper Triassic flysch deposits with basaltic pillow lavas [Shweminbon Group (Upper Triassic – Lower Jurassic turbidites), formerly part of Loi-an Group; Bawgyo Group (Upper Triassic) and their equivalents; Upper Triassic turbidites (Thanbaya/Pane Chaung group/formations)].

In conclusion, the comparative studies between Western and Eastern Tethys, and especially their geodynamic evolution, plate tectonic reorganizations in wider paleogeographical context and their influence to paleoceanographical changes are important to understanding of evolution of the whole Tethys Ocean during the Late Paleozoic – Mesozoic times. Therefore, we would like to propose to focus on the Tethys jigsaw from its creation to destruction in new IGCP Project as continuation of the IGCP-589 Project (Development of the Asian Tethyan Realm: Genesis, Process and Outcomes) and especially according to our discussion during last meeting in Poland (Kraków, 29 September – 5 October 2017).

Key words: Tethys Ocean, Alpine-Carpathians, SE Asia, orogenic systems, Late Paleozoic-Mesozoic, geodynamics, paleogeography

Proceedings of the Second International Symposium on Geoscience Resources and Environments of Asian Terranes (GREAT 2018)
19 - 23 November 2018 Bangkok, Thailand

Reworked conodonts from the Lower Permian carbonate turbidites in the Inthanon Terrane, Northern Thailand and their tectonic significance

Mongkol Udchachon[1]*, Hathaithip Thassanapak[1] and Clive Burrett[2,3]

1 Applied Paleontology and Biostratigraphy Research Unit, Department of Biology, Faculty of Science, Mahasarakham University, Mahasarakham, 44150, Thailand.

2 Paleontological Research and Education Center, Mahasarakham University, Mahasarakham, 44150 Thailand.

3 School of Physical Sciences, University of Tasmania, Hobart, Tasmania, 7001, Australia

* Corresponding author email: Mongkol.c@msu.ac.th

Abstract

Tectonic subdivision of northern Thailand has from west to east been included the Sibumasu, Inthanon, Sukhothai, terranes and Nan Suture. The Inthanon Terrane has been interpreted as autochthonous platform sediments of the Sibumasu Terrane overlain by thrusted allochthonous oceanic sediments and mafic igneous rocks. The allochthonous carbonates contain warm water Carboniferous-Permian faunas in contrast to the cool water faunas of the Permian carbonates of the Gondwana derived Sibumasu Terrane. A carbonate turbidite succession near Lamphun, to the south of Chiang Mai in Northern Thailand in the Inthanon Terrane contains Upper Devonian, Lower Caboniferous and Lower Permian conodonts. The turbidites, with common graded, convolute and plane laminations, are thin to medium bedded and overlie a 2 m thick basalt and a ribbon chert succession. Conodonts from the turbidite sequence include Gnathodus raisae, Idiognathoides tuberculatus, Lochriea glaber, Lochriea sp., Mesogondolella cf. monstra, Mesogondolella cf. arccuata, Mesogondolella cf. gutta, Neognathodus cf. symmetricus, Palmatolepis sp., Streptognathodus sp. and others.

Previous interpretations of this locality have been as a carbonate seamount or as blocks within an accretionary prism. We interpret these mixed faunas as a result of eroded carbonate grains from pre-existing strata of platform or continental shelf margin from the east. The German Geological Mission to Thailand also reported several localities in Northern Thailand where Devonian conodonts reworked into Carboniferous and Permian limestones. The underlying basalt is alkaline to sub-alkaline and is either a within-plate basalt or an OIB. None of these data provide strong support to the previous models but may suggest deposition on a carbonate platform and its margin with the basalts being formed in a north-south rift or embryonic ocean. The occurrence of thin chert layer intercalated in red quartz-rich siliciclastic sequence next to the turbidite section indicate shallow shelf environment during Late Palaeozoic. These evidences further suggest sea-level transgression on deep outer shelf/slope environment probably during late Early Permian or younger following relative sea-level low stand with shelf margin exposure.

Key words: Conodont, Inthanon Zone, Early Permian, carbonate turbidites, submarine slope

Proceedings of the Second International Symposium on Geoscience Resources and Environments of Asian Terranes (GREAT 2018)
19 - 23 November 2018 Bangkok, Thailand

U-Pb age dating of zircons and petrography of rocks along the contact zones between country rocks and intrusive igneous rocks from Khao Khi Nok Area, Tambon Pa Khai, Thong Saen Khan District, Uttaradit Province

Phattharawadee Wacharapornpinthu[1*] and Phisit Limtrakun[1]

1 Department of Geological Sciences, Faculty of Science, Chiang Mai University, Chiang Mai, 50200, Thailand

* Corresponding author email: Phattharawadee_w@cmu.ac.th

Abstract

The study area is located at Khao Khi Nok, Tambon Pa Khai, Thong Saen Khan District, Uttaradit Province. This area was the contact metamorphic zones where the country rocks of limestone interbedded with tuff, contacted with an igneous intrusion, resulting in metamorphism of limestone intercalated with tuff to calc-silicate rocks, marble, and hornfels along the contact zone. From the petrographic studies, the intrusive igneous rocks were monzogranite/granodiorite which composed of quartz, alkali feldspar and plagioclase as essential minerals. The accessory minerals composed of biotite, apatite, zircon/monazite, and hornblende. Due to the presence of hornblende, the intrusive igneous rocks can be referred to as I-type granite. The shallow intrusive igneous rocks exhibited plagioclase and clinopyroxene ophitic texture indicating of shallow intrusion nature. The metamorphic rocks included marble and calc-silicate rocks. Marble contained mostly of calcite whereas calc-silicate rocks composed of calcite, augite, quartz, wollastonite, and plagioclase. Tuff was also metamorphosed to hornfels, which major compositions were including actinolite, chlorite, albite, and quartz. Using the mineral assemblages, equilibrium estimation of the studied marble and calc-silicate rocks can be ranked into amphibolite facies. The equilibrium temperatures were estimated around 500-700°C, pressure of about 2-10 kbars corresponded to the depths of 10-40 kilometers. The contact hornfelsic rocks were albite-epidote hornfels facies which equilibrium temperature of 350-500°C, and pressure below 2 kbars with depths less than 10 kilometers. The U-Pb age dating of zircon from the studied intrusive igneous rocks

yields a magmatic age of 254.7±4.2 Ma. The Permo-Triassic I-Type granite possibly suggests continental rifting environment during, which should be further confirmed by geochemical analyzes.

Key words: Petrography, Metamorphism, U-Pb dating, Permo-Triassic, Uttaradit, Thailand

1. Introduction

The Khao Khi Nok area was a part of eastern belt granites of Thailand following to Granite Provinces and tectonic divisions in Thailand (figure 1a. ; (Hutchison, 2007); E. J. Cobbing, Ridd, Barber, and Crow (2011). The ages are ranged between 248 and 224 Ma, based on zircon U-Pb dating, E. J. Cobbing et al. (2011). Whereas, the oldest age of the Eastern Province Granites have been reported by (Booth, Sattayarak, Ridd, Barber, and Crow, 2011) for a hornblende granite, in well Yang Talat-1 (at a depth of 4125 m), forming the basement beneath the Khorat Plateau which gave an $^{40}Ar/^{39}Ar$ age of 329±3 Ma. According to mentioned above, the ages are wide range from Middle Carboniferous to Middle Triassic. In this work, the studied area is the contact metamorphic zone of Pha Huat limestone (Piyasin, 1985) and granitic rock. However, this area does not have the absolute age and the intensive study on the rock types. Therefore, we aim to study the petrography and absolute age of the rock in this area.

2. Geological background

The Khao Khi Nok area is located at 17°29'53.5"N 100°18'19.2"E, tambon Pa Khai, Thong Saen Khan district, Uttaradit province, Thailand, with a total area of 1 km^2, and is on combination maps between sheet 5043 I Amphoe Thong Saen Khan and 5044 II Ban Hat Ngio series L7018 edition 1-RTSD (Figure. 1b; Royal Thai Survey Department, 1999). This area is the contact zones between the country rocks of limestone of Pha Huat formation, Ratchaburi group (Piyasin, 1985) and contacted with Khao Yai granite, located at the northern part of Khao Khi Nok. The pluton is a part of Eastern granitic belt of Thailand that is Generally emplaced in Upper Paleozoic sedimentary and volcaniclastic sequences. Granitic activity was accompanied by volcanism which

persisted from Carboniferous to the Late Triassic Charusiri, Clark, Farrar, Archibald, and Charusiri (1993).

3. Sampling and petrography

In this study, twenty least altered samples were collected from the Khao Khi Nok. The petrographic studies were analyzed by polarizing microscope and counted 400 points by volume. They can be divided the rocks into three groups (figure 1b) which are; 1. Intrusive igneous rocks (pink), 2. Shallow intrusive igneous rock (green), 3. Contact metamorphic rocks (purple). (Figure 1c. hand specimen of each rock types)

3.1. Intrusive igneous rocks

The intrusive igneous rocks can be systematically classified into three groups such as monzogranite 4 samples, granodiorite 6 samples, monzodiorite/monzogabbro 1 sample. (following the classification of (Streckeisen, 1974))

Monzogranite (figure $2a_1$, $2a_2$) showed aphanitic texture which a seriated groundmass, that various in crystal sizes were ranged from 0.03-5.12 mm. They were clearly distinguished into two parts, which are coarse crystal granite and fine crystal granite. The rocks all composed of quartz, alkali feldspar, and plagioclase as essential minerals. Biotite, hornblende, zircon, apatite, and opaque mineral showed as accessory minerals but the presence of augite particularly shows in fine crystal granite. Quartz mostly exhibits subhedral to anhedral crystals and uneven in their boundary in such a type of consertal texture. Alkali feldspar, subhedral to euhedral crystals, showed Carlsbad twin, and almost grain was altered to sericite/clay minerals. Plagioclase was similar an alkali feldspar except for their polysynthetic twin and zoning. The anorthite content can be measured from the extinction angle and had the An-content range from 6-7, indicated to albite composition. Biotite and hornblende strongly exhibited dichroism, biotite showed brown to pale brown whereas, hornblende showed green to pale green. Both were partly altered to chlorite. Augite showed equigranular texture with a rounded shape and had crystal size ranged from 0.02-0.13 mm. Apatite showed euhedral to subhedral crystals with short prismatic shape, 0.01-0.15 mm. Zircon showed euhedral to subhedral crystals, usually represented zoning and pleochroic halo.

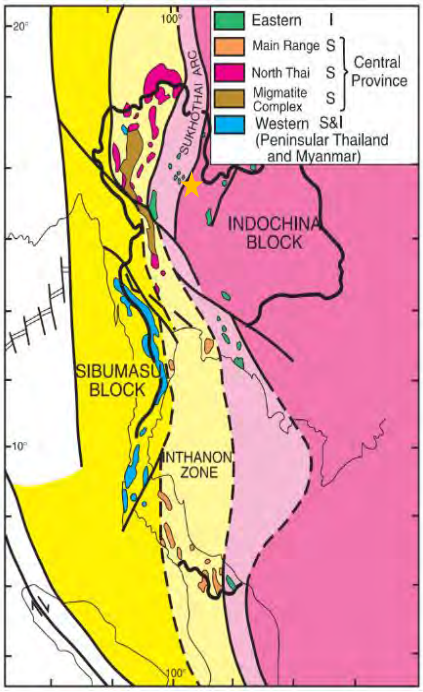

Figure 1a. Granite Provinces and tectonic divisions in Thailand (Cobbing et al., 1986; Hutchison 2007; Cobbing et al., 2011). Represented the Khao Khi Nok area with the yellow star.

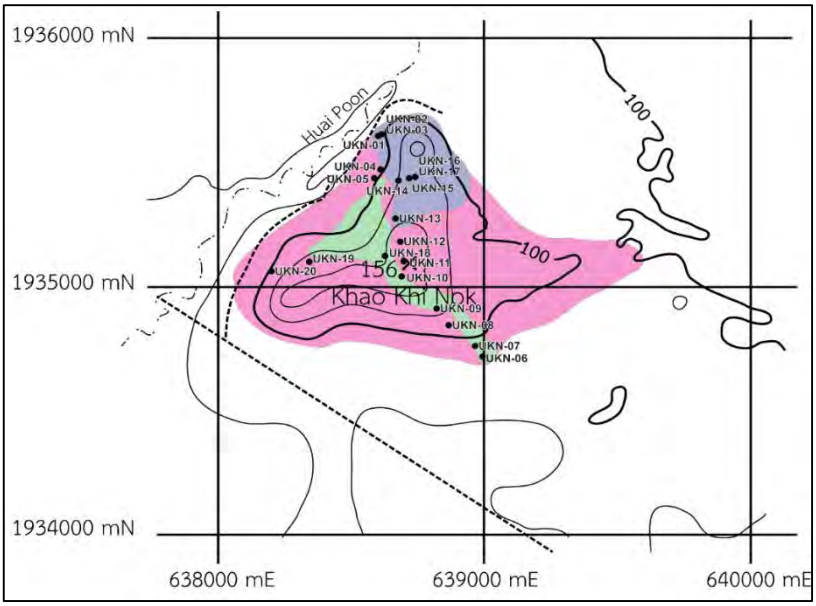

Figure 1b. Geological map of the Kaho Khi Nok area which composed of three rock units; 1.) Intrusive igneous rocks (pink), 2.) Shallow intrusive igneous rock (green), 3.) Contact metamorphic rocks (purple).

Figure 1c. Hand specimen of rock samples; a.) Monzogranite, b.) Granodiorite; c.) Monzodiorite/Monzogabbro, d.) Gabbro, e.) Marble, f.) Calc-silicate, g.) Hornfels

Granodiorite (figure 2b) showed aphanitic texture which a seriated groundmass, that had a crystal sizes ranged from 0.01-4.25 mm., and composed of quartz, alkaline feldspar, and plagioclase as essential minerals. Quartz, alkali feldspar, and plagioclase exhibited their characteristics similarly with monzogranite. Plagioclase showed bent twin that possibly caused by the external force. Granodiorite also had biotite, hornblende, apatite, and zircon as accessory minerals but did not have augite.

Monzodiorite/monzogabbro (figure 2c) also showed aphanitic texture which a seriated groundmass, that had a crystals sizes ranged from 0.01-2.75 mm., and composed of quartz, alkaline feldspar, and plagioclase as essential minerals. However, there were a few grains of quartz. The essential minerals were similarly to granodiorite except for bent twin. This sample had more difference about accessory minerals. It only presented most of the clinopyroxene, a few grains of titanite and zircon.

3.2 Shallow intrusive igneous rocks

There were 2 samples of shallow intrusive igneous rocks (figure 2d) that exhibited fine crystals, 0.02-0.38 mm., of groundmass of essential minerals which are the ophitic texture of plagioclase and clinopyroxene. These samples showed a porphyritic texture with plagioclase, 0.08-1.75 mm., and clinopyroxene, 0.45-0.78 mm., as phenocrysts. Most of the plagioclase was altered to sericite or clay minerals, hard to observe their polysynthetic twins. Clinopyroxene were mostly altered to chlorite and occurred of the new mineral around their grain boundary; the reaction rim. There were opaque minerals as accessory minerals.

3.3 Contact metamorphic rocks

The contact metamorphic rocks can be divided into two types according to their protoliths which were;

1) Metacarbonate rocks (6 samples)

From the mineral assemblages, there were two types of rocks can be divided;

1. Marble (figure 2e), and 2. Calc-silicate (figure 2f). These two types metamorphosed from limestone and exhibited the idiotopic texture. Marble was assembly only calcite with coarse crystals (0.08-8.25 mm.), whereas, calc-silicate composed of fine crystals (0.02-0.88 mm.) of calcite, augite, quartz, wollastonite, plagioclase, opaque minerals, and clay minerals.

2) Metabasite rock (1 sample)

Metabasite had very fine crystals, that was to be hornfels (figure 2g). from their assemblages, this rock possibly metamorphosed from andesitic tuff. There were assembly most of the very fine crystals of small columnar green to pale green actinolite and were altered to chlorite, small lath with polysynthetic twins of plagioclase and were altered to sericite.

4. Analytical zircon U-Pb isotopes

Selected five samples from granitic rocks such as sample no. UKN-03, UKN-07, UKN-10, UKN-11, and UKN-20, then, milled each sample to a powder. 100 grams of each were separated their zircons from gravity separation by using water and purified by hand-picking under the polarizing microscope and binocular microscope. Zircon grains were mounted in epoxy and polished to expose the biggest surface, half the mean grain thickness. The internal structures of the zircons and inclusions were checked by using transmitted and reflected optical microscopy.

Cathodoluminescence (Charusiri et al.) images and scanning electron microscope (SEM) images of zircons were taken by using a (FE-SEM JEOL JSM-7100F) for examining the internal structures of zircon grains and selecting optimum spot locations for U-Pb dating isotopic analysis. Zircon U-Pb isotopes were analyzed by using the Laser Ablation Inductively Coupled Plasma Mass Spectrometry (LA-ICP-MS) at the Institute of Earth Sciences, Academia Sinica, Taipei.

A total of 327 zircon grains from three samples of granodiorite and two samples of monzogranite were analyzed. All the zircon grains were pale brown to colorless with short prismatic crystals, <0.1-0.4 mm. Most of them exhibit a homogeneous and some of with oscillatory zoning. They showed Th (943-13 ppm) and U (926-6 ppm) contents with Th/U ratio of (0.24-2.36). According to the Th/U ratio, in magmatic origin generally showed the Th/U ratio of 0.1-1.0 (Belousova, Griffin, O'Reilly, and Fisher, 2002). However, the ratio can reached up to more than 1.0 due to the substitution of U^{4+} which is easily accepted into the zircon structure relative to Th^{4+} (Ahrens, Cherry, and Erlank, 1967) because its ionic radius was closer to that of Zr^{4+} (Shannon, 1976). 125 grains of zircon were analyzed for calculation of weighted average $^{206}Pb/^{238}U$ age (254.7±4.2 Ma) (figure 3a-3e).

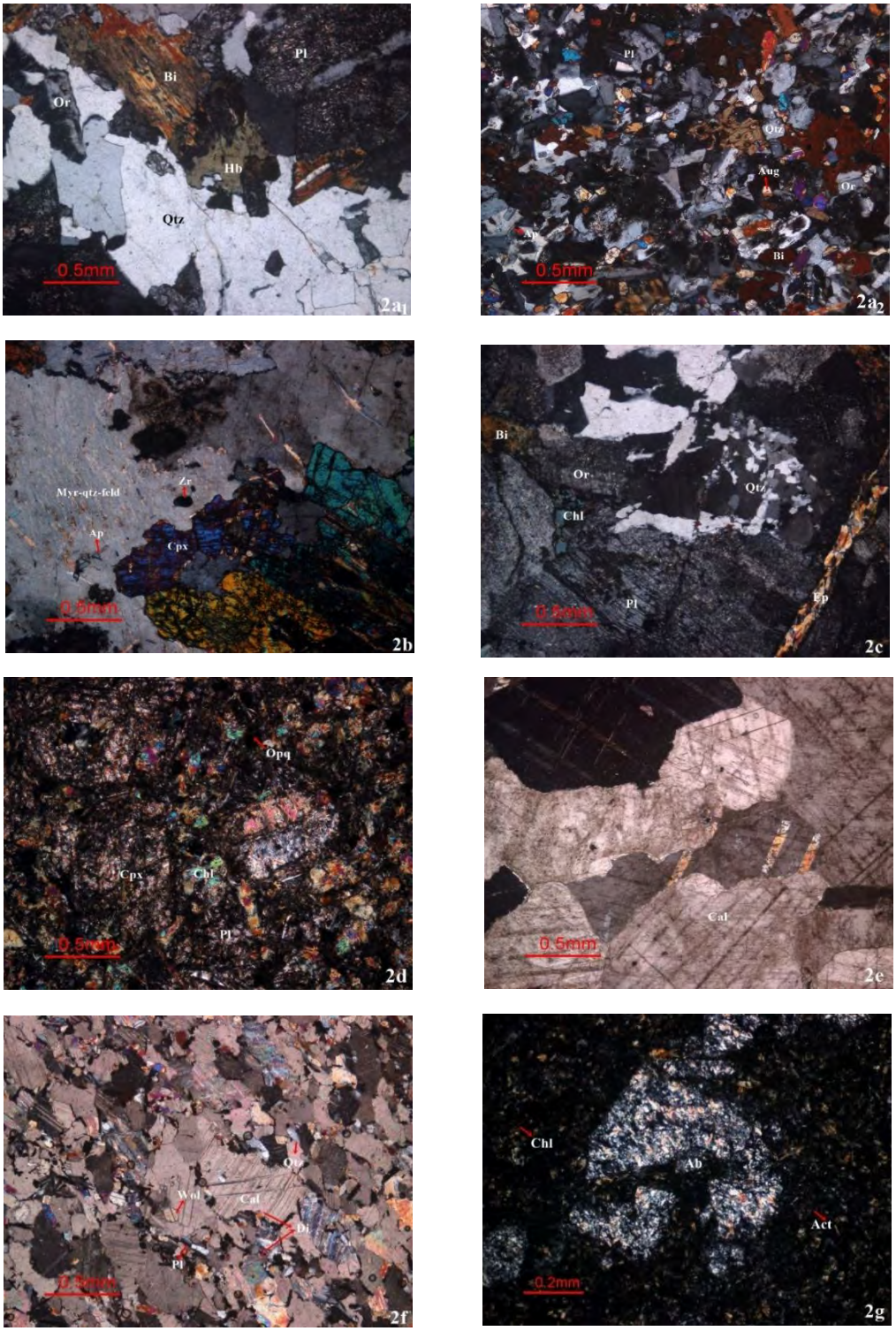

Figure 2. The petrographic studied of the Khao Khi Nok area, the rocks composed of; a_1.) Coarse crystal monzogranite, a_2.) Fine crystal monzogranite, b.) Monzodiorite/Monzogabbro, c.) Granodiorite, d.) Microgabbro, e.) Marble, f.) Calc-silicate, g.) Hornfels as seen in thin section under cross-polarized light.Mineral abbreviations: Qtz-Quartz, Or-Orthoclase, Pl-Plagioclase, Myr-qtz-feld-Myrmekitic quartz feldspar intergrowth, Hb-Hornblende, Bi-Biotite, Zr-Zircon, Ap-Apatite, Cpx-Clinopyroxene, Ep-Epidote vein, Chl-Chlorite, Aug-Augite, Cal-Calcite, Wol-Wollastonite, Ab-Albite, Act-Actinolite.

5. Discussion

As the mentioned above, the petrographic studied can be divided the rocks into three major types. First, the intrusive igneous rocks exhibit hornblende as an accessory mineral which can be indicated to I-type granite. However, there are various types of accessory minerals in the rocks. Monzogranite showed an equigranular augite, unusual accessory mineral in granitic rock. According to the contact metamorphic zone, intrusive igneous rocks were contacted with limestone and can possible the metasomatism of these rocks. In this case, the metasomatism can cause the exchange of the calc-silicate minerals into the pluton. Granodiorite represented alkaline feldspar and plagioclase intergrowth of vermicular quartz, myrmekitic texture, that usually occurs near the rim of plagioclase or between grains of perthitic alkaline feldspar or along the contact of alkaline feldspar and plagioclase crystals ((Turner, 1960); (Phillips, 1974), (L. Collins, 1983; Cox, Bell, and Pankhurst, 1979), (Sepahi and Collins, 2002)). Myrmekitic texture occurs adjacent to alkaline feldspar, it can result from metasomatism processes. ((Ramberg, 1952); (Peng, 1970); (Phillips, 1974); (Hibbard, 1980); (Best, 1982); (Hyndman, 1985); (L. G. Collins, 1988); (Philpotts, 1989); (Sepahi and Collins, 2002)). Monzodiorite/Monzogabbro showed a few grains of quartz and had more percentage of plagioclase. Moreover, the accessory minerals composed of large clinopyroxene crystals and wedge titanite that difference from other granitic rocks. The mineral compositions and their texture of intrusive igneous rocks can be referred to metasomatism processes and can be indicated this zone to endoskarn. From the studied intrusive igneous rocks by U-Pb age dating of zircon yields 254.7±4.2 Ma. The pluton was emplaced in the Permo-Triassic period.

Second, the shallow intrusive rocks showed plagioclase and clinopyroxene with an ophitic texture. This textural sequence is typically found at the margins toward the center in diabasic or doleritic rocks (basaltic dikes) or from the chilled surface to depth of basaltic flows.

For the contact metamorphic rocks, their mineral assemblages can be indicated to protolith, also, metamorphic facies. Metacarbonate rocks can be ranked to amphibolite facies which an equilibrium temperature around 500-700°C, and pressure of about 2-10 kbars with depths from 10-40 kilometers. Whereas, hornfelsic rocks, metabasite, indicate albite-epidote hornfels facies which equilibrium

temperature of 350-500°C, and pressure below 2 kbars with depths less than 10 kilometers. (following metamorphic facies series; (Winter, 2001))

Geochronology of these granodiorite/ monzogranite obtained from U/Pb age determination (254.7±4.2 Ma) were in a good agreement with stratigraphic. It was found that the limestone country rocks contain Textularia sp., Climacammina sp., Schubertella sp., Triticites sp., Pseudofusulinella sp., and Ammovertella sp. indicated the early Permian. The foraminifera were identified followed by (Department of Mineral Resources, 1969), (Schubert, 1908), (von Staff, 1910), (Thompson, 1951), (Girty, 1904), (Cushman, 1928), and (Nanan, 2017). This scenario could be depicted the shallow ground of the Lagoon to the back reef (Dew et al., 2018).

6. Conclusion

The Khao Khi Nok area composed of three major type of rocks which are intrusive igneous rocks, shallow intrusive igneous rocks, and contact metamorphic rocks.

1. Intrusive igneous rocks that emplaced during Permo-Triassic period, can be divided into three types following to their mineral compositions such as monzogranite, granodiorite, and monzodiorite/monzogabbro. Monzogranite and granodiorite mainly composed of quartz, alkaline feldspar, and plagioclase as essential minerals. They also have the similar accessory minerals which are biotite, hornblende, apatite, zircon but differ to the presence of augite in monzogranite that may cause by metasomatism processes. Monzodiorite/ monzogabbro exhibits a few grains of quartz and has clinopyroxene and titanite as accessory minerals domain. Due to the presence of hornblende, these rocks can be referred to I-type granite.

2. Shallow intrusive igneous rocks can be classified to gabbro from their composition and can be called dike from their ophitic texture.

3. Contact metamorphic rocks can be divided into two types following to their mineral assemblages such as marble and calc-silicate, metacarbonate, and hornfels, metabasite. Marble contains mostly of calcite whereas calc- silicate

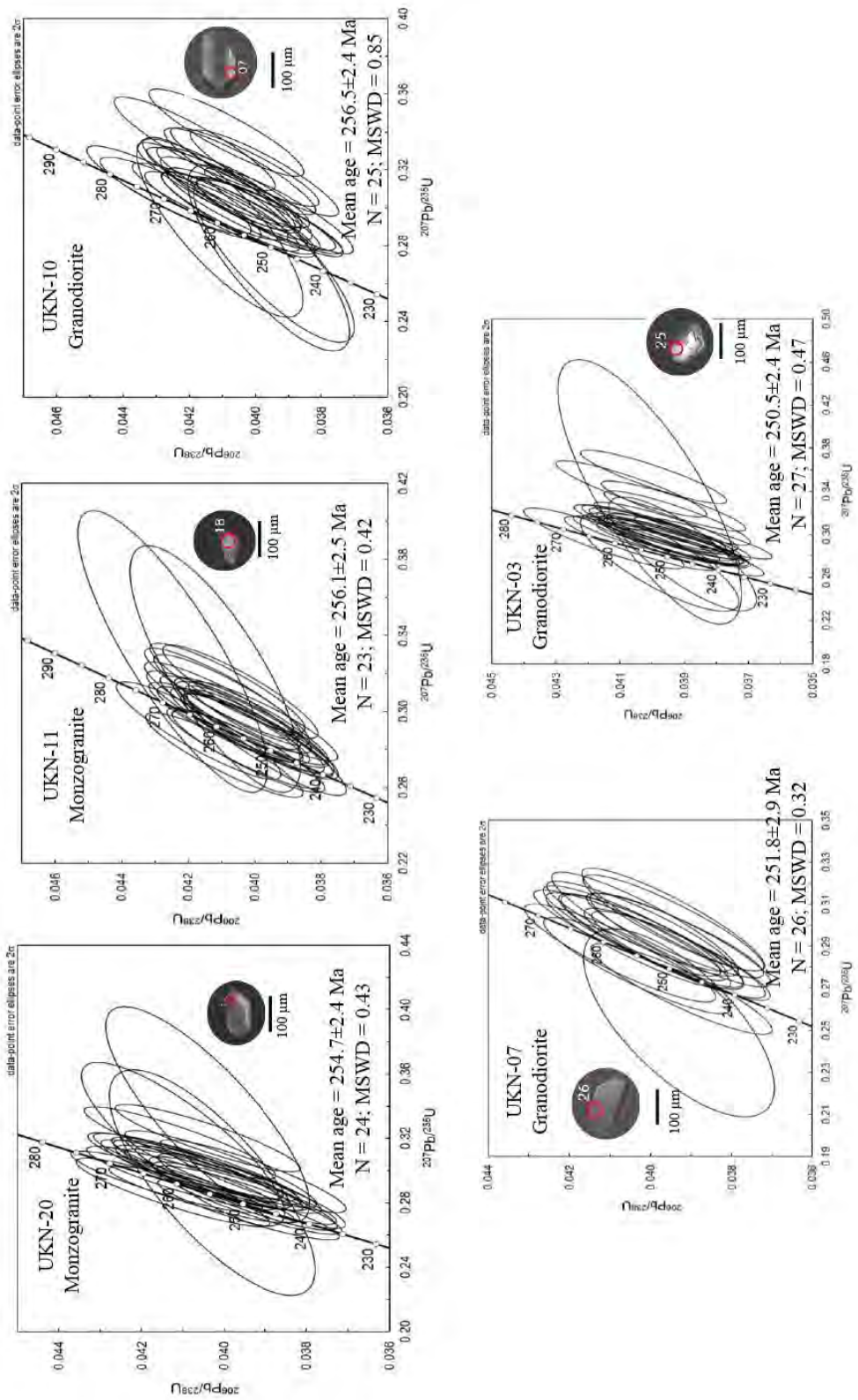

Figure 3(a-e). Concordia diagrams of zircons from the Khao Khi Nok area, Thong Sean Khan district, Uttaradit province, Thailand.

rocks composed of calcite, augite, quartz, wollastonite, and plagioclase. Hornfels composed of actinolite, chlorite, albite, and quartz. The studied marble and calc-silicate rocks can be ranked into amphibolite facies and hornfels indicate albite-epidote hornfels facies.

7. Acknowledgement

We thank the staff of the Institute of Earth Sciences, Academia Sinica, Taipei, for the advising about using the LA-ICP-MS laboratory. Thank for the Department of Geological Sciences, Faculty of Science, Chiang Mai University, Chiang Mai, Thailand, for many supporting during we did this research. This work was refunded by the Development and Promotion of the Gifted in Science and Technology Project (DPST).

8. References

Ahrens, L. H., Cherry, R. D., and Erlank, A. J. (1967). Observations on the Tn-U relationship in zircons from granitic rocks and from kimberlites. *Geochimica et Cosmochimica Acta, 31*(12), 2379-2387.

Belousova, E., Griffin, W., O'Reilly, S., and Fisher, N. (2002). Igneous zircon: trace element composition as an indicator of source rock type. *Contributions to Mineralogy and Petrology, 143*, 602-622.

Best, M. G. (1982). Igneous and metamorphic petrology. *W.H. Freeman, New York San Francisco*

Booth, J., Sattayarak, N., Ridd, M., Barber, A., and Crow, M. (2011). The Geology of Thailand.

Charusiri, P., Clark, A., Farrar, E., Archibald, D., and Charusiri, B. (1993). Granite belts in Thailand: evidence from the $^{40}Ar/^{39}Ar$ geochronological and geological syntheses. *Journal of Southeast Asian Earth Sciences, 8*(1-4), 127-136.

Cobbing, E., Mallick, D., Pitfield, P., and Teoh, L. (1986). The granites of the Southeast Asian tin belt. *Journal of the Geological Society, 143*(3), 537-550.

Cobbing, E. J., Ridd, M., Barber, A., and Crow, M. (2011). Granitic rocks. *The Geology of Thailand. Geological Society, London*, 441-457.

Collins, L. (1983). *Myrmekite formed by recrystallization of plagioclase and its implications for the origin of some granitic rocks.* Paper presented at the Geological Society of America Abstracts with Programs.

Collins, L. G. (1988). *Hydrothermal differentiation and myrmekite: a clue to many geologic puzzles*: Theophrastus publications.

Cox, K., Bell, J., and Pankhurst, R. (1979). The interpretation of igneous rocks, George Allen and Unwin. In: London.

Cushman, J. A. (1928). Additional genera of the Foraminifera. Contr. *Cushman Lab. For. Res, 4*(1), 1-8.

Department of Mineral Resources. (1969). *Fossil of Thailand*.

Dew, R. E., King, R., Collins, A. S., Morley, C. K., Arboit, F., and Glorie, S. (2018). Stratigraphy of deformed Permian carbonate reefs in Saraburi Province, Thailand. *Journal of the Geological Society, 175*(1), 163-175.

Girty, G. H. (1904). ART. XXI.--Triticites, a New Genus of Carboniferous Foraminifers. *American Journal of Science (1880-1910), 17*(99), 234.

Hibbard, M. (1980). Indigenous source of late-stage dikes and veins in granitic plutons. *Economic Geology, 75*(3), 410-423.

Hutchison, C. S. (2007). Geological Evolution of Southeast Asia. 2nd edn. *Geological Society of Malaysia, Kuala Lumpur, Malaysia.*

Hyndman, D. W. (1985). *Petrology of igneous and metamorphic rocks*: McGraw-Hill.

Nanan, K. (2017). *Classification of Foraminifera in Permian Limestone from Khao Na Pha Tang Area, Ban Tham Din, Tambon Bo Thong, Thong Saen Khan District, Uttaradit Province.* (Bachelor), Chiang Mai University, Unpublished B.Sc thesis.

Peng, C. C. (1970). Intergranular albite in some granites and syenites of Hong Kong. *American Mineralogist: Journal of Earth and Planetary Materials, 55*(1-2), 270-282.

Phillips, E. R. (1974). Myrmekite-one hundred years later. *Lithos, 7*(3), 181-194.

Philpotts, A. R. (1989). Petrography of igneous and metamorphic rocks. In. Englewood Cliffs, N.J. :: Prentice Hall.

Piyasin, S. (1985). *Geological Survey Report, scale 1: 250,000* (Vol. 38/1990). Bangkok: Economic Geology Division, Department of Mineral Resources.

Ramberg, H. (1952). Origin of igneous and metasomatic rocks. In: University of Chicago Press, Chicago.

Schubert, R. (1908). Zur Geologie des Osterreichischen Velebit. *Jahrbuch der Geologischen Reichsanstalt, Wien, 58*, 345-386.

Sepahi, A. A., and Collins, L. G. (2002). A study of intergrowth textures and their possible origins in the Alvand plutonic complex, Hamadan, Iran.

Shannon, R. (1976). Revised effective ionic radii and systematic studies of interatomic distances in halides and chalcogenides. *Acta Crystallographica Section A, 32*(5), 751-767. doi:doi:10.1107/S0567739476001551

Streckeisen, A. (1974). Classification and nomenclature of plutonic rocks recommendations of the IUGS subcommission on the systematics of igneous rocks. *Geologische Rundschau, 63*(2), 773-786.

Thompson, M. (1951). New genera of fusulinid Foraminifera. *Contributions from the Cushman Foundation for foraminiferal Research, 2*, 115-119.

Turner, F. J. (1960). *Igneous and metamorphic petrology / Francis J. Turner, John Verhoogen*. New York: McGraw-Hill.

von Staff, H. (1910). Der Oberkarbon Foraminiferensapropelit Spitzbergens. *Bulletin of the Geological Institution of the University of Upsala, 10*, 81-123.

Winter, J. D. (2001). *An introduction to igneous and metamorphic petrology. Prentice Hall, Upper Saddle River.*

Proceedings of the Second International Symposium on Geoscience Resources and Environments of Asian Terranes (GREAT 2018)
19 - 23 November 2018 Bangkok, Thailand

Crystallization temperature range of corundum from Yatkansin Taung area, Myanmar

Tawatchai Chualaowanich[1]*, Maung Maung Naing[2], Alongkot Fanka[3], Tanut Watcharamai[1], Myint Soe[2], Han Lynn Moe[2], Phyo Zaw Thwin[2] and Alin Suksawat[1]

1 Department of Mineral Resources, Thailand

2 Department of Geological Survey and Exploration, Myanmar

3 Department of Geology, Chulalongkorn University, Thailand

* Corresponding author email: t.chualaowanich@gmail.com

Abstract

New corundum occurences in Myanmar are located in between Madaya and Singu townships, north of Mandalay, in the vicinity of Yatkansin Taung. Light to dark sky-blue corundum variety is observed surfacially while rarer pink variety does not expose. The genesis of the corundum is closely related to pegmatite/syenite intrusion into the marble strata of the Mogok Metamorphic Suites. The concentration of TiO2 in the blueish variety corundum (<0.01 – 0.5 %wt.) trends to increase along with the color intensity of the stones. The Cr2O3 content of of the blueish variety (<0.01 – 0.07 %wt.) is discernibly lower than the pinkish variety (0.19 – 0.25 %wt.).

According to mica geothermometer, crystallization temperatures of the observed corundum fall in between 580-630 oC. Nevertheless, the crystallization process of the pinkisk variety ought to be initiated at slightly higher temperature than the blueish variety.

Key words: corundum, geothermometer, Mogok Metamorphic Suites, Yatkansin Taung, Myanmar

Proceedings of the Second International Symposium on Geoscience Resources and Environments of Asian Terranes (GREAT 2018)
19 - 23 November 2018 Bangkok, Thailand

Characteristics of mantle xenoliths enclosed in alkali basalt at Bo Phloi District, Kanchanaburi Province

Pornchanit Sawasdee[1], Prayath Nanthasin[1]*, Christoph Hauzenberger[2] and John Booth[1]

1 Department of Earth Sciences, Faculty of Science, Kasetsart University, Thailand

2 Institute of Earth Science, University of Graz, Austria

Abstract

The mantle xenoliths enclosed in alkali basalt were collected from Khao Lun Tom, Bo Phloi District, Kanchanaburi Province. Mineralogy, texture, and mineral chemistry of these samples were characterized under polarized microscope and EPMA (Electron probe micro-analyzer). The petrographic results show that the samples are equigranular texture and mainly consist of an assemblage olivine + orthopyroxene + clinopyroxene + spinel, however, plagioclase also presents in some xenolith samples. Based on modal percentage of mineral constituents, xenolith samples were classified to be spinel lherzolite and harzburgite. Note that some samples contain both spinel and plagioclase which indicate that such xenoliths originated at the transition zone between stability fields of these minerals at the depth of approximately 50 km. The mineral chemistry of olivine grains show that the Fosterite contents are in very narrow range with Fo 89.31-90.88. Spinel grains have a Cr# in the range of 0.13-0.14. Orthopyroxene grains show the composition of En87.79-89.36-Wo1.03-2.46-Fs8.62-10.41 while clinopyroxene grains have the compositional range of En45.63-48.55-Wo46.91-49.64-Fs4.35-5.10. Temperature and pressure were estimated based on the Ca partitioning between olivine and clinopyroxene which are approximately 1,113-1,232°C and 25 kbar on the other hands two-pyroxene method yields 1,035-1,050°C. Both methods indicate the condition of crust-upper mantle boundary which is consistent with the result from petrographic observation.

Key words: mantle xenolith, Bo Phloi, Kanchanaburi, alkali basalt

Proceedings of the Second International Symposium on Geoscience Resources and Environments of Asian Terranes (GREAT 2018)
19 - 23 November 2018 Bangkok, Thailand

Retrograde texture in calc-silicate rocks at Akarui Point, Lützow-Holm Complex, East Antarctica: Implication for metamorphic evolution

Bowornlak Amnatmetta[1], Prayath Nantasin[1]*, Sotaro Baba[2], Tomokazu Hokada[3], Atsushi Kamei[4], Ippei Kitano[5], Yoichi Motoyoshi[3], NugrohoSetiawan[6], Davaa-ochir Dashbaatar[7] and John Booth[1]

1 Department of Earth Sciences, Faculty of Science, Kasetsart University, Thailand

2 Department of Natural Environment, University of the Ryukyus, Japan

3 Geology Group, National Institute of Polar Research (NIPR), Japan

4 Department of Earth Science, Shimane University, Japan

5 Division of Earth Sciences, Faculty of Social and Cultural Studies, Kyushu University, Japan

6 Department of Geological Engineering, Gadjah Mada University, Indonesia

7 School of Geology and Mining Engineering, Mongolian University of Science and Technology, Mongolia

* Corresponding author email: fscipyn@ku.ac.th

Abstract

Calc-silicate rocks at Akarui Point, Lützow-Holm Complex, East Antarctica, occur as lens in hornblende-biotite gneiss and biotite-hornblende gneiss which are the dominant rocks in the area. All metamorphic rocks at Akarui Point was previously designated to be metamorphosed under an upper amphibolite facies condition during the Late Proterozoic supercontinent Gondwana assembly. But here, we report new petrographic evidences which suggest that the Akarui Point could possibly reached a granulite facies and consequently retrograded to amphibolites facies. Calc-silicate rocks mostly consist of an assemblage diopside + garnet + hornblende ± scapolite + phlogopite ± apartite±sphene. The crucial texture of relict diopside that is surrounded by hornblende generally found in the calc-silicate bodies. This texture could represent a retrograde event took place in the area. The anti-perthite texture in plagioclase feldspar, and K-feldspar altered to sericite are consistent with the replacement of hornblende over diopside. In addition, the second retrograde overprint of green schist facies on amphibolites facies which is marked by an assemblage muscovite + chlorite + actinolite also found in some samples. According to previous literatures, metamorphic rocks in Lützow-Holm complex shows a spatial variation of metamorphic grade ranking from amphibolites facies to the east and granulite facies to the west. Akarui Point situates in the transition zone between amphibolite facies and granulite facies. Hence, most previous authors tend to conclude that such metamorphic variation might indicate a different P-T during the Pan-African orogeny of Gondwana assembly. But here we prefer to conclude that the Akarui Point has been experienced the granulite facies metamorphism as same as other localities in the western part of Lützow-Holm Complex and retrograde to lower grade afterward.

Key words: Antarctica, Akarui Point, Retrograde, calc-silicate, Pan-African Orogeny

Proceedings of the Second International Symposium on Geoscience Resources and Environments of Asian Terranes (GREAT 2018)
19 - 23 November 2018 Bangkok, Thailand

Ruby-bearing calc-silicate at West Ongul Island, Lützow-Holm Complex, East Antarctica

Penchan Thaworndumrongsakul[1], Prayath Nantasin[1]*, Sotaro Baba[2], Tomokazu Hokada[3], Atsushi Kamei[4], Ippei Kitano[5], Yoichi Motoyoshi[3], Nugroho Setiawan[6], Davaa-ochir Dashbaatar[7] and John Booth[1]

1 Department of Earth Sciences, Faculty of Science, Kasetsart University, Thailand

2 Department of Natural Environment, University of the Ryukyus, Japan

3 Geology Group, National Institute of Polar Research (NIPR), Japan

4 Department of Earth Science, Shimane University, Japan

5 Division of Earth Sciences, Faculty of Social and Cultural Studies, Kyushu University, Japan

6 Department of Geological Engineering, Gadjah Mada University, Indonesia

7 School of Geology and Mining Engineering, Mongolian University of Science and Technology, Mongolia

* Corresponding author email: fscipyn@ku.ac.th

Abstract

Ruby-bearing calc-silicate rocks at the West Ongul Island in Lützow-Holm Complex of East Antarctica occur as elongate lens within charnockitic rocks. Previous works point out that the area has been metamorphosed under amphibolite to granulite facies. Calc-silicate lens is approximately 1 m. wide and 100 m. long. Corundum formed as a narrow band at the middle of this calc-silicate lens with various thicknesses ranging from few mm. up to 20 cm. The grain size of corundum also varies from less than 1 mm. in the southern part up to approximately 5 cm. in the northern side. This calc-silicate body shows a well symmetric variation of lithology that could be defined as 4 zones named scapolite-rich zone, clinopyroxene-rich zone, epidote-rich band and corundum-bearing zone, from outer to inner, respectively. The scapolite zone is characterized by very coarse-grained, elongate scapolite crystals which align perpendicular to the contact between the lense and charnockite. It is made up of an assemblage scapolite + clinopyroxene + biotite + phlogopite. The corundum-bearing zone is made up of an assemblage clinopyroxene + biotite + phlogopite + corundum + calcite + amphibole + plagioclase + sericite. The texture of phase transformation of phlogopite to be corundum is obviously preserved in this zone. The presences of scapolite along both rims of calc-silicate body and the distinct reddish epidote layers might indicate a metasomatism between charnockite and calc-silicate body during the peak metamorphism. Meanwhile such corundum formation reaction could be taken place during this metamorphic event.

Key words: Ruby, Calc-silicate, Lützow-Holm Complex, West Ongul Island, Antarctica

Proceedings of the Second International Symposium on Geoscience Resources and Environments of Asian Terranes (GREAT 2018)
19 - 23 November 2018 Bangkok, Thailand

Mineral chemistry of cordierite, plagioclase and biotite in the cordierite-bearing tonalite in Bokeo Province, Lao PDR

Srett Santitharangkun[1] and Burapha Phajuy[1*]

1 Department of Geological Sciences, Faculty of Science, Chiang Mai University, Chiang Mai, 50200, Thailand

* Corresponding author email: buraphaphj3@gmail.com

Abstract

Bokeo Province located in the northwest of Lao PDR is believed to be a part of Sukhothai terrane. The tonalite samples exhibit a seriate texture with a slightly foliated characteristic. The rock samples consist of plagioclase + quartz + biotite ± muscovite + cordierite ± opaque mineral ± K-feldspar ± apatite + zircon. Secondary minerals; sericite, clay minerals and chlorite altered from plagioclase, K-feldspar and biotite, respectively. Cordierite is present in only a few studied samples and shows no chemical zone. The most of them altered to white mica. Chemical composition of cordierite is made up of Si content from 4.93 to 5.24 apfu. and high in Al (Al_{tot} from 3.75 to 4·18 apfu.). Mg# of cordierite is between 0.56-0.63. Mineral chemistry of plagioclase indicates range of Anorthite content from andesine to labradorite (An_{34-59}). The study mineral chemistry of biotite represents temperature and pressure of crystallization at 708±12 °C to 779±12 °C and 2.96±0.33 to 3.75±0.33 kbar respectively.The anorthite content of plagioclase might refers to evidence of tonalitic magma source. The Mg# of cordierite is slightly higher than S-type granitoid (mg-number < 0·6). Cordierite-bearing tonalitic rocks can rarely be found in volcanic arc tectonic setting. They are similar to the experimental results of High-Al Tonalite and Trondhjemites at the cornucopia Stock, Blue Mountains, Northeastern Oregon. The tonalite samples are an evidence for volcanic arc resulting from the closure of closing of paleo-Tethys in the Bokeo Province area.

Key words: Cordierite-bearing rock tonalite, Minerals chemistry, Volcanic arc, Lao PDR

1. Introduction

Sibumasu and Indochina blocks were separated by Inthanon zones, the main suture zone of the Paleotethyan Ocean during Late Paleozoic to Early Mesozoic (Sone and Metcalfe, 2008; Peng et al., 2013; Fan et al., 2015; Metcalfe et al., 2017). Other suture zones separated from Late Carboniferous until Late Permian might refer to back-arc basin called Nan-Sra Kaeo suture zone (Barr and Macdonald,1987, Singharajwarapan and Berry, 2000). In between the main sutures were discovered terrane/arc called Sukhothai terrane. (Metcalfe, 2011; Sone and Metcalfe, 2008) (Figure 1).

Many researchers have proposed the granitoid rock in Southeast Asia related to post-collisions of Sibumasu and Indochina (Searle et al., 2012; Wang et al., 2016; Qian et al., 2017). Granitoid belts in Southeast Asia are divided into three main part running from southwest of China through northern Thailand and northwest of Lao PDR into Malay Peninsula. They are designated as Western-, Central-, and Eastern-Granitoid Belts. The age of granitoid rocks believed to be the Late Paleozoic to Mesozoic. (Charusiri et al., 1993; Cobbing, 2011; Kawakami et al., 2014; Oliver et al., 2014; Searle et al., 2012; Wang et al., 2016; Qian et al., 2017).

This study focuses on minerals characteristics in cordierite-bearing granitoid rock in Bokeo province Lao PDR. The results may apply for some of evolution the volcanic arc in the north of Southeast Asia.

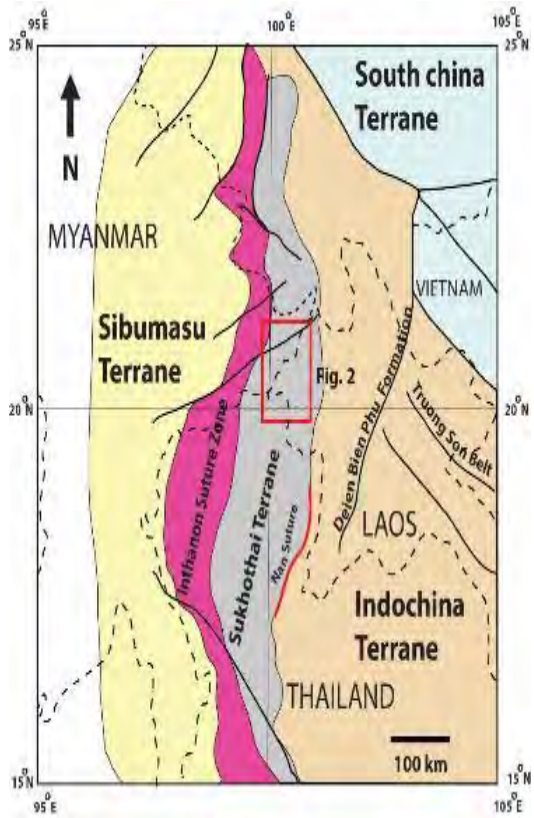

Figure 1. Distribution map of tectonic zone in the study area (modified from Sone and Metcalfe, 2008).

2. Geological background

The study area locates in Sukhothai terrane. It contains with difference age of volcanic rocks, plutonic rocks and sedimentary rocks (Figure 2). Precambrian to Lower Cambrian sedimentary rocks represent low- to medium- grade metamorphic rocks. They contain quartzite and mica schist and sedimentary rocks consisted of metasandstone, mudstone and greywacke. The Devonian to Lower Permian rocks represent shallow marine sedimentary rocks that contain sandstone, muddy limestone and mudstone. The Upper Permian to Lower Triassic sedimentary rocks is characterized by shallow marine deposit and continental deposit. It contains widespread of dark grey limestone, siltstone, mudstone, shale, conglomerate, red bed sandstone interbedded with siltstone and volcaniclastic sandstone. The Jurassic to Cretaceous sedimentary rocks is shown continental sedimentary rocks such as red bed sandstone interbedded with siltstone. The Cenozoic sedimentary sequences are featured by non-marine sequences and alluvium deposit.

In part of igneous rocks, they include volcanic rocks and plutonic rocks. The Mesozoic rocks comprise of volcanic rocks (rhyolite and andesite) and pyroclastic rocks (rhyolitic tuff and andesitic tuff). The Permo-Triassic plutonic rocks are characterized by granitoid rocks and diorite. The Cenozoic volcanic rocks contain alkali basalt (Department of Geology and Mines, 1990; Sutherland et al., 2002; Department of Mineral Resources, 2007; Myanmar Geoscience Society, 2014).

3. Methodology

The rock samples are selected from field work that located in middle part of Bokeo Province. The rock samples were randomly collected from out crops that distribution near main road, tracks, steams and Mekong River.

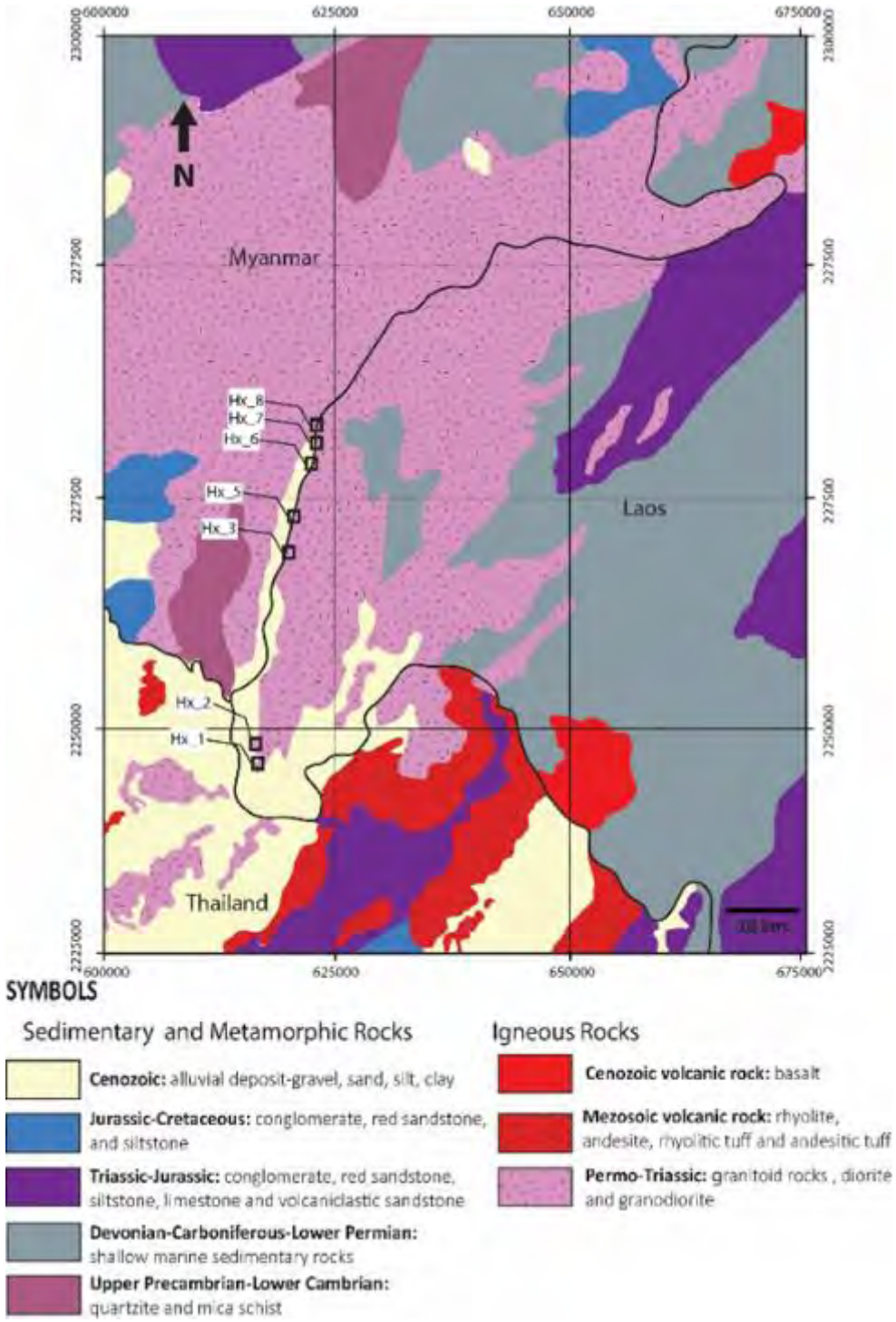

Figure 2. Geologic map of the study area and sample location (modified from Department of Geology and Mines, 1990; Department of Mineral Resources, 2007; Myanmar Geoscience Society, 2014).

Lithology of rock samples were investigated by cross section of the slab that polished by 200 mesh of silicon carbide powders. After that, the rock samples were dyed by intensive hydrofluoric acid solution and saturated solution of sodium cobalt nitrite and solution of amaranth. The samples that stained with yellow color indicate the components of potassium feldspar and stained with pink color indicate the components of plagioclase. Petrography of rock samples were observed by thin section. Petrographic analysis is investigation of the rock types, interpreted by rock textures, components, mineral alteration, and other physical features. The rock sample was classified by 1000 time counting of essential and accessory minerals shown in thin section. The amounts of essential minerals were calculated in percentage by volume and separate group of the rock samples by IUGS Sub-commission on the Systematics of Igneous Rock (Streckeisen, 1976).

Preparation of minerals chemical analysis for rock samples were started from polished thin sections and then investigated by a combination of reflected polarizing microscope. After a first petrography, the samples of special interest were selected for further observations. Quantitative mineral analyses were performed on gold coated polished sections, using a JEOL JSM-5910LV scanning electron microscope equipped with a LINK Systems EDS at Chiang Mai University (measurement time for energy dispersive elements 30 sec).

4. Result

4.1 Lithology and Petrography

Lithology characteristics of rocks sample show gray colored with large grains enough to be visible with the unaided eye. The samples exhibit seriate grain-size distribution with slightly foliated characteristic. The crystal size ranges from fine grain crystal to moderate-large grain crystal. Remarkable feature of the rock samples are almost dyed by pink color of amaranth solution indicated plagioclase content. (Figure 3).

Table 1. Mineral modal analyses of the representative of the tonalite samples in the Bokeo Province.

	Hx_01	Hx_02	Hx_03	Hx_04	Hx_05	Hx_06	Hx_07	Hx_08
Minerals component								
Quartz	35.8	33.6	30.0	31.6	34.2	33.4	30.2	32.4
Plagioclase	30.4	38.4	35.2	28.6	24.8	29.0	35.0	35.0
K-feldspar	0.4	3.4	-	trace	-	trace	-	-
Biotite	24.6	19.4	15.4	18.6	21.4	18.6	18.0	20.6
Muscovite	4.2	3.8	-	3.4	1.4	4.0	3.8	6.6
Cordierite	4.4	1.4	18.6	17.0	18.2	14.2	12.2	5.0
Zircon	0.2	trace	0.4	0.6	trace	0.2	0.4	0.4
Opaque	-	-	0.4	-	trace	-	trace	trace
Apatite	-	-	-	0.2	-	0.6	0.4	-

Petrographic study, the minerals assemblage (table 1) of rocks sample consist of unzoning plagioclase (24.8-38.4 modal%) + quartz (30.0-35.8 modal%) + biotite (15.4-24.6 modal%) ± muscovite (0-6.6 modal%) + cordierite (1.4-18.6 modal%) ± opaque mineral (0-0.4 modal%) ± K-feldspar (0-3.4 modal%) ± apatite (0-0.4 modal%) + zircon (trace-0.6 modal%). Classification name of rock samples used percentage by volume of quartz, plagioclase and potassium feldspars is tonalite (Figure 4, 5). Secondary minerals include sericite, clay minerals and chlorite/clay mineral altered from plagioclase, K-feldspar and mica respectively. Least altered cordierite present in only a few samples. The cordierite are most altered to white mica.

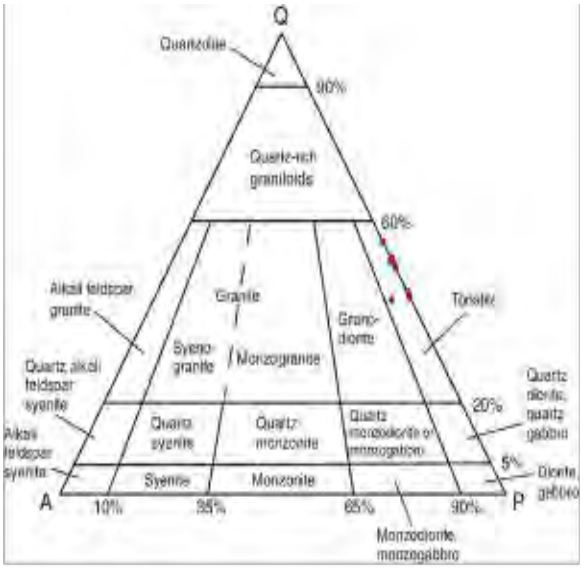

Figure 3. Rock sample number Hx_1 (A) and Hx_3 (B)

Figure 4. Plots of the studied sample (red circle) in the tonalite field in QAP diagram (Streckeisen, 1976).

4.2 Minerals Chemistry

Plagioclase is characterized by SiO_2 (53.80-62.56 wt%), TiO_2 (0-0.29 wt%), Al_2O_3 (23.88-33.30 wt%), Fe_2O_3 (0-0.02 wt%), FeO (0-0.21 wt%), MnO (0 -0.39 wt%), MgO (0-0.16 wt%), CaO (6.37-10.13 wt%), Na_2O (3.72-6.80 wt%) and K_2O (0-0.25 wt%) (see also at table 2). The compositions of plagioclase in Bokeo area are broad range of anorthite-content (An_{34-59}) (Figure 6). They present range in Si content from 2.39 to 2.76 atoms per formula unit (apfu.), Na content from 0.32 to 0.58 apfu. and Ca content from 0.30 to 0.49 apfu.

Chemical composition of biotite is featured by SiO_2 (33.97-38.66 wt%), TiO_2 (1.29-4.02 wt%), Al_2O_3 (18.29-26.59 wt%), Fe2O3 (0.58-1.01 wt%), FeO (17.71-23.22 wt%), MnO (0-0.50 wt%), MgO (8.63-9.88 wt%), CaO (0-0.65 wt%), Na_2O (0-0.80 wt%) and K_2O (6.38-9.82 wt%) (see also at table 3). They exhibit range in Si content from 4.84 to 5.57 apfu. and they show Al content from 3.13 to 4.47 apfu. Mg# of biotite is between 0.46-0.90. The study minerals chemistry of biotite represents temperature and pressure crystallization of magma. Ti-saturation surface can be reformulated as the geothermometric expression: $T=\{[\ln(Ti)-a-c(Mg\#)^3]/b\}^{0.333}$, which T is temperature in C°, Ti is the number of apfu. normalized on the basis of 22 O atoms, Mg# is Mg/ (Mg + Fe), a = -2.3594, b= 4.6482×10^{-9} and c = -1.7283 (Darrell et al., 2005). From application of the Ti-biotite geothermometer represents temperature of crystallization at 708±12 °C to 779±12 C°. Geobarometer can be calculated

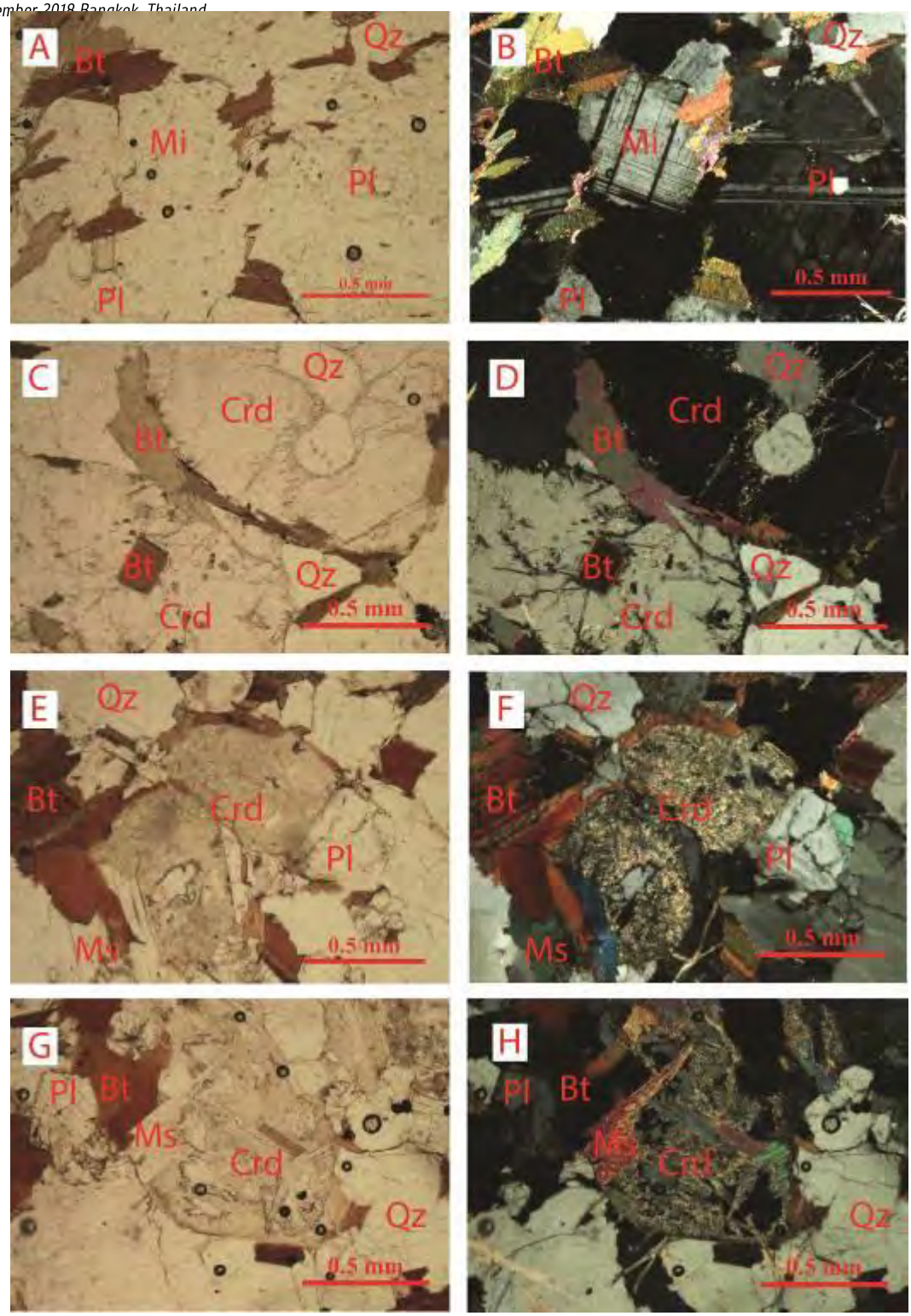

Figure 5. Representative photomicrographs of tonalite at Bokeo Province area shown seriate texture with medium to large grain crystal. Mineral abbreviations: Qz-Quartz, Mi -Microcline, Pl – Plagioclase, Bi – Biotite, Ms – Muscovite and Crd – Cordierite. A. and B. is sample no. Hx_1, C. and D. is sample no.Hx_3, E. and F. is sample no. Hx_5, G. and H. is sample no. Hx_7. Picture A, C, E and G as seen under plain-polarized light and picture B, D, F and H as seen under cross-polarized light.

from Al_{tot} apfu. content of biotite. rocks. The following empirical equation was obtained: P (kbar) = 3.03 × Al_{tot}-6.53 (±0.33) (Uchida et al., 2007). From application of the Al_{tot}-biotite geobarometer represents pressure of crystallization at 2.96±0.33 to 3.75±0.33 kbar.

Mineral chemistry of least-altered cordierite is characterized by SiO_2 (48.54-52.00 wt%), TiO_2 (0-0.63 wt%), Al_2O_3 (31.37-34.93 wt%), Fe_2O_3 (0.19-0.21 wt%), FeO (8.07-8.84 wt%), MnO (0.12-0.46 wt%), MgO (6.87-7.90 wt%), CaO (0-0.26 wt%), Na_2O (0-0.34 wt%) and K_2O (0-0.09 wt%) (see also at table 4). They exhibit a narrow range in Si content from 4.93 to 5.24 apfu. and they are high in Al (Al_{tot} from 3.75 to 4·18 apfu.). Mg# (Mg number =Mg/Mg+Fe_{tot}) of cordierite is between 0.56-0.63 (Figure 6).

5. Discussion

5.1 Origin of tonalitic magma

Tonalitic rocks in Brokeo Province indicate characteristics of derivation from a mafic or mantle-derivative source. Mineral content of the rock samples consists of low K

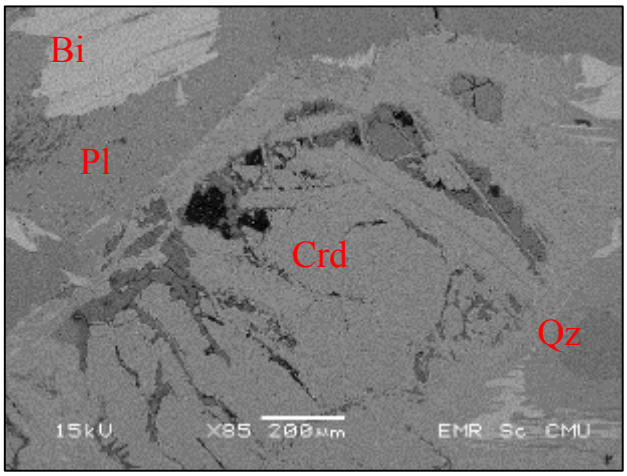

Figure 6. Backscattered electron minerals; image of sample number Hx_1 contains with cordierite (Crd), plagioclase (Pl), Biotite (Bi) and Quartz (Qz).

minerals (0-3.4 modal% of K-feldspar). In addition, mineral chemistry of the plagioclase revealed an An-content value of 34 to 59 that indicate andesine to labradorite variety. The plagioclase represents crystallization in intermediate or mafic rock. However, the presence of highly quartz content refer to felsic composition. Evidently, minerals component analyses indicate that the rocks were not primary magma.

The minerals characteristic of tonalitic rocks in Brokeo Province mimic in the Archean,

relatively hot oceanic lithosphere is subducted (Defant and Drummond, 1990). However, some of study suggested that Phanerozoic high-Al tonalite-trondhjemite (Barnes et al., 1996; Petford and Atherton, 1996) and Mesozoic high-Al Tonalite and Trondhjemites at the cornucopia Stock, Blue Mountains, Northeastern Oregon (Johnson et al., 1997) can be generated by partial melting of lower-crust and volcanic-arc basement rocks, respectively.

5.2 Cordierite in the tonalitic magma

One of the evidences of tonalitic magma in Brokeo Province is the emerging of magmatic cordierite in tonalite. Cordierite is referred to a pelitic sedimentary source (S-type granite or pegmatite; Green, 1976 and Miller, 1985). However, the low component of minerals contained potassium and Mg-number value of cordierite are slightly higher than typical of cordierite from S-type granite (Mg# < 0·6). In addition, the rock samples argue against pelitic source. Moreover, cordierite in tonalite present lacks resorption texture, euhedral shape and larger size than the rare cordierite shown in metasedimentary wall rock. There reasons argue against a xenocrystic origin for the cordierite in the tonalite sample. Previous experimental study on peraluminous granites demonstrated that cordierite occurs as a biotite geobarometer of rock samples (2.96±0.33-3.75±0.33 kbar). The cordierite that present euhedral phase in early mineral suggests that cordierite was near liquidus phase. It implies shallow depths crystallization (Taubeneck, 1964; Clemens and Wall, 1981).

5.3 Tectonic implications of tonalite in Brokeo province

Out crop distribution of tonalitic rock in Brokeo Province is believed that tonalitic rock emerges in Sukhothai terrain. The tonalitic rock in Brokeo Province might be interpreted as the Chiang Khong-Lampang-Tak igneous zone. Some of study have identified that the Middle Triassic (241–239 Ma) volcanic rocks in the Central Chiang Khong-Lampang-Tak igneous zone formed at transition from sub-duction to initial collision (Qian et al., 2017). Moreover, studying of Wang et al. (2016) indicate syn-

Table 2. Major oxides and structural formula of plagioclase

Sample no.	9-pl-1	9-pl-2	19-pl-1	19-pl-3	29-pl-1	29-pl-2	29-pl-3
Major oxide (wt.%)							
SiO_2	61.02	62.56	61.04	59.23	56.52	53.80	60.76
TiO_2	0.00	0.29	0.00	0.22	0.26	0.00	0.00
Al_2O_3	25.07	23.88	25.54	26.30	27.87	33.30	25.62
Fe_2O_3	0.02	0.00	0.00	0.00	0.01	0.01	0.02
FeO	0.21	0.00	0.00	0.00	0.10	0.15	0.19
MnO	0.00	0.00	0.00	0.39	0.09	0.34	0.14
MgO	0.00	0.00	0.11	0.13	0.00	0.16	0.00
CaO	6.80	6.37	9.59	8.48	10.13	8.38	7.46
Na_2O	6.72	6.80	3.72	5.07	4.80	3.80	5.81
K_2O	0.15	0.10	0.00	0.18	0.22	0.07	0.00
total	100.00	100.00	100.00	100.00	100.00	100.00	100.00
Cations per 8 oxygens							
Si	2.70	2.76	2.69	2.63	2.53	2.39	2.69
Ti	0.00	0.01	0.00	0.01	0.01	0.00	0.00
Al	1.31	1.24	1.33	1.38	1.47	1.75	1.34
Fe^{3+}	0.00	0.00	0.00	0.00	0.00	0.00	0.00
Fe^{2+}	0.01	0.00	0.00	0.00	0.00	0.01	0.01
Mn	0.00	0.00	0.00	0.01	0.00	0.01	0.01
Mg	0.00	0.00	0.01	0.01	0.00	0.01	0.00
Ca	0.32	0.30	0.45	0.40	0.49	0.40	0.35
Na	0.58	0.58	0.32	0.44	0.42	0.33	0.50
K	0.01	0.01	0.00	0.01	0.01	0.00	0.00
total	4.93	4.90	4.80	4.89	4.94	4.90	4.89
An	0.36	0.34	0.59	0.47	0.53	0.55	0.42
Ab	0.64	0.65	0.41	0.51	0.45	0.45	0.58
Or	0.01	0.01	0.00	0.01	0.01	0.01	0.00

Table 3. Major oxides and structural formula of biotite

Sample no.	1-bt-01	3-bi-02	3-bi-04	3-bi-04	3-bi-05	8-bt-01	8-bt-02	8-bt-03	8-bt-04
Major oxide (wt.%)									
SiO_2	38.66	38.40	36.56	37.06	36.06	37.26	37.27	38.46	36.55
TiO_2	4.02	2.63	1.74	2.53	1.82	2.41	2.59	2.49	2.38
$Al2O_3$	20.19	18.29	19.42	19.74	25.90	19.62	19.80	18.61	24.10
$Cr2O_3$	0.00	0.00	0.00	0.00	0.00	0.00	0.00	0.00	0.00
$Fe2O_3$	0.89	1.01	0.98	0.86	0.64	0.92	0.91	0.94	0.68
FeO	17.71	21.51	23.22	22.26	18.27	20.15	19.35	19.34	17.80
MnO	0.04	0.00	0.00	0.20	0.00	0.42	0.50	0.50	0.04
MgO	8.69	8.98	8.95	9.88	8.63	9.51	9.52	9.77	9.29
CaO	0.08	0.00	0.09	0.13	0.65	0.01	0.11	0.14	0.51
Na_2O	0.35	0.26	0.39	0.00	0.80	0.00	0.14	0.34	0.34
K_2O	9.37	8.92	8.66	7.36	7.23	9.70	9.82	9.40	8.32
Cations per 22 oxygens									
Si	5.51	5.57	5.36	5.36	5.10	5.41	5.40	5.56	5.19
Ti	0.43	0.29	0.19	0.28	0.19	0.26	0.28	0.27	0.25
Al	3.39	3.13	3.36	3.36	4.32	3.36	3.38	3.17	4.03
Cr	0.00	0.00	0.00	0.00	0.00	0.00	0.00	0.00	0.00
Fe^{3+}	0.10	0.11	0.11	0.09	0.07	0.10	0.10	0.10	0.07
Fe^{2+}	2.11	2.61	2.85	2.69	2.16	2.45	2.35	2.34	2.11
Mn	0.00	0.00	0.00	0.02	0.00	0.05	0.06	0.06	0.00
Mg	1.85	1.94	1.96	2.13	1.82	2.06	2.06	2.10	1.96
Ca	0.01	0.00	0.01	0.02	0.10	0.00	0.02	0.02	0.08
Na	0.10	0.07	0.11	0.00	0.22	0.00	0.04	0.09	0.09
K	1.70	1.65	1.62	1.36	1.30	1.80	1.82	1.73	1.51
total	15.21	15.38	15.58	15.31	15.28	15.49	15.50	15.45	15.31
Mg#	0.46	0.71	0.66	0.76	0.82	0.81	0.84	0.86	0.90

Table 4. Major oxides and structural formula of cordierite

Sample no.	1-crd-01	1-crd-02	1-crd-03	3-crd-1	3-crd-2	3-crd-3	3-crd-4
Major oxide (wt.%)							
SiO_2	50.19	50.09	50.33	48.54	52.00	49.64	51.63
TiO_2	0.02	0.00	0.12	0.17	0.27	0.63	0.00
Al_2O_3	32.53	33.07	32.63	34.93	31.68	32.64	31.37
Cr_2O_3	0.00	0.00	0.00	0.00	0.00	0.00	0.00
Fe_2O_3	0.21	0.19	0.20	0.19	0.21	0.21	0.24
FeO	8.43	8.10	8.46	8.63	8.07	8.84	9.47
MnO	0.46	0.29	0.12	0.32	0.32	0.36	0.17
MgO	7.74	7.90	7.77	6.87	7.01	7.62	6.93
CaO	0.03	0.03	0.04	0.26	0.00	0.00	0.03
Na_2O	0.32	0.33	0.33	0.00	0.34	0.06	0.06
K_2O	0.09	0.00	0.00	0.09	0.09	0.00	0.09
Cations per 18 oxygens							
Si	5.09	5.06	5.09	4.93	5.24	5.04	5.23
Ti	0.00	0.00	0.01	0.01	0.02	0.05	0.00
Al	3.89	3.94	3.89	4.18	3.77	3.91	3.75
Cr	0.00	0.00	0.00	0.00	0.00	0.00	0.00
Fe^{3+}	0.02	0.01	0.02	0.01	0.02	0.02	0.02
Fe^{2+}	0.71	0.68	0.72	0.73	0.68	0.75	0.80
Mn	0.04	0.03	0.01	0.03	0.03	0.03	0.01
Mg	1.17	1.19	1.17	1.04	1.05	1.15	1.05
Ca	0.00	0.00	0.00	0.03	0.00	0.00	0.00
Na	0.06	0.07	0.06	0.00	0.07	0.01	0.01
K	0.01	0.00	0.00	0.01	0.01	0.00	0.01
total	10.99	10.99	10.98	10.97	10.89	10.96	10.89
Mg#	0.62	0.63	0.62	0.58	0.60	0.60	0.56

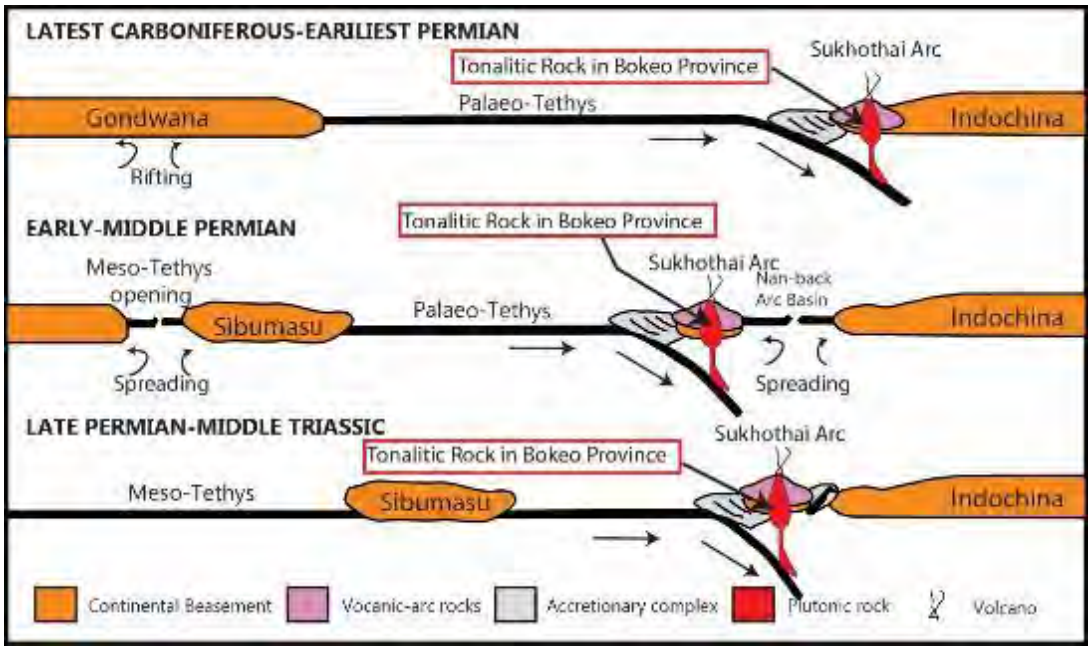

Figure 7. Schematic tectonic cratons showing tectonic evolution of tonalitic rocks in Bokeo Province, Lao PDR. They might emerge in volcanic-arc tectonic setting.at Sukhothai terrain (modified from Sone and Metcalfe, 2008)

Triassic (~237 Ma) and abundant post-collisional at Late Triassic (230-200 Ma) igneous rocks in northern Thailand. However, the evidence of minerals assemblage, texture and minerals chemistry argue against syn/post-collisional granitoid rocks. The rock samples show slightly foliated texture. On the other hand, granitoid rocks nearby the study area do not indicate metamorphic texture. This reasoning supports that the study area occurs before the granitoid rocks in adjacent area. Moreover, the minerals assemblage and minerals chemistry occur that the tonalitic rock in Brokeo province originate from volcanic-arc tectonic setting. In consequence, tonalitic rock in Brokeo province might be resulted from the closure of volcanic arc between closing of Paleo-Tethys since the Latest Carboniferous (Figure 7).

6. Conclusion

Petrographic and minerals chemistry observations of the rock samples in Brokeo Province suggest that they relate to tonalitic rocks. The study of minerals chemistry

represents temperature and pressure of crystallization at 708±12 °C to 779±12 °C and 2.96±0.33 to 3.75±0.33 kbar respectively. They indicate crystals crystallized at a depth of about 11 km. The tonalite in Brokeo Province were induced by the derivation from a mafic or mantle-derivative source in a volcanic-arc setting possibly related to subduction of Paleo-Tethys into Sukhothai terrain.

7. Acknowledgement

We thank the staff of the Department of Geological Sciences, Faculty of Science, Chiang Mai University, Chiang Mai, Thailand, for the advice about using all of instrument and supporting during we did this research. This study was refunded by the Development and Promotion of the Gifted in Science and Technology Project (DPST).

8. References

Barr, S.M. and Macdonald, A.S. 1987. Nan River suture zone, northern Thailand. *Geology*, 15,.907-910.

Barnes, C. G., Petersen, S. W., Kistler, R. W., Murray, R. and Kays, M. A. 1996. Source and tectonic implications of tonalite–trondhjemite magmatism in the Klamath Mountains. *Contributions to Mineralogy and Petrology*, 123, 40-60.

Charusiri, P., Clark, A.H., Farrar, E., Alchibald, D. and Charusiri, B. 1993. Granite belts in Thailand: evidence from the $^{40}Ar/^{39}Ar$ geochronological and geological syntheses. *Journal of Southeast Asian Earth Sciences*, 8, 127–136.

Clemens, J. D. and Wall, V. J. 1981. Origin and crystallization of some peraluminous (S-type) granitic magmas. *Canadian Mineralogist*, 19, 111-131

Cobbing, E.J. 2011. Granitic rocks. In: Ridd, M.F., Barber, A.J. and Crow, M.J. (Eds.), The Geology of Thailand. *Geological Society*, London, p. 441–457.

Department of Geology and Mines, 1990. Lao P.D.R. Geological and Mineral Occurrence Map 1:1000000. Department of Geology and Mines, Lao P.D.R., Vientiane.

Department of Mineral Resources, 2007. Geologic Map of Thailand by Province 1:250,000. Department of Mineral Resources, Thailand, Bangkok.

Drummond, M. S. and Defant, M. J. 1990. A model for trondhjemite-tonalite-dacite genesis and crustal growth via slab melting: Archean to modern comparisons. *Journal of Geophysical Research*, 95, 21503-21521.

Fan, W.M., Wang, Y.J., Zhang, Y.H., Zhang, Y.Z., Jourdan, F., Zi, J.W. and Liu, H.C. 2015. Paleotethyan subduction process revealed from Triassic blueschists in the Lancang tectonic belt of Southwest China. *Tectonophysics*, 662, 95-108

Green, T. H. 1976. Experimental generation of cordierite or garnet bearing granitic liquids from a pelitic composition. *Geology,* 4, 85–88.

Henry, D.J., Guidotti, C.V., and Thomson, J.A.2005. The Ti-saturation surface for low-to-medium pressure metapelitic biotites: Implications for geothermometry and Ti-substitution mechanisms.*American Mineralogist*, 90, 316-328.

Johnson, K., Barnes, C.G. and Miller, C.A. 1997. Petrology, Geochemistry, and Genesis of High-Al Tonalite and Trondhjemites of the Cornucopia Stock, Blue Mountains, Northeastern Oregon. *Journal of Petrology*, 38, 1585-1611.

Kawakami, T., Nakano, N., Higashino, F., Hokada, T., Osanai, Y., Yuhara, M., Charusiri, P., Kamikubo, H., Yonemura, K. and Hirata, T. 2014. U-Pb zircon and CHIME monazite dating of granitoids and high-grade metamorphic rocks from the eastern and peninsular Thailand-a new report of Early Paleozoic granite. *Lithos*, .200–201, 64–79.

Metcalfe, I., Henderson, C.M. and Wakita, K. 2017. Lower Permian conodonts from PalaeoTethys ocean plate stratigraphy in the Chiang Mai-Chiang Rai suture zone, northern Thailand. *Gondwana Research*, 44, 54–66.

Miller, C. F., 1985. Are strongly-peraluminous magmas derived from pelitic

sedimentary sources? *Journal of Geology*, 93, 673–689.

Myanmar Geoscience Society, 2014. Geologic Map of Myanmar 1:2,250,000. Myanmar Geoscience Society, Yangon, Myanmar.

Oliver, G., Zaw, K., Hotson, M., Meffre, S. and Manka, T. 2014. U–Pb zircon geochronology of Early Permian to Late Triassic rocks from Singapore and Johor: a plate tectonic reinterpretation. *Gondwana Research*, 26, 132–143.

Peng, T.P., Wilde, S.A., Wang, Y.J., Fan, W.M. and Peng, B.X. 2013. Mid-Triassic felsic igneous rocks from the southern Lancangjiang Zone, SW China: petrogenesis and implications for the evolution of Paleotethys. *Lithos*, 168-169, 15-32.

Petford, N. and Atherton, M. 1996. Na-rich partial melts from newly underplated basaltic crust: The Cordillera Blanca batholith. *Journal of Petrology,* 37, 1491–1521.

Qian, X., Feng, Q.L., Wang, Y.J., Zhao, T.Y., Zi, J.W., Udchachon, M. and Wang, Y.K. 2017. Late Triassic post-collisional granites related to Paleotethyan evolution in SE Thailand: Geochronological and geochemical constraints. *Lithos*, 286–287, 440–453.

Searle, M.P., Whitehouse, M.J., Robb, L.J., Ghani, A.A., Hutchison, C.S., Sone, M., Ng, S.W.P., Roselee, M.H., Chung, S.L. and Oliver, G.J.H. 2012. Tectonic evolution of the Sibumasu Indochina terrane collision zone in Thailand and Malaysia: constraints from new U-Pb zircon chronology of SE Asian tin granitoids. *Journal of the Geological Society*, 169, 489–500

Singharajwarapan, S. and Berry, R., 2000. Tectonic implications of the Nan suture zone and its relationship to the Sukhothai fold belt, northern Thailand. *journal of Asian Earth Sciences,* 18, 663–673.

Sone, M. and Metcalfe, I. 2008. Parallel Tethyan sutures in mainland Southeast Asia: new insights for Paleo-Tethys closure and implications for the Indosinian orogeny. *Geoscience*, 340, 166–179.

Sutherland, F. L., Bosshart, G., Fanning, C.M., Hoskin, P.O.W. and Coenraads, R.R. 2002. Sapphire crystallization, age and origin, Ban Huai Sai, Laos: Age based on zircon inclusions. *Journal of Asian Earth Sciences*, 20, 841–849.

Taubeneck, W. H. 1964. Cornucopia stock, Wallowa Mountains, northeastern Oregon: field relationships. *Geological Society of America Bulletin*, 75, 1093-1116.

Uchida, E., Endo, S and Makino M. 2007. Relationship Between Solidification Depth of Granitic Rocks and Formation of Hydrothermal Ore Deposits. *Resource Geology*, 57, 47-56.

Wang, Y.J., He, H.Y., Cawood, P.A., Srithai, B., Feng, Q.L., Fan, W.M., Zhang, Y.Z. and Qian, X. 2016. Geochronological, elemental and Sr-Nd-Hf-O isotopic constraints on the petrogenesis of the Triassic post-collisional granitic rocks in NW Thailand and its Paleotethyan implications. *Lithos*, 266–267, .264–286

Proceedings of the Second International Symposium on Geoscience Resources and Environments of Asian Terranes (GREAT 2018)
19 - 23 November 2018 Bangkok, Thailand

Characteristics of gold mineralization in Huai Kham On gold deposit in Sukhothai Fold Belt, Northern Thailand

Ladda Tangwattananukul[1]*, Daizo Ishiyama[2] and Punya Charusiri[3]

1 Department of Earth Sciences, Faculty of Science, Kasetsart Univerisity, Bangkok, Thailand

2 Faculty of International Resource Sciences, Akita University, Japan

3 Department of Geology, Faculty of Science, Chulalongkorn University, Bangkok, Thailand

* Corresponding author email: fscildt@ku.ac.th

Abstract

Huai Kham On deposit is located in the Lampang-Phrae mineral belt, Northern Thailand. The Lampang-Phrae mineral belt is a part of Sukhothai fold belt that extends from south of China (Yunnan province) to north of Thailand (Lampang province) through central of Thailand (Sukhothai province). Ore veins are characterized by veins, veinlets and strockwork breccias which are hosted by andesite lava, monomictic andesitic breccia, polymictic andesitic breccia and volcanic sedimentary breccias. The gold-bearing quartz veins can be divided into five stages based on cross-cutting relationship and mineral assemblage. Intense of electrum occurred in Stages I and II that coexists with pyrite, galena, chalcopyrite and sphalerite. The mineral assemblage of the gold-bearing quartz veins of Stages I and II are characterized by quartz-calcite-adularia-illite-sulfide minerals. The hydrothermal solution forming the gold-bearing quartz veins are at the temperature of 350° to 400°C based on the δ18O values of altered andesite lava range from +9.8 to +11.0‰. The gold-bearing quartz veins of the Huai Kham On gold deposit were formed from the magmatic water interacted with metamorphic rock or sedimentary rock during derived of hydrothermal solution from deeper to shallow levels.

Key words: Gold deposit, Oxygen isotope, Huai Kham On, Sukhothai Fold Belt

Subsurface Late Quaternary ironstones in Northwest Bangladesh: A Geochemical Review

Ismail Hossain[1]*, Md. Sazzadur Rahman[1], Md. Abdur Rahim[2], Pradip Kumar Biswas[3], A.S.M. Mehedi Hasan[3] and Md. Ibrahim Adham[1]

1 Department of Geology and Mining, University of Rajshahi, Rajshahi 6205, Bangladesh

2 Department of Disaster Resilience and Engineering, Patuakhali Science and Technology University, Patuakhal, Bangladesh

3 Institute of Mining, Mineralogy and Metallurgy (IMMM), BCSIR, Joypurhat, Bangladesh

* Corresponding author email: Ismail_gm@ru.ac.bd

Abstract

The present research deals with the geochemistry of subsurface Late Quaternary ironstones in Northwest Bangladesh. These subsurface ironstones are composed of varying proportions of siderite and goethite with some manganese-rich silicate, quartz and clay fraction. These rocks have been analyzed with XRF, XRD and optical microscopy. The ironstones contain major oxides as Fe_2O_3* (* total Fe) (avg. 66.6 wt%), SiO_2 (avg. 15.3 wt%), Al_2O_3 (avg. 4.0 wt%), MnO (avg. 7.7 wt%) and CaO (avg. 3.4 wt%). The higher percentage of Fe_2O_3* along with Al_2O_3 and MnO indicate the ironstones as goethite and siderite. Comparatively higher percentage of SiO_2 indicates the presence of the relative amounts of clastic quartz and manganese-rich silicate or clay in these rocks. These ironstones also have significant amount of MnO (avg. 7.7 wt%) suggesting their depositional environments under oxygeneted condition.

According to Principal component analysis (PCA), first principal component (PC1) accounts for 76% of the total variance and it shows that PC1 is dominated by the strong factor loadings for Fe_2O_3*, Al_2O_3, SiO_2 and MnO, while moderate factor loading for CaO. Second principal component (PC2) accounts for 21% of the total variance and is dominated by moderate factor loading for Al_2O_3 and CaO. The moderate factor loadings are for these two oxides present in both the PC1 and PC2, which indicating that it is predominant oxides of the samples. From these statistical analyses, PCA shows remarkable affinities of Fe_2O_3* and MnO with CaO versus SiO_2 and Al_2O_3. The trends of Fe_2O_3* and MnO shows similar geochemical affinities which expanded iron and manganese minerals to develop ironstones.

Overall, chemical data of these ironstones suggest that the source rock suffered deep chemical weathering and iron was mostly carried in association with the clay fraction and organic

matter. Iron concretion was mostly formed by bacterial build up in swamps and marshes, and was subsequently embedded in clayey mud. Within coastal environments, fluctuation of water table goethite and siderite with mud and quartz became dry and compacted to form ironstone. Later these ironstones were subjected to the weathering and transported to form the present ironstones.

Key words: Ironstone, Geochemistry, Siderite, Goethite, Bangladesh

Proceedings of the Second International Symposium on Geoscience Resources and Environments of Asian Terranes (GREAT 2018)
19 - 23 November 2018 Bangkok, Thailand

Variation in chemical weathering intensity in the Mekong River basin over the past 30,000 years

Thanakorn Jiwarungrueangkul[1]*, Zhifei Liu[1] and Karl Stattegger[2,3]

1 State Key Laboratory of Marine Geology, Tongji University, Shanghai 200092, China

2 Institute of Geosciences, University of Kiel, 24118 Kiel, Germany

3 Institute of Geology, Adam Mickiewicz University, 61-712 Poznań, Poland

* Corresponding author email: thanakorn-ji@hotmail.com

Abstract

The Mekong River basin is an ideal area for the Earth surface process study because of its unique geographic and climatic settings. In this study, we present high-resolution clay mineralogy and major element geochemistry of Core SO18383-3 collected off the Mekong River mouth in the southern South China Sea, aiming to reconstruct sediment provenance and chemical weathering intensity since the last glaciation. Clay mineral analysis suggests that the Mekong River is a major sedimentary source for the studied area. Smectite/(illite + chlorite) and smectite/kaolinite ratios coupled with TiO2/K2O ratio reveal the temporal variation in chemical weathering intensity in the Mekong River basin. The relatively lower ratios around the Last Glacial Maximum (LGM) (30.2–15.2 cal ka BP), the Younger Dryas interval (12.0–11.5 ka), and mid to late Holocene (8.0–1.5 ka) indicate weak chemical weathering intensity. In contrast, the higher ratios occurring during the period of main deglaciation (15.2–8.0 ka) indicate stronger chemical weathering in the Mekong River basin. The good correlations between these proxies and the available proxy records of the East Asian Summer Monsoon (EASM) intensity suggest that the intensity of chemical weathering in the Mekong River basin over the last 30,000 years is significantly controlled by the EASM evolution. This study provides insight into chemical weathering intensity as response to the evolution of the EASM system and increases our understanding of the principal forcing factor on continental weathering in the Mekong River basin since the LGM.

Key words: Chemical weathering intensity, Clay mineralogy, Geochemistry, Mekong River

Proceedings of the Second International Symposium on Geoscience Resources and Environments of Asian Terranes (GREAT 2018)
19 - 23 November 2018 Bangkok, Thailand

Geologic significance of Iranian Zagros for World Diffusion of Homo sapiens

Ken-ichiro Hisada[1]*

1 Division of Earth Evolution Sciences, Graduate School of Life and Environmental Sciences, University of Tsukuba, Japan

* Corresponding author email: hisadak@geol.tsukuba.ac.jp

Abstract

It is better known that there are a lot of ruins of Paleolithic ages in the southern part of the Iranian Zagros Mountains. The Arsanjan area is situated 80 km northeast of Shiraz, a largest city of the Iranian Zagros Mountains. The author gained the opportunity to study the geological field survey with archeological team of University of Tsukuba from 2011 to 2016. As a result, he could get valuable geological information on middle Paleolithic stone tools and their raw material (Hisada, 2016).

The stratigraphy of the Dalnesin valley, of which our archaeological target site Cave K9-5 is located near the entrance, was established in this study. Three lithological units could be recognized; fossiliferous limestone, radiolarite units and bedded limestone. The fossiliferous limestone unit is characterized by the occurrence of stromatoporoids and corals. The limestone is thickly bedded and dark gray in color and is supposed to be mainly Upper Jurassic. The radiolarite unit is distributed in the Dalnesin valley and on the southern side. The radiolarite unit can be divided into the lower alternation of brown shale and radiolarite and the upper alternation of limestone and radiolarite subunits. The radiolarite unit presents folded structure on the outcrop scale and flat-lying structure on the large scale. The depositional ages of the radiolarite unit is latest Jurassic to Early to Cretaceous according to radiolarian identification (Hisada et al, 2017). The bedded limestone unit, which is correlatable to the middle Cretaceous Salvak Formation, occurs extensively on the northern side of the Dalnesin valley. This unit is making a spectacle landform, that is, a cliff more than 500 m high. On the foot of this cliff, there are isolated smaller hills where argillaceous bedded limestone is distributed. The Cave K9-5 is developed in this unit. Therefore, the present study reveals that the stratigraphy of the High Zagros in the Arsanjan area is the fossiliferous limestone unit, radiolarite unit and bedded limestone unit and in ascending order.

The birth place of Homo sapiens is said to be East Africa 200,000-100,000 years ago. After that ancient people moved to West Asia and then spread to the world. From East Africa to West Asia, there are two routes, that is, north and south routes. The north and south routes correspond to Sahara-Sinai Peninsula-Levant, and Bab al Mandeb-Arabian Peninsula-Strait of Hormuz, respectively. Ancient people taking the south route entered to the Zagros Mountains and probably

reached to the Arsanjan area. The traverse of the Zagros Mountains was accomplished without a lot of troubles by whale back structure (= not continuous ridge) and presence of salt domes.

Radiolarite seems to have been preferable to the bedded chert as stone tools. Bedded chert consists of chert beds no more than 10 cm thick separated by mudstone films a few millimeters thick. This chert would not have yielded pieces of stone large enough to manufacture a full range of tools. However, radiolarite beds are thick enough to yield pieces suitable for flake production using the Levallois technique. Accordingly, co-occurrence of radiolarite for stone tools and limestone for residence caves is considered to be convenient resources for ancient people. In fact, the distance between the Cave K9-5 and the outcrops of the radiolarite unit is just a few kilometers.

Such a limestone-radiolarite association can be regarded as paleogeographic and tectonic results. During the Jurassic, the continents of Laurasia and Gondwana were separated by the shallow Neotethys ocean. Present-day West Asia was located at the innermost part of the Neotethys near the paleo-equator at a favorable location for upwelling currents, resulting in high faunal productivity (Baumgartner, 2013). Thus, an extensive carbonate platform developed on the Arabian continental margin. After the Arabia plate separated from the Africa plate and collided with the Eurasia plate, the limestone-radiolarite association was folded and uplifted to form the Zagros Mountains.

Vahdate Nasab et al. (2013) compiled the distributions of Upper, Middle and Lower Paleolithic sites in Iran. It is noteworthy that Middle and Upper Paleolithic sites are more concentrated in the Zagros Mountains than in the Alburz Mountains and they are exclusively located near Kermanshah and Neyriz. It is well-known that the Mesozoic ophiolite accompanied with radiolarite is distributed at Kermanshah and Neyriz (Gholami Zadeh et al., 2017). In both areas, the occurrence of the limestone-radiolarite association is also confirmed. This means that ancient people used limestone caves as residences and radiolarite as raw materials for stone tools. In other words, ancient people they might try to find limestone and radiolarite positively for their lives in the Zagros Mountains. Also ancient people learned more how to make stone tools from radiolarites there, and then they left the Zagros for the world diffusion.

Key words: Paleolithic, Zagros, radiolarite, limestone, stone tool, Arsanjan

Proceedings of the Second International Symposium on Geoscience Resources and Environments of Asian Terranes (GREAT 2018)
19 - 23 November 2018 Bangkok, Thailand

Preliminary study on causes and impacts of urban salinity in Khon Kaen City, Northeast Thailand

Romyupa Srikraiwest[1], Rungroj Arjwech[1]* and Mark E. Everett[2]

1 Department of Geotechnology, Faculty of Technology, Khon Kaen University, THAILAND

2 Department of Geology and Geophysics, Texas A&M University, College Station, Texas, USA

* Corresponding author email: rungroj@kku.ac.th

Abstract

Dryland salinity is recognized to be a significant problem across the world. The province of Khon Kaen is the most salt-affected region in northeast Thailand, while Khon Kaen City is undergoing a rapid phase of building construction and urbanization. The urban development by necessity is expanding into areas of high soil salinity. In this study, we analyzed satellite imagery, field observations, and borehole lithological logs to explore the spatial relationship between geological structure and hydrogeology. This is done to identify the cause of salinity in the Khon Kaen region and to evaluate its potential societal impact. The salinity found in the soil is a natural occurrence that is sourced from rock salt formations that are widely distributed over the region at various depths. The upward migration of dissolved salt in groundwater is controlled by fluctuations in the water table, and follows pathways defined by subsurface geological structures and fractures. The dissolved salt ions migrate toward the ground surface via deep groundwater flow systems. Human activities such as deforestation in upland regions and poor soil management strategies can exacerbate soil salinity problems by raising the groundwater table. Salinity impacts steel-reinforced concrete structures in built-up areas where salt has migrated to the surface. Salt-affected soils may become hidden due to changes in land use from low-lying agricultural fields to residential areas.

Key words: Dryland salinity, Urban salinity, Khon Kaen province

1. Introduction

Dryland salinity has become a major environmental problem in Northeast Thailand. The province of Khon Kaen is the most salt-affected, while Khon Kaen City is undergoing a rapid phase of building construction and urbanization (Arjwech and Everett, 2017). By necessity, the urban development is expanding into areas of high soil salinity. Urban salinity occurs as a result of a combination of excess water and salt in the environment (Ryan, 2003). Some of this

excess occurs naturally, but the way we use and manage our land and water resources has a large impact on salinity (Department Natural Resources, 2006). The installation of roads, buildings and other infrastructure can also alter natural drainage patterns, while other sources of excess water may result from leaking sewerage, stormwater and water pipes. The salts can break down materials such as concrete and prevent plants from taking up water (Collings, 2002). This research was a preliminary study of the causes and impacts of salinity that affects building areas in Khon Kaen City. The information presented in this study can be used for making managements that can reduce the growth of salt-affected soil areas due to human activities.

2. Study Area

The study area covers approximately 20.5 sq km to the west of Mittraphap Road in Khon Kaen City. In the past, local salt production in this area caused and distributed anthropogenic salinization processes. Currently, land reclamation for construction purposes involves backfilling severely salt-affected soil areas. However, salt crust and salinity indicator plants are still found in swampy areas as shown in Figure 1.

Figure 1. Photos of study area with deployment of the ERT line 1 and line 2

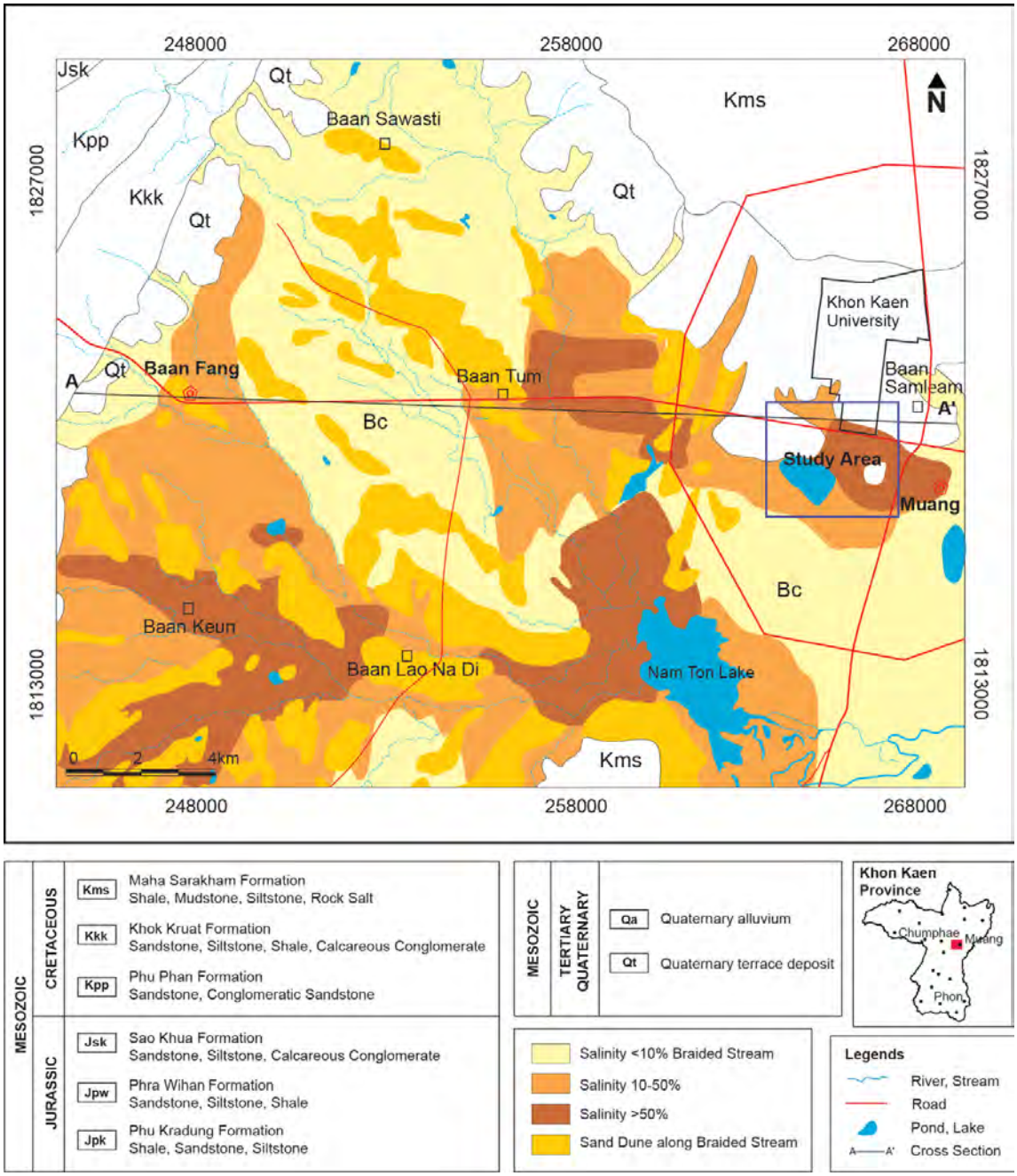

Figure 2. Geologic map with level of salinity distribution in Khon Kaen basin, Khon Kaen province (updated from Arjwech et al., 2014; 2018)

3. Geological Setting

Khon Kaen City is located in the Khon Kaen basin at the west rim of the Khorat Plateau. The geology is composed of Quaternary terrace (Qt), gravels found around the rim of the basin. Loess deposit found outstandingly covers the campus of Khon Kaen University. Quaternary alluvium (Qa) is sparely found in lower plains in the discharge area. Bedrock is not found crop-outed in the basin. The Quaternary sediments overlie the rock salt bearing Maha Sarakham Formation. Salinity is

classified into three categories in the basin (Arjwech et al., 2014; 2018). Most of the study area is located in severely salt-affected soils.

4. Methodology

An interpretation of aerial photography was conducted to examine the relationship between geomorphology and saline soil distribution over the area. Land use change was examined by satellite imagery between the year of 2002 and 2018 and field observation. Lithology well logs and rock salt data are available from 20 core holes, combined as cross sections to identify rock salt and subsurface structures. Two lines of 2D Electrical Resistivity Tomography (ERT) were carried out over the earthen berm through a lower plain.

5. Results

1. Causes of urban salinity

Factors that contribute to urban salinity include:

1.1 Geology

From three potash wells (K50, K58 and K107) in the study area, rock salt rises to a minimum depth of 105 m. Rock salt is located at various depths from 105 to 230 m as shown in Figure 3, depending on the controlled structures such as anticline and syncline. Salinity naturally occurs due to existing of rock salt bearing the Maha Sarakham Formation. These results imply that the thickness and depth of the rock salt layer and pathways, subsurface geological structures and fractures, play important roles in determining the surface soil salinity distribution.

1.2 Hydrogeology

The ERT survey was conducted to examine the depth and wide distribution of saline groundwater under the earthen berm through the lower plain. Brackish groundwater and saline groundwater exist underneath the earthen berm with low resistivity values (<6 ohm-m), as shown in Figure 4 and 5. However, diffusion and capillary can raise the salinity up to near the surface of the berm layer, as shown in ERT line 1 at ~90-110 m. Saline groundwater presents near the surface through the lower plain in ERT line 2.

A fresh artesian well located nearby ERT line 1 supports the idea that saline groundwater is related to geomorphology within the area. The existence of rock salt, including shallow and deep flow systems, contribute to salinity. Saline groundwater exists deeper on the higher terrace as a recharge area. Salt crust and salt tolerant plants also indicate the boundary of the saline soils. Results from the ERT were used to support the aerial interpretation and identify the saline soil boundary.

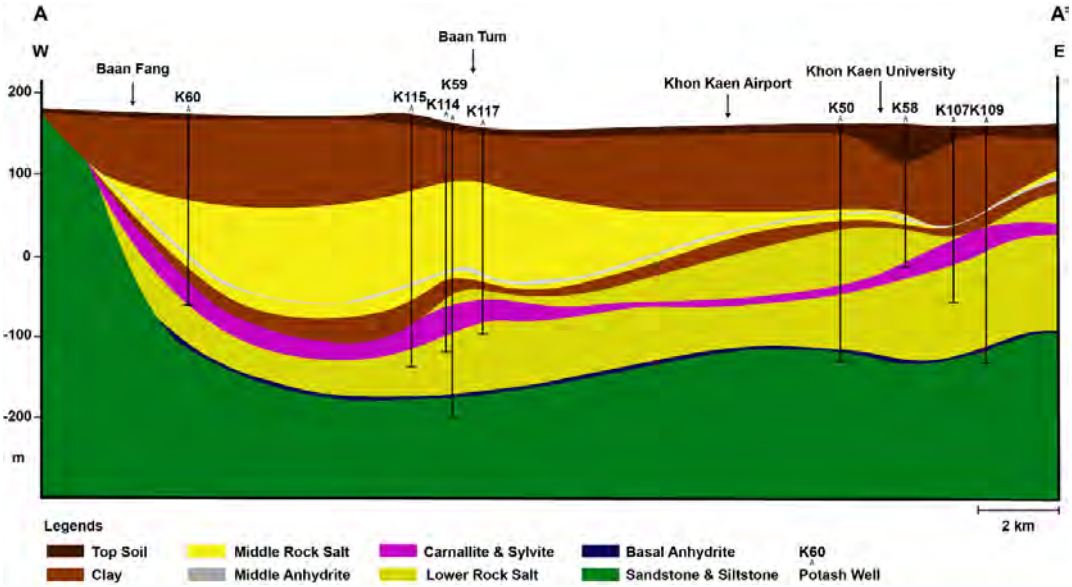

Figure 3. Cross section showing characteristic of subsurface rock salt

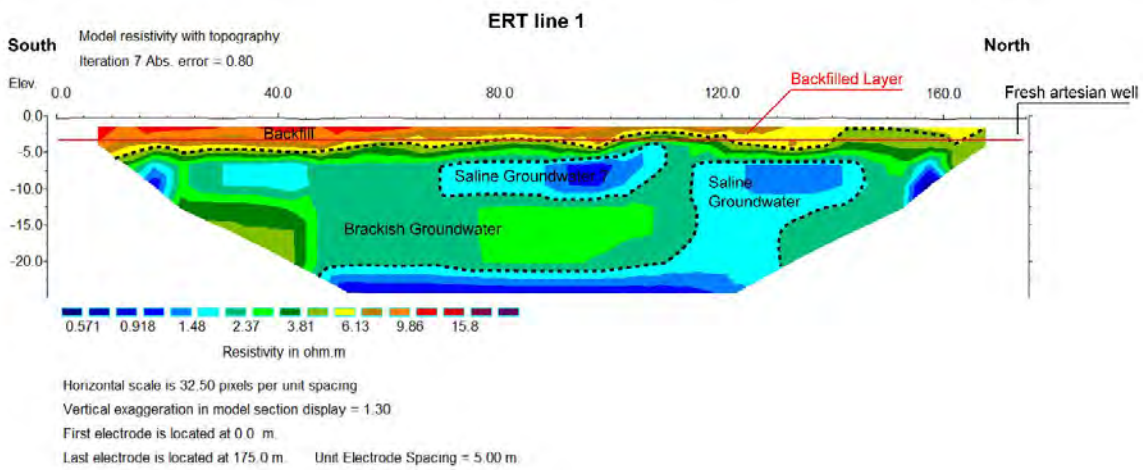

Figure 4. Inversion image and interpretation of line 1

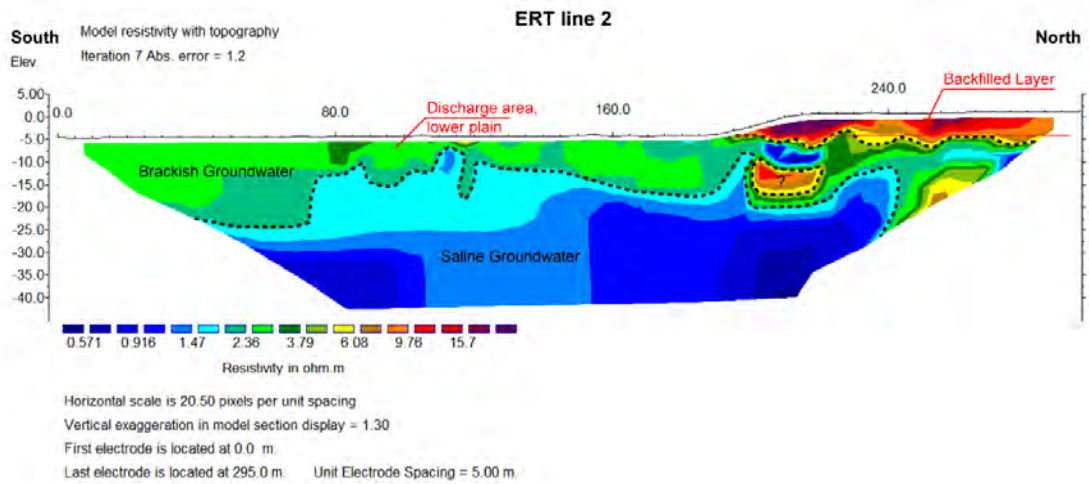

Figure 5. Inversion image and interpretation of line 2

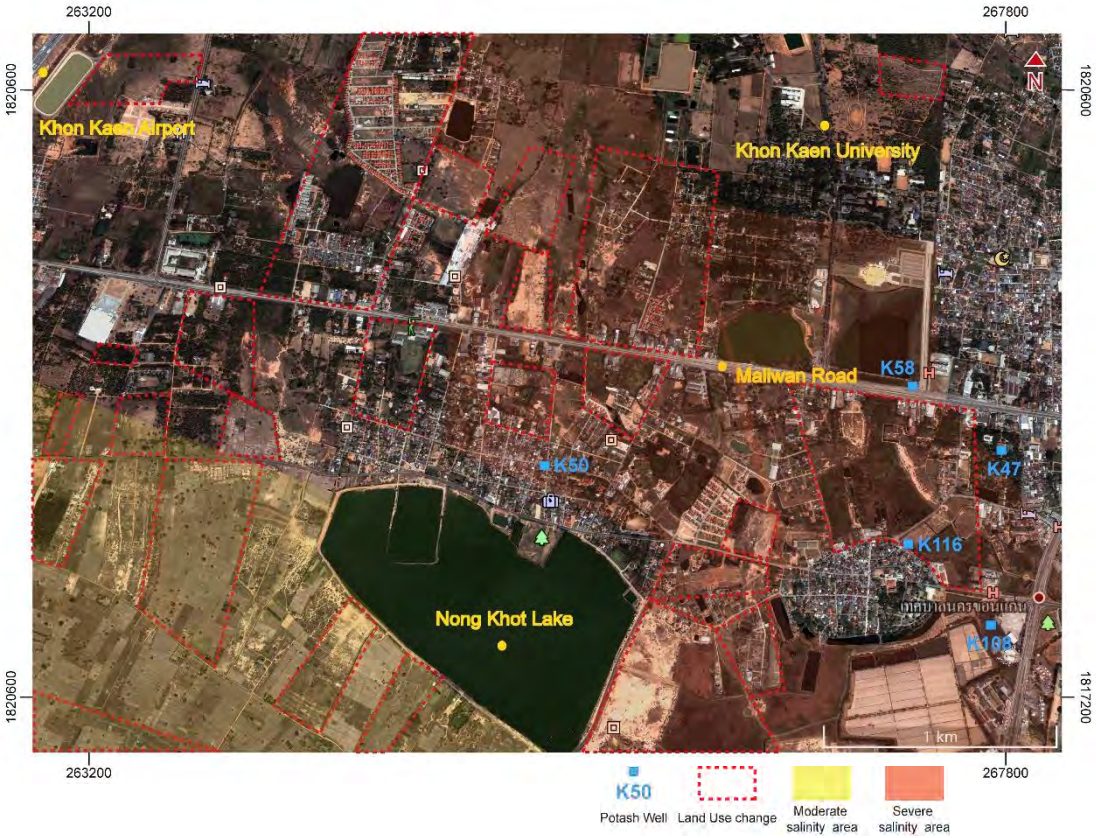

Figure 6. Satellite imagery taken in 2002 of study area with zone of severe salinity

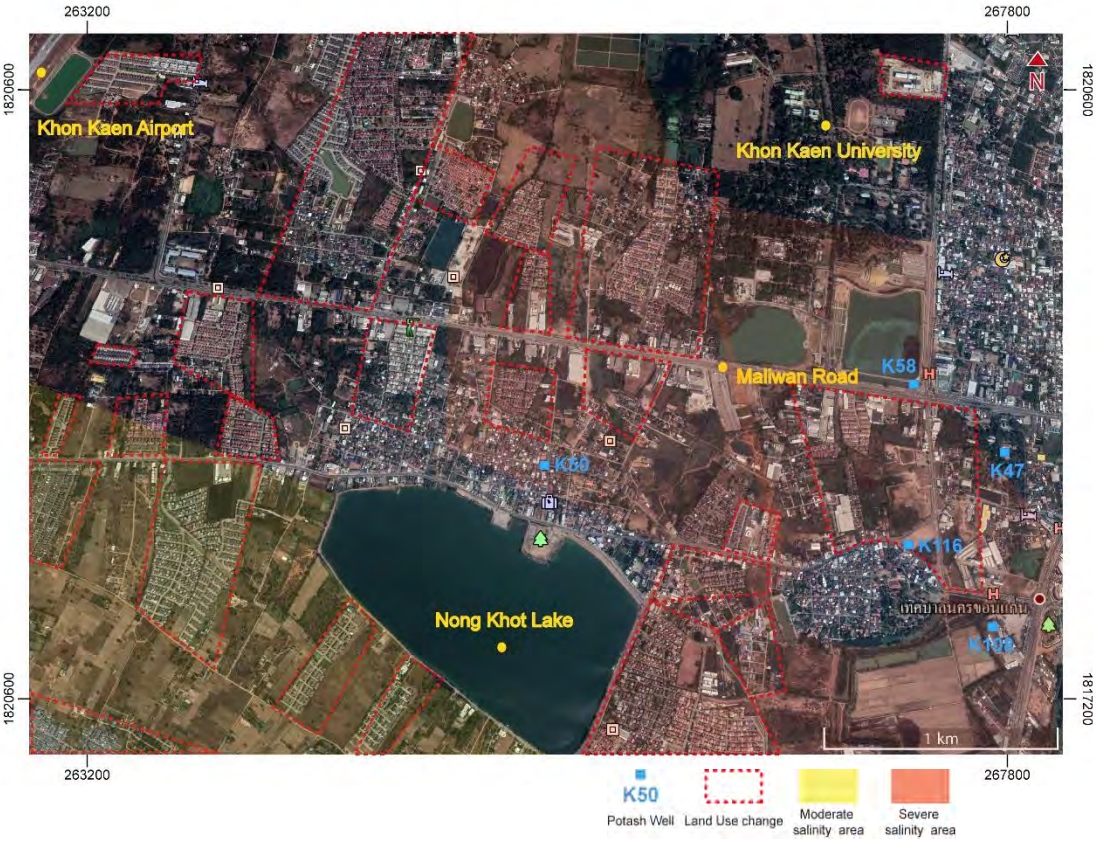

Figure 7. Satellite imagery taken in 2018 of study area with zone of severe salinity

1.3 Land use change

Satellite imageries of the study area taken in 2002 and 2018 are shown in Figure 6 and 7, respectively. Urbanization has gradually expanded from 2002 through 2018. Use of earthen berm for construction purposes has been implemented over areas of salt affected soils. Previously empty farm lands have been converted to residential areas and community marketplaces. Consequently, building foundations were constructed on the earthen berm and soaked in saline groundwater. Human activities such as deforestation in upland regions and poor soil management strategies can have likely also exacerbated soil salinity problems.

2. Impacts

Concrete structures have been built over the berm in saline soil areas, and periodic wetting of the concrete causes rising damp, where the saline groundwater is drawn into the brick or cement by capillary action. As the building materials undergo periodic wetting and drying cycles, salt crystals often grow within the confined pore spaces, as shown in Figure 8. In severe cases, these crystals can cause deterioration of the brick and concrete and can result in cracked bricks or mortar and concrete turning to dust.

Figure 8. Damage of bricks and mortar caused by salinity

6. Conclusions

Urban salinity in Khon Kaen City is caused by (1) geology due to existing rock salt in the subsurface, (2) hydrogeology due to migration of dissolved salt in groundwater controlled by fluctuations in the water table and pathways defined by subsurface geological structures and fractures, and (3) land use change from agricultural areas to residential areas. These contribute salinity and cause concrete structure deterioration.

7. Acknowledgements

This work was supported by Research fund for supporting lecturer to admit high potential student to study and research on his expert program year 2018, Graduated School, Khon Kaen University.

8. References

Arjwech, R., Everett, M. (2017). The Relationship between Geological Factors and the Distribution of Saline Soil; a case study around Khon Kaen University, Thailand. Songklanakarin Journal of Science and Technology (In press).

Arjwech, R., Wannakao, P., Archwichai, L., and Wannakao, L. (2014). The Relationship between Geological Structures and the Distribution of Saline Soil in Downstream Impacted Area of Ubonratana Dam, Khon Kaen Province. KKU Research Journal, 19(6), 834-842.

Arjwech, R., Evereet, M., and Wannakao, P. (2018). Geological Factors Controlling the Distribution of Saline Soil in Khon Kaen Basin, Thailand. The EGU General Assembly 2018, Vienna, Austria.

Collings, A. (2002). Indicators of Urban Salinity. NSW Department of Land and Water Conservation, Sydney, New South Wales.

Department Natural Resources. (2006). Introduction to Urban Salinity. NSW Department of Infrastructure, Planning and Natural Resources, Sydney, New South Wales.

Ryan, M. (2003). Introduction to Urban Salinity. NSW Department of Infrastructure, Planning and Natural Resources, Sydney, New South Wales.

Proceedings of the Second International Symposium on Geoscience Resources and Environments of Asian Terranes (GREAT 2018)
19 - 23 November 2018 Bangkok, Thailand

Mapping of shallow rock salt using seismic refraction and 2D electrical resistivity topmography methods at Borabue, Maha Sarakham, Thailand.

Rungroj Arjwech[1]*, Thunyatorn Sarntima[1] and Mark E. Everett[2]

1 Department of Geotechnology, Faculty of Technology, Khon Kaen University, THAILAND

2 Department of Geology and Geophysics, Texas A&M University, College Station, Texas, USA

* Corresponding author email: rungroj@kku.ac.th

Abstract

Natural swamps and lakes in the northeast of Thailand show evidence of rock salt dissolution. A knowledge of the depths and the structures of the rock salt would be useful to achieve a better understanding of the impact of its dissolution on the environment and to facilitate effective land management strategies. Geophysical methods can provide key subsurface information. Three seismic refraction profiles and one electrical resistivity tomography (ERT) profile were carried out at Nong Bo reservoirs in the salt-affected Borabue district of Maha Sarakham province. The seismic results indicate the top of shallow rock salt beneath Nong Bo reservoir by a diagnostic zone of high P-wave velocity >3,400 m/s at depths >20 m. The ERT investigation shows electrical resistivity values 9 ohm.m at similar depths, indicative also of shallow rock salt. Zones interpreted to be saline groundwater are electrically conductive, identified by electrical resistivity values 5 ohm.m in the ERT images. The combined seismic-ERT interpretation suggests that shallow rock salt lies beneath the reservoir in the Borabue district.

Key words: seismic refraction survey, electrical resistivity tomography, shallow rock salt.

1. Introduction

The ultimate cause of soil salinization in northeast Thailand is the presence of rock salt in the shallow subsurface. While the Maha Sarakham evaporite-bearing formation (Yumuang et al., 1986) is widely distributed at ~100-300 m depths (Satarugsa et al., 2005; Arjwech et al., 2014) over much of the Khorat basin of northeast Thailand, it can become readily mobilized (Warren, 1989). The salt can flow upward to form domes, pedestals, and elongated salt walls, canopies, and other

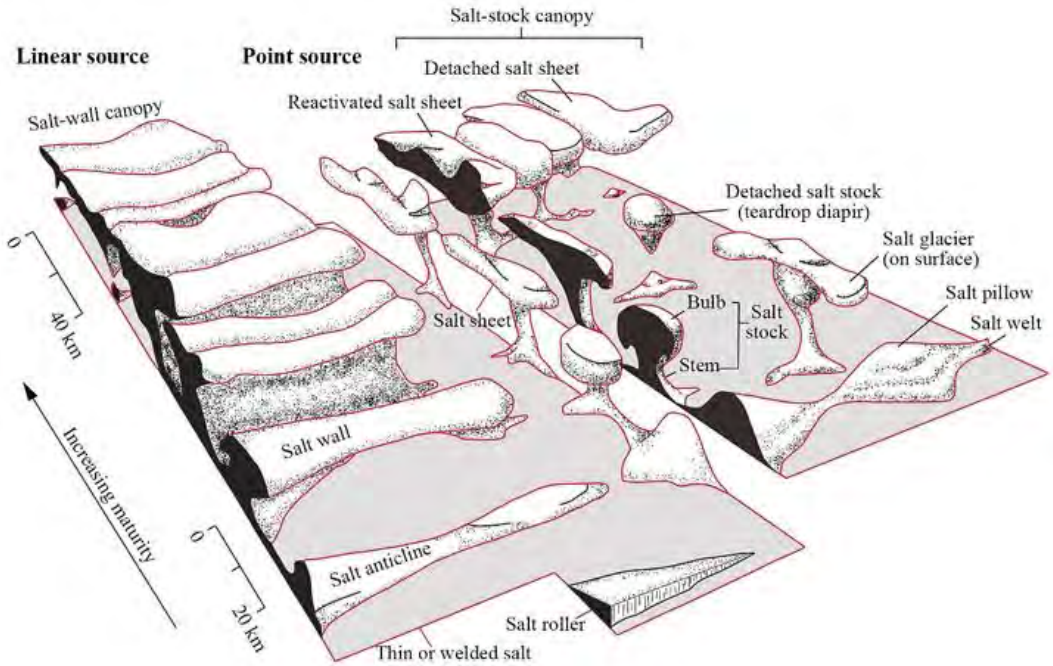

Figure 1. Types of rock salt structures developed from linear sources and point sources (Hudec and Jackson, 2007).

discordant bodies of various geometries (Hudec and Jackson 2007; see also Figure 1). Supajanya et al. (1 9 9 2) has recognized numerous shallow salt domes across northeast Thailand by their surface topographic expressions.

Geophysical surveys can be designed to achieve a specified penetration depth over wide areas at low cost. Herein electrical resistivity tomography (ERT) and seismic refraction ground-based geophysical efforts were used to determine shallow salt body in the Borabue district, Maha Sarakham, northeast Thailand. The geophysical results, analyzed in conjunction with borehole data, provide insight into the causation of soil salinization and saline groundwater in this salt-affected area.

2. Study area

Nong Bo reservoir, shown in Figure 2 , is located in Borabue district, Maha Sarakham province. It is naturally formed by the collapse of a shallow salt dome into a sinkhole due to dissolution of the salt by groundwater. The primary accumulation of saline soil is in direct correspondence with the existence of rock salt that belongs to the lower salt layer of the Maha Sarakham formation, whcih is widely distributed at various depths across northeast Thailand (DMR 2005).

Due to differential loading that was likely generated by regional compressive tectonic forces during the Cretaceous or Tertiary periods (e.g. Lovatt Smith et al., 1996; Morley 2012), the lower layer of rock salt from the Maha Sarakham formation intruded

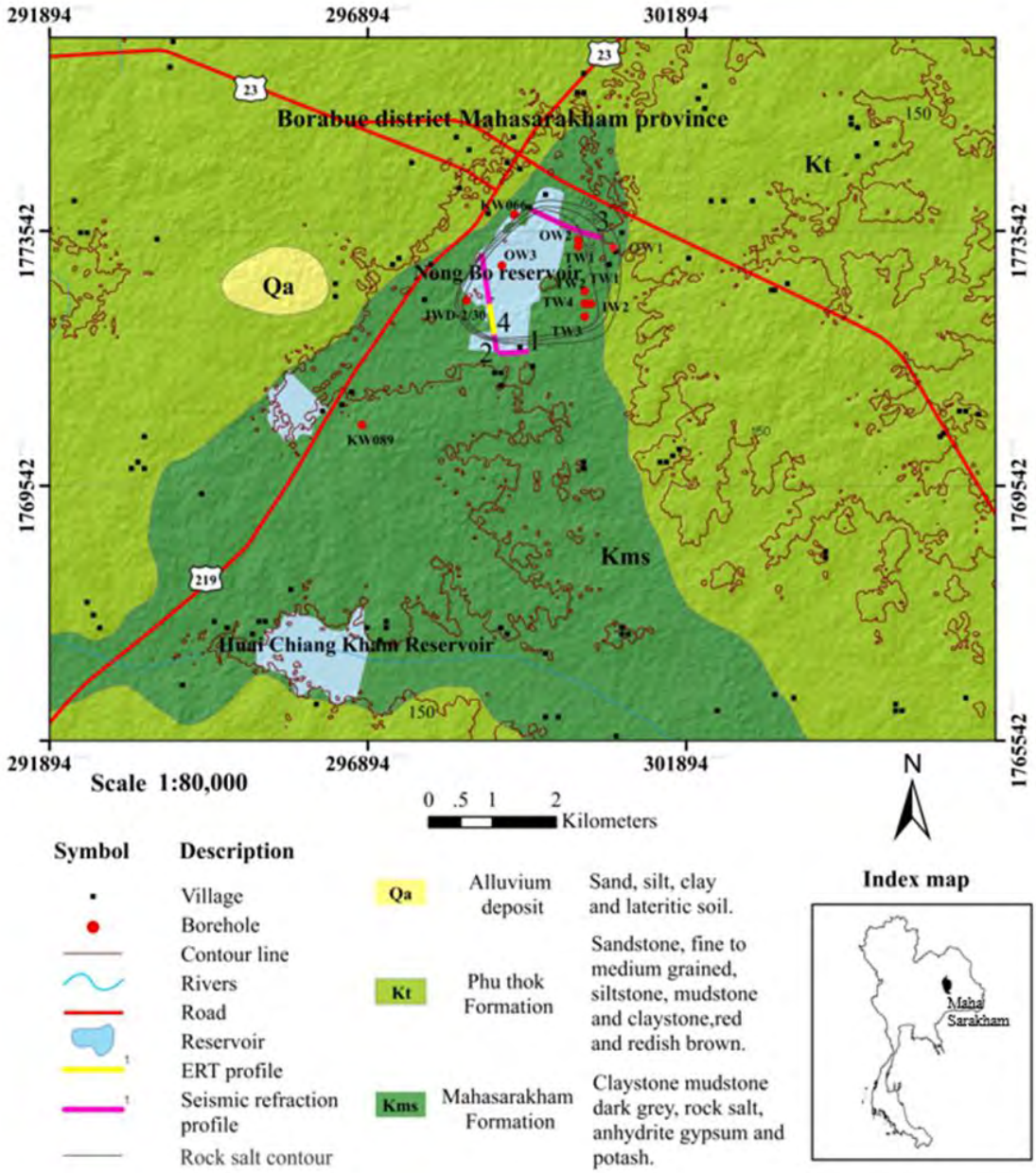

Figure 2. Geological map of the study area, Borabue district, Maha Sarakham province (modified from DMR, 2009) showing location of study area and seismic and ERT measurement profiles.

upward through the overlying clastic Phu Tok formation. The regional-scale geometry of the salt intrusion, whether it is in the form of isolated domes or else a continuous, elongate salt wall or canopy, is not known.

3. Methodology

The seismic refraction and electrical resistivity tomography (ERT) methods were used in this study to map the shallow salt distribution in the Borabue district. The seismic refraction measurements were

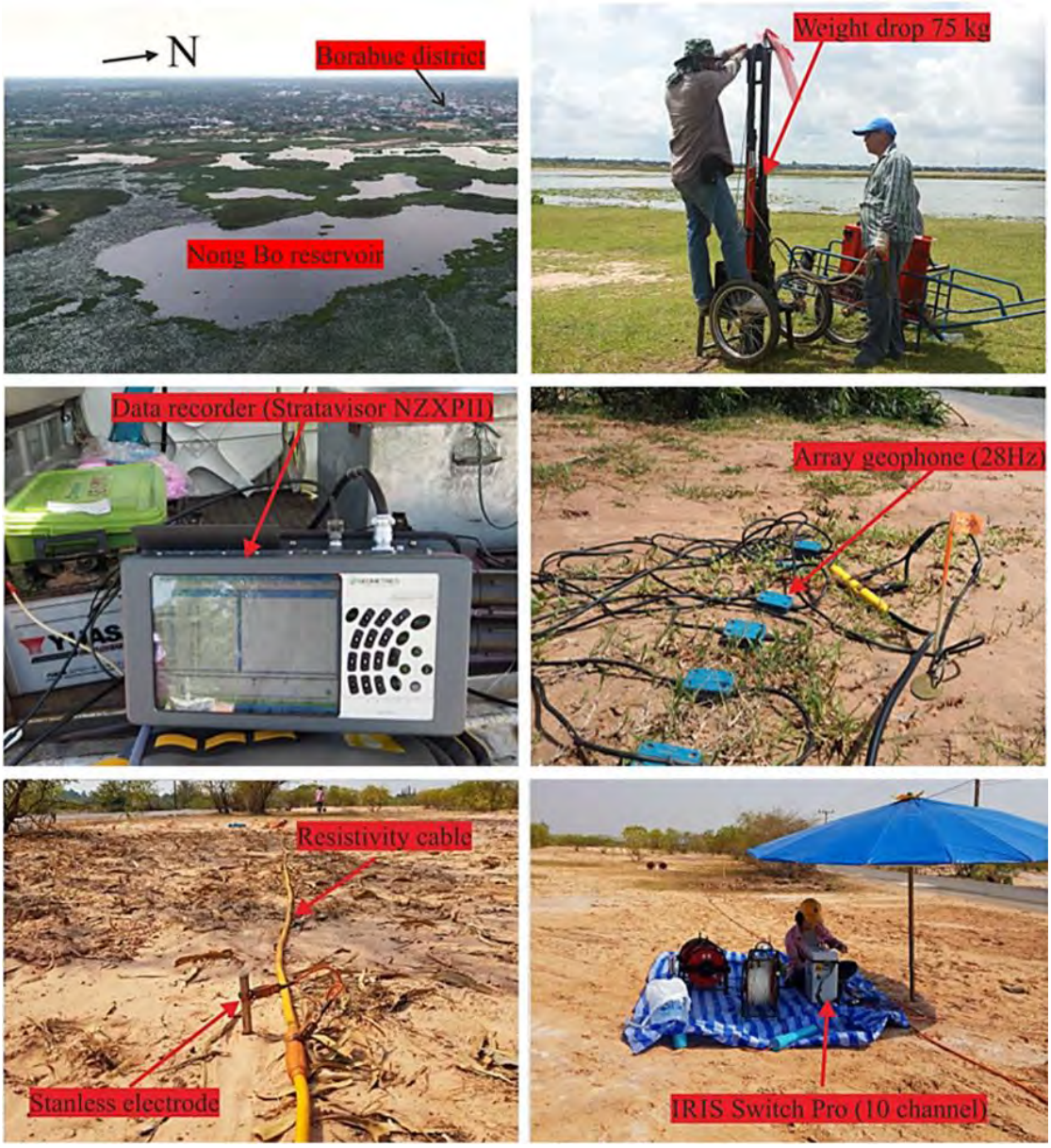

Figure 3. Some representative photographs of sudy area, equipment and field deployment.

collected along three lines (labeled 1-3) using the 48-channel Geometric StrataVisor NZXPII seismograph. A 75-kg accelerated weight drop was used as the source, with the resultant signals recorded by an array of geophones at 10 m spacing. The ERT data were collected one lines (labeled 5) using the Syscal Pro multi-electrode imaging system with internal switchbox and an array of 96 steel electrodes. The dipole-dipole array configuration was used with electrode spacing 5 m. The locations of the seismic refraction and ERT survey lines (Figure 2) were selected according to the available site accessibility in the vicinity of the Nong Bo reservoir. Some representative photographs of the field deployment are shown in Figure 3.

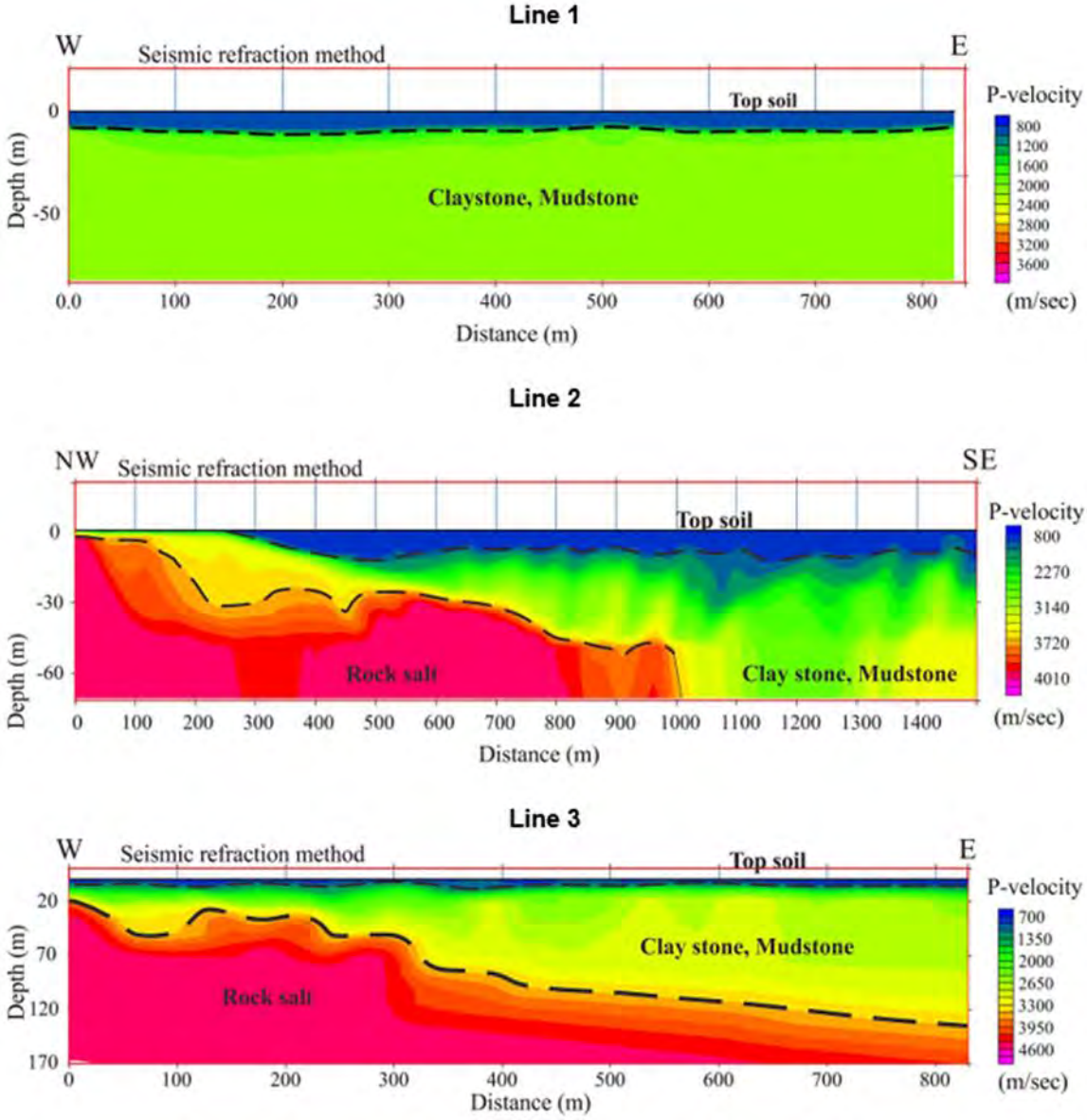

Figure 4. Interpretation of the velocity sections of seismic refraction line 1, 2, and 3.

4. Results

The refraction tomograms constructed from the seismic data acquired along lines 1, 2 and 3 are shown in Figures 4 a, 4b and 4 c, respectively. The P-wave information contained in the tomograms is calibrated with information from the nearby boreholes. It is convenient, for the sake of providing a simple geological interpretation, to zonate the tomograms based on P-wave velocity ranges. Zone (1) is defined as regions within which wave velocity is very low, 400-800 m/s. Such low values are indicative of the weathered overburden that is found at the surface to about 20 m depth. Zone (2) is defined as regions within which wave velocity lies between 1400-3400 m/s. Such intermediate values are supposed to be due to the presence

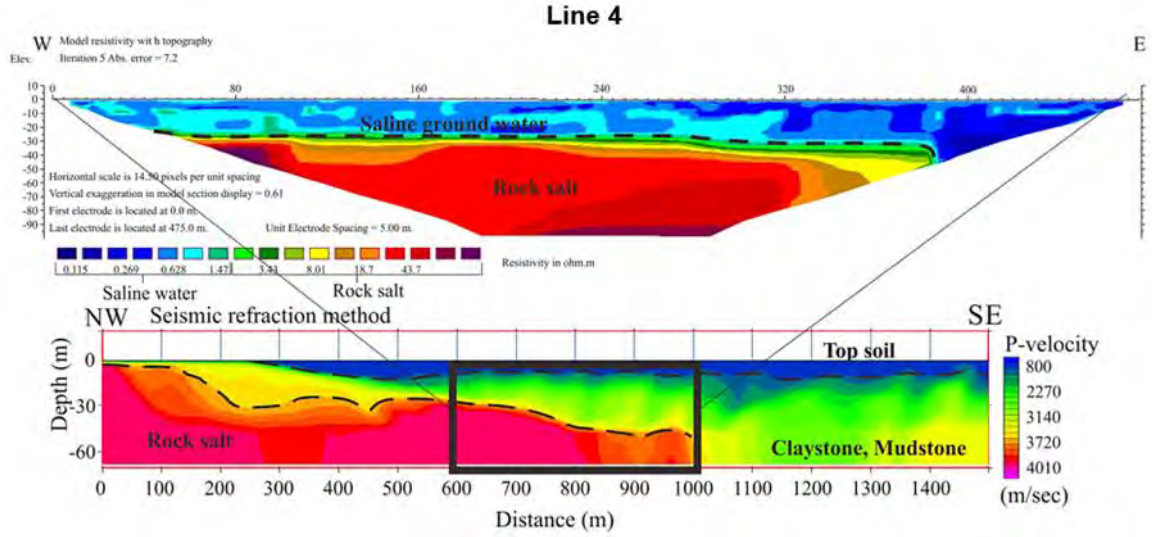

Figure 5 Interpretation of the geoelectrical sections of the ERT line 4 and seismic refraction line 2.

of claystone and/or mudstones. Zone (3) is defined by very high wave velocities >3,400 m/s. Such values are interpreted as due to the presence of rock salt.

The ERT tomogram from line 4 is shown in Figure 5. This tomogram may be directly compared with the seismic refraction tomogram from line 1 (Figure 4a) since the former is co-located with the central part of the latter (see map, Figure 2). On the resistivity tomogram, a zone of high resistivity >40 Ωm (in red) underlies a surficial low-resistivity layer (in blue). The low-resistivity layer is likely the weathered overburden that is saturated, or partially saturated, with saline groundwater. The top of the high-resistivity zone occurs at depth ~25-30 m. This would be consistent with the seismic imaging of rock salt on the line-1 tomogram

5. Discussion

The results of the seismic refraction and ERT surveys carried out at Nong Bo reservoir are consistent with the lithological logs and previous studies that have suggested the existence of shallow salt dome whose top is ~20 m below the surface. However, it appears that the shallow salt dome is restricted to the immediate vicinity of the Nong Bo reservoir (Figure 1). This information about the subsurface distribution of shallow salt is useful to land management efforts since the formation of sinkholes and other environmental effects such as salinization are normally coupled with the presence of shallow salt.

6. Conclusion

Seismic and ERT surveys were successfully applied to delineate the geometry of the shallow

rock salt in certain parts of the Borabue district permitted by site accessibility and time constraints. The seismic refraction tomograms provide sharp contrasts between rock salt and the surrounding overburden, claystone and mudstones. However, the interpretation of the ERT tomograms proved more subtle. The imaged resistivity of the rock salt appeared to be unrealistically low compared to published values for dry rock salt. We hypothesize that the very high conductivity of the overlying saline groundwater has minimized the electric current that passes through the layer of rock salt. This causes the ERT method to under-estimate the resistivity of the rock salt since its sharp transition with the overlying saline groundwater zone is not resolved.

7. Acknowledgments

This work was financially supported by Department of Geotechnology, Faculty of Technology and Graduate School, Khon Kean University.

8. References

Arjwech R., Wanakao P., Archwichai L. and Wanakao L. 2014. The relationship between geological structures and the distribution of saline soil in downstream impacted area of Ubon Ratana dam, Khon Kaen province (in Thai). Asia-Pacific J. Sci. Technol. 19, 834-842.

DMR (Department of Mineral Resources). 2005. The study on an effect of geological factor to saline soil distribution in Northeast of Thailand; 2004 (Full Report of the Study on Geology and Hydrogeology). Ministry of Natural Resources and Environment.

DMR (Department of Mineral Resources). 2009. 12:56 Geological map of Changwat Maha Sarakham Scale 1: 250,000. Ministry of Natural Resources and Environment.

Hudec M. R. and M.P.A. Jackson. 2007. Terra infirma; Understanding salt tectonics. Earth-Sci. Rev. 82, 1-28.

Lovatt Smith P.F., R.B. Stokes, C. Bristow and A. Carter. 1996. Mid-Cretaceous inversion in the Northern Khorat Plateau of Lao PDR and Thailand, in Hall, R. and Blundell, D. (eds) Tectonic Evolution of Southeast Asia, Geol. Soc. Sp. Publ. 106, 233-247.

Morley C.K. 2012. Late Cretaceous–Early Palaeogene tectonic development of SE Asia. Earth-Science Rev. 115, 37–75.

Satarugsa P., Youngmee W. and Meesawat S. 2005. New regional boundary of Maha Sarakham formation in northeastern Thailand: results from 2D seismic mapping, Proc. GEO-INDO 2005, Khon Kaen, Thailand.

Supajanya T., Vichapan K. and Sri-israporn S. 1992. Surface expression of shallow salt dome in northeast Thailand. Proc. Nat. Conf. Geol. Resources for Thailand, Bangkok.

Warren J.K. 1989. Evaporite Sedimentology. Prentice Hall, New Jersey, 285 pp.

Yumuang S., Khantaprab C. and Aiyag M.T. 1986. The evaporite deposits in Baronet Narong area, Northeastern Thailand. Geol. Soc. Malaysia Bull. 20, 249-267.

Proceedings of the Second International Symposium on Geoscience Resources and Environments of Asian Terranes (GREAT 2018)
19 - 23 November 2018 Bangkok, Thailand

Utilization of pumice aggregate blended with serpentinite and palm oil fuel clinker in lightweight mortar

Benjawan Prajaklertwittaya[1] and Danupon Tonnayopas[1]*

1 Department of Mining and Materials Engineering, Prince of Songkla University

* Corresponding author email: danupon.t@psu.ac.th Tel. 083-7150978

Abstract

Lightweight mortar containing pumice aggregate (PA) blended with serpentinite and palm oil fuel clinker (POFC) was investigated. Cubic specimen was carried out in size of 50×50×50 mm. Ground serpentinite (GS) and POFC were replaced partially ordinary Portland cement (OPC), type 1 in proportion of 0%, 10%, 20% and 30wt.% with water to binder ratio (w/b) performed of 0.35. Whole specimens were cured in ambient temperature (temperature of 25-28 ^{o}C and relative humidity of 75-80%) for 3, 7, 28, 56 and 90 days. Assessment of mortar specimens including bulk density, water losing, dimensional stability, electrical resistance and compressive strength were determined. Microstructure were analyzed via scanning electron microscope (SEM). Testing results revealed that mortar specimen was blended with 10% POFC provided highest compressive strength value of 17 MPa at curing ages 28 days which met threshold as structural lightweight aggregate concrete. Moreover, mortar specimens mixed with GS had highest dimensional stability value and can considered as insulating lightweight aggregate concrete. SEM can be observed mineral phases embedded matrix of portlandite, ettringite, brucite and shape like a honeycomb of C-S-H. It was indicated that GS and POFC can be supplementary pozzolanic materials.

Key words: Pumice, Serpentinite, Palm oil fuel clinker, Lightweight mortar, Pozzolanic material.

1. Introduction

Nowadays, the price of crude oil is continuous rising. Using oil from agriculture as alternative fuel instead crude oil and it seems suitable for agricultural countries like Thailand. Oil palm plantation is a well-known industrial agriculture in southern Thailand and usually produced as biodiesel [1]. Mesocarp palm fiber is waste from oil extraction process which is recycled as fuel for electrical generation using in palm oil factories and by produced was a palm oil fuel clinker (POFC). Most factories often used POFC for landfill that affected to environmental problems. Silicon dioxide is mainly component of POFC that supplied mechanical performance to concrete [2,3].

Serpentinite is an asbestos rock which altered from serpentine composed mainly of silicon dioxide and magnesium dioxide. It is often applied to produce thermal resistance material due to it has high heat-resistance property [4].

Silica or silicon dioxide (SiO_2) reacted with calcium hydroxide ($Ca(OH)_2$), product of hydration activity, formed calcium silicate hydrate (C-S-H) that developed strength and physical properties of concrete [5] such as, decreased porosity [6]. The POFC characterization has been high silica content and amorphous material. It is high potential supplementary pozzolanic material. [7]

Pumice is a volcanic rock and highly porous so gain pumice has low density [8]. Moreover, it composed of high silica element. So lightweight aggregate is interesting alternative to use for construction material, especially in concrete [9]. Lightweight concrete or mortar can be transport easily and saving energy consumption.

Thus, utilization of pumice aggregate blended with serpentinite and POFC in lightweight mortar is interesting alternative. It is not only reduced environmental problem but also added value for POFC and serpentinite. Furthermore, reduced cost of construction and increased the rapid of building due to the favorable composition and transportation.

The chief goal of this research is to study the influence of using pumice as lightweight aggregate and blended serpentinite and POFC with ordinary Portland cement in regard to physico-mechanical properties and microstructure of lightweight mortar.

2. Experimental program

2.1 Material used

Ordinary Portland cement (TIS Type 1) was used in this research. POFC is collected from heating boiler of the Palm Pattana Southern Border Co., Ltd. It is situated in Pattani province (Fig 1.).

Fig 1. Palm oil fuel clinker from waste of power generator at palm oil mill.

Serpentinite sample supported by the Asia Mineral Processing Co., Ltd. from an open pit mining at Narathiwat province, Thailand (Fig 2). POFC and serpentinite lump samples were crushed with rotary crusher, ball mill and grounded with jar mill for reducing size then sieved pass through 45 μm. For pumice aggregate is derived from Indonesia under commercial agent. Pumice aggregate was sieved pass through 4.75 mm and retaining 150 micron assign as fine aggregate.

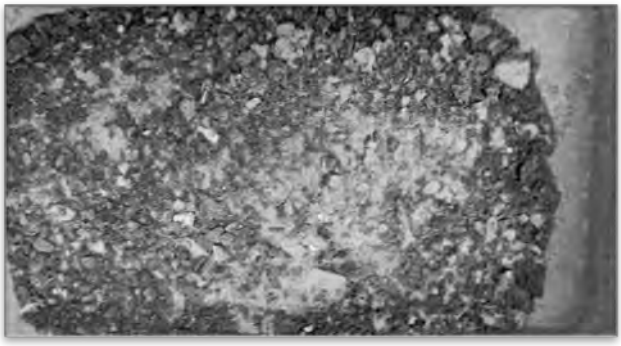

Fig 2. Serpentinite sample is derived from Narathiwat

2.2 Sample preparation

Ordinary Portland cement (OPC), type 1 was replaced partially with POFC and GS at proportion of 0, 10, 20 and 30wt.%. All mixtures of POFC, GS and OPC were decreased size by ball mill. The pre-wet pumice aggregate was soaked in water for 6 hours before batching. Then, mopped water from pre-wet pumice with clean textile for 1 hour. Pumice has the capacity of water absorption about 40%. In this ingredient is used pumice as fine aggregate of 100 kg/m^3. Proportion of water to binder (w/b) is 0.35 and constant throughout this study. List of mixing categories is shown in Table 1. Casted mortar cube specimen was in size of 50×50×50 mm. Whole specimens were cured in ambient temperature (temperature of 25-28 ^{o}C and relative humidity of 75-80%) for 3, 7, 28, 56 and 90 days.

Table 1. Mortar mixing design in this study.

Mix	Code	Content (kg/m^3)		
		OPC	POFC	GS
OPC	A	250	-	-
POFC10	B	225	25	-
POFC20	C	200	50	-
POFC30	D	175	75	-
GS10	E	225	-	25
GS20	F	200	-	50
GS30	G	175	-	75
POFC5GS5	H	225	12.25	12.25
POFC10GS10	I	200	25	25
POFC15GS15	J	175	37.5	37.5

Note: OPC = Ordinary Portland cement, POFC= Palm oil fuel clinker, GS = Grounded serpentinite

2.3 Characterization materials and testing methods

Cured specimens were investigated including bulk density, water losing, dimensional stability, electrical resistivity (ER) and compressive strength. The compressive strength was tested with compression testing machine (TTR-080G capacity 1500 kN) according to ASTM C109 [10]. The ER was measured with a Fluke True-rms multimeter. Chemical compositions of POFC and GS were analyzed via X-ray fluorescence spectrometer (XRF) (Zetium Panalytical) which is shown in Table 2.

Table 2. Chemical analysis of POFC and GS by XRF.

Chemicalcomposition (%)	POFC	GS
Silicon dioxide (SiO_2)	53.6	37.9
Aluminium oxide (Al_2O_3)	0.9	2.1
Ferric oxide (Fe_2O_3)	1.9	8.0
Magnesium oxide (MgO)	7.1	36.6
Calcium oxide (CaO)	15.2	0.2
Potassium oxide (K_2O)	9.9	-
Titanium dioxide (TiO_2)	-	0.1
Sulfur trioxide (SO_3)	0.5	0.2

Microstructure was also analysis on dominant specimens using scanning electron microscope (SEM) (XMAX – Quanta400)

2.3.1 Bulk density

The bulk density (D) of mortar specimen is calculated from the mass of a unit volume of the specimen, can be expressed in equation (1).

$$D = M/V \quad (1)$$

Where M is weight and V is volume

2.3.2 Water losing

The percentage of the estimated water content difference between before and after curing periods of mortar specimens, computation given in equation (2)

$$W_t = ((W_b - W_a)/ W_b) \times 100 \quad (2)$$

where W_t is the percentage of water losing, W_b and W_a is weight of mortar specimens before and after curing periods, respectively.

2.3.3 Electrical resistivity

Electrical resistivity (ER) that measuring electrical resistance value passed from onside a body through the other side, relationship can be determined as equation (4)

$$ER = rA/d \quad (3)$$

where r is electrical resistance in ohm, A is the area and d is the length of the electricity flowing through specimen.

2.3.4 Specific strength

Specific strength (SS) is defined as a proportion between compressive strength to its bulk density of the mortar specimens at certain age, can be reformed in equation (4).

$$SS = F/D \quad (4)$$

Where F is compressive strength value in MPa and D is bulk density value in kg/m^3 of the same specimen.

3. Result and discussion

3.1 Bulk density

Bulk density of mortar specimens after long-term curing found that its bulk density decreasing compared before. Owing to mortar specimens have lost weight due to water evaporation (Fig 3.)

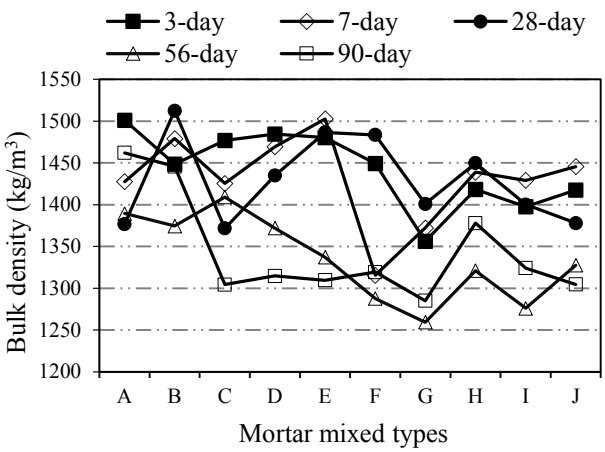

Fig 3. Bulk density of mortar specimens after curing at difference ages.

3.2 Water losing

When curing duration of mortar specimens increased given water losing increased too Fig 4. Besides, POFC and volumetric after curing and before curing, respectively. It can be noticed water losing value had closely relationship with bulk density value.

GS in mortar specimen effects on water losing properties. Increasing amount of POFC and GS contents induced water losing increased. Mortar specimens blended with GS have highest water losing value. However, mortar specimen with 10% POFC at curing age of 28 days having lowest water losing value of 1.137%. It could be attributed reducing porosity due to pozzolanic and hydration activity. However, more excessive percentage of POFC resulted instead of increasing pore of mortar specimens.

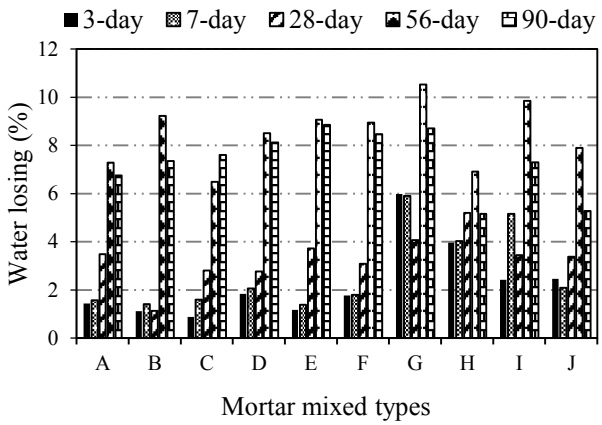

Figure 4 Water losing of mortar specimens at difference ages.

3.3 Dimensional stability

Each curing periods of mortar specimen occurred shrink and expand differently. Increase in POFC content in cured mortar expand. Moreover, the experimental displayed that mortar specimens with 10% GS has lowest volumetric changing value is 0.045%, 0.044% and -0.223% (plus is expansion and minus is shrinkage) at curing ages 28, 56 and 90 days, respectively (Fig 5). Comparison between volumetric changing values

of GS specimens provided lower than POFC mortar specimen. It considered these contributions from magnesium in form M-S-H gel. Minimizing the dimensional stability of mortar specimens were depended on cementitious material types and content amounts and mixture design (Table 1).

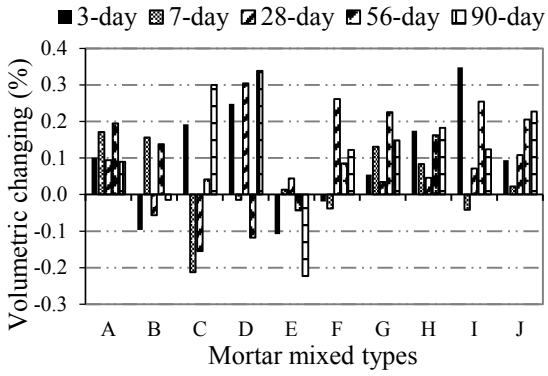

Figure 5 Dimensional stability of mortar specimens at difference ages.

3.4 Electrical resistivity

Experimental measuring on electrical resistance of control and 10% OPFC mortar specimens at age of 28 days is 16.38 Ω.cm. ER value increased according to increment of long-term curing ages and depicted in Figure 6. It can be noted water losing had also relationship with electrical resistivity.

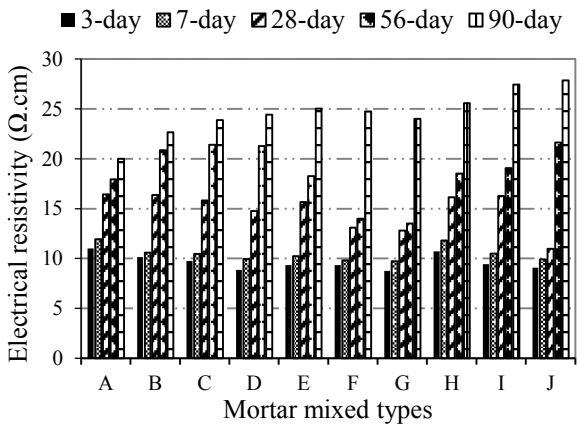

Figure 6 Electrical resistivity of mortar specimens at difference ages

3.5 Compressive strength

At early ages of mortar specimens blended with POFC and GS found their compressive strength values lower than control mortar (Figure 7). The compressive strength value slightly increased according to curing age increasing. Because of POFC composition can be formed hydration and pozzolanic material. This result is the decreasing of porosity caused lower water losing value (Figure 4). Therefore, mortar specimens have enough water for pozzolanic and hydration activity. Testing results revealed that optimizing formulation of mortar specimen was blended with 10% POFC provided highest compressive strength value of 17.48 MPa and 18.05 MPa at curing ages of 28 and 56 days, respectively. Nevertheless, replacing partially OPC in proportion of higher than 10% POFC and 10% GS contents gain decreasing strength. Effect of high GS contained in mortar specimens on dimensional stability (Fig 5), electrical resistivity (Fig 6) and compressive strength values (Fig 7). However, mortar specimen combining 5% POFC and 5%GS obtained gently lower of 28-day compressive strength of 16.22 MPa (Fig 8.). Specific strength derived from comparing between compressive strength and bulk density values. It indicated 10% POFC seem highest at curing ages of 28 and 56 days (0.012 and 0.013 m^2/s^2, respectively). It met threshold as

structural lightweight aggregate concrete [11]. On the other hand, mortar specimens were blended with GS can be characterized as insulating lightweight aggregate concrete according to ASTM C332 [12].

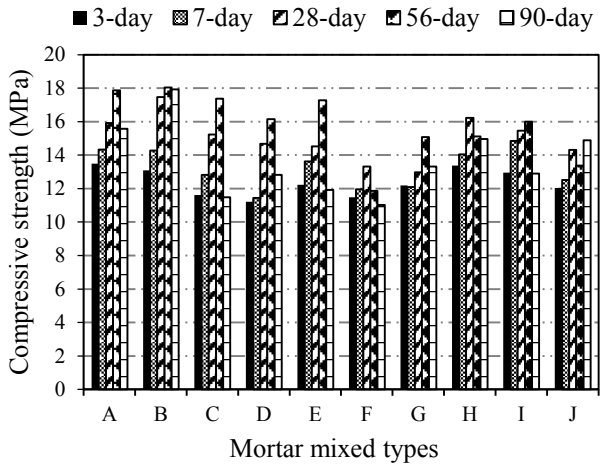

Fig 7. Compressive strength of mortar specimens at difference ages.

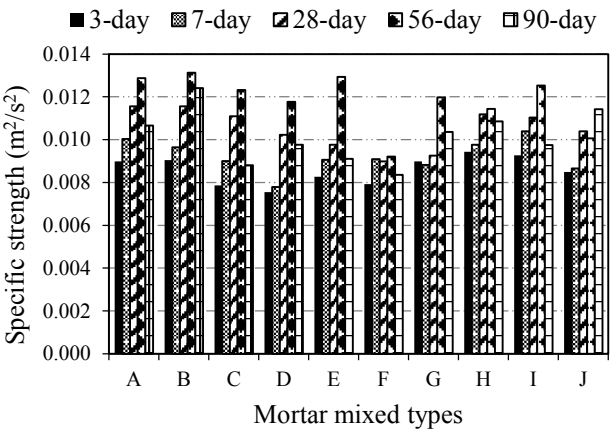

Fig 8. Specific strength of mortar specimens at difference ages

3.6 Microstructure analysis

Microstructure of dominant POFC mortar specimens via scanning electron microscope observed mineral phases of calcite, portlandite, ettringite and calcium silicate hydrate (C-S-H).

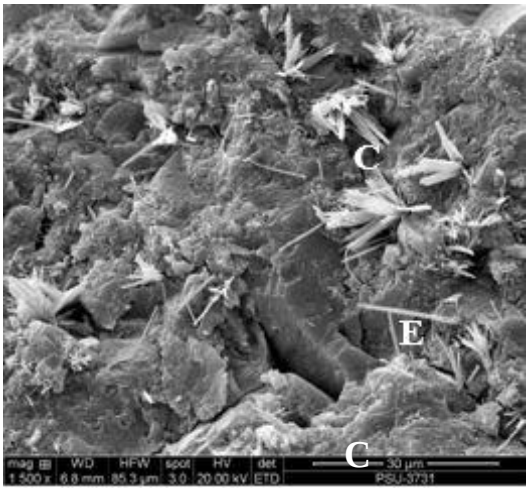

Fig 9. SEM microphotograph of ettringite (E) and calcite (C) in 10% POFC mortar specimen.

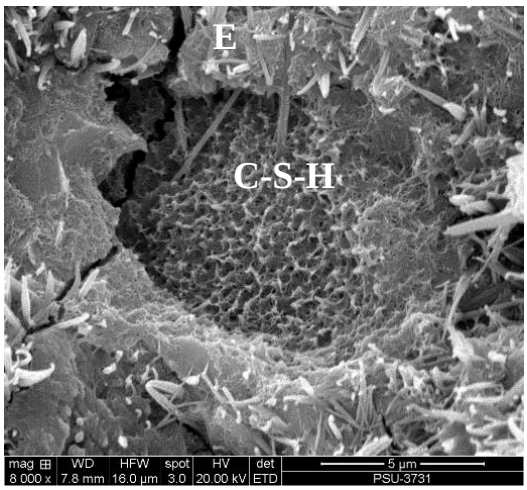

Fig 10. SEM microphotograph shown honeycomb C-S-H and ettringite in 5%POFC and 5%GS mortar specimen.

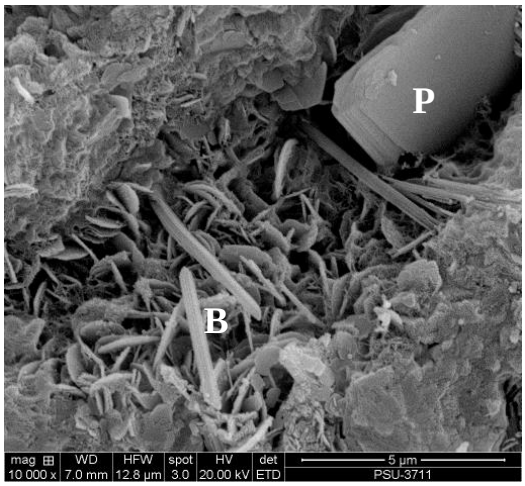

Fig 11. SEM microphotograph of portlandite (P), brucite (B) in 10 % GS mortar specimen.

Several ettringite and portlandite are occurred in POFC mortar specimens (Fig 9). It may be affected of volumetric changing on expansions. Pozzolanic and hydration activities formed shape like a honeycomb of C-S-H [13] in 10% POFC specimens (Fig 10) which contributed strength and physical properties. But increasing of POFC content decreased compressive strength assumed that this expansion resulted in internal micro-crack of mortar specimens. On the other hand, mortar specimens blended 10% GS occurred portlandite (calcium hydroxide – $Ca(OH)_2$) and brucite (magnesium hydroxide – $Mg(OH)_2$) [14] which is product of hydration activity (Fig 11).

4. Conclusion

In this study, pumice lightweight aggregate mortar blended with GS and POFC can be delineated. The experimental result can be concluded that mortar incorporating with 10% POFC has lowest water losing value and has highest compressive strength value. Besides, mortar specimen blended 10% GS has achieved lowest volumetric changing value. Thus, GS and POFC with appropriate content can be use as supplementary cementitious material. Particularly, GS can be sustained dimensional stability of lightweight aggregate concrete.

5. Acknowledgements

This research was supported raw materials used by the Palm Pattana Southern Border Co., Ltd. and the Asia Mineral Processing Co., Ltd, respectively. And this research was financially supported by Office of the Higher Education, Center of Excellence in Materials Engineering (CEME) and was funded for thesis dissertation funding annual 2017 by PSU Graduate School and a scholarship for Bachelor and Master Program 5 years annual 2017 by Faculty of Engineering, Prince of Songkla University.

6. References

[1] Wangrakdiskul, U., Yodpijit, N. 2015. Trends Analysis and Future of Sustainable Palm Oil in Thailand, *KMUTNB Int J Appl Sci Technol*, 8, 1, 21-32.

[2] Karim, M., Hashim, H., Razak, H. 2016. Thermal activation effect on palm oil clinker properties and their influence on strength development in cement mortar. *Construction and Building Materials,* 125, 670 – 678.

[3] Ranjbar, N., Behnia, A., Alsubari, B., Birgani, P., Jumaat, M. 2016. Durability and mechanical properties of self-compacting concrete incorporating palm

oil fuel ash. *Journal of Cleaner Production*, 112, 723 – 730.

[4] Orlov A., Chernykh. T, 2016. Research of water resistance and heat resistance of magnesium phosphate cements. *Procedia Engineering,* 150, 1623 – 1626.

[5] Chong, J., Sutan, N., Yakub, I., 2012. Characterization of early pozzolanic reaction of calcium hydroxide and calcium silicate hydrate for nanosilica modified cement paste. *UNIMAS e-Journal of civil engineering,* 4, 3, 6 – 10.

[6] Zeyad, A., Johari, M., Tayeh, B., Yusuf, M., 2017. Pozzolanic reactivity of ultrafine palm oil fuel ash waste on strength and durability performances of high strength concrete. *Journal of Cleaner Production,* 144, 511-522.

[7] Karim, M., Hashim, H., Razak, H. 2016. Assessment of pozzolanic activity of palm oil clinker powder. *Construction and Building Materials*, 127, 335 – 343.

[8] Gqndqz, L., Ugur, I. 2005. The effects of different fine and coarse pumice aggregate/cement ratios on the structural concrete properties without using any admixtures. *Cement and Concrete Research*, 35, 1859 – 1864.

[9] Hawa A. and Tonnayopas D. 2013. Lightweight aggregate concrete blended with rice husk ash and para rubber wood fly ash, The 11th Conference on Mining, Materials and Petroleum Engineering and the 7th International Conference on Earth Resources Technology, Nov. 11-13, Chiang Mai, Thailand, 1-6.

[10] ASTM C109 / C109M-16a, 2016. Standard Test Method for Compressive Strength of Hydraulic Cement Mortars (Using 2-in. or [50-mm] Cube Specimens), ASTM International, West Conshohocken, PA.

[11] ASTM C330/C330M-17a, 2017. Standard Specification for Lightweight Aggregates for Structural Concrete. ASTM International, West Conshohocken, PA.

[12] ASTM C332-17, 2017. Standard Specification for Lightweight Aggregates for Insulating Concrete, ASTM International, West Conshohocken, PA.

[13] Franus, W., Panek, R., Wdowin, M., 2015. SEM investigation of microstructures in hydration products of portland cement. In E.K. Polychroniadis et al. (eds.), *2nd International Multidisciplinary Microscopy and Microanalysis Congress,* Switzerland, P. 105-112

[14] Tonelli, M., Martini, F., Calucci, L., Geppi, M., Borsacchi, S., Ridi, F., 2017. Traditional Portland cement and MgO-based cement: a promising combination. *Physics and Chemistry of the Earth,* 99, 158 – 167.

Proceedings of the Second International Symposium on Geoscience Resources and Environments of Asian Terranes (GREAT 2018)
19 - 23 November 2018 Bangkok, Thailand

AFT age datings of the Mesozoic clastic rocks of the Phu Phan Range, NE Thailand: Constrains for their tectonic exhumation

Apivut Veeravinantanakul[1], Noriko Hasebe[3], Pitsanupong Kanjanapayont[2] and Punya Charusiri[1]*

1 Department of Geology, Chulalongkorn University

2 Basin Analysis and Structural Evolution Special Task Force for Activating Research (BASE STAR), Department of Geology, Faculty of Science, Chulalongkorn University

3 Institute of Nature and Environmental Technology, Kanazawa University

* Corresponding author email: cpunya@chula.ac.th

Abstract

Mesozoic clastic rocks (3,600 m-thick) of the Phu Phan mountain range (PPR), NE Thailand have been investigated for their Apatite Fission Track (AFT) age determination. The prime aim is to decipher the uplift rates of the Khorat region. Therefore, geologic transects have been performed over the PPR area. Results on current and previous fieldwork in conjunction with remote sensing and air-borne magnetic investigations reveal series of anticlinal and synclinal fold structures mainly in the NW-SE trend. These folds have been displaced by NE-SW, short-left lateral strike slip faults. Samples of 21 very fine- to medium-grained silicic clastic rocks have been collected for AFT dating. A total of 120 apatite grains from 6 samples have been discovered to be qualified for AFT dating estimation. The current AFT results and those of the previous studied of the PPR rocks reveal 3 AFT age groups; i.e. 78 to 60 Ma, 55 to 42 Ma, and younger than 37 Ma. The first AFT age group (78 - 60 Ma) has a close similarity with the tectonic movement in response to the NE-SW compressive stress with in the Khorat region, leading to the major deformation structures including the Phu Phan fold structures. Two successive basins have been also formed at this episode. The second episode (55 - 42 Ma) is considered to be the event of the extensive exhumation with in the Khorat region, giving rise to the Khorat Plateau. The last episode (<37 Ma) is marked by minor movement along the NE-SW-trending fault in response to the clockwise rotation of the Indochina block. It should be pointed out that the younger event (23 Ma) from several previous geochronological dates also exist, but not affecting the study area. Our current AFT results and other geochronological dates support the average exhumation rate of the PPR to be ca. 0.0139 mm/yr (or 13.9 m/Ma).

Key words: Apatite fission track dating, Sandstone, Khorat Group, Exhumation, Phu Phan Ranges

Proceedings of the Second International Symposium on Geoscience Resources and Environments of Asian Terranes (GREAT 2018)
19 - 23 November 2018 Bangkok, Thailand

Facies analysis of igneous rocks, alteration patterns and feldspar deposits in Tak Province, Thailand

Boontarika Srithai[1]*, Weerapan Srichan[1], Tanapoom Khositanont[2], Thunyaluck Wongwai[2], Phattranit Sungprasit[1] and Panadda Saokhamkhet[3]

1 Department of Geological Sciences, Chiang Mai University, Chiang Mai, Thailand

2 Department of Groundwater, Bangkok, Thailand

3 Pipatkorn Company Limited, Tak, Thailand

* Corresponding author email: boontarika.s@cmu.ac.th

Abstract

Feldspar deposits at Rom Yen, Boon Bundal and Nam Saeng mines locate in Tambon Wang Prachop, Mueang Tak, Tak Province operated by Pipatkorn company limited are among major depostis supplying sodium feldspar to domestic and international markets. The deposits associated with intrusive and volcanic/pyroclastic deposits including monzogranite, granodiorite and quartz-rich granitoid with minor portion of rhyolite/rhyolitic tuff. An andesitic dyke was also observed in Nam Saeng mine. Petrographically, the least deformed and least altered host granitic rocks were medium-grained and non porphyritc texture. The major mineral constiutents were quartz, plagioclase and alkali feldspar, with subordinate amount of muscovite, biotite, hornblende, allanite, apatite, tourmaline, titanite, zicon and opaque minerals. Rhyolite/rhyolitic tuff, only found in Rom Yen mine, were strongly deformed and appeared brecciated. However, a narrow area of highly altered spherulite-rich and spherulite-poor alternated layers observed in the field were an indicative of high temperature devitrification of vitrophyre or vitriclastic rocks. Geochemical analyses revealed that these granitic rocks were subalkalic affinities and peraluminous compositions. Tectonically, these granitic rocks intruded in syn-collision to within plate envirionment. Albitzed rocks resulted from highly to pervasive alteration where sodium feldspar compositions were albite to oligoclase (An2-An12). Minor amount of quartz, calcite, epidote and occasionally pyrite were among alteration assemblages. The NW/SE foliation in these three mines were very much constant with orientation varied from 280/40SW to 300/80SW, where the steeper dipping was observed both SW and NE directions. The second set orientated nearly perpendicular to the first set, 020/50SE to 040/80SE. These NW/SE foliations coincided with orientation of the Mae Moei (Mae Ping) Fault Zone, which is interpreted to be the major lineament governed the region that allowed hydrothermal influx to albitized country rocks.

Key words: Sodium feldspar deposit, Albitization, Alteration, Volcanic Facies, Tak

Proceedings of the Second International Symposium on Geoscience Resources and Environments of Asian Terranes (GREAT 2018)
19 - 23 November 2018 Bangkok, Thailand

Geochemistry of granitoids in the Kyaing Tong Area, Eastern Shan State, Myanmar: Implications for Tectonic Setting

Khine Zar Wai[1]*, Khin Zaw[2], Min Aung[3] and Zin Maung Maung Thein[4]

1 Department of Geology, University of Yangon, Myanmar

2 CODES, Centre of Ore Deposits and Earth Sciences, Hobart, Tasmania, Australia

3 Maubin University, Maubin, Myanmar

4 Department of Geology, Magway University, Myanmar

* Corresponding author email: khinezarwai585@gmail.com

Abstract

Three granitoid belts in Myanmar are north-south linear trending from east to west, Eastern Granitoid Belt, Central Granitoid Belt and Western Granitoid Belt. The three belts are different in geological, geochemical and geotectonic setting. The Kyaing Tong area is located at the north easternmost part of the Eastern Granitoid Belt of Myanmar in the western part of the Shan-Thai Block or SIBUMASU Terrane and lies north of the Triassic granitoids Belt of Thailand. This area is mainly made up of granitoids as batholithic scale with varying magmatic differentiation characteristics. The Kyaing Tong batholith mainly consists of biotite granite, porphyritic biotite granite, foliated granite, hornblende granite, granodiorite and leucogranite. The host rocks are pelitic and psammitic rocks. Major oxides and trace elements compositions of fourteen representative samples indicate CIPW norms with hypersthene contents from 2.50 % to 14.05% and corundum values with (0.03-6.97%). Magnetite contents (0.52-2.62%), ilmenite contents (0.04-1.71%), apatite (0.14-0.72%), pyrite (0.02-0.38%), chromite (0.03 and below) and zircon content (0.03-0.06%) are noted. Total alkali content (Na_2O+ K_2O) ranges from 4.48% to 7.71%, whereas (Na_2O+ K_2O+CaO) contents are (6.68%-10.22%) and (Al_2O_3+Na_2O+ K_2O) contents are (18.42%-21.72%). The most notable geochemical characteristics of the Kyaing Tong granitoids are high abundance of Cr, Rb and Sr in all analyzed samples. The granitoid rocks in the study area are mostly in peraluminous field. High peraluminousity of the granites also indicate that more pelitic sediments may have contributed in the magma. According to Harker variation diagrams, negative correlation between TiO_2, MgO, MnO, Fe_2O_3, CaO, P_2O_5 versus SiO_2 suggests that the granites are likely formed due to the result of fractional crystallization during magmatic evolution. Differentiation Index (D.I) values 73.8 to 92.7 supports that these granitoids are well fractionated and more felsic in composition. According to the results of field, petrographic and geochemical evidences, the granitoid rocks of the study area are both I-type and S-type affinity. On the basis of the trace elements data, the granitoids of the study area are mostly within plate granitoids (WPG) with some volcanic arc granitoids (VAG) and syn-collision granitoids (syn-COLG). Tectonically, the Kyaing Tong Granitoids may have occurred under a subduction related setting during the Late Triassic.

Key words: Eastern Granitoid Belt, Kyaing Tong batholith, geochemical characteristics

Proceedings of the Second International Symposium on Geoscience Resources and Environments of Asian Terranes (GREAT 2018)
19 - 23 November 2018 Bangkok, Thailand

Tectonic models in South East Asia – the importance of fieldwork

Hathaithip Thassanapak[1], Mongkol Udchachon[1] and Clive Burrett[2]*

1 Applied Palaeontology and Biostratigraphy Research Unit, Department of Biology, Faculty of Science, Mahasarakham University, Mahasarakham 44150, Thailand

2 Palaeontological Research and Education Centre, Mahasarakham University, Mahasarakham 44150, Thailand

* Corresponding author email: cfburrett@gmail.com

Abstract

Recent field and laboratory work in South East Asia have produced some surprising results that underline the importance of field-work in order to understand the tectonic evolution of South East Asia.

In Myanmar, we, with Professor Punya Charusiri and EGAT colleagues have found Ordovician conodonts in a succession of hitherto unmapped limestones northeast of Hpa-an. These are overlain by probably Carboniferous sandstones which in turn, near Hpa-an, are unconformably overlain by Early Permian mudstones. The Palaeozoic succession and Latest Carboniferous-Earliest Permian deformation episode is similar to that at Uthai Thani in Thailand but its cause is mysterious and does not fit in any published tectonic model.

In Cambodia, we have found the extension of the Permian Sa Kaeo Suture at Pailin. Radiolaria show an Early Permian age and mapping shows that the suture extends in an east-west rather than a northwest-southeast direction. In the north of Pailin a probable metamorphic sole is succeeded northwards by probable back-arc Permian sediments and a volcanic succession overlain by extremely fossiliferous limestones at Sisophon. The Early Permian volcanics may be traced westwards into Thailand.

In Lao PDR, a succession of Ordovician through to Permian has been examined at Sepon and northwards to Khamouanne. Conodonts of Ordovician through to Carboniferous age are present and with sedimentological and structural data define the southern margin of the Truong Son Terrane. Our palaeontological, structural and detrital zircon data suggest that the Truong Son Terrane derived from the Himalayan sector of Gondwana possibly in the Ordovician and drifted during the Silurian and Devonian, suturing with the remainder of Indochina in the Early-mid Carboniferous. Silurian radiolarians, graptolites and zircon data suggest a deep pelagic environment with an Early Silurian volcanic arc extending eastwards into Vietnam. Late Silurian deep marine sediments at Sepon contrast strongly with marginal marine to terrestrial sandstones (as at Do Son) further north on the Truong Son Terrane.

In Thailand, conodont, radiolarian, chert geochemistry and sedimentological work confirms the Mae Yuam fault zone in Mae Hong Son Province as the eastern margin of Sibumasu (Shan-Thai) or the western margin of the Inthanon Zone. The eastern margin of the Inthanon Zone-the Chiang Rai Line either does not exist where it is supposed to be (or is buried under Triassic volcanics) or is much more complicated that simple allochthonous nappe models have proposed. Other tectonic models are equally, if not more, plausible.

Key words: Radiolarians, conodonts, tectonics, terranes, Myanmar, Laos, Thailand, zircons

Proceedings of the Second International Symposium on Geoscience Resources and Environments of Asian Terranes (GREAT 2018)
19 - 23 November 2018 Bangkok, Thailand

Tube-like inclusions in cat's eye from Ilakaka, Madagascar

Janyaporn Witthayarat[1]* and Phisit Limtrakun[1]

1 Department of Geological Sciences, Faculty of Sciences, Chiang Mai University, Chiang Mai, Thailand

* Corresponding author email: dana_mul@hotmail.com

Abstract

Cat's eye is one of the phenomenon variety of chrysoberyl ($BeAl_2O_4$). It contains ultra-fine parallel rutile needles that are oriented very close together which causes the cat's eye effect. The sample from Ilakaka, Madagascar was examined using gemological instruments and advanced techniques. Microscopic examination revealed many oriented hollow tubes pass through the sample. When the sample is turned, a thick light band of cat's eye effect moves from side to side perpendicular to the oriented inclusions. To investigate the cause of the cat's eye effect, SEM-EDS was carried out and the corresponding images of inclusion were taken. Sample was cut perpendicular to the elongate oriented inclusions. SEM image revealed a crossed section of hollow tubes on the surface of sample. The tube wide less than 10 μm and thickness about 3 μm. EDS analysis was chosen to compare the two analyses point between inclusion and the host gem. It is shown that the inclusion has the main composition as same as normal chrysoberyl, and have no sign of the TiO_2 composition. Also, the low TiO_2 content in EPMA result normally found in chrysoberyl variety.

Key words: Cat's eye effect, chrysoberyl, tube-like inclusions, SEM-EDS

1. Introduction

Cat's eye variety occurs in various shades of yellow, green and brown but the highly priced is cat's eye alexandrite. Its chatoyancy is produced by reflection of light from minute, parallel, hollow tubes within the gem, and is best seen in a cabochon cut stone. The term cat's eye when used without any accompanying mineral name refers to cat's eye chrysoberyl.

In jewelry industry, the cat's eye variety of chrysoberyl is more popular due to its appealing optical phenomena. The cat's eye effect in chrysoberyl is caused by many types of inclusions even from the same country. The study on the cause of cat's eye effect from Sri Lanka and Madagascar will be useful for origin determination.

Some minerals display their unusual optical phenomena such as play of color in opal,

adularescence in moonstone, and labradorescence in labradorite feldspar. Another type of phenomenon results from reflection of lights that caused by internal structures or inclusions within the host mineral. This effect will be seen when stone is cut en cabochon and oriented inclusions are parallel to the base of the stone (Liddicoat, 1989). As the stone is turned, the beam of light moves from side to side like the eye of cat, then it is so called "cat's eye" or "chatoyancy". The cat's eye effect results from the scattering of light by parallel needle-like inclusions (Wüthrich and Weibel, 1981) or closely packed parallel fibers (Hurlbut and Kammerling, 1991). All oriented inclusions are perpendicular to the "eye" effect (Figure 1). In cat's eye variety, some literatures mentioned that the cause of this effect is due to various mineral inclusions such as rutile (Tang and Tay, 1999) or sillimanite (Soman and Nair, 1985). Thus, the cat's eye from other localities may be caused by different inclusion.

Cat's eye crystallized from granitic pegmatite (Groat, 2007) such as in Borboerema, Brazil and south Datoka. In addition, this gem variety can also grow in the aluminium-rich country rock near pegmatite or granulites and charnockite which Ratnapura, Sri Lanka and Ilakaka, Madagascar are sample deposits of these host rocks (Simonet *et al.,* 2008). Ilakaka is a town in Ihorombe region in the south western part of Madagascar. The entire west coast is blanketed by Mesozoic to Cenozoic sediments and originated from the Precambrian high-grade metamorphic rock. This giant placer is in the Isalo Group. The Group represents the upper part of the rift sequences, 1 to 6 km thick, made up conglomerates and white sandstones, capped by Lower Triassic red-bed sequences. These detrital sediments marked an active period of rifting and terrestrial sedimentation with the formation of giant gem paleoplacers in the Isalo sandstones. Chrysoberyl and cat's eye were found associated with ruby and fancy color sapphires (Giuliani *et al.,* 2007).

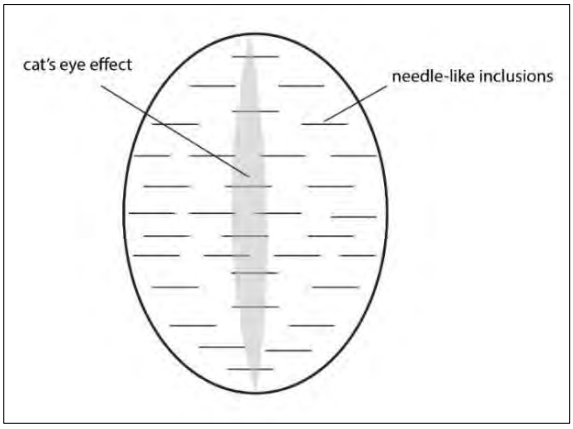

Figure 1. Schematic drawing of cat's eye, paralleled needle-like inclusions are perpendicular to the effect

Cat's eye effect is an optical phenomenon in gemstone. When such a gemstone is cut in cabochon, its surface displays a band of light at right angles to the length of the inclusions. As the stone is turned, the narrow beam moves from side to side as does a cat's eye. The cat's eye effect caused by parallel

needle-like inclusions (Wüthrich and Weibel, 1981) or closely packed parallel fibers (Hurlbut and Kammerling, 1991).

Soman and Nair (1985), revealed the chatoyancy effect in pegmatitic chrysoberyl from southern India may be due to the presence of acicular crystal of sillimanite along micro-fractures. Whereas Tang and Tay (1999) reported that Indian cat's eye (from Orissa and Kerala) owes its chatoyancy to oriented rutile silk because of the high Ti content.

V-shape twins of chrysoberyl from Brazil were studied using transmission electron microscopy and x-ray diffraction technique (Drev *et al.,* 2015). To investigate the rutile precipitation in twin boundary, the research found that the increase of titanium probably occurred after twin formation.

Until recently study, Schmetzer *et al.* (2016) explained the cat's eye effect caused by many different types of inclusion, especially rutile needles. Using combination techniques including optical microscopy, micro-Raman spectroscopy, and electron microprobe analysis employing backscattered imaging, point analysis, and titanium mapping were applied. The results indicated that rutile inclusions were various form of needle-like and/or V-shape platelets, sometimes rectangular and triangular. These inclusions were elongated perpendicular to a-axis, parallel to c-axis, and parallel to symmetry-equivalent <011> directions. The four-ray star chrysoberyl caused by ilmenite particles oriented parallel to c-axis. Milky appearance in cat's eye is caused by a combination of needles and platelets inclusion.

2. Methodology/Experimental design

Rough cat's eye sample was defined using physical characteristic, that they have a cloudy area. To test if the sample is cat's eye or not; drop oil or water on the cloudy surface and use a light source (Figure 2). The sample will show a band of light as the cat's eye on the oil or water drop. This method was suggested by a Thai gem cutter. Some of cat's eye samples were then cut to prove this method.

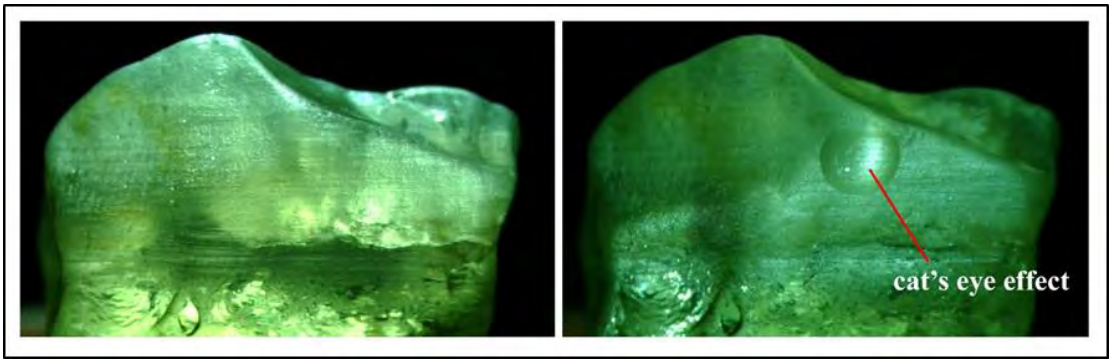

Figure 2 The cat's eye effect testing

All samples were cleaned by soaking in hydrochloric acid, to dissolve any carbonate materials that may be present, and washed with water. Most chrysoberyl samples were cut and polished in a direction perpendicular to the c-axis, while some samples were cut and polished in another direction because of their flat shape. Cat's eye samples were cut perpendicular or parallel to the inclusion.

Basic gemological study

Cat's eye sample was characterized using basic gemological instruments. The specific gravity was determined hydrostatically. Polariscope was used to determine the optic character of sample. Refractometer was used to measure the refractive indices and birefringence. Ultraviolet luminescence was examined using both long-wave (365.4 nm) and short-wave (253.7 nm) ultraviolet radiation. Gemological microscope was used to examine the inclusions.

Spectroscopic study

Chemical analysis of the cat's eye samples was carried out in an attempt to identify the composition of the mineral phase(s) that are responsible for the cat's eye effects. The chemical composition of cat's eye was analyzed using electron probe microanalysis (EPMA). EPMA-WDS was applied using spreading analysis points for the sample. The oxides are determined for all samples including Al_2O_3, FeO (as total Fe), Cr_2O_3, V_2O_3, TiO_2, SiO_2, MnO, CaO, and MgO, while the BeO contents were calculated using matrix-correction programs. Cat's eye sample was also imaged using backscattered scanning electron microscope, JEOL JSM-5910LV, and analyzed for the chemical composition of the inclusion in low vacuum mode.

3. Results and Discussion

Basic gemological study

A Madagascan cat's eye sample was analyzed for gemological properties. The samples are corroded, but also reveal twinning. The Madagascan cat's eye is 1.52 carats in weight with a dimension 6.6 x 6.5 x 4.8 millimeters. The specific gravity is 3.73 which in the range of chrysoberyl. Refractive indices are from 1.746 to 1.755, with a birefringence of 0.009. The sample shows inert to both long- and short-wave ultraviolet radiation.

Madagascan sample showed many paralleled tube-like inclusions. Some tubes are partially filled with tiny reflected particles (Figure 3) under the reflected light. Besides, there are numerous tube-like inclusions with orientation slightly perpendicular to the most of inclusions (Figure 4).

Spectroscopic study

To investigate the chemical composition of the sample, sample was cut perpendicular to the oriented inclusion and fixed the area for identification. A total of 4 analysis points were

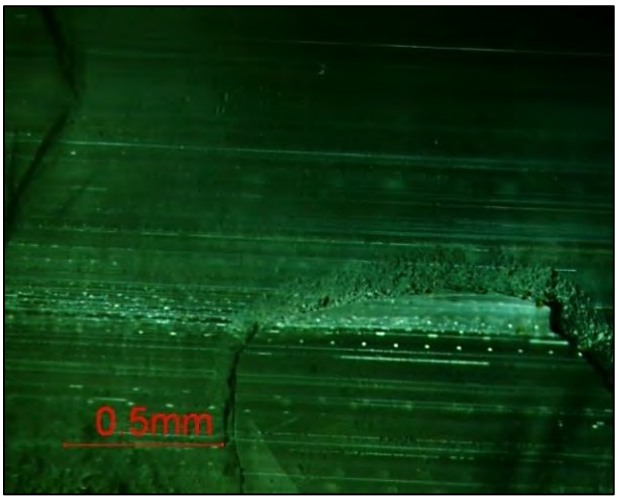

Figure 3. Tube-like inclusion are filled with reflected particles in sample under reflected light

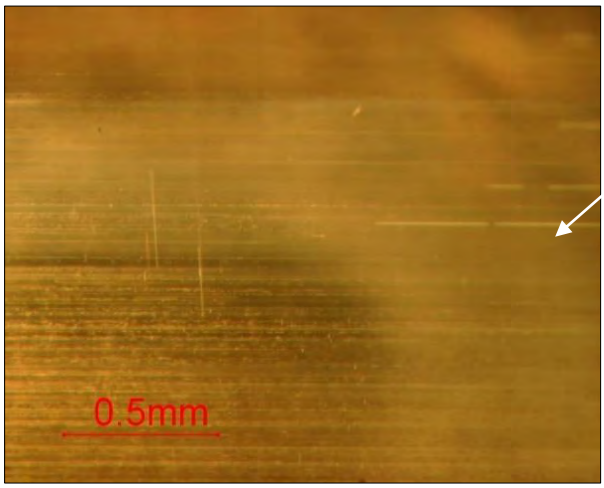

Figure 4. Tube-like inclusions are oriented perpendicular to the major inclusion under dark field illumination

assigned using EPMA-WDS (Figure 5) with a random selection. Al and Be contents, as the principal components of chrysoberyl (normal and cat's eye), are calculated. As presented in Table 1, Al_2O_3 content ranges from 76.349 to 77.273 wt% ($\bar{x}$ = 77.0 wt%), while BeO content ranges from 20.38 to 20.748 wt% ($\bar{x}$= 20.53 wt%). The FeO (as total Fe) content ranges from 0.959 to 1.074 wt% ($\bar{x}$ = 1.46 wt.%). There are two analysis points devoid of TiO_2 in sample. Other two analysis points are 0.017 and 0.062 wt% which are low value and normally found in chrysoberyl (Schmetzer *et al.,* 2013 and Mitpang, 2007).

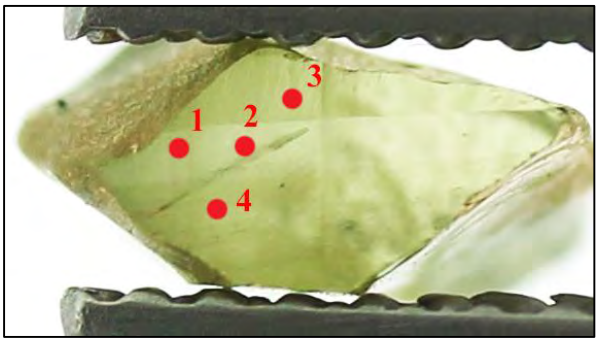

Figure 5. All 4 analysis points were analyzed using Electron Probe Microanalysis

Table 1. Chemical properties of cat's eye sample with 2 distinct zone, from Ilakaka, Madagascar

Point No.	Al_2O_3	BeO	FeO	Cr_2O_3	V_2O_3	TiO_2	SiO_2	MnO	CaO	MgO	Total
#1	76.349	20.574	1.016	0.052	bdl	bdl	0.202	0.006	0.08	0.034	98.313
#2	77.125	20.748	0.978	bdl	bdl	0.017	0.005	bdl	bdl	bdl	98.873
#3	77.122	20.38	1.074	0.015	0.013	bdl	0.025	0.06	bdl	bdl	98.689
#4	77.273	20.422	0.959	bdl	0.001	0.062	0.061	bdl	0.004	0.024	98.806

Further investigate the cause of the cat's eye effect, SEM-EDS was carried out and the corresponding images of inclusion were taken. SEM image revealed crossed section of hollow tubes on the surface of the sample. The tube width is less than 10 μm and the thickness is about 3 μm (Figure 6).

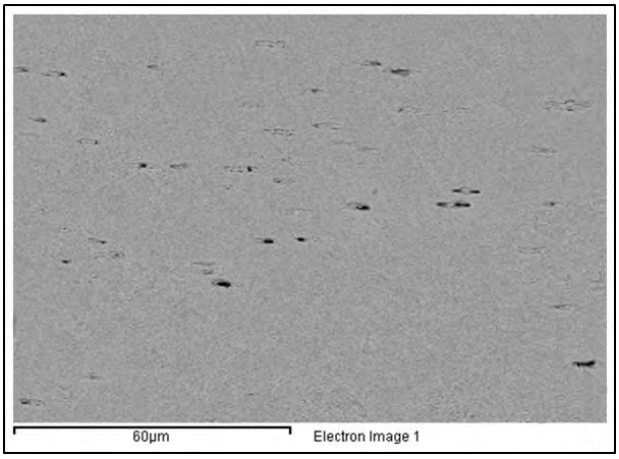

Figure 6. SEM image shows the oriented inclusions which were cut across the oriented inclusions

SEM image was shown in Figure 7. The cross-section of long tube wide less than 10 μm and thickness about 3 μm. EDS analysis was chosen to compare the two analysis points between the inclusion and the host gem. It is shown that the inclusion has the same main components as normal chrysoberyl, and no sign of the TiO_2 composition appeared.

4. Conclusion

The cat's eye sample from Ilakaka, Madagascar show a numerous of oriented tube-like inclusion under the gemological microscope. While SEM image presents the cross-section of tubes. Also, chemical composition result from EMPA support this scheme with low content of TiO_2, different from other literatures. It can be indicated that the cause of cat's eye effect in chrysoberyl caused by not only rutile needles but also tube-like inclusions.

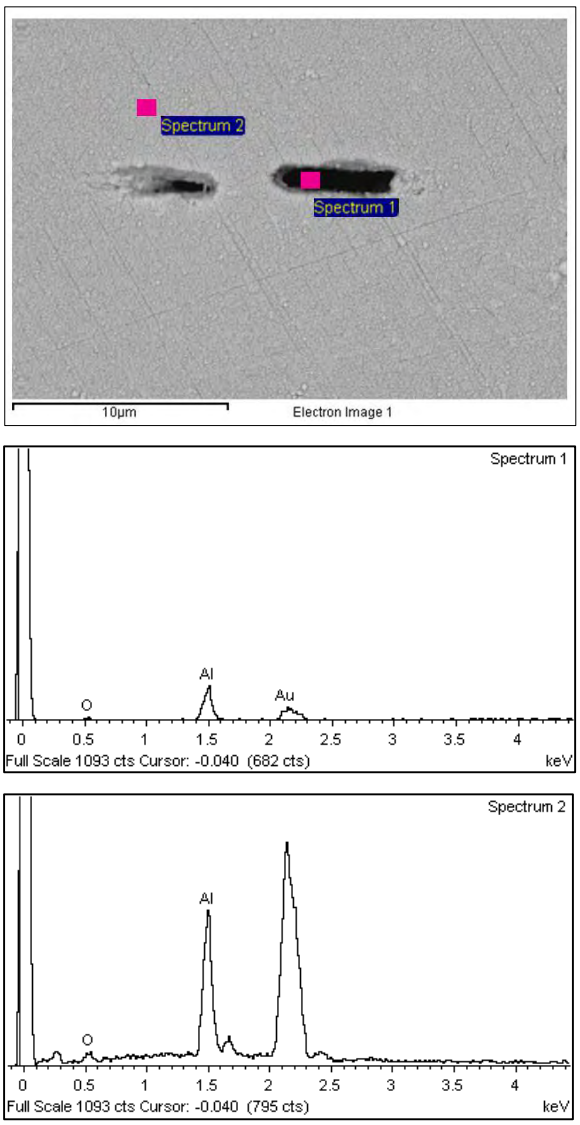

Figure 7 Enlargement of tube-like inclusion and EDS analysis points in sample

5. References

Drev, S., Komelj, M., Mazaj, M., Daneu, N., and Recnik, A., "Structural investigation of (130) twins and rutile precipitates in chrysoberyl crystals from Rio das Pratinhas in Bahia (Brazil)", American Mineralogist, Vol.100, 2015, pp. 861-871.

Groat, L.A., "Geology of Gem Deposits", Mineralogical Association of Canada, Vol.37, 2007, pp. 145-152.

Giuliani, G., Fallick, A., Rakotondrazafy, M., Ohnenstetter, D., Andriamamonjy, A., Ralantoarison, T., Rakotosamizanany, S., Razanatseheno, M., Offant, Y., Garnier, V., Dunaigre, C., Schwarz, D., Mercire, A., Ratrimo, V., and Ralison, B., "Oxygen isotope systematics of gem corundum deposits in Madagascar: relevance for their geological origin", Mineral Deposita, Vol.42, 2007, pp. 251-270.

Hurlbut, C.S., and Kammerling, R.C., Gemology second edition, John Wiley & Sons, Inc., New York, 1991, 337 p.

Liddicoat, R.T., Handbook of Gem Identification 12th edition, Gemological Institute of America, Santa Monica, United States of America, 1989, 362 p.

Mitpang, T., Mineralogy of gemstones associated with corundum from Ilakaka, Madagascar, Thesis for Master of Science, Chiang Mai University, 2007, 129p.

Schmetzer, K., Krzemnicki, M.S., Hainschwang, T., and Bernhardt, H.J., "Natural and synthetic vanadium-bearing chrysoberyl", The Journal of Gemmology, Vol.38, No. 7-8, 2013, pp. 223-238.

Schmetzer, K., Bernhardt, H.J., and Glig, H.A., "Characterization of oriented inclusions in cat's-eye, star and other chrysoberyls", The Journal of Gemmology, Vol.35, No.1, 2016, pp. 28 – 54.

Simonet C., Fritsch, E., and Lasnier, B., "A classification of gem corundum deposits aimed towards gem exploration", Ore Geology Reviews, Vol.34, pp. 127-133.

Soman, K., and Nair, N.G.K., "Genesis of chrysoberyl in the pegmatites of southern Kerala, India", Mineralogical Magazine, Vol.49, 1985, pp.733-738.

Tang, S.M., and Tay, T.S., "Radioactivity of neutron-irradiated cat's eye chrysoberyls",

Nuclear Instruments and Methods in Physics Research, Vol.150, 1999, pp. 491-495.

Wüthrich, A., and Weibel, M., Optical theory of asterism, Physics and Chemistry of Minerals, Vol.7, 1981, pp. 53-54.

Proceedings of the Second International Symposium on Geoscience Resources and Environments of Asian Terranes (GREAT 2018)
19 - 23 November 2018 Bangkok, Thailand

Tectonic Evolution of granitoid rocks in the Thetkaw-Sakangyi area, Thanbyuzayat Township, southern Myanmar: Constraints from Geochemistry and U-Pb zircon age

Mi Paik[1]*, Khin Zaw[2], Hla Kyi[3] and Thein Win[3]

1 Department of Geology, Dagon University, Yangon, Myanmar

2 CODES ARC Centre of Excellence in Ore Deposits, University of Tasmania, Hobart, Tasmania, Australia

3 Department of Geology, Yangon University, Yangon, Myanmar

* Corresponding author email: mimipaik1977@gmail.com

Abstract

The Thetkaw-Sakangyi area is covered by medium- to high-grade metamorphic rocks of the lower part of Mergui Group (Late Paleozoic to Early Paleozoic), low grade metamorphic rocks of Taungnyo Group (Early Carboniferous) and Mesozoic granitoid rocks (Mi Paik, 2013; Mi Paik, 2017). These granioids are biotite granite, garnet-bearing muscovite-biotite granite, quartz microdiorite and pegmatite. The field evidence together with petrological and geochemical characteristics suggest that the granitoid rocks in the area are calc-alkaline and mostly peraluminous in composition. The biotite granite has I-type character, whereas garnet-bearing muscovite-biotite granite gives S-type affinities. The LA ICP-MS U-Pb zircon dating of granitoid rocks in the area indicates an Early Cretaceous age (121.3±1.1-106.8±1.6 Ma). Based on the tectonic discrimination diagrams of Y+Nb Vs Rb, biotite granite falls within the volcanic arc granite (VAG), and pegmatite and garnet-bearing muscovite-biotite granite are in syn-collision granites (Syn-COLG) field. In this paper, we present the new tectonic model that can explain how I and S-types graintoids with tin mineralization in pegmatites were emplaced during Early Cretaceous in the Thetkaw-Sakangyi area. During about 121 Ma, the meso-tethys slab subducted beneath the Sinbumasu Terrane (including the research area) (Metcalfe, 1999) that caused the partial melting of mantle wedge and that melts ± interacted with continental crust, which produced the melts of I-type volcanic arc granites (VAG).The slab is continuously subducted and it would be initially started roll back and followed by crustal thickening due to collision of the Sibumasu Terrane with Indochina Terrane during about 118 Ma. This happening produced the extra-heat. That heat is enough to partial melting of crustal rocks. And then, magma mixing, assimilation and fractional crystallization, which were produced the melts of S-type syn-collision granites (Syn-COLG) over the area. The continued roll back of subducted slab could be capable of upwelling underplating of mantle derived magma, to form quartz microdiorite during about 113 Ma in the area. Later, the hydrothermal activities carrying with tin mineralization which formed in the pegmatites and quartz veins are intruded into the early formed granitoids and along the country rocks during about 106 Ma. Thus, the age of tin mineralization appears to be new age of mineralization in central granitoids of Myanmar.

Key words: I- and S-type granite; Early Cretaceous; collision granitoids; tin mineralization

Proceedings of the Second International Symposium on Geoscience Resources and Environments of Asian Terranes (GREAT 2018)
19 - 23 November 2018 Bangkok, Thailand

Bi-modal Volcanic Rocks of the Lam Narai Area, Lopburi Province

Nuchit Siritongkham[1], Weerapan Srichan2*, Phisit Limtrakun[2] and Somboon Khositanont[1]

1 Department of Mineral Resources, Bangkok

2 Department of Geological Sciences, Faculty of Science, Chiang Mai University

* Corresponding author email: weerapan.s@cmu.ac.th

Abstract

Volcanic rocks in the Lam Narai area are located 6 km south of Chai Badan district, Lop Buri province, central plain Thailand. Field relationship, petrography, geochemistry and tectonic setting of these volcanic rocks can be separated into mafic and felsic rocks. The mafic rocks include basaltic layer and mineralizing zone. The basaltic layer composes of porphyritic and aphanitic texture in glassy groundmass and plagioclase microlites whereas the mineralizing zone is composed of smectite clay mineral. Geochemically, the basaltic layer plots in trachybasalt and basaltic-trachyandesite fields. The Zr/Ti against Nb/Y ratio plot of the basaltic layer is in range of 0.0139 to 0.0155 and 0.4631 to 0.6389, respectively. Their REE patterns of the basaltic layer and mineralizing zone are flat HREE from Sm to Yb with chondrite-normalized Sm/Yb [herein (Sm/Yb)n] = 1.74 – 2.36, and LREE enrichment with chondrite-normalized La/Sm [herein (La/Sm)n] = 2.58-2.79. These compositional ranges correspond to within-plate tholeiites and transitional tholeiites. The felsic rocks are glassy layer and altered glassy layer. The glassy layer shows porphyritic texture in the glassy groundmass with few perlitic crack. The altered glassy layer is porphyritic texture in glassy groundmass with few spherulitic texture. These layers are plotted in rhyolitic field. The Zr/Ti against Nb/Y ratio plot of these layers are in range of 0.1483 to 0.1943 and 0.3682 to 0.6901, respectively. Their REE pattern has relatively flat HREE with chondrite-normalized Sm/Yb [herein (Sm/Yb)n] = 1.11-0.76, and slightly LREE enrichment with chondrite-normalized La/Sm [herein (La/Sm)n] = 4.48-5.86. These compositional ranges correspond to calc-alkaline rhyolite affinity. The silica contents and REE patterns of the Lam Narai volcanic rocks are grouped in mafic and felsic compositions which are possibly derived from different magmatic source in within-plate environment during the Cenozoic evolution of SE Asia.

Key words: Lam Narai area, Mafic and felsic rocks, Volcanics, Lop Buri, Cenozoic, Thailand

Proceedings of the Second International Symposium on Geoscience Resources and Environments of Asian Terranes (GREAT 2018)
19 - 23 November 2018 Bangkok, Thailand

Mineralogical and geochemical variation of kaolin deposit at Chae Hom District, Lampang Province, Thailand

Patcharin Kosuwan Jundee[1]*, Kittikorn Tima[1] and Burapha Phajuy[1]

1 Department of Geological sciences, Faculty of Science, Chiang Mai University, Chiang Mai, 50200, Thailand

* Corresponding author email: patcharinkosuwan.j@cmu.ac.th

Abstract

The Chae Hom kaolin deposit was occurred both residual deposit in Permo-Triassic igneous rock boundary and sedimentary deposit in Quaternary sedimentary rock boundary. The kaolin samples were collected from the area of Tambon Ban Sa, Chae Hom District, Lampang Province for mineralogical and geochemical studied. Mineralogical variation shows that most of samples composed of residual primary and secondary minerals. It can be separated into three groups base on clay minerals as vermiculite, vermiculite-kaolinite and nontronite. Vermiculite group composed mainly of quartz subordinated potassic feldspar and albite with minor amount of vermiculite and muscovite. Vermiculite-kaolinite group consist largely of quartz subordinated vermiculite and kaolinite with small amount of potassic feldspar and albite. Nontronite constitute largely of quartz, subordinated nontronite, albite and potassic feldspar. The variation of geochemistry show that the vermiculite group is low SiO_2 content that have affected from vermiculitzation more than silicification. The Al_2O_3, Na_2O, K_2O contents in vermiculite and vermiculite-kaolinite groups were high cause of effected from vermiculitzation and kaolinitzation. The nontronite show high quartz and SiO_2 content because silicification have high influence in this group. The origin of kaolin deposit in the area of Chae Hom district related with rhyolite source rock and hydrothermal alteration. The silicification was high influent more than vermiculitzation and kaolinitzation. The origin of source rock is volcanic rock that erupted in within plate. Therefore, the source rock of clay minerals is the Chae Hom rhyolite that the part of the Chiang Khong–Lampang–Tak Volcanic Belt.

Key words: Chae Hom rhyolite, kaolin deposit, hydrothermal alteration, ceramic material

1. Introduction

Clay minerals (kaolin) reserves in Thailand were reported by Department of Mineral Resource (2003) that they were about 182.79 million tones and were discovered in many places such as Lampang, Uttaradit, Prachin Buri, Ranong, Surat Thani and Nakhon Si Thammarat Provinces. In northern Thailand, Lampang is the largest deposit with 32 resources and 103.47 million tones reserve. The important ceramic clays deposits are in Chae Hom, Mae Tha, and Muang District, Lampang Province that are large high-quality white clays supply for ceramic manufactory in Thailand. The ceramic clays including fire clays that clay with after fired color is white or light (kaolin, white clays, pottery clays and china clays). Therefore, many ceramic industries were established in Lampang area that is the result of main ceramic product of Lampang. The studies of clay minerals deposit in term of mineral and geochemical characteristics are important for ceramic industry and relate industry materials.

Kaolinite, $Al_2[Si_2O_5](OH)_4$, is the main phase of the kaolin. The kaolinite crystal structure is composed of a plane of SiO_4 tetrahedra linked by oxygen atoms parallel to a plane of $AlO_2(OH)_4$ octahedra. It is formed when anhydrous aluminosilicate found in rock rich in feldspar is altered by weathering or hydrothermal processes. The clay minerals deposit can occur two ways that is residual deposit and secondary deposit. Residual deposit is commonly found in mountain area or feldspar resource and occurred by weathering and hydrothermal alteration. Sedimentary deposit of clay minerals resource is occurred by redeposition of residual deposit in floodplain.

Arunsrisanchai and Potisat (1992) mention that the alteration in rhyolite and rhyolitic tuff in Lampang Province dominantly by silicification and well support by Donmuang et al., (2014a) that was studied clay deposit at Teerayuth Mine, Amphoe Muang, Lampang Province and concluded that the clay minerals are alteration product of rhyolite though hydrothermal alteration. The degrees of alterations were related with SiO_2 content. The low alteration has higher SiO_2 content than high alteration. In addition, Donmuang et al., (2014b) were studied mineralogy of sedimentary clay deposit in Mae Than Mine, Amphoe Mae Tha, Lampang Province. The clay minerals were deposit in basin overlie rhyolitic tuff basement rocks. The major clay minerals are quartz, kaolinite, illite, potassium feldspar and montmorillonite. The kaolinite and illite were found in lower layer and montmorillonite were found in upper layer.

The study area is located in Ban Sa Phae village, Chae Hom District, Lampang Province and appear on topographic map scale 1:50,000 sheet 4946 III (Amphoe Chae Hom) series L7018 between latitude 18°36'15" to 18°36' 21" and longitude 99°33'7" to 99°35'20" with approximately 12 square kilometers. The Department of Mineral

Resources (2007) separated rocks in the study area into four rock units as follows: Middle Triassic sedimentary rocks, Tertiary sedimentary rocks, Quaternary unconsolidated sediments, and Permo-Triassic igneous rocks (Figure 1). The Triassic sedimentary rocks consist of sandstone, conglomerate and limestone in the lower parts; gray-greenish gray mudstone, and interbedded sandstone, siltstone and shale, with limestone lenses are in the upper parts. Fossils of Halobia sp., Posidonia sp., and Paratrachycerus sp. are observed in the upper parts. The Triassic sedimentary rocks are unconformably overly the Permo-Triassic volcanic rocks, and both unconformably and conformably overly the Permian strata. The Tertiary sedimentary rocks are composed of red sandstone, shale, mudstone, claystone, lignite, calcareous shale, clayey mudstone, conglomerate and diatomite with gastropods and ostracods, leaves, stems, fish bones, and Viviparus sp.. They overly the Permo-Triassic igneous rocks and Triassic sedimentary rocks. The Quaternary unconsolidated sediments and the Quaternary semi-consolidated sediments are gravel, sand, silt, clay and mud, and conformably overly the Tertiary sedimentary rocks. The Upper Triassic, Chae Hom volcanic rocks are constituted by flows, dikes, tuff and agglomerate of rhyolitic and andesitic compositions. The kaolin in Chae Hom area was residual deposit in Permo-Triassic igneous rock boundary and sedimentary deposit in Quaternary sedimentary rock boundary.

2. Materials and methods

2.1 Sample collection

Ten kaolin samples were randomly collected from Ban Sa Phae area, Chae Hom district, Lampang province. The representative kaolin samples were collected from both residual deposit and secondary deposit. 1 kg per samples were collected from B-horizon with depth 5-10 cm from surface. Mineralogical and geochemical analysis of clay minerals samples were done by X-Ray Fluorescent (XRF) method and X-Ray Diffractometer (XRD) method.

2.2 Sample preparation for mineralogical and geochemical analysis

The clay minerals samples were dried at 100 °C in an electric oven for 24 hours and then take it out and cooled down to room temperature. The dried samples were prepared for geochemical and mineralogical analysis by grinding into 200 mesh size or 44 micron.

Gechemical analyses of major oxides (SiO_2, TiO_2, Al_2O_3, total iron (FeO and Fe_2O_3) as Fe_2O_3, MnO, MgO, CaO, Na_2O, K_2O and P_2O_5) and some certain trace elements (Ba, Rb, Sr, Y, Zr, Nb, Zn, Ni, Cr, Sc and Th) were carried out using PANalytical Zetium X-ray fluorescence (XRF) spectrometer (wavelength dispersive system), installed at the Kanchanaburi campus, Mahidol University, Thailand. These chemical species were measured from fusion discs prepared with 0.5 g sample

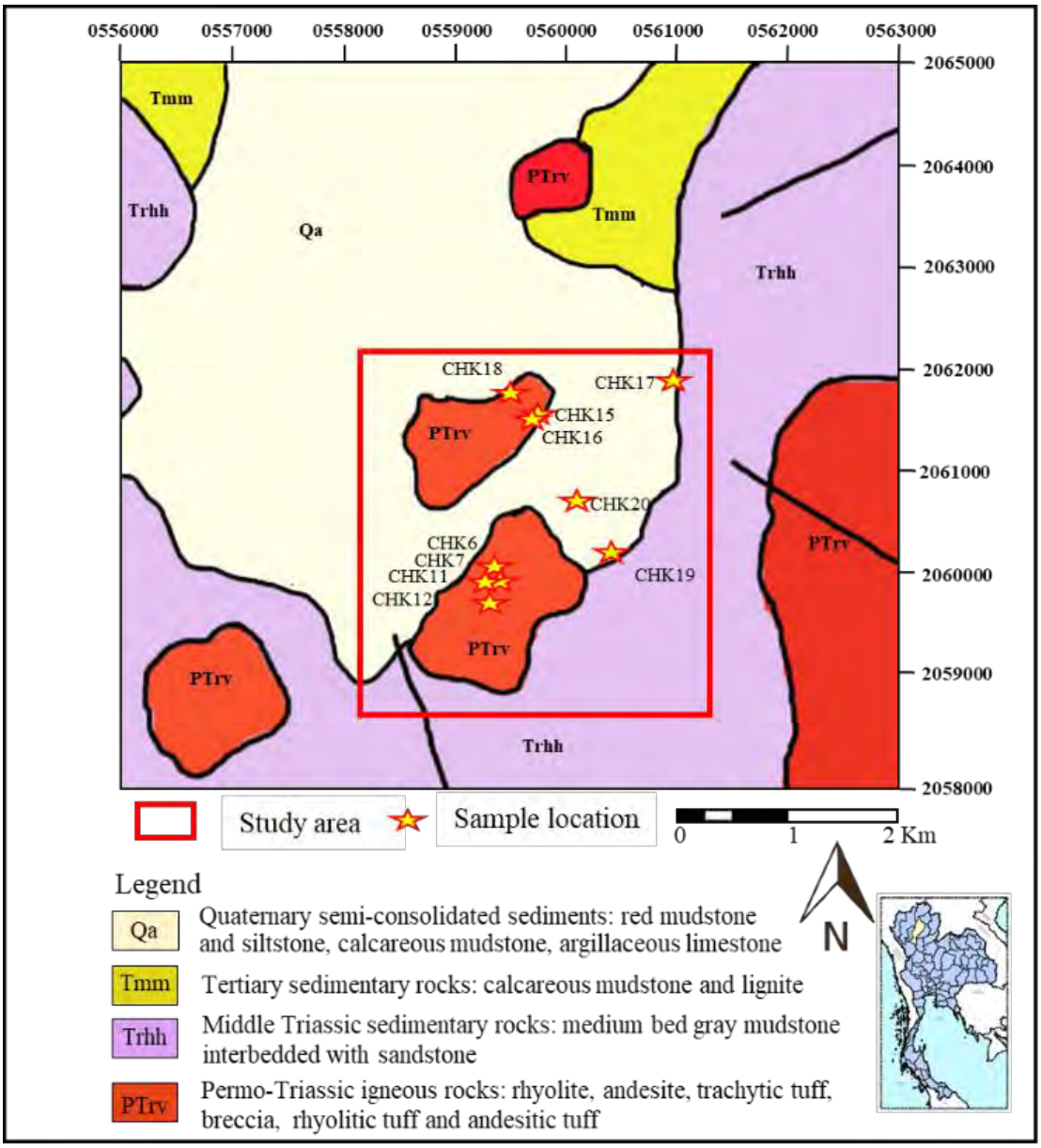

Figure 1. Geologic map of studied area and sample locations at Chae Hom District, Lampang Province modified from Department of Mineral Resources (2007).

powder and 6.5 g mixer materials (anhydrous lithiumtetraborate (Li2B4O7) 49.75%, lithium metaborate (LiBO2) 49.75% and lithiumbromide (LiBr) 0.5%). Ignition loss was measured at, Chiang Mai University by heating approximately 1 g of powered samples at 1000 ºC for 8 hours.

Mineralogical analysis was carried out using Philips X-ray diffractometer (XRD) spectrometer, installed at the Ceramic Indusial Material Group, Lampang, Thailand. Mineralogical analysis was done by mixing the 200-mesh dried sample with treatments included air drying,

glycolation with ethylene glycol, and heating to 550 °C were used for this analysis. The clay fraction was separate from bulk sample by sedimentation and mounted as an oriented aggregate for clay-mineral identification (Poppe et al., 2012).

3. Results and Discussion

3.1 Mineralogical Analysis

The XRD result show that the bulk mineralogical variation of kaolin deposit in the research area were show in Table 1 and Figure 2. They are composed of quartz, vermiculite, kaolinite, nontronite, potassium feldspar, albite, and muscovite. Quartz are the major minerals in this kaolin deposit.

The samples can be separated into three groups based on clay minerals that found in bulk composition as vermiculite, vermiculite-kaolinite and nontronite. The vermiculite group (CHK7, CHK11, CHK18 and CHK19) are composed of quartz, vermiculite, potassium feldspar, albite, and muscovite (Figure 3). The vermiculite-kaolinite group (CHK6, CHK16, CHK17 and CHK20) are consist of quartz, vermiculite, kaolinite, potassium feldspar, albite, and muscovite (Figure 4). The nontronite group (CHK12 and CHK15) are compose of quartz, notronite, potassium feldspar and albite (Figure 5).

Table 1. Mineralogical XRD analysis (%) of kaolin samples.

Group	Vermiculite Group				vermiculite-kaolinite Group				Nontronite Group	
Sample No.	CHK-7	CHK-11	CHK-18	CHK-19	CHK-6	CHK-16	CHK-17	CHK-20	CHK-12	CHK-15
Quartz	77.67	79.43	79.64	50.60	86.01	81.13	82.40	79.71	85.14	90.13
Vermiculite	9.67	6.55	8.40	17.35	6.62	8.56	6.34	9.93	-	-
Kaolinite	-	-	-	-	2.52	2.38	6.79	4.09	-	-
Nontronite	-	-	-	-	-	-	-	-	4.68	4.29
Potassium feldspar	-	5.82	6.13	11.82	2.21	2.14	1.21	4.09	2.38	3.33
Albite	9.25	8.20	5.83	14.23	2.65	5.79	3.26	-	7.80	2.28
Muscovite	3.41	-	-	6.01	-	-	-	2.19	-	-

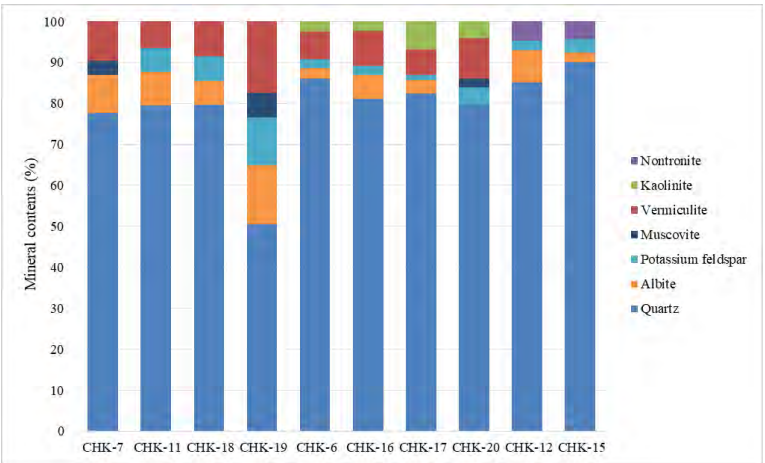

Figure 2. The mineral contents in kaolin samples by XRD analysis.

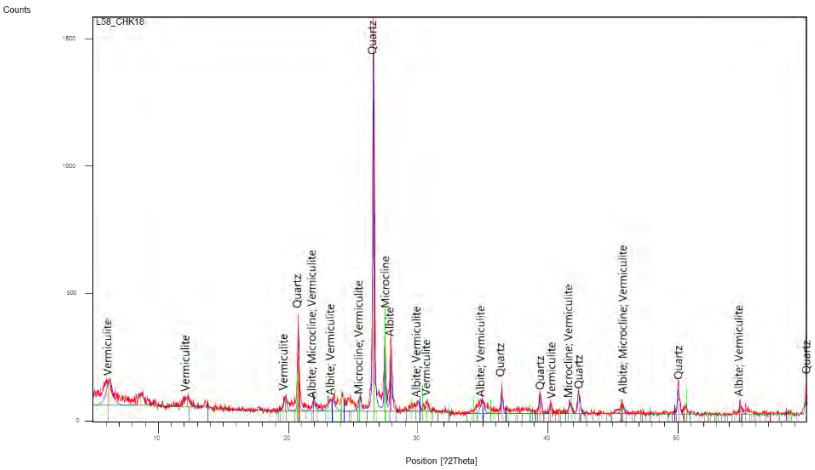

Figure 3. XRD pattern of representative vermiculite group (sample no. CHK18)

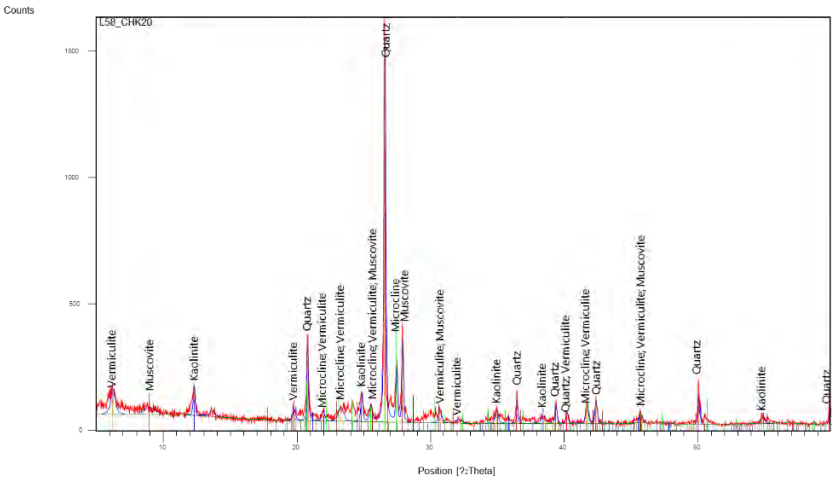

Figure 4. XRD pattern of representative vermiculite-kaolinite group (sample no. CHK20)

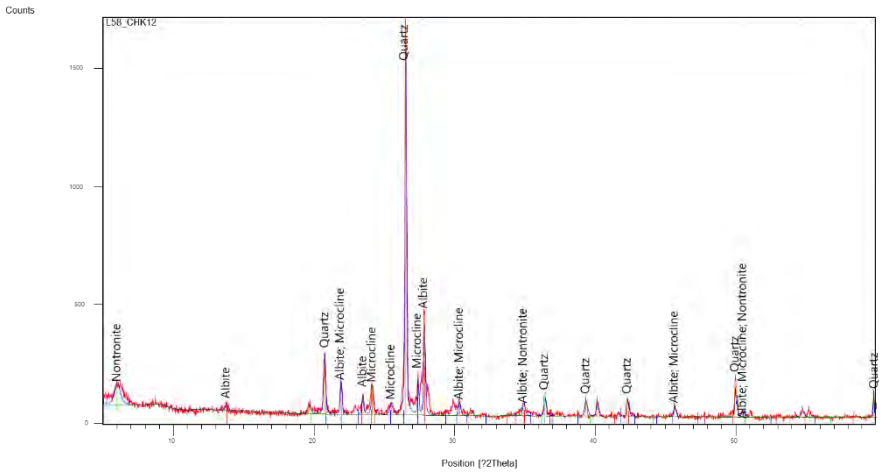

Figure 5. XRD pattern of representative nontronite group (sample no. CHK12)

3.2 Geochemical Analysis

The Geochemical analyses form XRF for major oxides, some trace elements and LOI (Loss on Ignition) of the kaolin samples were reported in table 2. The samples composed mainly of SiO_2 (71-80%), subordinated with Al_2O_3 (14-19%), K_2O (1-6%), LOI (1-6%) and Na_2O (0-5%), respectively with minor amount of TiO_2, Fe_2O_3, CaO, MnO, MgO and P_2O_5. SiO_2, LOI is high in nontronite group, with subordinated vermiculite-kaolinite and vermiculite groups, respectively. TiO_2, Fe_2O_3 and MgO contents are high in vermiculite-kaolinite group, subordinated nontronite and vermiculite groups, respectively (figure 6). While, Vermiculite group show high Al_2O_3, Na_2O, K_2O, CaO, MnO, and P_2O_5 contents, with subordinated vermiculite-kaolinite and notronite groups, respectively.

Some trace elements were determined for source rock of kaolin deposit. They concentration of Ni, V, Rb, Y, Nb, Th, Cr, Sr, Ba, Sc and Zr is 3-26, 20-150, 163-520, 92-143, 29-58, 3-18, 0-130, 65-244, 614-831, 0-3, 105-946 ppm, respectively. Ni, V, Nb, Th, Cr and Zr are high in vermiculite-kaolinite group and subordinated vermiculite and nontronite groups, respectively (figure 7). Rb, Y, Sr and Ba are high in vermiculite with subordinate in vermiculite-kaolinite and nontronite groups, respectively. Sc are high in nontronite group with subordinated vermiculite and vermiculite-kaolinite groups, respectively.

3.3 Mineralogical and geochemical variation of kaolin deposit

The variation of mineralogy and geochemistry of kaolin deposit are depended on primary minerals and texture of source rock and secondary process such as alteration. Jundee *et al.* (in Press) conclude that the source rock in Chae Hom area is seriated rhyolite that were dominantly effected with sericititzation and silicification and secondary

process was dominated than source rock constituents.

Accordingly, the degree of alteration depended on alteration process. Donmuang *et al.,* (2014a) suggest that the degree of alteration (kaolinitzation) is based on SiO_2 content. So that the nontronite group in the Chae Hom kaolin deposit is low degree of alteration, vermiculite-kaolinite group is moderate to high degree of alteration and vermiculite is high degree of alteration. Therefore, the variation of mineralogy in Chae Hom kaolin deposit show that vermiculite and kaolinite rich in high degree of alteration, while nontronite was found only in low degree of alteration.

Vermiculite and nontronite occur as weathering product of volcanic glass/material under alkaline condition and in quartz and opal vein. Vermiculite in soil kaolins from Thailand is a common minor constituent of these clay fractions and its average structural formula derived from EDS data indicates that it was formed by Al replacing K in muscovite (Hart et al., 2003). Kaolinite are residual deposit formed by weathering or low-temperature hydrothermal alteration of feldspar, muscovite, and Al-rich silicates in acid rocks. Quartz was found both as residual primary minerals from weathering process in source rock and secondary minerals by alteration process (silicification). Potassic feldspar and albite were found in most of groups and they were residual mineral in source rock.

The variation of geochemistry (major oxide) in this studied show that the vermiculite group is low SiO_2 content that have effected from vermiculitzation more than silicification. The Al_2O_3, Na_2O, K_2O and LOI contents in vermiculite and vermiculite-kaolinite groups were high cause of effected from vermiculitzation and kaolinitzation. The nontronite show high quartz and SiO_2 content because silicification have high influence in this group.

3.4 The source rock of clay minerals

While, the rocks have undergone variable degrees of alteration and low-grade metamorphism, the concentrations of immobile elements may be changed, due to the dilution or enrichment of the mobile elements. However, the ratios of immobile elements in the primary rock and altered rock remain constant. Accordingly, only the elements considered as immobile elements and immobile-element ratios are used to interpret the geochemical data in this study. Furthermore, TiO2, Zr, Nb, Y and Rb are an incompatible immobile element, therefore it will be used as a parameter for the studied rock samples.

The least-mobile Zr/TiO2 and Nb/Y ratios of the clay minerals samples in ranges of 0.087-0.239 and 0.255-0.527 in respective manner, however, imply that the source rocks of clay

Table 2. Geochemical XRF analyses (recalculated to 100 wt% on volatile-free basis) and LOI of the clay minerals (kaolin) samples.

Group	Vermiculite Group				vermiculite-kaolinite Group				Nontronite Group	
Sample no.	CHK7	CHK11	CHK18	CHK19	CHK6	CHK16	CHK17	CHK20	CHK12	CHK15
Major oxide (wt%)										
SiO_2	71.17	74.00	73.27	67.35	79.84	74.75	76.45	74.41	77.34	77.06
TiO_2	0.08	0.07	0.08	0.17	0.09	0.11	1.08	0.13	0.05	0.07
Al_2O_3	18.40	15.87	18.98	22.43	14.09	17.48	18.76	18.21	14.68	16.45
Fe_2O_3	1.25	0.48	1.35	1.27	0.73	1.97	1.66	0.93	0.93	1.28
MnO	0.14	0.02	-	0.03	-	0.03	-	-	-	-
MgO	0.29	0.13	0.23	0.16	0.23	0.26	0.25	0.11	0.44	0.16
CaO	0.31	0.40	0.11	0.36	0.06	0.23	0.03	0.13	0.40	0.15
Na_2O	3.53	4.43	1.15	2.29	0.86	1.32	0.12	1.25	3.02	1.24
K_2O	4.79	4.60	4.84	5.93	4.10	3.81	1.63	4.82	3.15	3.59
P_2O_5	0.04	-	-	0.02	-	0.03	0.02	-	-	-
LOI	2.56	1.15	5.33	4.58	3.29	5.02	6.04	4.22	3.18	4.93
Original sum	102.56	101.15	105.33	102.40	103.29	105.02	106.04	104.22	103.18	104.93
Trace Element (ppm)										
Ni	6	5	8	26	10	9	30	3	9	5
V	24	21	24	34	22	26	150	27	20	21
Rb	520	439	472	558	386	395	163	487	299	393
Y	142	110	119	143	110	104	97	136	92	104
Nb	58	29	45	44	58	56	25	45	32	40
Th	18	3	10	7	4	9	33	4	3	5
Cr	4	11	2	2	16	4	130	-	-	4
Sr	195	244	105	141	73	120	65	120	195	113
Ba	823	826	831	820	810	775	614	810	808	773
Sc	2	3	2	2	2	2	0	1	3	2
Zr	181	102	138	158	126	128	946	140	105	108
Some select ratio										
Zr/TiO_2	0.239	0.153	0.179	0.095	0.134	0.114	0.087	0.109	0.218	0.145
Nb/Y	0.406	0.265	0.380	0.305	0.527	0.536	0.255	0.329	0.351	0.379
Nb+Y	200	139	164	187	168	160	122	180	125	144

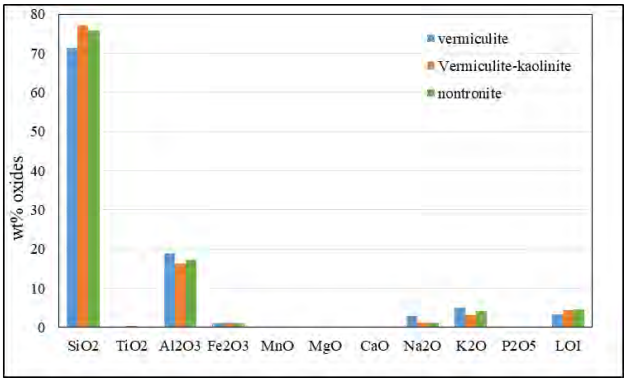

Figure 6. Average major oxide concentration (wt%) of vermiculite, vermiculite-kaolinite and nontronite groups.

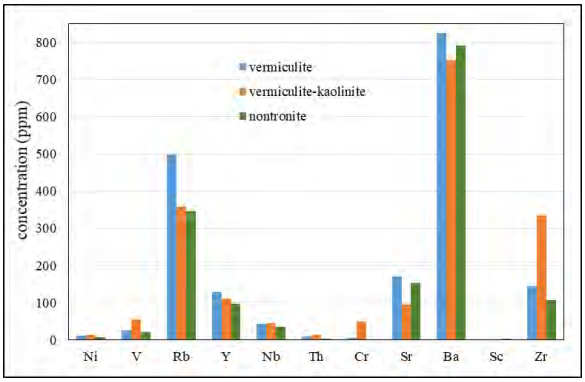

Figure 7. Average trace elements concentration (ppm) of vermiculite, vermiculite-kaolinite and nontronite groups.

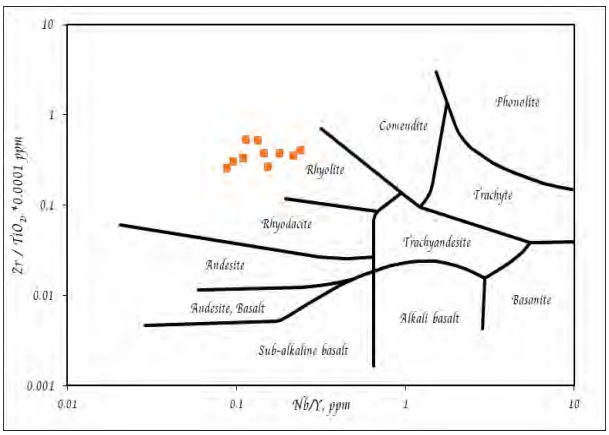

Figure 8. A plot of Zr/TiO_2 against Nb/Y for the studied clay minerals samples. Field boundaries for different rock types are taken from Winchester and Floyd (1977).

minerals is rhyolite (Winchester and Floyd, 1977) (Figure 8).

The Rb and Nb+Y of the studied clay minerals samples in ranges of 163-558 ppm and 122-200 ppm, and Nb and Y in rang of 25-58 ppm and 92-143 ppm in respectively. The plot of Rb against Nb+Y (Figure 9) and Nb against Y (Figure 10) (Pearce *et al.,* 1984) indicating that the origin of source rock is volcanic rock that erupted in within plate. The source rock and their origin of clay minerals in Chae Hom was supported by Jundee *et al.* (In press) suggest that Chae Hom rhyolite have been alteration (sericitization and silicification) to kaolinite. In addition, they have rather flat REE patterns and light REE enrichment, typical of calc-alkalic rocks. They mention that Chae Hom rhyolite is the part of the Chiang Khong–Lampang–Tak Volcanic Belt. The geochemistry features of volcanic rocks in the Chiang Khong–Lampang–Tak Volcanic Belt are strong compositional analogies with other post-collisional magmatic suites and are more typical of volcanic belts formed in a rapidly evolving post-collisional, basin-and range-type extensional setting.

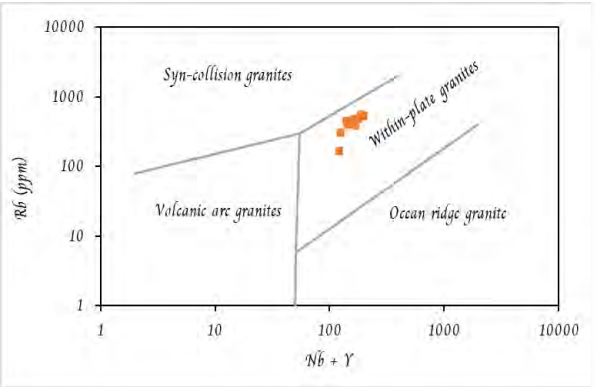

Figure 9. A plot of Rb against Nb+Y for the studied clay minerals samples. Field boundaries are taken from Pearce *et al.* (1984).

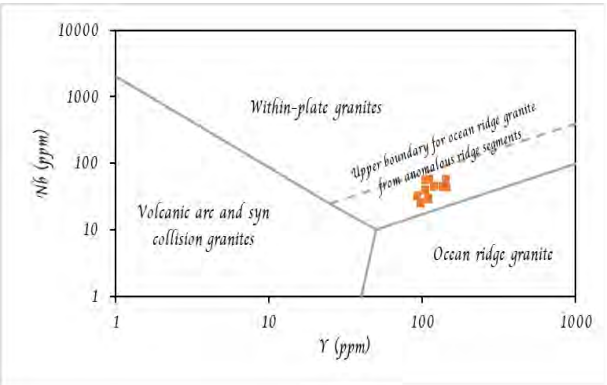

Figure 10. A plot of Nb against Y for the studied clay minerals samples. Field boundaries are taken from Pearce *et al.* (1984).

4. Conclusions

The Chae Hom kaolin deposit was occurred both residual deposit in Permo-Triassic volcanic rock boundary and sedimentary deposit in Quaternary sedimentary rock boundary. The variation of mineralogy and geochemistry of clay minerals deposit are depended on alteration process. The clay minerals was classified as vermiculite, vermiculite-kaolinite and nontronite groups. The origin of source rock is volcanic rock that was erupted in within plate. Therefore, the source rock of kaolin is the Chae Hom rhyolite that the part of the Chiang Khong–Lampang–Tak Volcanic Belt.

5. Acknowledgements

The authors acknowledge financial support provided by the Faculty of Science, Chiang Mai University and Chiang Mai University. We would like to thank Miss Janjira Srayungthong, staff of Mahidol University, Kanchanaburi Campus for her kindness in XRF analysis and Dr. Keadsuda Donmuang for her kindness in XRD analysis.

6. References

Arunsrisanchai, W., and Potisat, S. 1992. Preliminary investigation of primary gold occurrences in northern Thailand. In Charoen Phiancharoen (eds.), *Proceedings of the National Conference on "Geologic Resource of Thailand: Potential for future development"*, Bangkok, Resources Mineral of Department, Thailand, p. 110-107.

Department of Mineral Resource. 2003. Kaolin deposit in Thailand. Geological Survey Division, Bangkok.

Department of Mineral Resources. 2007. Geological map of Changwat Lampang, scale 1: 1,000,000. Geological Survey Division, Bangkok.

Donmuang, K., Asnachinda, P., Limtrakun, P., Rattanasatien, B., and Khandarosa, W. 2014a. Geochemical and mineralogical variation of hydrothermally altered rhyolite at Teerayuth mine, Ban Laeng, Amphoe Muang, Lampang Province, Thailand. *IOSR Journal of Applied Geology & Geophysics*, 2, 2 (II), 77-84.

Donmuang, K., Asnachinda, P., Limtrakun, P., Rattanasatien, B., and Khandarosa, W. 2014b. Mineralogical variation of sedimentary clay deposit at Mae Than mine, Ban Mae Than, Lampang Province, Thailand. *IOSR Journal of Applied Geology & Geophysics*, 2, 6 (I), 16-21.

Hart, R. D., Wiriyakitnateekul, W., and Gilkes, R. J. 2003. Properties of soil kaolins from Thailand. *Clay Minerals*. 38, 1, 71-94.

Jundee, P.K., Phajuy, B., Panjasawatwong, Y. Sericitization-Silicification of Chae Hom Volcanics, Lampang, Northern Thailand. *Songklanakarin Journal of Science and Technology.* in Press.

Pearce J.A., Harris N.B.W. and Tindle A.G. 1984. Trace element discrimination diagram for the tectonic interpretation of granite rock. Journal of Petrology, 25, 956-983.

Poppe, L., Paskevich, V.F., Hathaway, J.C., and Blackwood, D.S. 2012. A laboratory manual for X-Ray powder diffraction. U.S. Geological Survey. open-file report 01-041.

Winchester, J.A., and Floyd, P.A. 1977. Geochemical discrimination of different magma series and their differentiation products using immobile elements. Journal of Chemical Geology, 20, 325-343.

Proceedings of the Second International Symposium on Geoscience Resources and Environments of Asian Terranes (GREAT 2018)
19 - 23 November 2018 Bangkok, Thailand

Middle Ordovician Ostracods from Sri Sawat district, Kanchanaburi province: implication for paleogeographic interpretation

Patteera Ketmuangmoon[1]*, Thitikan Junrattanamanee[2], Nitipon Noipow[3] and Anisong Chitnarin[1,2]

1 Georesources Research Group, Institute of Engineering, Suranaree University of Technology, Nakhon Ratchasima

2 School of Geotechnology, Suranaree University of Technology, Nakhon Ratchasima

3 Faculty of Science and Technology, Valaya Alongkorn Rajabhat University under the Royal Patronage, Pathum Thani

* Corresponding author email: nikpatteera@gmail.com

Abstract

Fossil ostracods are recovered from limestones at the Wat Mong Krathae locality, a part of the Tha Manoa Limestone Formation, in Sri Sawat district, Kanchanaburi province. The exposure of stylolitic limestones showing thin-to thick beds was investigated and rock samples were collected. The age of Middle Ordovician (Darriwilian age) is designated by associated macrofossils: Armenoceras chediforme (Kobayashi, 1958) and Teiichispirina sp. Four from 27 rock samples yielded the ostracods; however, 80% of specimens were recovered from a single grainstone in the middle part of the section. Most of the carapaces are poorly preserved although ten species can be recognized. This fauna is dominated by members of Families Drepanellidae, Aparchitidae, Healdiidae, Longisculidae, Beecherellidae, but is different from the Thong Pha Phum fauna previously described. The fauna shows biogeographical relations to Iran, Argentina and NW China at the generic level, which supports the close palaeogeographic position of these continents during the Middle Ordovician.

Key words: Perigondwana, Sibumasu, Ostracoda, Thung Song Limestone

Proceedings of the Second International Symposium on Geoscience Resources and Environments of Asian Terranes (GREAT 2018)
19 - 23 November 2018 Bangkok, Thailand

Remnant of the Pleistocene debris flows at Khao Din: Implication for the paleo-environment of Ban Laem Chabang, Sri Racha District, Chonburi Province, Eastern Thailand

Prinya Putthapiban[1], Wasuporn Phupatwibun[1], Parisa Nimnate[1], Narongsak Kaewdum[1], Piyatida Saengthong[1] and Sutatcha Hongsresawat[1]

1 Geoscience Program, School of Interdisciplinary Studies, Mahidol University Kanchanaburi Campus, 199 Moo 9, Lumsum, Sai Yok, Kanchanaburi, 71150, Thailand

Extended Abstract

Khao Din Hill is located in Sri Racha District, Chonburi Province and found in a 1:50,000 topographic map series L7018, sheet 5135 II with a coordinate UTM grit 7116/14507. It is an N-S trending elongated hill approximately 900 m long and 500 m wide. At the center of the ridge, the highest peak is at 123 m above mean sea level (AMSL). The flat ground at the foothill is 20 m AMSL, and the nearest shoreline is about 6 km to the west. In this paper, we present our discoveries of the remnant of Pleistocene debris flows and propose that they were primary sources responsible for forming the Khao Din landform.

The rock-face cutting for private land use along the SSE tip of Khao Din revealed at least four distinct sub parallel, unconsolidated sedimentary strata labeled as units A, B, C and D (Figures 2 and 3). All strata have similar orientation of strike N 23 W and dip 20 W. Measurements of total true thicknesses of the top strata indicate that they are slightly greater than 15 m. Nonetheless, the total thicknesses of the whole area can be much greater than 15 m. The lowermost stratum (Unit A), > 6 m thick, consists of a few sub flows. The sediments are mainly gravel size (64-256mm) with very high angularity to sub-angular, very poorly sorted and low to moderate sphericity. These gravels include 15% quartzite, 30% quartz schist, 50% vein quartz and 5% feldspars. Sediments of Unit B, ~1.5 m thick, are mainly gravelly coarse sands with less than 20% silt and clay. These gravelly sands are angular to sub-round, poorly sorted and low to high sphericity. Their material contents are 10% quartzite, 30% quartz schist, 55% mineral and vein quartz and 5% feldspars. Sediments of Unit C, ~2.5 m thick, are very angular to sub round, poorly sorted with high to low sphericity. Their material contents include 25% quartzite, 30-35% quartz schist, 45-50 % vein quartz and 2-3 % feldspars. The sediments of top most layer, apart from the top soil, Unit D, > 4 m thick, are mainly gravelly coarse sands ~30 – 35 % gravel, 60 – 63 % coarse

sands and < 10 silt and clay (Figure 4). Their shapes are angular to sub round, poorly to moderate sorted with low to high sphericity. Their material contents are 10 % quartzite, 30-35 % quartz schist, 50-60 % vein quartz and 5 % feldspars.

The slope depositional nature of the Khao Din sediment layers includes (i) low-angle incline orientation, (ii) coarsening upward sequences, (iii) high angularity, (iv) poorly sorted with inter-bedded gravel and coarse sand layers and (v) very small amount of silt and clay particles. We propose that these sedimentary sequences were formed by paleo-debris flows along the slope of relatively high viscosity and relatively slow. With information previously mentioned and source rock identifications, it is indicated that the source rocks of Khao Din hill were derived from (a) Permo-Carboniferous metamorphic rocks and (b) Triassic granite bodies at much higher elevation, perhaps, hundreds of meters higher than the present, by extensive weathering, erosion, transportation and deposition processes from the northern and north-northeastern directions.

The Pleistocene age of the Khao Din debris flows was earlier proposed based on the discovery of primitive human-made pebble tools similar to some of those Oldowan pebble tools during Paleolithic period or 2.6 – 1.7 million years before present (Figure 5).

Acknowledgements

We thank Dr. Amnat Jareerat, Chairman of the School of Disciplinary Studies and Asst. Professor Dr. Thatchavee Leelawat, Vice President of Information Technology and Kanchanaburi Campus, Mahidol University, for their encouragements and supports.

References

Anderson, D.D. (1987) A Pleistocene-Early Holocene Rock Shelter in PeninsularThailand, National Geographic Research 3: 184-198.

Department of Mineral Resources (2007) Geologic map of Changwat Chonburi, 1:250,000.

Shepard, F.P., 1954. Nomenclature based on sand–silt–clay ratios. Journal ofSedimentary Petrology 24 (3), 151–158.

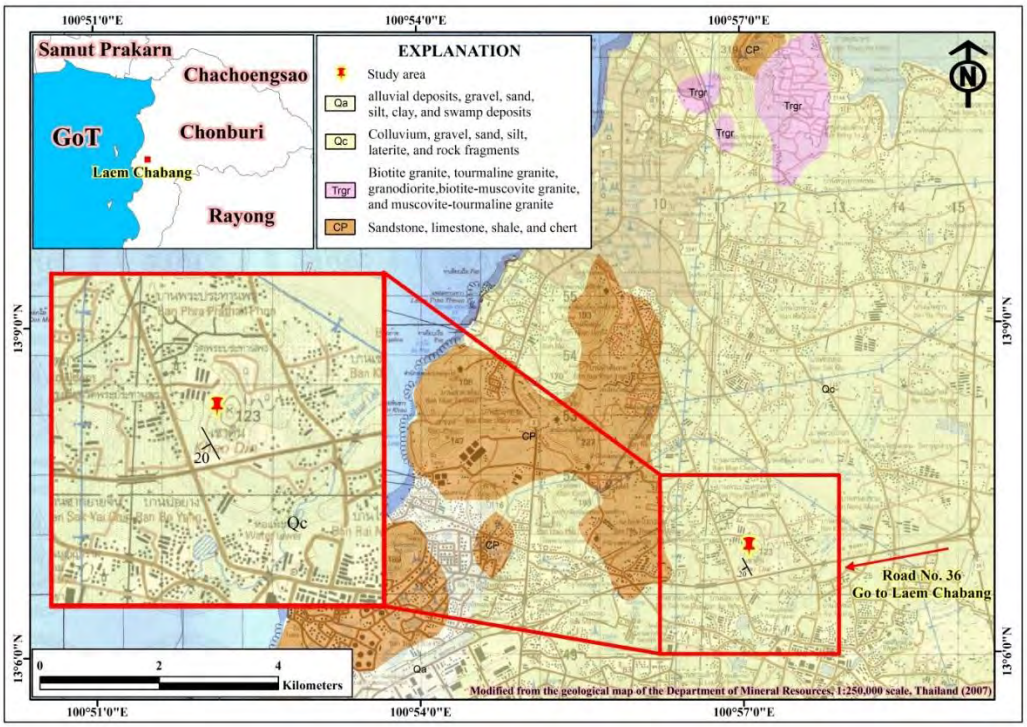

Figure 1. The topography of Khao Din and its relation to regional geology modified after Geological Map of Changwat Chonburi, 1:250,000 scale, Department of Mineral Resources, 2007.

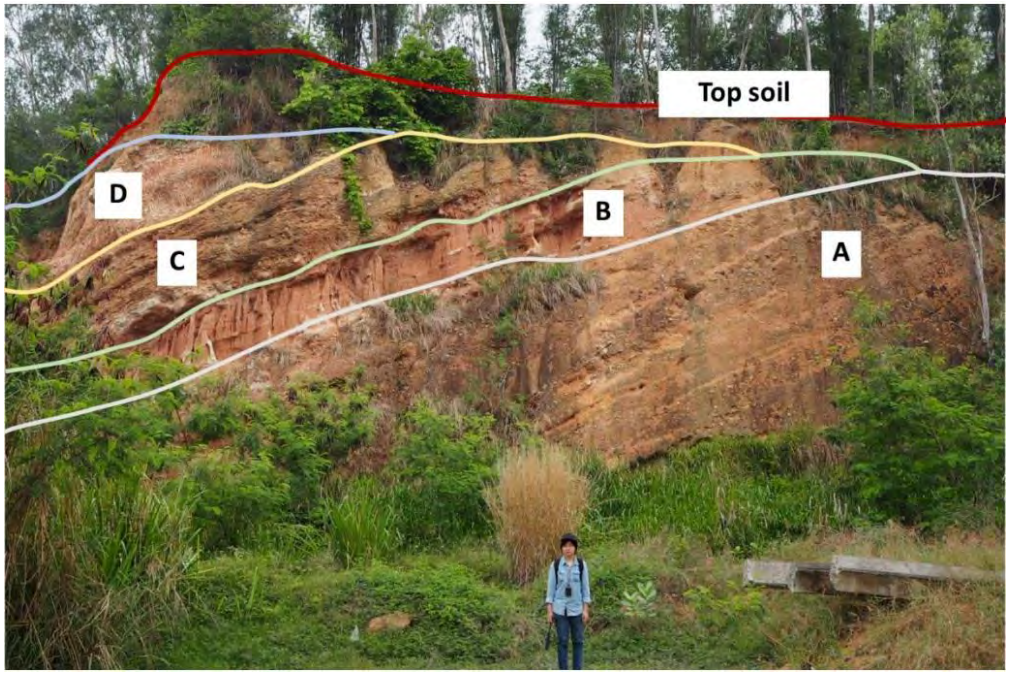

Figure 2. The rock-face cutting for private land use along the SSE tip of Khao Din. Big boulders can be observed scatter at the upper part of Units A, B, C and D.

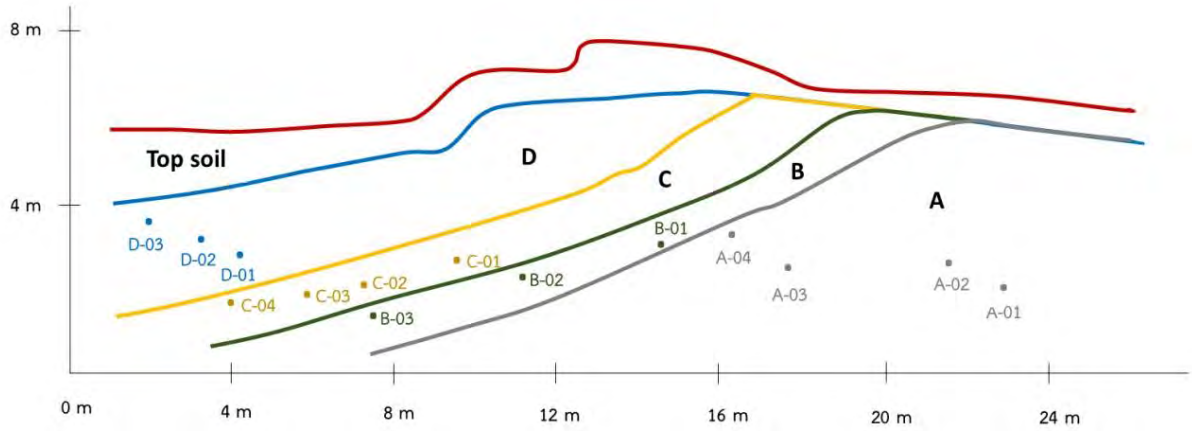

Figure 3. Sketched map showing four distinct sub parallel, unconsolidated sedimentary stratra labeled as unit A, B, C and D and the sample locations used in this study.

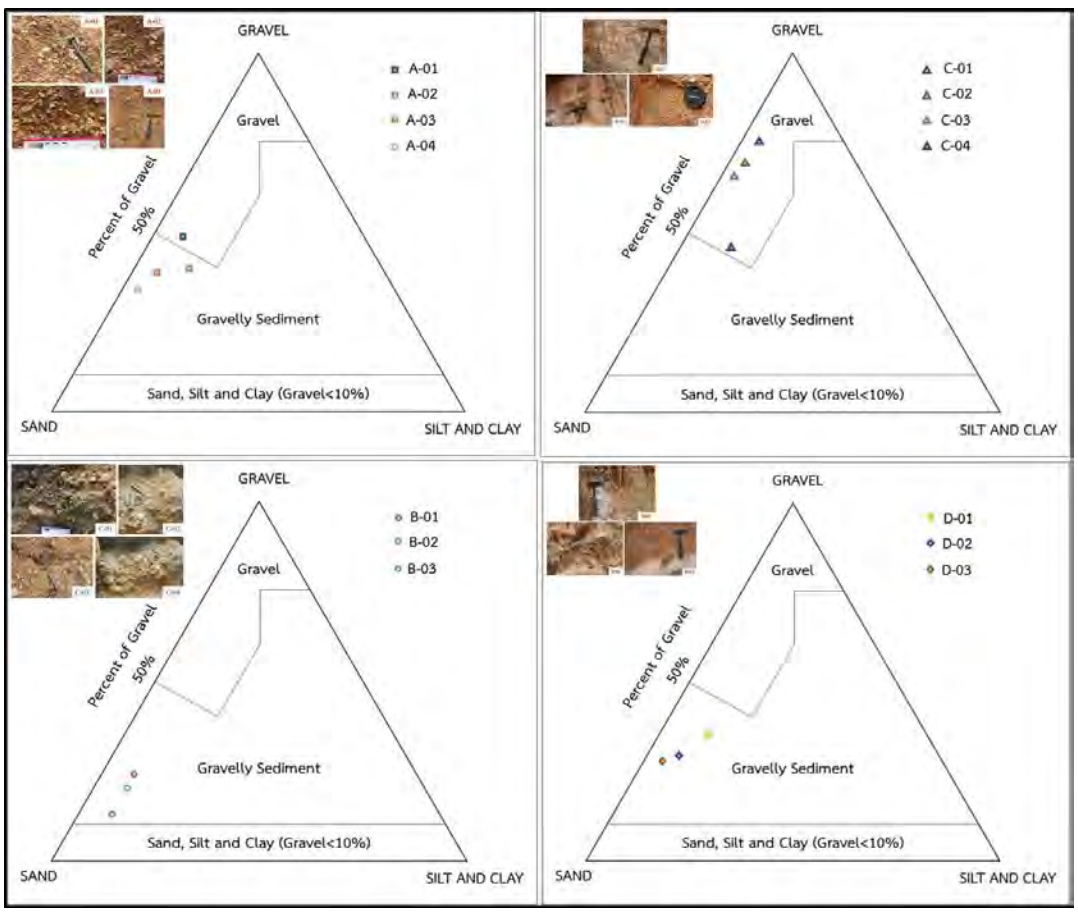

Figure 4. Grain size distribution of the studied samples from the four strata, followed Shepard's classification system (Shepard, 1954).

Figure 5. Map of Afro-Eurasia showing important sites of the Oldowan industry, Wikipedia, the free encyclopedia website and the potential Oldowan pebble tools at Sri Racha, Eastern Thailand.

Proceedings of the Second International Symposium on Geoscience Resources and Environments of Asian Terranes (GREAT 2018)
19 - 23 November 2018 Bangkok, Thailand

Architecture, depositional environment and tectonics implication of the Triassic deposits in Pong District, Phayao Province

Rattanaporn Fongngern[1], Pitaksit Ditbanjong[1], Aphisit Seangdang[2] and Wittaya Kandharosa[1]

1 Department of Geological Sciences, Chiang Mai University

2 Siamphan Enterprise Public Company Limited, Bangkok

* Corresponding author email: rattanaporn.f@cmu.ac.th

Abstract

This study investigated the Triassic sedimentary rocks in Ban MaeTai Tombon Aoi Pong District, Phayao Province. The rock unit is composed of gray mudstones interbedded with siltstones and sandstones. From approximately 60 m thick measured section and hand specimens collected every 2 m, the strata were divided into four lithofacies: thin-bedded mudstone and siltstone (A), thin-bedded sandstone (B), thick-bedded sandstone (C), and deformed rock (D). Facies A, B and C occur in upward-fining sequences in which structureless beds, parallel laminations, ripples, mudclasts, flames and load casts can be observed. The fining upward pattern and sedimentary structures are characteristic of turbidite's Bouma sequence formed by turbidity currents. Flames and load casts are indicative of high depositional rates. The thick succession of turbidites, rare bioturbation, and occurrence of soft-sediment deformation suggest the depositional environment as deepwater and probably on the slope. The U-Pb age dating of zircons from three sandstone samples indicates minimum depositional age around 240-210 Ma (middle-late Triassic). Thus, these turbidites are interpreted to be deposited in the deep basin along the Sukhothai zone, i.e. forearc basin, existing before the collision between the Sibumasu and Indochina Blocks was completed. This is in agreement with the previous studies.

Key words: Turbidite, Deepwater slope, U–Pb dating, Sukhothai zone, Triassic

Proceedings of the Second International Symposium on Geoscience Resources and Environments of Asian Terranes (GREAT 2018)
19 - 23 November 2018 Bangkok, Thailand

Early Carboniferous Ostracods from Tham Pha Tha Phon, Noen Maprang district, Phitsanulok province

Sataporn Kongsat[1] and Anisong Chitnarin[2, 3*]

1 Development and Promotion of Science and Technology Talents Project, Suranariwittaya school, Nakhon Ratchasima

2 School of Geotechnology, Suranaree University of Technology, Nakhon Ratchasima

3 Georesources Research Group, Institute of Engineering, Suranaree University of Technology, Nakhon Ratchasima

* Corresponding author email: anisong@sut.ac.th

Abstract

Tham Pha Tha Phon is one of the outstanding geosites in northern Thailand representing beautiful karst topography and abundant fossils. It is located about 6 km Southeast of Noen Maprang city in Phitsanulok province and is protected by wildlife conservation office. The rocks are predominated by bedded and massive limestones with a few sandstone beds in the lower part. Limestones are fossiliferous, both macro- and microfossils such as corals, brachiopods, algae and foraminifers indicate the age of Early Carboniferous (Vesian age) and probably up to Middle Carboniferous. In this study, many ostracods are recovered from a single wackestone collected from Tham Rue in the lower part of the succession. They comprise of 20 species which belong to Aparchitidae, Paraparchitidae, Kirkbyidae, Bairdiidae, Cytherideidae, Microcheilinellidae, Polycopidae Families. The ostracod assemblage represents organisms living in carbonate substrates with normal salinity, deposited on the middle part of continental shelf.

Key words: Indochina, Ostracoda, Khao Pha Tha Phon Limestone

Proceedings of the Second International Symposium on Geoscience Resources and Environments of Asian Terranes (GREAT 2018)
19 - 23 November 2018 Bangkok, Thailand

Classification of the Upper Paleozoic Trilobites from Doi Tu Pu, Chiang Rai Province, Northern Thailand: Preliminary result

Siwakorn Maneethein[1], Pitaksit Ditbanjong[2]*, Yupa Thasod[2], Arnaud Bignon[3,4], Phornphen Chanthasit[5], Woratham Bubpha[2]

1 Yupparaj Wittayalai School, Chiang Mai 50200, Thailand.

2 Department of Geological Sciences, Faculty of Science, Chiang Mai University. Chiang Mai 50200, Thailand.

3 Universidad Nacional de Córdoba. Facultad de Ciencias Exactas, Físicas y Naturales. Córdoba, Argentina.

4 Consejo Nacional de Investigaciones Científicas y Tecnológicas (CONICET), Centro de investigaciones en Ciencias de la Tierra, (CICTERRA). Córdoba, Argentina.

5 Sirindhorn Museum, Department of Mineral Resources, Sahatsakhan, Kalasin 46140, Thailand.

* Corresponding author email: pitaksit.d@cmu.ac.th

Abstract

Several Upper Paleozoic successions sparsely crop out in Northern Thailand. Most of them are Permian carbonate rock while fossiliferous siliciclastic strata with continue succession is rare and not wildly distribute. The study area, Doi Tu Pu, is an about 110x120 m2 old quarry, located at Taweerat Community, Rimkok Sub-district, Mueang Chiang Rai District. According to previous works, this area was Carboniferous (Braun and Hahn, 1976), Permian (DMR, 2007). Sedimentary succession is dominantly composed of black mudstone/siltstone interbedded with very thin- to thin-bedded sandstone. A facies study reveals a relatively shallow environment. Fossil remains commonly include brachiopods, gastropods, crinoids, corals, bryozoans, plants and trilobites. Trilobites were found in black silty mudstone, at least from three different beds. Totally, 109 specimens were randomly collected from those three fossiliferous mudstone beds. Trilobite sample consists of 24 cephalons, 1 thorax and 84 pygidiums. The majority are incomplete and/or disarticulated. A preliminary analysis of the systematics identified them as order Proetoida. They show similar morphological features to Thaiaspis setthabutti Kobayashi (1961) and Brachymetopus nakornsri found from Middle-Upper Carboniferous in Loei Province and described by Kobayashi and Hamada (1989). These species are restricted to the Moscovian age. Since the trilobites from Doi Tu Pu can be comparable to trilobite assemblage from Loei Province, the age of Doi Tu Pu succession can be suggested to Middle-Upper Carboniferous. Moreover, the wide sample of pygidia allows an analysis of their size (length over width, number of axial rings and pleural lobes). This

study highlights the presence of several ontogenetical instars. Consequently, a geometric morphometrics analysis will be performed in order to describe precisely their developmental trajectory. This work is a special project of a high school student under the Development of Promotion Sciences and Technology (DPST). The project objective is to apply the scientific method to the palaeontological study and to participate in the research working group of geologists. The selected topic allows the student to understand how to collect prepared and classify the fundamental fossils, Trilobita.

Key words: Trilobite, Upper Paleozoic, Doi Tu Pu, Chiang Rai Province, Northern Thailand

Proceedings of the Second International Symposium on Geoscience Resources and Environments of Asian Terranes (GREAT 2018)
19 - 23 November 2018 Bangkok, Thailand

Preparation of standard material for EPMA techniques for Uranium and Thorium analyses

Sopit Poompuang[1]

1 Department of Geology, Faculty of Science, Chulalongkorn University, Bangkok 10330, Thailand

Abstract

Uranium (U) and thorium (Th) are radioactive elements that constitute trace amount in the nature. They are important elements used in determination age of rocks using Electron Probe Micro Analyzer (EPMA) methods. The method is used on polished surface of solid sample and required standard samples that normally need to be imported at high prices. This study aims at developing a standard sample particularly for uranium and thorium analyzes for our domestic use.

The certified standard powdered material of uranium and thorium are used in preparation of our uranium and thorium standards samples, the powdered material is melted at temperatures about 1200° C to make a homogeneous solid before it is molded by resin and then surface get polished. Standard samples are then analyzed by LA-ICP-MS and EPMA. The obtained values are compared to the certified standard material. The results indicate that the values of uranium and thorium are similar reflecting the standard samples are homogeneous which is a characteristic feature of standard materials. This developing of standard samples for EPMA at cheaper price for domestic uses is proved possible.

Key words: Standard materials; Radioactive substances radiographs; EPMA

Proceedings of the Second International Symposium on Geoscience Resources and Environments of Asian Terranes (GREAT 2018)
19 - 23 November 2018 Bangkok, Thailand

Beach morphodynamic response to Northeast monsoon surge at the Gulf of Thailand

Sumet Phantuwongraj[1]* and Montri Choowong[1]

1 Morphology of Earth Surface and Advanced Geohazards in Southeast Asia Research Unit (MESA RU), Department of Geology, Faculty of Science, Chulalongkorn University

* Corresponding author: phantuwongraj.s@gmail.com

Abstract

Coastal area along the southern part of Thailand at the Gulf of Thailand side was normally affected by the Northeast (NE) monsoon surge during the winter season. The high energy wave impact at the coastline, resulting from strong wind, is usually causing the geomorpholocigal change at the coastal area. Erosional features such as beach scarp, scour, and breached sand barrier are commonly observed after the NE monsoon surge event. After the event, the erosional area, especially at the beach, were commonly recovered themselves by landward deposition of sediments from the nearshore processes. However, the rate of beach recovery is not the same throughout the coastline but it's different from place-to-place. At the area of high recovery rate, it can get the sediment to deposit and fill up the erosional space in one year. In contrast, at the area of low recovery rate, it might take several years to get the sediment back at the same place. Thus, the erosional features such as scour or breached beach or dune are still preserved.

This study we used field survey data including beach profiles and sedimentary characteristics of surficial beach sand to investigate the beach morphodynamic in the affected area of NE monsoon surge. The rate of beach recovery will calculate and then compare throughout the study sites. Coastal topography and geomorphological units of the area will be classified by using remote sensing data and field survey data. Beach profiles data were collecting by total station before-during-and after the NE monsoon surge for observe the change of beach topography. Surficial beach sediment also collected at the same area of beach profile for comparing the change of its characteristic.

After the NE monsoon surge events, most of the study sites showed erosional features such as beach scarp. Beach in the study sites were eroded at the average distance of 7 meters. However, at some sites, beach profile data show the depositional behavior of sediment after the monsoon surge event. Beach morphodynamic change are including; beach erosion, nearshore sand bar movement, foreshore deposition, and backshore deposition. Beach recovery characteristics in the study area can be devided into two major type including foreshore recovered and backshore recovered.

Key words: Beach morphodynamic, Coastal erosion, Beach recovery, Northeast monsoon surge, Gulf of Thailand.

Proceedings of the Second International Symposium on Geoscience Resources and Environments of Asian Terranes (GREAT 2018)
19 - 23 November 2018 Bangkok, Thailand

2-D gravity data modelling and interpretation of Mae Suai Basin, Chiang Rai Province

Suebchat Kanthiya[1], Niti Mangkhemthong[1]* and Christopher K. Morley[1]

1 Department of Geological Sciences, Chiang Mai University, Chiang Mai, 50200, Thailand.

*Corresponding author e-mail: niti.ace@gmail.com

Abstract

The Mae Suai Basin, an intermountain basin in Northern Thailand, became an area of interest in 2014 after an occurrence of the M6.1 earthquake that epicenter locations may associate with basin-bounding fault structures. Total 627 gravity stations with a spacing of ~500 m were collected; standard gravity correction methods were applied to produce the residual Complete Bouguer anomaly (CBA). The residual CBA shows gravity lows are located within the basin that are bounded by gravity highs in regions of granite and metasedimentary basement to the west and east, respectively. Analysis of geophysical lineaments and basin depth estimates indicate fault lineaments lie along the eastern, northern, and southern parts of the basin. The 2-D gravity models suggest that the MSB is an asymmetrical half-graben geometry with the maximum basin depth of ~700 m controlled by the Mae Suai Fault on the eastern boundary. Interpreted normal fault patterns show the Mae Suai Fault lies in a releasing bend configuration, linked by the NE-SW strike-slip faults of the northern and southern boundaries.

Key words: Thailand Cenozoic basins, Gravity, 2-D geophysical model, Mae Suai Basin, Mae Lao faults.

1. Introduction

Subsurface geology of the Mae Suai Basin (MSB) is poorly defined due to the absence of surface exposures, and only shallow geophysical data (<100 m) of resistivity interpretations provided by Department of Mineral Resources, DMR (2014) and Department of Groundwater Resources, DGR (2009). Based on a surficial data interpretation, Uttamo, Elders, and Nichols (2003a) suggested the MSB is an extensional basin within the zone of Cenozoic rifts in northern Thailand (Figure 1a). The associated left-lateral strike-slip Mae Lao Fault (MLF) to the northeast of the Mae Suai area may have been activated during the high magnitude (M6.1) earthquake on May 5th, 2014 (U.S. Geological Survey, 2014), even though the epicenter location of the main shock was

located in Pan District, Chiang Rai province (Noisagool et al., 2016). Consequently, understanding the basin geometry and related fault geometries has become important for understanding the context of seismicity in the area. In order to understand the subsurface geometry and structure in the basin, a ground gravity survey is the first key method to determine the geometry of MSB where density lows are related to the basin fill and density highs are present over the surrounding basement terrain. Gravity measurement can utilize variations in the gravitational field where density contrasts are present, particularly lateral variations associated with geology of subsurface (Hinze et al., 2012).

This study reveals the subsurface geometry of the MSB using a ground-based gravity survey that covers part of the Mae Suai District. Numerical geophysical filtering techniques were applied to the gravity data to enable the production of 2-D cross-section models of the basin morphology. Gravity data filtering and modeling were processed on the Geosoft Oasis montaj® software package. The aims of the processing were to detect the basin boundaries and estimate the basin depth. Geophysical processing techniques of total horizontal derivative, Euler deconvolution, the second order (2nd) of horizontal derivative, radial spectral analysis, and depth to basement were applied to better constrain the basin boundaries and for fault detections. Four 2-D forward models were generated using the 2DGM-SYS Module® in order to construct a subsurface model of the MSB. We also compared our 2-D gravity modeling results to geological information to help confirm the MSB's subsurface structures.

2. Background Geology

The MSB is one of around forty intermountain basins in Basin and Range Province of Northern Thailand that graphically trends N-S. The basin is 30 km long and 60 km wide (DMR, 2007; Uttamo et al., 2003a, Figure 1a). The low-relief region of the basin area is mostly filled with Tertiary and Quaternary accumulations in an intermountain basin. The basin sediments were locally derived from the topographically high terrains of the granite pluton to the west and metasedimentary-sedimentary assemblages to the east. The metasedimentary assemblage comprises Silurian-Devonian units composed of phyllite, calc-silicate phyllite, and chert (DMR, 2007). Piyasin (1972) estimated the thickness of this basement at 1500 m. The Carboniferous unit of sandstone, shale, and limestone that is exposed

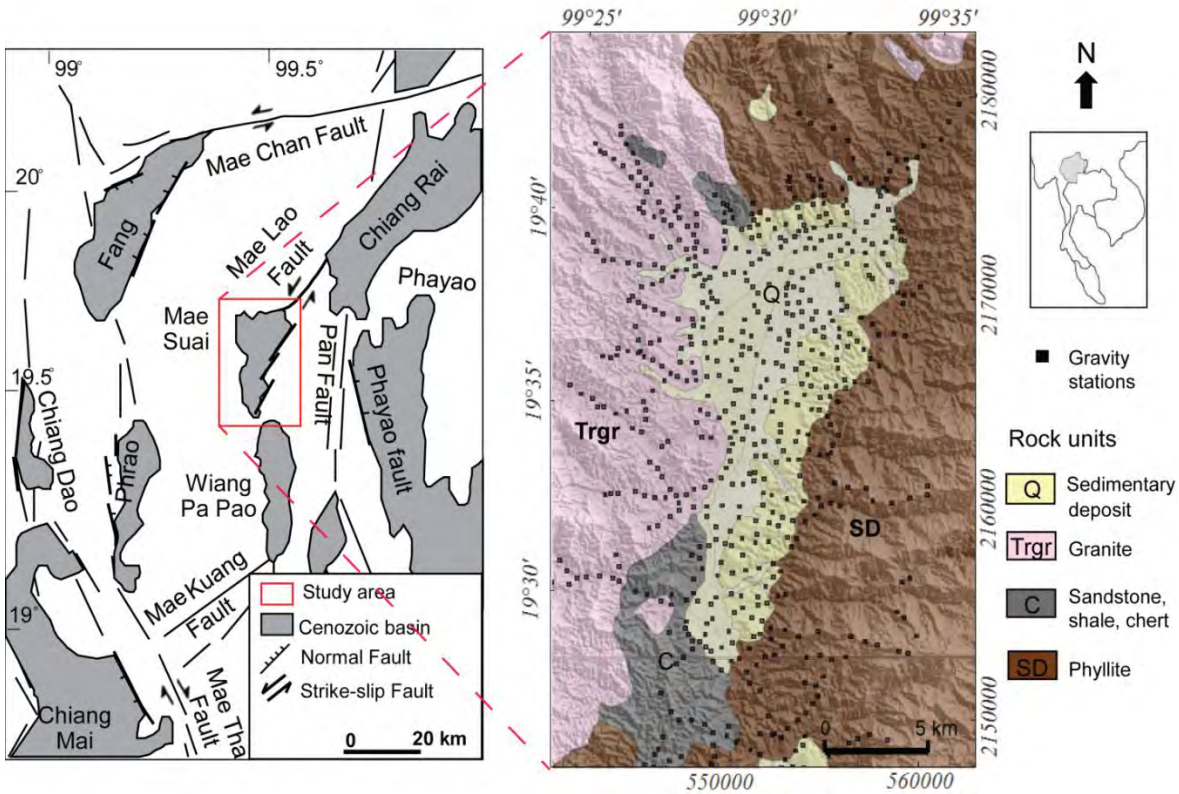

Figure 1. (a) Structural relationship between strike-slip faults, normal faults, and the Cenozoic rift basins in Northern Thailand (modified from Uttamo et al., 2003a). A red rectangle marks a surveyed area of MSB. (b) Simplified geologic map of MSB and surrounding area is overlain by collected gravity stations (modified from DMR, 2007).

in small patches in the western region was mapped as unconformably overlying the Silurian-Devonian unit (Barr et al., 1990). The Carboniferous clastic rocks found to the southwest are Mae Tha Formation which has a thickness of about 400 m (Bunopas, 1981). The granite intrusion is interpreted as the youngest basement unit which is grouped as the Triassic Fang Batholith (Cobbing, 2011) (Figure 1b).

The Cenozoic Basin and Range provinces in Northern Thailand have formed under the major strike-slip fault systems that caused the opening of N-S trending rift basins. The faults trend ENE-WSW and NW-SE (Rhodes et al., 2004), e.g. the NNW-trending Phayao Fault zone (PFZ), and the ENE-trending Mae Chan Fault zone (MCFZ), (DMR, 2014; Uttamo et al., 2003a) (Figure 1a). The PFZ trends N-S, is 35 km long and acts as an oblique slip fault with dextral and normal motion, the fault runs parallel to the western margin of the southern part of Chiang Rai Basin. The MCFZ is 150 km long and acts as a sinistral movement along the ENE-WSW direction in the northernmost part of

Thailand (Morley, 2007). This fault terminates at the northern tip of Fang basin (Uttamo et al., 2003a). One major fault that lies parallel to MCFZ is the left-lateral strike-slip Mae Lao Fault (MLF) which runs along the northern part of the MSB (Uttamo et al., 2003b).

3. Materials and Methods

3.1 Gravity data collection and data reduction

The gravity data collected for this study covers an area of 600 km2 in the Mae Suai District. The data was acquired using a CG-3 Autograv gravity meter with data survey accuracy of 0.01 mGal, to obtain a total of 627 gravity stations with an observation spacing of around 500 m. A high accuracy differential GPS was used to control the vertical elevations of all gravity stations. The GPS has a post-processing accuracy of less than 0.2 m. The collected gravity data contained temporal variations ranging around 0.05-0.2 mGal per a 3-5-hour survey loop due to the Earth tidal and measurement drift that had to be linearly eliminated (Robinson and Crouch, 1998). The Latitude correction was applied to minimize the gravity effect of the Earth's elliptical shape and rotation. The 1967 International Gravity Formula (IGF67) for datum reference was used for Free-air and Bouguer slab corrections where an applied reduction in density of 2.67 g/cm3 was used. Mass effects due to topography surrounding the observation site have to be minimized. The Terrain correction method described by Whitehead and Musselman (2006) added to the SBA yields the Complete Bouguer Anomaly (CBA). The trend analysis has to be processed to ideally eliminate the long wavelength gravity anomaly generated from deep regions. Therefore, the residual CBA (Figure 2) has been produced for geophysical interpretation and analysis using the minimum curvature gridding method with a grid cell size of 270 m.

3.2 Gravity data processing

The structural boundaries of the MSB in the 2-D modeling process are constrained using the edge detection techniques for gravitational field data consisting of the Total horizontal derivative, the Euler deconvolution, and the 2nd horizontal derivative. The horizontal derivative (THDR) method produces maximum ridge of anomaly gradients over the contacts between different densities among subsurface rock units that are caused by features such as stratigraphic or structural contacts which juxtapose units of different densities (Whitehead and Musselman, 2006). We applied the Euler Deconvolution technique of three

orthogonal gradients along x, y, and z axes of potential field to integrally estimate subsurface locations in both horizontal and vertical (depth) dimensions of an anomaly source (Reid et al., 1990). In practice, Structure Index and Window Size are run together with gradient data in the least-square inversion to deconvolve the subsurface location (Hinze et al., 2012). Note that appropriate parameters of Euler calculation for ideal fault contacts were set at a Structure Index of 0 and a Window Size of 15 (Whitehead and Musselman, 2006). Moreover, determination of fault trends associated with the interpreted faults of previous surface studies (e.g. MLF and MSF) could be achieved by a zero trending of the 2nd horizontal derivative method in the appropriated gradient directions (e.g. azimuths 135o and 100o) (Whitehead and Musselman, 2006) perpendicular to the structural target of fault strikes. These possible fault lineaments can be identified and mapped. In order to determine the basin depth to basement, we also applied a semi-automatic source detection using the technique of Analytic Signal Amplitude called the Pdepth method to yield subsurface depth constraints along the 2-D profiling data. The depth to basement solutions are calculated by discrete depth solutions of assumed structural contacts (Nabighian, 1972; Thurston and Smith, 1997; Whitehead and Musselman, 2006) and represented as clustered points of the structural contact locations. The used parameters for computing discrete depth solutions by moving spatial window were set between 500 m to 2000 m of the minimum and maximum window operator length, respectively, with a 100 m expansion increment.

3.3 2-D Forward gravity modeling

The 2-D forward modeling of gravity data was constructed to reveal the subsurface geometry information based on the Talwani et al. (1959) method. Four profiles of 2-D gravity models have been constructed extending about 10 km in a NW-SW direction perpendicular to a basin orientation. Because of the non-uniqueness limitation of gravity modeling and the absence of other subsurface data, all available surface and subsurface data constraints from the integration of earlier gravity data analysis are considered in the forward modeling to minimize gravity misfits between observed and calculated gravity anomaly data and accomplish the most reasonable geological model. Appropriate densities from 12 rock samples and standard rock's density information (e.g. Telford et al., 1990; Wattananikorn et al., 1994) were used as

Table 1 Rock density estimations for 2-D forward gravity modeling.

Rock units	Rock density (g/cm^3)		
	Density estimation from rock samples	Telford et al. (1990)	Wattananikorn et al. (1995)
Triassic granite (3 samples)	2.64 ±0.03#	2.64	2.62
Silurian-Devonian metasedimentary rocks (5 samples)	2.69 ±0.05#	2.71	-
Carboniferous Sedimentary rocks (4 samples)	2.55 ±0.07#	2.35	-
Tertiary Sediments	-	2.2#	2.15 to 2.3

#densities were used for 2-D forward gravity modeling.

modeling parameters (Table 1). Four density blocks have been modeled comprising: 1) Cenozoic sediments with density of 2.2 g/cm3, 2) Silurian-Devonian metasedimentary rocks with a density of 2.68 g/cm3, 3) Carboniferous sedimentary rocks with a density of 2.55 g/cm3, and 4) Triassic granitic rocks with a density of 2.65 g/cm3. Note that these pseudo-geological models were created with an assumption that the Earth has no curvature and the model can be extended to an infinite distance to unconsidered lateral edge effects of the density body (Taiwani and Heirtzler, 1964).

4. Results and Interpretation.

4.1 Gravity anomaly interpretation and data analysis

The residual CBA (Figure 2) reveals the regions of gravity anomaly variation of -13 to 7 mGal associated with density contrasts due to different lithologies. This gravity anomaly map roughly classifies features over the basin and pre-Cenozoic basements. By comparison with the geologic map (Figure 1b), gravity anomaly lows (L) correspond well to a basin locality which is associated with Cenozoic sediment units. Whereas gravity highs (H) bound the basin to the northern, eastern and southern margins and correspond with relatively high-density Paleozoic metasedimentary rocks. The moderate gravity anomalies (M) fit to the felsic basement rock type which is compatible to the lower density of Triassic granite intrusion.

The Total horizontal derivative (THDR) that was applied to the residual CBA represents the lateral boundary of basin anomalies and the contact boundaries of rock units. The

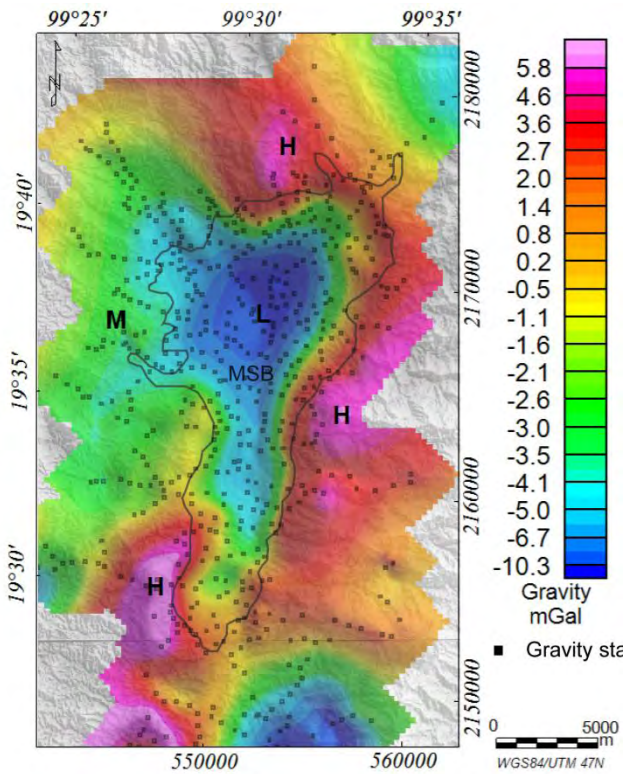

Figure 2. Residual Complete Bouguer anomaly map of Mae Suai area overlying a DEM data. Gravity variations of lows, moderates, and highs are labeled as L, M, and H, respectively.

interpreted lineament results, which are showed by largest gradient anomalies, clearly separate the basin area from the surrounding rocks at the northern, southern, western, and eastern basin edges (Figure 3a). These structural contact anomalies are oriented in NNE-SSW, NNW-SSE, NE-SW, and NW-SE directions.

Figure 3b illustrates Euler's depth solutions of clustered points that are located at structural contacts bounding the basin in subsurface. The clustered depth solutions along the western margin are calculated between 300 and 500 m (Figure 3b). The depth solutions of the northern margin yielded average depths as deep as 1000 m (Figure 3b). The eastern margin with depths between 700 to 1300 m suggests the presence of normal boundary faults as identified in a previous study (Uttamo et al., 2003a).

The 2nd horizontal derivative map along the SE-gradient (azimuth 135o) interprets two main fault striking systems that trend NE-SW and lie at the northern and southern margins of the basin (Figure 3c). The structural interpretation of zero-trending lineaments represents faults following the orientation of the sinistral movement of MLF (Uttamo et al., 2003b). The 2nd horizontal derivative along the ESE-gradient (azimuth 100o) enhances the structural fault contact interpretations along the straight, nearly NNE-SSW oriented lineaments at the eastern and western basin margins (Figure 3d). The normal-slip of Mae Suai Fault (MSF) may be related to the interpreted linear segments in the east.

A combination of qualitative gravity interpretations indicates the presence of ten structural lineaments (Lineaments F1 to F10) (Figure 4a) that corresponds with the recognized basin boundaries that may, or may not be controlled by faults. Based on a relation

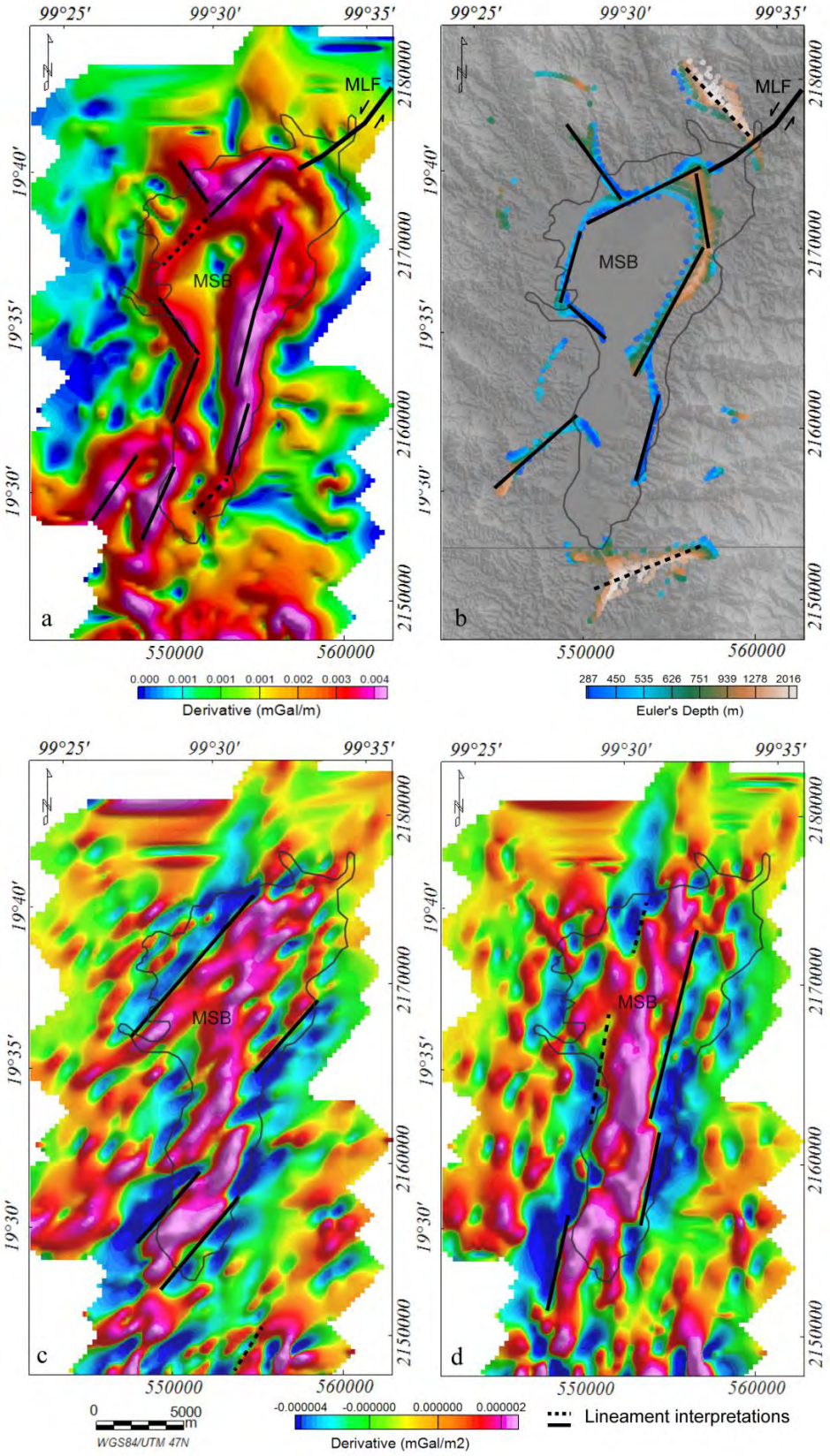

Figure 3. Lineament interpretations displaying on (a) the total horizontal derivative anomaly, (b) the Euler deconvolution's cluster solutions, (c) the 2nd horizontal derivative anomaly along the SE-gradient direction (azimuth 135°), and (d) the 2nd horizontal derivative anomaly along the ESE-gradient direction (azimuth 100°). The interpretations relate to either fault or unconformity contacts.

to known major faults and geological features (Figures 1 and 4), we suggest Lineaments F3 and F5 are fault segments related to the MLF that may displace as the sinistral movement (Uttamo et al., 2003b, Figure 1a). Lineaments F6 and F7 to the east are possibly related to the segments of normal-slip of MSF (Khamphira, 2016; Uttamo et al., 2003b, Figure 1a). On the western margin, other lineaments (F2, F4, F8, F9, and F10) mark unconformity contacts between basin sediments and pre-Cenozoic basement rocks (Barr et al., 1990) (Figure 4b).

4.2 Pseudo geological interpretation of the 2-D gravity models

The 2-D models from gravity data produce the representative subsurface geometry of MSB that suggest the MSB exhibits a maximum basin depth of about 700 m on the northern profiles of Profiles MS1 and MS2 and about 600 m on the southern profiles (Profiles MS3 and MS4) (Figure 6). The basin is bounded by metasedimentary, sedimentary, granite intrusion of basement along the eastern, western, westernmost boundaries, respectively (Figure 6). The steep eastern basin boundary is locally controlled by major west-dipping faults (F6 and F7) and their parallel intra-basin fault (F6S). A Silurian-Devonian metasedimentary unit is modeled as the main lithology underlying the basin. A small block of the Carboniferous sedimentary unit is constructed as an unconformable layer resting on the older Silurian-Devonian unit (Barr et al., 1990). The younger Triassic granite pluton with unconstrained shaped crosscuts the two older basement units to the west. In terms of basin depth, geometry, and structure, our interpretations seem to be reasonable and associated with the well-known Cenozoic basins that have been investigated previously, for example, Li Basin (DMR, 2001; Morley et al., 2000) and Mae Moh Basin (Morley and Racey, 2011).

5. Discussion

The gravity gradient map exhibits NE-SW trending contours at the northern and southern parts of the MSB, which are probably related to fault segments that run parallel to the major MLF (F3 and F5, Figure 4b). The strike-slip interpretation of the MLF at the northeastern part (Uttamo et al., 2003a and b) possibly links through the extensional bounding fault system with the southern fault segment (F5, Figure 4b) based on gravity data interpretation. Interpretation of left lateral displacement of the moment tensor solution by Noisagool et al. (2016) and the larger scale high conductive fault zone of the Magnetotellurics

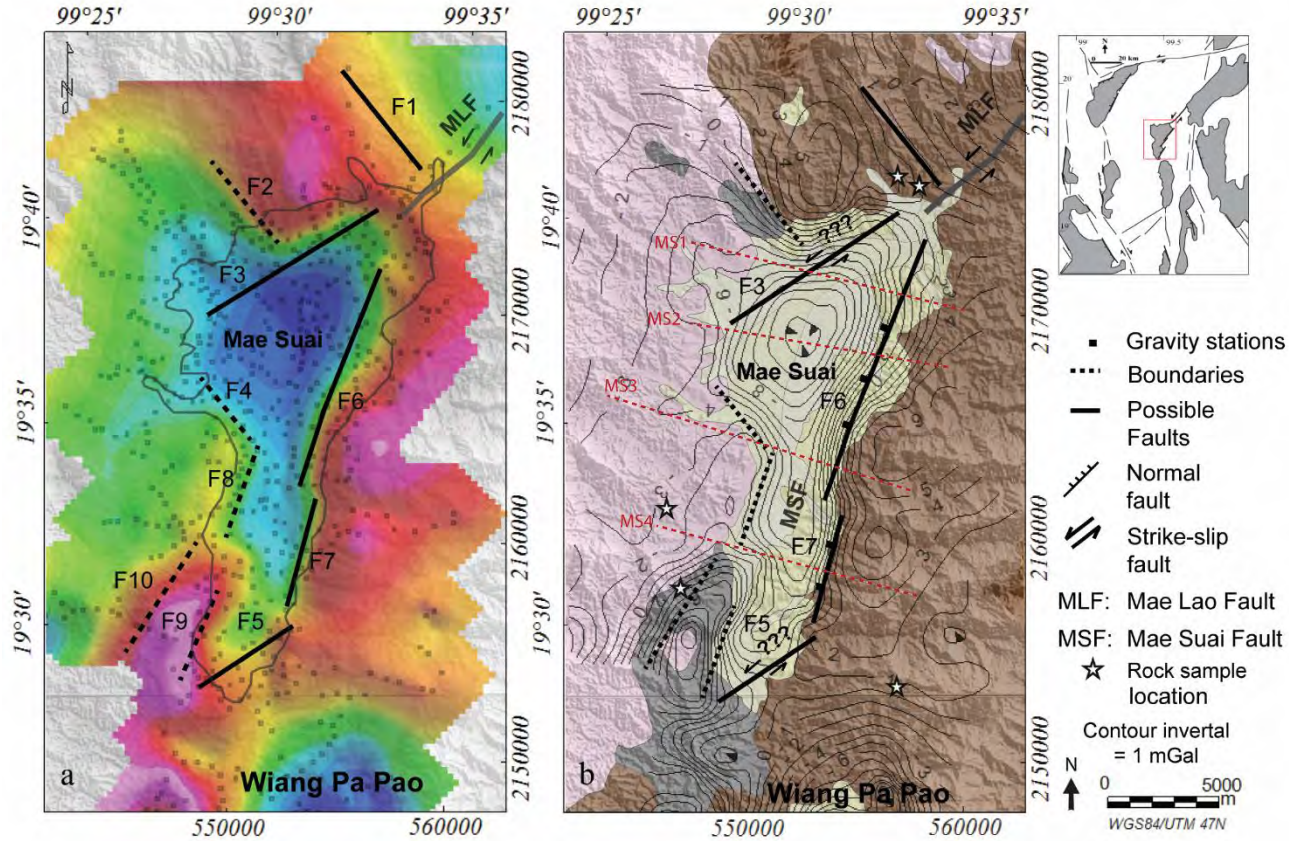

Figure 4. (a) Ten structural lineaments interpreted from integrated gravity edge detection techniques overlying the residual CBA. (b) Possible fault interpretations and senses of movement overlying the geologic map with the residual CBA contour patterns. Black dashed lines F2, F4, F8, F9, and F10 are probably unconformity contacts. Red dashed lines are the 2-D forward gravity modeling profiles.

inversion solution by Boonchaisuk et al. (2017) also seem compatible with the orientation of northern fault (F3, Figure 7b). However, the relationship between the northern segment (F3) and these previous study interpretations of MLF is ambiguous due to the inadequate surface evidence of a fault.

A pseudo E-W geological cross-section shows the MSB forms a half-graben structure controlled by the eastern boundary fault system of the MSF (F6 and F7, Figures 6 and 7). The 2-D gravity models suggest at least two normal fault segments with its systems comprise the west dipping normal faults at the eastern basin boundary (Figure 7) which is called the MSF system. The MSF system interpretation is also consistent with the structural lineaments based on Landsat satellite imagery (Khamphira, 2016) (Figure 7b). We interpret the western boundary of the basin as a nonconformity contact with the

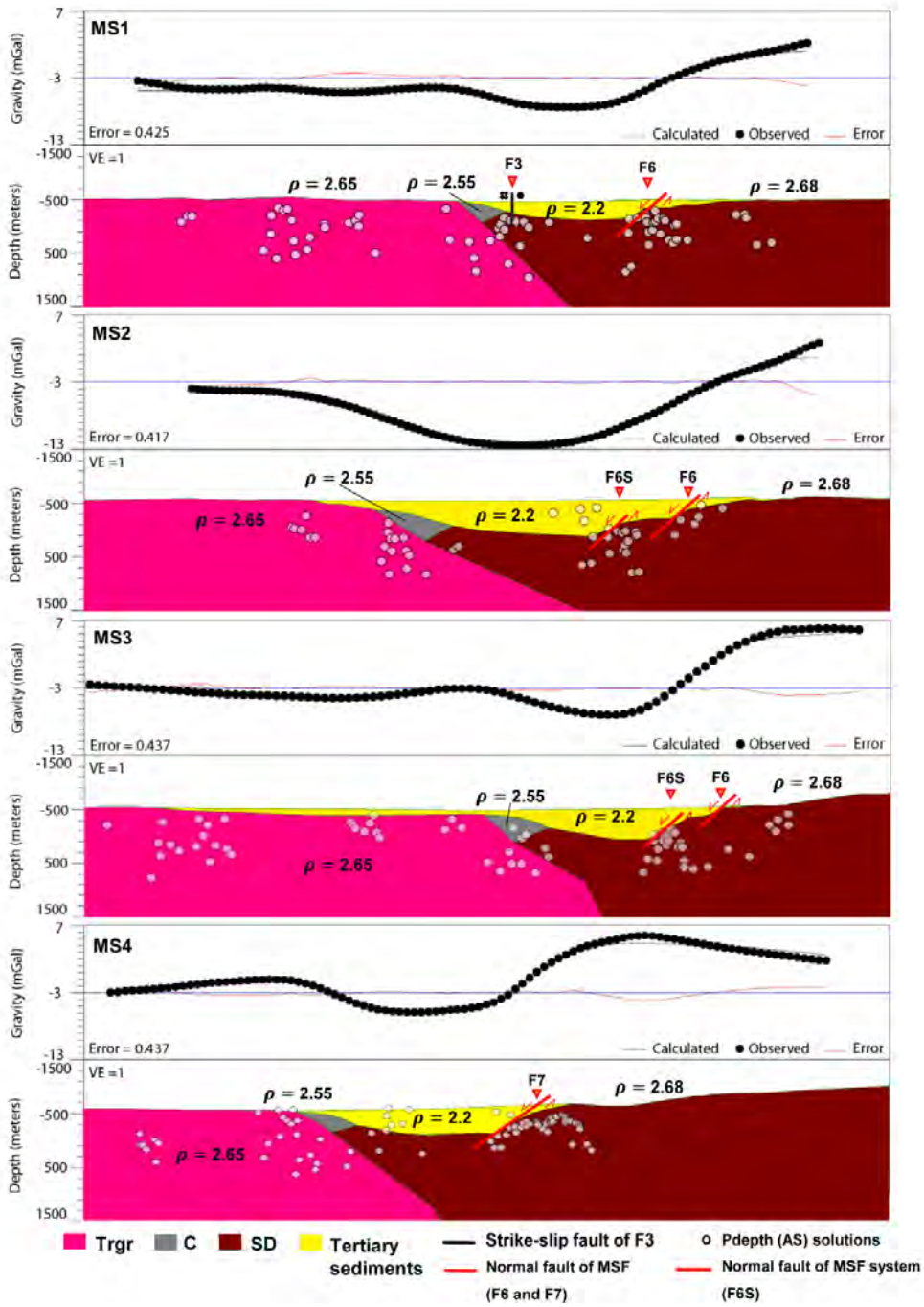

Figure 5. 2-D forward gravity profiles representing a half-graben geometry with the maximum basin depth of about 700 m. Densities are in g/cm3. Fault interpretations are based on gravity anomaly interpretation and analysis. White circles are depth estimation of the Pdepth method.

Triassic granite intrusion (Cobbing, 2011). However, these fault systems in the west need a further geological investigation to better understand their structures and association with the basin margin.

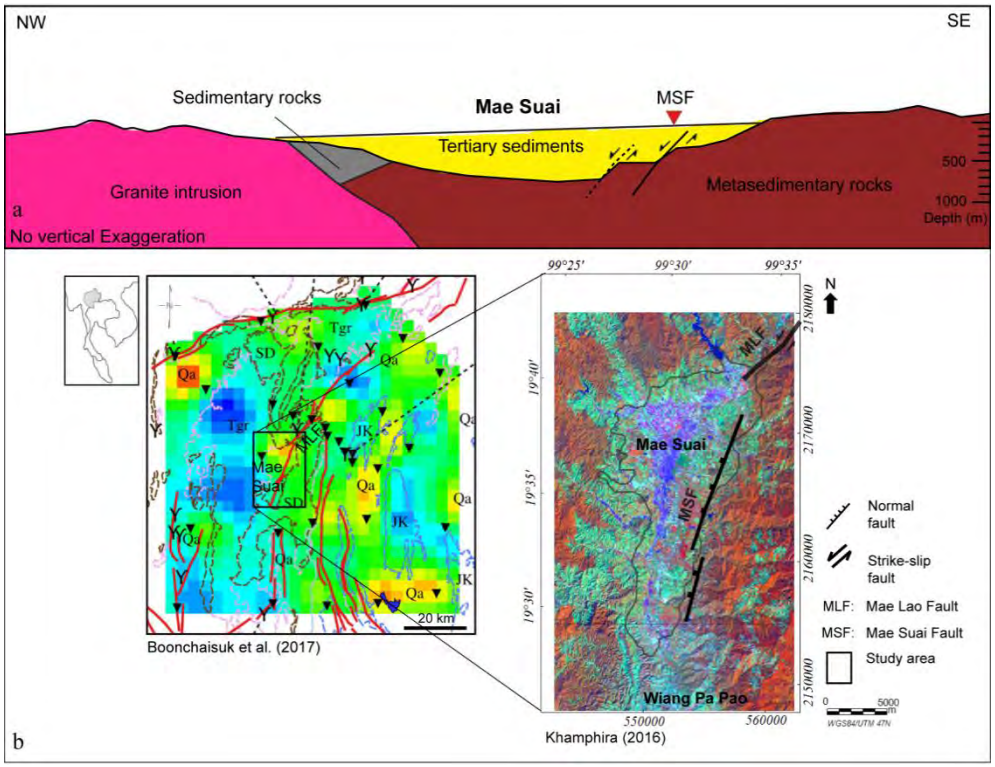

Figure 6. (a) Simplified geologic cross-section showing a half-graben structure controlled by the eastern boundary fault of Mae Suai Fault. (b) The fault interpretations correspond well with previous studies of Boonchaisuk et al. (2017) and Khamphira (2016) who have mentioned the faults on the eastern part of the basin.

6. Conclusions

Geologic cross-sections of the subsurface geometry of the MSB and related fault structures were created based on new gravity anomaly data analysis and 2-D gravity modeling. These results show that the maximum basin depth of the MSB is approximately 700 m. The basin boundary and fault locations corresponded well with previous studies that identified bounding faults on the northern, southern, and eastern parts of MSB. The NE-SW trending strike-slip faults at the northern margin of the basin correspond with the Mae Lao Fault orientation. A similarly trending strike-slip fault zone is interpreted on the southern margin. The eastern margin is dominated by a NNE-trending normal fault zone related to the Mae Suai Fault. Therefore, the MSB has an extensional half-graben structure where the eastern margin is bounded by the NNE-trending Mae Suai Fault. Consequently, the basin formation can be interpreted to form an extensional transfer zone where the strike-slip faults at the northern

and southern margins link with the normal faults system at the eastern margin.

7. Acknowledgments

We are thankful to Chaisri, S. and Tulyatid, D. for discussions related to geophysical and geological backgrounds. We extremely thank for Yawichai A., Minin, T., and Sangthip C. for gravity data acquisition support. We acknowledge the DPST Graduate with First Placement and CMU Graduated Research scholarships for financial supports. This research was also funded through the supporting of the gravity processing software from the Geophysics Research Laboratory at Department of Geological Sciences, Chiang Mai University.

8. References

Barr, S. M., Tantisukrit, C., Yaowanoiyothin, W., Macdonald, A. S. 1990. Petrology and tectonic implications of Upper Paleozoic volcanic rocks of the Chiang Mai belt, northern Thailand. Journal of Southeast Asian Earth Sciences, 4(1), 37-47.

Boonchaisuk, S., Noisagool, S., Amatyakulb, P., Rung-Arunwan, T., Vachiratienchaic, C., Siripunvaraporn, W. 2017. 3-D magnetotelluric imaging of the Phayao Fault Zone, Northern Thailand: evidence for saline fluid in the source region of the 2014 Chiang Rai earthquake. Journal of Asian Earth Sciences, 147, 210-221.

Bunopas, S. 1981. Paleogeographic history of western Thailand and adjacent parts of Southeast Asia-A plate tectonics interpretation: Victoria University of Willington, (unpublished Ph.D. thesis), reprinted 1982 as Geological Survey Paper no.5, Geological Survey Division, Department of Mineral Resources, Bangkok, 810.

Cobbing, E. J. 2011. Granitic rocks. In M. F. Ridd, Barber, A. J., and Crow, M. J. (eds.), The geology of Thailand, Geological Society, London, pp. 441-458.

Department of Groundwater Resources. 2009. Potential groundwater potential assessment project. (Chiang Rai-Phayao). Department of Groundwater Resources, Bangkok (in Thai).

Department of Mineral Resources. 2001. Geology of Thailand. Department of Mineral Resources, Ministry of Natural Resources and Environment, Bangkok (in Thai).

Department of Mineral Resources. 2007. Geological map of Thailand 1:250,000.

Department of Mineral Resources, Bangkok.

Department of Mineral Resources. 2014. Report of geophysical survey in active fault area at Chiang Rai Province, 5th May 2014, Department of Mineral Resources, Bangkok (in Thai).

Hinze, J. W., Vonfrese, R. R. B., Saad, A. H. 2012. Gravity and Magnetic Exploration-Principles, Practice and Applications, Cambridge University, New York.

Khamphira, C. 2016. Geomorphologic and earthquake evidence for faulting in Wiang Pa Pao – Mae Suai Basin, Chiang Rai Province. Chiang Mai University (in Thai).

Morley, C. K. 2007. Variations in Late Cenozoic-Recent strike-slip and oblique-extensional geometries, within Indochina: the influence of pre-existing fabrics. Journal of Structural Geology, 29, 36-58.

Morley, C. K., Racey, A. 2011. Tertiary stratigraphy. In M. F. Ridd, Barber, A. J., and Crow, M. J. (eds.), The geology of Thailand, Geological Society, London, pp. 223-271.

Morley, C. K., Sangkumarn, N., Hoon, T.B., Chonglakmani, C., Lambiase, J. 2000. Structural evolution of the Li Basin, Northern Thailand. Journal of the Geological Society, 157, 483-492.

Nabighian, M. N. 1972. The analytic signal of two-dimensional magnetic bodies with polygonal cross-section: Its properties and use for automated anomaly interpretation. Geophysics, 37(3), 507-517.

Noisagool, S., Boonchaisuk, S., Pronsopin, P., Siripunvaraporn, W. 2016. The regional moment tensor of the 5 May 2014 Chiang Rai earthquake (Mw = 6.5), Northern Thailand, with its aftershocks and its implication to the stress and the instability of the Phayao Fault Zone. Journal of Asian Earth Sciences, 127, 231-245.

Piyasin, S. 1972. Geology of the Changwat Lumpang Sheet NE 47-7, Scale 1:250000, Report of Investigation, No. 14. Department of Mineral Resources, Bangkok (in Thai).

Reid, A. B., Allsop, J. M., H. Granser, H., Millet, A. J., Somerton, I. W. 1990. Magnetic interpretation in three dimensions using Euler deconvolution. Geophysics, 55(1), 8-91.

Rhodes, B. R., Perez, R., Lamjuan, A., Kosuwan, S. 2004. Kinematics and tectonic

implications of the Mae Kuang Fault, northern Thailand. Journal of Asian Earth Sciences, 24, 79-89.

Robinson, E. S., Crouch, C. 1998. Basic Exploration Geophysics. United States.

Talwani, M. J., Worazel, J. L., Landisman, M. 1959. Rapid gravity computations for two-dimensional bodies with application to the Mendocino submarine fracture zone. Journal of geophysical research, 64(1), 49-59.

Talwani, M., Heirtzler, J. R. 1964. Computation of gravity anomalies caused by two dimensional structures of arbitrary shapes. Geological Sciences, 9, 464-480.

Telford, W. M., Geldart, L. P., Sheriff, R. E. 1990. Applied Geophysics. Cambridge University.

Thurston, J. B., Smith, R. S. 1997. Automatic conversion of magnetic data to depth, dip, and susceptibility contrast using the SPI (TM) method. Geophysics, 62, 807-813.

Whitehead, N., Musselman, C. 2006. Montaj Gravity and Terrain Correction, Gravity Data Processing Extension for Oasis montaj v6.3, Tutorial and User Guide Geosoft Inc., Unpublished document, Toronto.

Uttamo, W., Elders, C., Nichols, G. 2003a. Relationships between Cenozoic strike-slip faulting and basin opening in northern Thailand. In F. Storti, Holdsworth, R. E., and Salvini, F. (eds.), Intraplate Strike-Slip Deformation Belts, Geological Society, London, Special Publications, pp. 89-108.

Uttamo, W., Singharajwarapan, S., Kantaroj, W., Chantarapaserd, S. 2003b. Tectonic settings and mineral deposits at Mae Suai-Wiang Pa Pao Area, Northern Thailand. Chiang Mai University (in Thai).

U.S. Geological Survey. 2014. M 6.1-13km NNW of Phan, Thailand. Retrieved from http://earthquake.usgs.gov/earthquakes/eventpage/usb000qack#shakemap

Wattananikorn, K., Beshir, J. A., Nochaiwong, A. 1994. Gravity interpretation of Chiang Mai Basin, northern Thailand: concentrating on Ban Thung Sieo area. Southeast Asian Earth Science, 12(1-2), 53-64.

Proceedings of the Second International Symposium on Geoscience Resources and Environments of Asian Terranes (GREAT 2018)
19 - 23 November 2018 Bangkok, Thailand

Carbon isotope profile for Guadalupian–Lopingian paleo-atoll carbonates in Japan

Teruyuki Maruoka[1]* and Yukio Isozaki[2]

1 Faculty of Life and Environmental Sciences, University of Tsukuba, Ibaraki, Japan

2 Department of Earth Science and Astronomy, The University of Tokyo, Meguro, Tokyo, Japan

* Corresponding author email: maruoka.teruyuki.fu@u.tsukuba.ac.jp

Abstract

A mass extinction event occurred around the Guadalupian–Lopingian (or Middle–Late Permian) boundary (G-LB; 260 Ma). Immediately before the G-LB, a significant change in the global carbon cycle occurred in the superocean Panthalassa, as indicated by the extremely high δ13C values for carbonate (up to + 6 ‰). This carbon isotopic signal was named as the "Kamura event" after the Kamura section in Japan. In order to understand the environmental conditions during the Kamura event, we analyzed the secular changes in the carbon isotopic ratio of the bulk organic matter in the Middle-Upper Permian carbonates of an accreted mid-oceanic paleo-atoll complex in Japan, where the Kamura event was first documented. The isotopic signatures from the mid-Panthalassan paleo-atoll complex provide valuable information within a global context of the extinction-related environmental changes around the G-LB. The high δ13C values of carbonate during the Capitanian (late Guadalupian) were associated with large isotopic differences between carbonate and organic matter (Δ13C = δ13Ccarbonate – δ13Corganic). Correlations were observed between δ13Ccarbonate and Δ13C during the Capitanian and Wuchiapingian (early Lopingian); however, their slopes and intercepts were observed to be different. Based on the analysis for the δ13Ccarbonate–△13C correlations proposed by Rothman et al., we infer that the Capitanian Kamura event involved an unusually large amount of dissolved organic matter (DOC), which possibly was retained in the expanded oxygen minimum zone (OMZ) at mid-depth; such a DOC reservoir likely disappeared at the G-LB. As the decline in Middle Permian marine biodiversity started during the early half of the Capitanian, the decline might be related to the expansion of OMZ.

Key words: Guadalupian–Lopingian mass extinction, Panthalassa, Extremely high δ13C Kamura event

Proceedings of the Second International Symposium on Geoscience Resources and Environments of Asian Terranes (GREAT 2018)
19 - 23 November 2018 Bangkok, Thailand

An evidence of large paleo-earthquake of the Mae Chan Fault in Mae Chan, northern Thailand

Weerachat Wiwegwin[1]*, Suwith Kosuwan[1], Jutamas Junpangngern[1], Rawee Phumsonklin[1], Piyaporn Hinsaeng[1], Ray Weldon[2], Elise (LiLi) Weldon[2] and Shi Xuhua[3]

1 Department of Mineral Resources, Thailand

2 Earth Science Department, University of Oregon, Eugene, USA

3 Earth observatory of Singapore, Singapore

*Corresponding author email: Weerachatto23@gmail.com

Abstract

We applied remote sensing and aerial photographic techniques to a study of the NE-SW trending Mae Chan Fault, located in the Mae Chan, Chiang Rai, northern Thailand. The main morphotectonic landforms associated with the Mae Chan Fault are fault scarps, offset streams, linear valleys, offset ridge crests, beheaded streams, hot springs, and linear mountain fronts. The trench sites crossed the Kio Sa Tai segment of the Mae Chan Fault, at Ban Pong Pa Kham (this study) and Bang Pong Khom (by Weldon et al., 2016), to the west of Ban Pong Pa Kham trench site were compiled, and used to analyse the history of fault movement in the area. The results of trenching of this study and Weldon et al. (2016) revealed young sediments with charcoal, and evidence for at least four ground-rupturing earthquakes on the fault. Based on C14 ages, OSL and TL ages, preliminary ages of the paleo-earthquake events are: (1) 20,000 yr BP; (2) 10,000 yr BP; (3) 8,000 yr BP; (4) 4,000 yr BP and (5) 1,500 yr BP. It is possible that the recurrence interval of seismic event on the Mae Chan Fault appears to be 1,000-3,000 years, and slip rate was roughly estimated as ca. 1.2-1.4 mm/yr. We also estimated paleo-magnitude of paleo-seismic generated by the Mae Chan Fault, using Equation of Wells and Coppersmith (1994), and the paleo-magnitude of the latest paleo-seismic event (possibly occurring at ca. 1,500 yr BP) on the Kio Sa Tai segment was Mw 6.9. Thus, we concluded that the Mae Chan Fault is still active, and it is considered that the Mae Chan area and vicinity may have a high chance for future moderate to large earthquakes.

Key words: Mae Chan Fault, paleo-earthquake, Kio Sa Tai segment, active fault

Proceedings of the Second International Symposium on Geoscience Resources and Environments of Asian Terranes (GREAT 2018)
19 - 23 November 2018 Bangkok, Thailand

Palaeodiet of Some Miocene Proboscidea in Thailand

Yupa Thasod[1]* and Supanut Santikoon[1]

1 Department of Geological Sciences, Chiang Mai University

* Corresponding author email: yupa161@gmail.com

Abstract

Twenty samples proboscidean teeth from Miocene basins in Thailand were carefully analysis on the occlusal surface for microwear characteristics. Each sample was cast and examined by low-magnification microscopy and scanning electron microscopy for the characteristic of the pit and scratches for paleodiet interpretation and the angles of scratch were measure for study the evolution of chewing styles.

The Miocene proboscideans were classified into three groups by quantitative microwear analysis which are browser, more pits and fewer scratches, including Stegolophodon nasaiensis from Na Sai subbasin and Prodeinotherium pentapotamiae from Khorat basin; mixed-feeders, the number of microwear between browsers and grazers, including Stegolophodon cf. latidens from Mae Moh basin and Tetralophodon cf. xiaolongtanensis from Chiang Muan basin; grazers, scratches and fewer pits, including Stegolophodon cf. stegodontoides and cf. Protanancus macinnesi from Khorat basin.

The angle of chewing suggested that S. nasaiensis is the most primitive Stegolophodon follow by S. cf. latidens and S. cf. stegodontoides, respectively. T. cf. xiaolongtanensis was more primitive than S. cf. latidens. P. pentapotamiae is primitive than cf. P. macinnesi and S cf. stegodontoides.

Key words: Microwear analysis, Paleodiet, Miocene Proboscidean, Thailand

Proceedings of the Second International Symposium on Geoscience Resources and Environments of Asian Terranes (GREAT 2018)
19 - 23 November 2018 Bangkok, Thailand

Tectonic Evolution of granitic rocks in the Salam area and Its Environs, Kawthaung Township, Tanintharyi Region, southern Myanmar: Constraints from Petrology, Geochemistry and U-Pb zircon age

Zin Mar Oo[1]*, Khin Zaw[2] and Aung Kyaw Htoon[3]

1 Department of Geology, Mawlamyine University, Mon State, Myanmar

2 CODES Centre of Excellence in Ore Deposits, University of Tasmania, Hobart, Tasmania, Australia

3 Department of Geology, Dagon University, Yangon, Myanmar

* Corresponding author email: misshnin2020@gmail.com

Abstract

The Salam area is mainly composed of metasedimentary rocks (Mergui Group) and NNW-SSE trending granitic rocks. The major rock types of granitic rocks are biotite granite, muscovite-biotite granite and porphyritic biotite granite. Metagreywacke, slate, quartzite and hornfels of metasedimentary rocks (Mergui Group) are commonly observed. In the area, original pelitic, and psammitic rocks were transformed into metasedimentary rocks by two types of metamorphism; regional metamorphism reinforced by local contact metamorphism. The petrochemical analyses of the rocks of the recent studies suggest that the igneous rocks from the study are calc-alkaline and mostly peraluminous types. According to K2O Vs SiO2 diagram, granitoid rocks from the study area fall in High K calc-alkaline to Shoshonite field. The molecular Al2O3/(CaO + Na2O + K2O) ratio of porphyritic biotite granite and biotite granite are mainly (>1.1) and the normative corundum of porphyritic biotite granite and biotite granite mostly >1 wt %; hence, these biotite granites are of S-type granites. The molecular Al2O3 / (CaO + Na2O + K2O) ratios of muscovite-biotite granites are >1.1; the normative corundum of muscovite-biotite granite >1 wt %; hence, these rocks are of undoubtedly S-type granites. Based on the trace elements tectonic discrimination diagram, the granitoid rocks are fitted in the syn-COLG (syn-collision granite) and WPG (within-plate granite). According to Rb/30-Hf-Ta3 triangular plot, the tectonic affinities of granites of the study area show Syn-collosional and late and post-collosional. The granitic rocks are appeared to have been derived from a magmatic process as forceful injection under mesozonal emplacement by the evidences of field occurrences, petrographic and geochemical character. Radiometric dating by U-Pb Zircon age method indicates that the age of Kt.2-Biotite granite

(79.47±0.89 Ma), muscovite-biotite granite (79.36±0.96 Ma) and porphyritic biotite granite (79.01±0.91 Ma). The magmatism in the area is attributable mainly to Indian oceanic subduction and later collision between Sino-Myanmar Ranges during Late Cretaceous.

Key words: metamorphism, metamorphic facies, mesozonal, magmatism, Radiometric dating

Proceedings of the Second International Symposium on Geoscience Resources and Environments of Asian Terranes (GREAT 2018)
19 - 23 November 2018 Bangkok, Thailand

Structural and Deformation of Metamorphic Rocks in the Doi Phuk Sung Area, Wiang Sa District, Nan Province

Thikapong Thata[1*] and Phisit Limtrakun[1]

1 Department of Geological Sciences, Faculty of Science, Chiang Mai University, Chiang Mai, 50200, Thailand

* Corresponding author email: thikapong_thata@cmu.ac.th

Abstract

The Nan-Uttaradit suture is the most complex suture in Thailand. It has been interpreted to mark the boundary between the Sibumasu block located in the west of Thailand (Sukhothai Zone) and the Indochina block located in the east of Thailand. The Mafic and Ultramafic and Metamorphic rocks are exhumed along the Nan River and are evidenced by the subduction zone. The amalgamation of these two blocks may have occurred in the Permian-Triassic. The study area is located in the south of Nan province and covers an area of approximately 22 km^2. The purpose of this study is to characterize deformation event of metamorphism and define structural geology by using petrography and structural analyses. The geological setting of the study area can be divided into 3 rock units. All rock units are not conformable and bounded with thrust faults. (1) The Limestone unit includes bedded limestone. (2) The Mélange block unit consists of metapelite, metabasite, and pyroclastic rocks. The relationship of rocks is a block in matrix fabrics. The metapelite is stilpnomelane quartz schist and phyllite. The metabasite is metaperidotite and metagabbro block in the serpentine matrix. (3) The Red bed sedimentary rocks unit comprises reddish brown conglomerate, sandstone, siltstone and volcanic rock. Metapelite in the mélange block unit recorded two events of deformation, S_1, and S_2 events. The S_1 is foliation showing in metapelites while the S_2 evidence in crenulation and folded of foliation (S_1). The controlled tectonic in the study area is the convergent plate boundary. The evidence in this study is a thrust fault and mélange unit. Thrust faults make the older rock unit overlying on the younger rock unit. The mélange unit had two events of deformation including foliation (S_1) and folding (S_2). The studied schist contains mineral assemblages of stilpnomelane + chlorite + phengite + albite + tremolite + quartz + K-feldspar ± biotite that formed under P - T conditions of 250 - 400 °C, and 2 - 9 kbars. The equilibrated P - T condition is stable in blueschist facies. The studied metabasite contains mineral assemblages of magnesite + quartz that formed under P - T conditions of 220 - 400 °C, and 4 - 6 kbars. The equilibrated P - T condition is stable in greenschist facies.

Key words: Structural, Deformation, Metamorphism, Nan Suture, Tectonics, Thailand

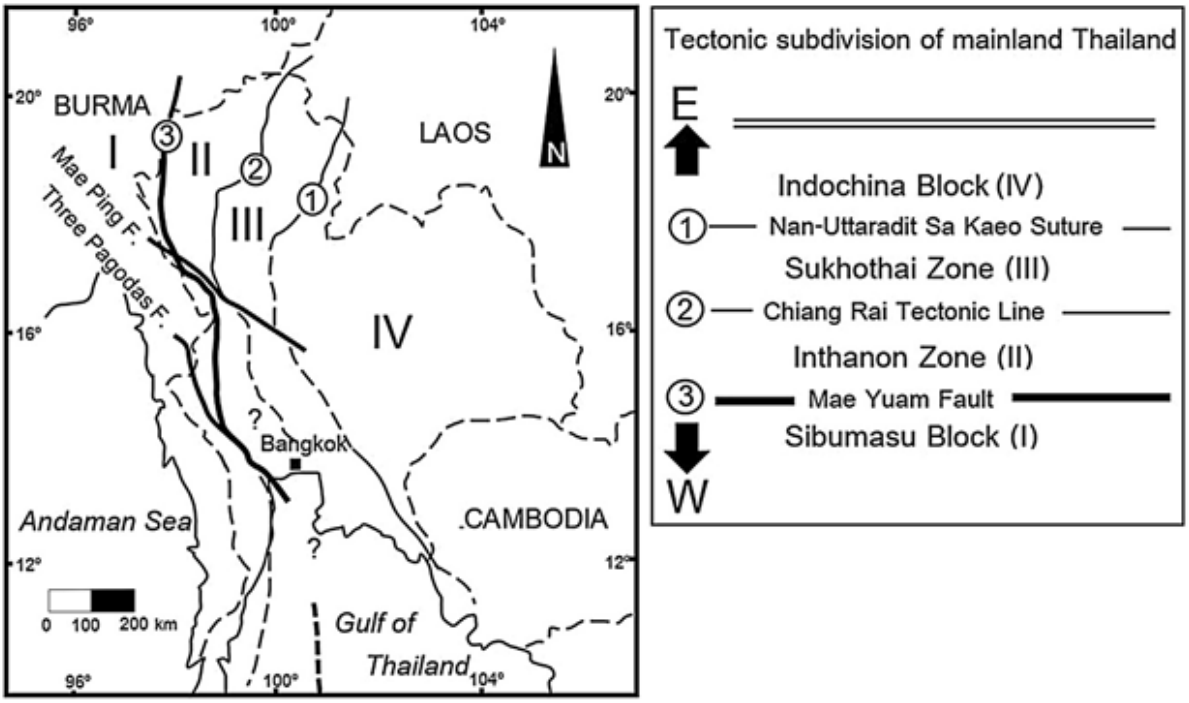

Figure 1. Geotectonic subdivisions of Thailand (modified from Ueno and Hisada, 2001).

1. Introduction

Thailand including two principle blocks which comprise Sibumasu block in the west and Indochina block in the east. The zone between them is the Sukhothai Zone (Sukhothai Fold Belt or Sukhothai Arc) (Figure 1). The suture between the Sukhothai Arc and Indochina block is the Nan Suture (Ueno and Charoentitirat, 2011). The Nan Suture is extended from Nan to Uttaradit. This suture zone was later referred to the Nan River Suture Zone, Nan Suture, or Nan-Uttaradit Suture. The Nan - Uttaradit Suture has previously been proposed to be the main Paleo - Tethyan suture (Bunopas, 1981; Barr and Macdonal, 1987 and Singharajwarapan and Berry, 1999) and a remnant of a closed back-arc basin (Sone and Metcalfe, 2008; Ueno and Hisada, 2001; Metcalf, 2002). The geometry and timing of the collision have been debated. The geometry of the collision between the terranes has been proposed as westward subduction of the Indochina Terrane underneath the Sibumasu Terrane (Barr and Macdonald, 1987; Bunopas and Vella, 1978; Charusiri et al., 2002) or eastward subduction of the Sibumasu Terrane under the Indochina Terrane (Beckinsale et al., 1979; Mitchell, 1986). The Nan - Uttaradit metamorphic belt lies roughly coincide with the Nan - Uttaradit suture zone. The metamorphic rocks in this belt are

probably subduction related and consist of metamafic to acid volcanic rocks characterized by a lesser evolved material. The imprint of the IP/ IT greenschist facies over the HP/ LT blueschist facies in Nan may connote other unknown tectonic movements rather than ordinary adjustment of the PT regime by uplifting. The IP/ IT greenschist to ampholite facies in the eastern part of Thailand reflects a different PT condition. Age differences between the Early Carboniferous in Nan and the Devonian-Carboniferous in east Thailand may suggest their differences in subduction regimes (Barr and Macdonald, 1987; Singharajwarapan, 1994; Singharajwarapan and Berry, 1993; 2000). The Nan River Volcanic Belt is the mafic and ultramafic rocks along with The Nan – Uttaradit Suture Zone. There are identified as a likely ophiolite (Macdonald and Barr, 1984). Subsequently, the discovery of blueschist associated with belt supported its role as a major suture (Barr et al., 1985; Barr and Macdonald, 1987). The Nan River Volcanic Belt includes not only oceanic mafic and ultramafic igneous rocks, but also the Pha Som Metamorphic Complex. This unit consists of volcanic rocks, greywacke – dominated metasedimentary units, piedmontite – quartz schist and serpentinite mélange. The metagraywacke has high detrital plagioclase content and was likely derived from a continental volcanic arc (Singharajwarapan, 1998; Singharajwarapan and Berry, 2000). This unit is at pumpellyite – actinolite facies. There is a correlation with the rocks further north along the belt containing high – pressure blueschist assemblages (the study area) as reported by Barr and Macdonald (1987). The associated but fault – bounded piedmontite – quartz schist unit was interpreted by Singharajwarapan and Berry (1993) as metamorphosed manganiferous hemipelagic or pelagic chert. The age of the Pha Som metasedimentary rocks is a Permian to Carboniferous age (Hess and Koch, 1975). The metamorphic age of 269 ± 12 Ma by K – Ar age for actinolite from mafic schists (Mid – Permian) (Barr and Macdonald, 1987). The ophiolitic rocks in the Nan River Belt (Hutchison, 1975; 1983; Thanasuthipitak, 1978; Bunopas and Vella, 1978; 1983; Sengor, 1979; Ridd, 1980; Huang, 1984) is associated with chromite (Orberge et al., 1995). The ultramafic sequence and its various chromitite deposits represent the mantle part of a supra – subduction zone ophiolite (Macdonald and Barr, 1984, 1987; Crawford and Panjasawatwong, 1996).

2. Geological setting

The study area is located in Baan Nam Muap, Wiang Sa and Na Noi districts, southern part of Nan province. It covers the area of

approximately 22 square kilometers. The boundary is between latitude 18°19'55.25" N to 18°23'10.36" N and longitude 100°55'49.35" E to 100°58'39.61" E. The area is encompassed in the 1:50,000 scale map sheet 5145I (Ban Nam Muap) (Figure 2).

Geological setting in the study area is controlled by convergent plate boundary. Rocks in the study area show three different lithologies (Figure 2). The rock units consist of (1) the Limestone Unit, (2) the Mélange Block Unit and (3) the Red Bed Sedimentary Rocks Unit. All rock units are not conformable and bounded with thrust faults. These faults strike trending NE – SW. The Mélange Block Unit is an elongate shape and parallel alignment to the thrust faults.

2.1 The Limestone Unit

The limestone unit is located in the eastern part of the study area. This unit includes grey to dark grey bedded limestone (Figure 3a and 3c). The limestone beds thickness vary from a few centimeters to a massive outcrop. There are close-folded locally and occasionally interbedded with thin carbonaceous meta – argillaceous layers. The limestone generally striking in N-S direction trend and dipping angle 20° – 40° in west direction.

2.2 The Mélange Block Unit

The mélange block unit is located in the middle of the study area. This unit can be subdivided into two type of rocks, (1) the metabasic rocks mélange consist of mafic – ultramafic rock blocks surrounded by serpentinite matrix (Figure 3d) . This subunit includes mafic volcanic rocks (gabbro). (2) The metasedimentary rocks mélange contains schist blocks and pyroclastic rock blocks surrounded by phyllite and mudstone (Figure 3b) . Blocks are ranging in size from centimeters to hundreds of meters. They have elongated and lens shapes. The bottom of this unit is the gray conglomerate, grey to greenish grey volcanic clastic sandstone medium to thin bed interbedded with shale (Figure 3e). The conglomerate clasts include volcanic rocks, chert, limestone and quartz. The clasts size is granular to boulder.

2.3 The Red Bed Sedimentary Rock Unit

The red bed sedimentary rocks unit located in the northern and southern part of the study area. This unit comprises red to reddish brown conglomerate, agglomerate, conglomerate, sandstone, siltstone and volcaniclastic rocks (Figure 3f). In the northern part, this unit shows NW – SE strike and 20° – 40° dipping angle, while in the southern part showing NE – SW strike and 60° – 80° dipping angle.

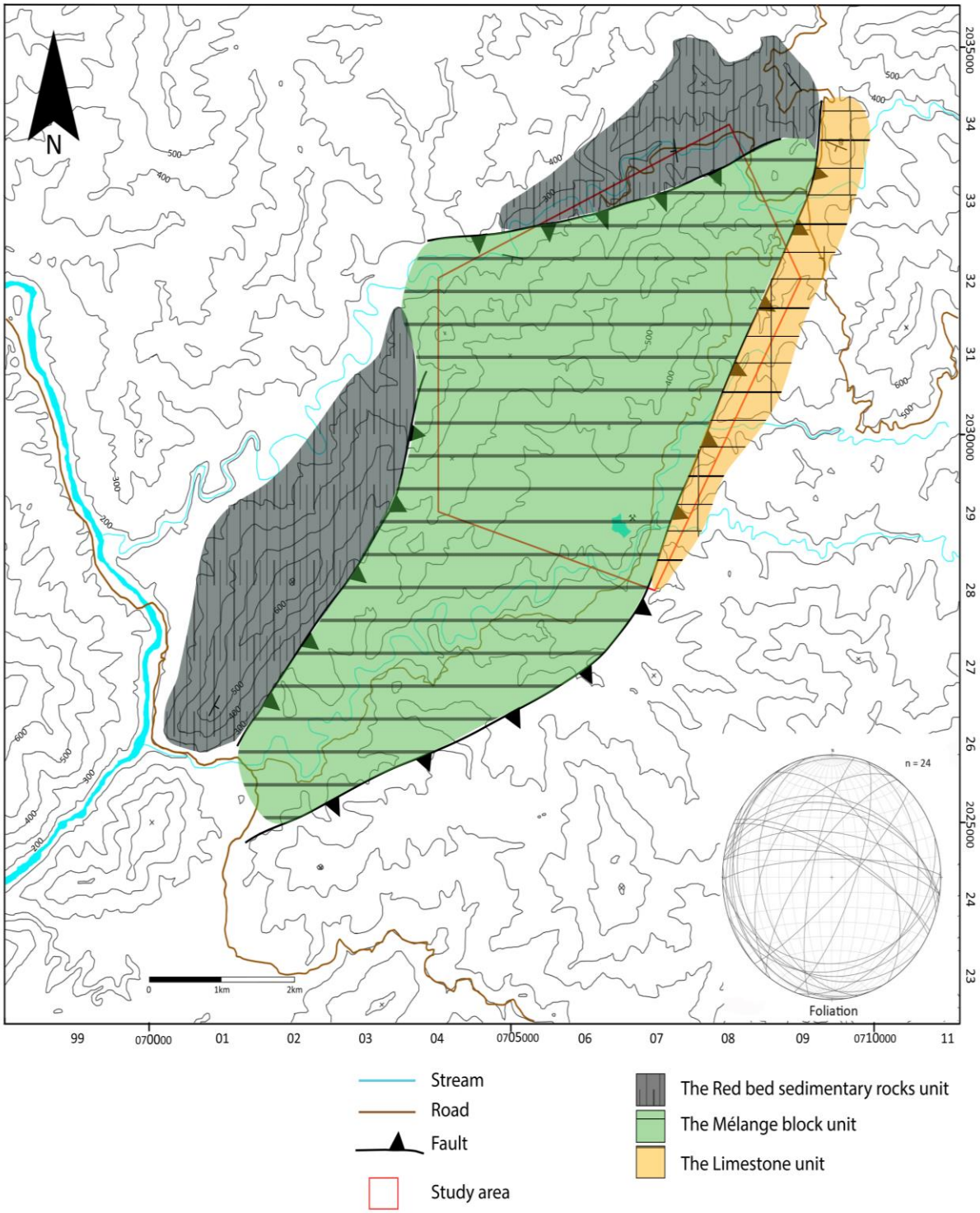

Figure 2. Geologic map of the study area and stereonet plot of foliation from the mélange block unit

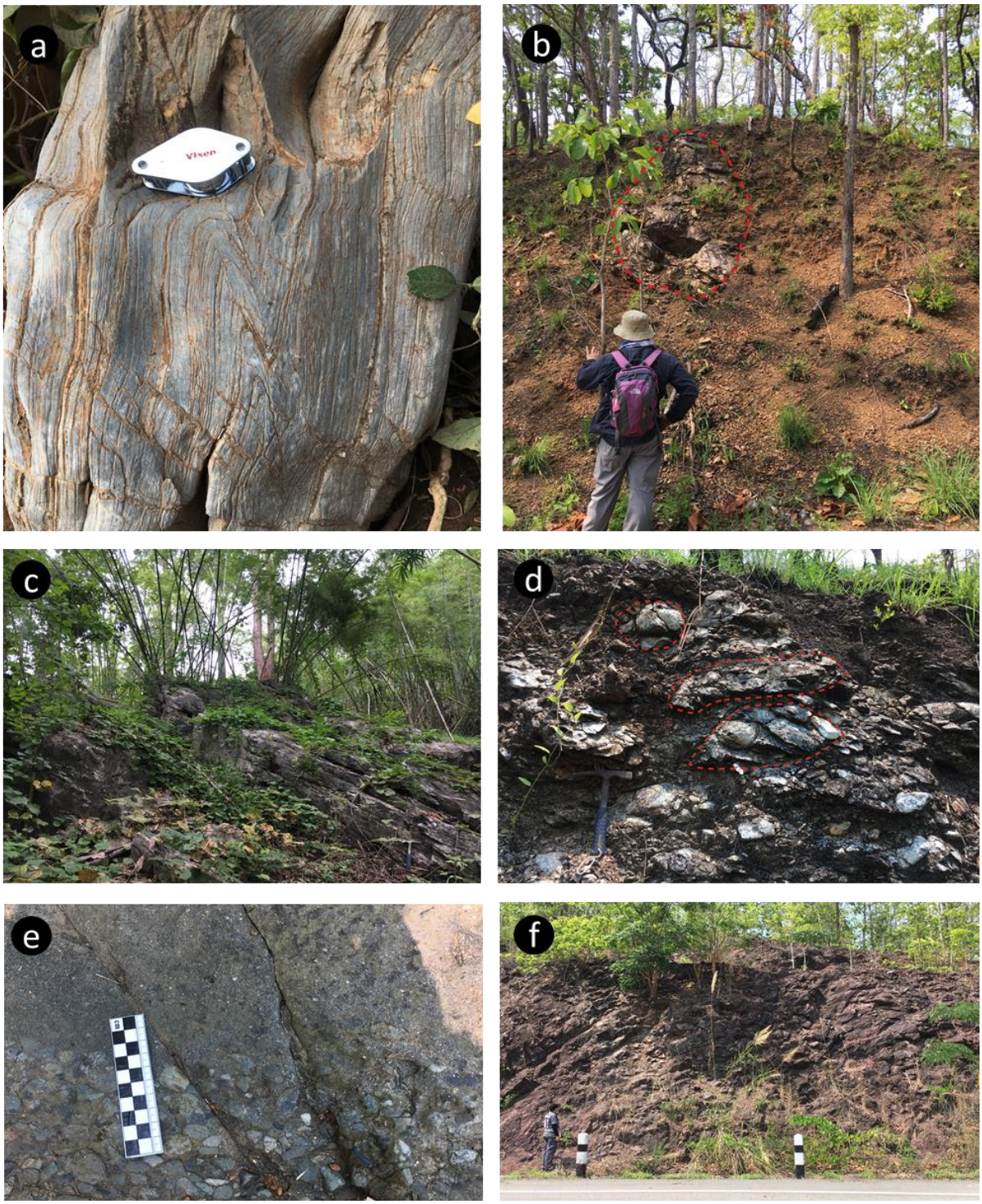

Figure 3. Photographs of rock units in the study area a.) close folded in the limestone unit. b.) metasedimentary rocks of the mélange blocks unit located in the Doi Phuk Sung. c.) limestone bed located in the Doi Tham Sali. d.) metamafic-ultramafic rocks in the serpentinite matrix of the mélange blocks unit. e.) conglomerate and sandstone underlie the mélange blocks unit. f.) red bed sandstone in the southern part of the study area.

3. Petrography

The petrography study focuses on the mineral assemblages of metamorphic rocks in the study area. The metamorphic rocks in the study area comprise metabasites and metapelites.

3.1 Metabasites

The metabasic rocks are from sample No. HL06 (Figure 4a-b), and HL07 (Figure 4c-4d). The two samples are located in the Doi Phuk Sung. The HL06 sample consists of magnesite, dolomite, quartz and chromite. The quartz, and magnesite formed by CO_2 rich hydrothermal contact metamorphism with ultramafic rocks. The chemical reactions are described in reaction 1a and 2a (Kelemaen et al., 2011).

$4Mg_2SiO_4$ (Mg-olivine) + $4H_2O$ + $2CO_2$ = (1a) $2Mg_3Si_2O_5(OH)_4$ (serpentine) + $2MgCO_3$ (magnesite)

$4Mg_2SiO_4$ (Mg-olivine) + $8CO_2$ = $4SiO_2$ (1b) (quartz) + $8MgCO_3$ (magnesite)

The samples HL07-1 (Figure 4c) and HL07-2 (Figure 4d) are peridotite and mafic rocks respectively. They comprise olivine, recrystallized chlorite, orthopyroxene which surrounded by serpentine.

3.2 Metapelites

The thin sections are made from mica quartz schist samples No. HL01 (Figure 4e) and HL08 (Figure 4f). The sample HL01 located in the old mine reservoir and the sample HL08 located in Doi Phuk Sung. The sample HL01 includes microcrystalline quartz, muscovite, biotite, prehnite and clay mineral. The sample HL08 comprises quartz, stilpnomelane, muscovite, biotite, blue amphibole, actinolite and titanite.

4. Deformation

All rock units boundaries are thrust faults. The structure exhibits the mélange blocks unit. The deformation occurs in metasedimentary rocks. The structural orientation in outcrops may not affect in the same direction when they are deformed. There are two events of deformation in these rock units. The first deformation (D_1) creates foliation following by the second deformation (D_2) that made the foliation folding and crenulation.

4.1 Deformation 1 (D_1)

The D_1 formed the foliation (S_1) (Figure 5) in the metasedimentary rocks of the mélange blocks unit. There are several orientations of foliations because of the direction of blocks in the mélange zone. The mica quartz schist sample HL01 (Figure 5a) shows striking foliation of 037/70NW. The sample HL08 (Figure 5b) is blue amphibole stilpnomelane quartz schist that show the orientation of foliation 329/48NE.

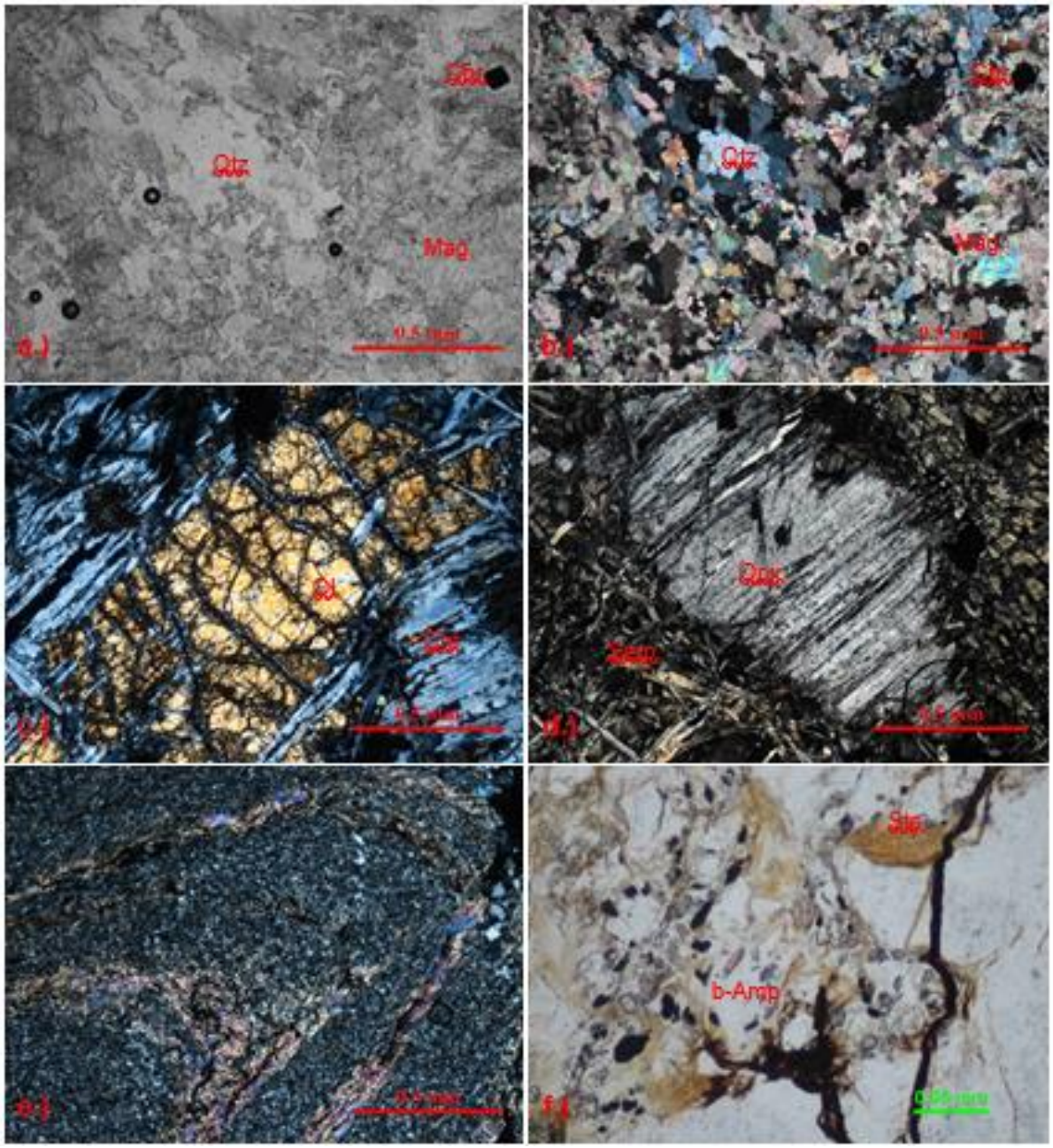

Figure 4. Photomicrographs showing mineral assemblage of the two main metamorphic rocks in microscope scale. a.) non – polarized and, b.) cross – polarized photomicrographs of metabasites containing magnesite, quartz, and chromite. c.) metabasites comprise olivine and recrystallized chlorite. d.) metabasites show orthopyroxene surrounded by serpentine. e.) close fold in microscope scale form microcrystalline quartz schist. f.) blue amphibole in stilpnomelane quartz schist. Mag = magnesite Qtz = quartz Chr = chlorite Ol = olivine b-Amp = blue amphibole Stp = stilpnomelane

4.2 Deformation 2 (D_2)

The D_2 formed the folding and crenulation (S_2) (Figure 5) in metasedimentary rocks in the mélange blocks unit. The orientation of S_2 is both perpendicular and parallel to the S_1. The evidences of folding are clearly demonstrated in the sample HL01, and crenulations are shown in the sample HL08.

5. Discussion

The study area has controlled by thrust faults as identified by the rock unit boundary. The mafic – ultramafic rocks in the mélange blocks unit are ophiolitic rocks. The ultramafic rocks consist of peridotites and variably amphibolitized layered gabbro and diabase that defined sheeted – dike complex. The mafic sequences are crosscut by different types of rocks such as coarse – grained orthopyroxene, plagioclase in gabbroic rocks, basalts and pillowed lavas with their sedimentary covered, most characteristic of Supra – Subduction Zone of (Orberge et al., 1995). The mélange related to subduction mainly occur in two types (Figure 6), the mass-transport deposits at the wedge front, and the broken formation and tectonic mélanges (Festa et al., 2010).

5.1 Mass-transport deposits at wedge front

The different degrees of stratal disruption are related to the state of consolidation at the stage of the slope failure and their runout the distance. Pinch and swell, boudinage, slump folds and ‘ slump balls, represent the most common structures affecting the intrabasinal sediments. Local imbrication of beds and bed packages, contractional and extensional duplexes, thrust systems, and intrafolial, isoclinal folds are also present. As for the passive margin – related mélanges, deformation of these sediments seems to have occurred when they were wet and unconsolidated. The extrabasinal rocks are present as blocks, bed chunks and entire bed packages that preserving their subduction-related tectonic fabric inside a fine-grained, commonly argillaceous matrix (Festa et al., 2010).

5.2 Broken formation and tectonic mélange

The broken formation and tectonosomes are characterized by a block in – matrix fabric in which part of the same coherent stratigraphic unit can be recognized and in which no ‘exotic’ blocks are present. Beds and bed fragments show a planar orientation consistent with an internal order at the outcrop to map – scale that coincides with a structural fabric. Various types of structures may have formed from the interaction of different subduction related processes. Mélange and broken formation – tectonosomes display lithological and structural evidence for different degrees of mixing and deformation depending on the

rheology of the rocks involved, superposition of different tectonic episodes, and different degrees of involvement in subduction processes (Festa et al., 2010).

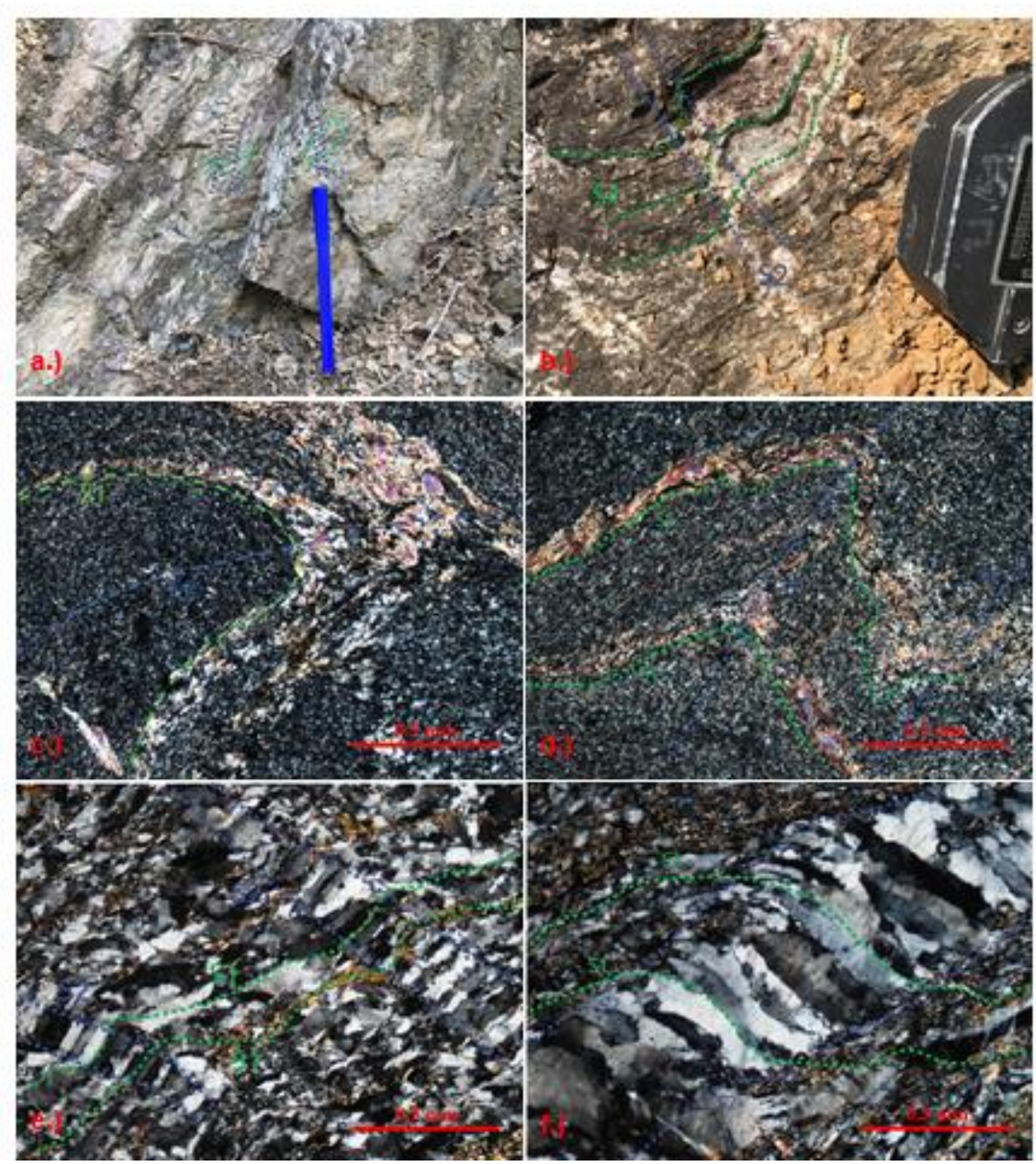

Figure 5. Photographs and photomicrographs showing structural features of the two main deformations in outcrop scale and microscope scale. a.) the outcrop sample HL01. b.) the outcrop sample HL08. c.) the sample HL01 showing deformation parallel to foliation. d.) the sample HL01 showing deformation perpendicular to foliation. e.) the sample HL08 showing deformation parallel to foliation. f.) the sample HL08 showing deformation perpendicular to foliation.

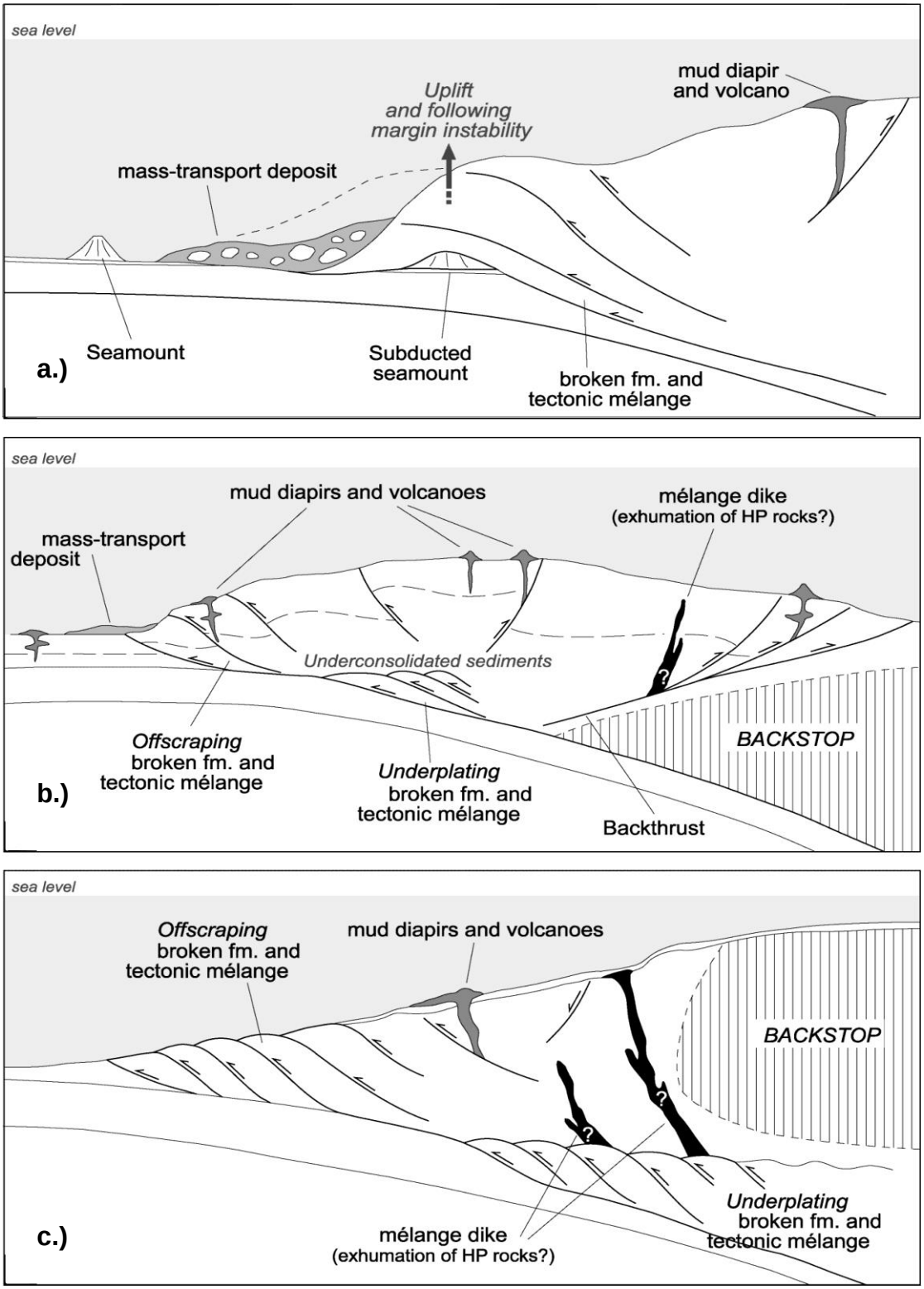

Figure 6. Conceptual models for the formation and emplacement of the mélanges associated with subduction zone processes, a.) seamount subduction, b.) large double-verging wedge with a low elevation of the backstop; c.) smaller wedge with a high elevation of the backstop. (modified from Festa et al., 2010).

6. Conclusion

The study area controls by convergent plate boundary (supra – subduction). Two types of the mélange related to subduction are the mass-transport deposits at the wedge front, and the broken formation and tectonic mélanges type. The lithology in the study area can be divided into three rock units. All rock units are not conformable and bounded with thrust faults. (1) The Limestone unit includes bedded limestone. (2) The Mélange block unit consists of metapelites, metabasites and pyroclastic rocks. (3) The Red bed sedimentary rocks unit comprises reddish brown conglomerate, sandstone, siltstone and volcanic rock. There are two events of deformation in these rock unitd. The first deformation (D_1) creates foliation while the second deformation (D_2) made the foliation folding and created crenulation. The mineral assemblages in metabasites are magnesite + quartz that formed under P – T conditions of 220 – 400 °C, and 4 – 6 kbars. The equilibrated P – T condition is stable in greenschist facies. The magnesite and quartz are formed by hydrothermal contact metamorphism. The studied schists contain the mineral assemblages of stilpnomelane + chlorite + phengite + albite + tremolite + quartz + K-feldspar ± biotite that formed under P – T conditions of 250 – 400 °C, and 2 – 9 kbars. The equilibrated P – T condition is stable in blueschist facies.

7. Acknowledgements

This study was supported by the Science Achievement Scholarship of Thailand (SAST). The members of Igneous Rocks and Related Ore Deposits Research Laboratory (IROL) , Department of Geological Sciences, Faculty of Science, Chiang Mai University, both staff and students, are thanked for supporting and suggestions.

8. References

Barr, S. M., Macdonald, A. S., Yaowanoiyothin, W. and Panjasawatwong, Y. , 1985, Occurrence of blueschist in the Nan River mafic-ultramafic belt, northern Thailand. *Warta Geologi*, 11, 47-50.

Barr, S. M. and Macdonald, A. S., 1987, Nan River suture zone, Northern Thailand. *Geology*, 15, 907 – 910.

Bunopas, S., 1981, Paleogeographic history of western Thailand and adjacent parts of Southeast Asia-A plate tectonics interpretation (PhD. thesis): Wellington, New Zealand, Victoria University, 810.

Bunopas, S., and Vella, P., 1978, Late Paleozoic and Mesozoic structural evolution of Thailand, in Nutalaya, P., ed., *Proceedings of the 3rd Regional Conference on Geology and*

Mineral Resources of Southeast Asia, Bangkok, Thailand, Asian Institute of Technology, p. 133-140.

Bunopas, S. and Vella, P., 1983, Tectonic and geologic evolution of Thailand, In Nutalaya, P. (eds.), *Proceedings of Workshop on Stratigraphic Correlation of Thailand and Malaysia*, Haad Yai, Geological Society of Thailand and Geological Society of Malaysia, 1, 307 – 322.

Charusiri, P., Daorerk, V., Archibald, D., Hisada, K. and Ampaiwan, T. 2002. Geotectonic evolution of Thailand: A new synthesis. *Journal of the Geological Society of Thailand*, 1, 1 – 20.

Crawford, A. J. and Panjasawatwong, Y. 1996. Ophiolite, ocean crust, and the Nan suture in NE Thailand. In Lee T. – Y.(eds.) *Proceeding of the International Symposium on Lithosphere Dynamics of East Asia*, Geological Society of China, Taipei, 84 – 9.

Festa, A., Pini, G. A., Dilek, Y. and Codegone, G., 2010, Mélanges and mélange – forming processes: a historical overview and new concepts. *International Geology Review*, 52, 1040 – 1105.

Hess, A. and Koch, K. E. (compilers) 1975. Geologic Map of Northern Thailand, Scale 1: 250,000, Sheet 1 (Nan), Federal Institute for Geosciences and Natural Resources, Germany.

Huang, J., 1984, New researches on the tectonic characteristics of China, in Yanshin, A. L., *et al.* (eds.), *Tectonics of Asia; colloquium 05, 27th International Geological Congress*, Moscow, Reports, 5, 13 – 28.

Hutchison, C. S., 1975, Ophiolite in Southeast Asia, *Geological Society of America Bulletin*, 86, 797 – 806.

Hutchison, C.S., 1983, Multiple Mesozoic Sn-W-Sb granitoids of Southeast Asia, In Roddick, J. A. (eds.), *Circum-Pacific plutonic terranes, Geological Society of America Memoir*, 159, 35 – 60.

Macdonald, A. S. and Barr, S. M., 1984, The Nan River mafic-ultramafic belt, northern Thailand: Geochemistry and Tectonic Significance. *Geological Society of Malaysia Bulletin*, 17, 249-281.

Kelemen, P. B., Matter, J., Streit, E. E., Rudge, J. F., Curry, W. B. and Blusztajn, J., 2011, Rates and Mechanisms of Mineral Carbonation in Peridotite: Natural Processes and Recipes for Enhanced, in situ CO_2 Capture and Storage. The Annual Review of Earth and Planetary Sciences, online at earth.annualreviews.org, 39, 545 – 576.

Metcalfe, I. 2002, Permian tectonic framework and paleogeography of SE Asia. *Journal of Asian Earth Science*s, 20, 551 – 566.

Orberger, B., Lorand, J. P., Girardeau, J., Mercier, J. C. C. and Pitragool, S. 1995. Petrogenesis of ultramafic rocks and associated chromitites in the Nan Uttaradit ophiolite, Northern Thailand. *Lithos*, 35, 153 – 182.

Ridd, M. F., 1980, Possible Paleozoic drift of SE Asia and Triassic collision with China, *Geological Society of London Journal*, 137, 635 – 640.

Sengor, A. M. C., 1979, Mid – Mesozoic closure of Permo – Triassic Tethys and its implications, *Nature*, 279, 590 – 593.

Singharajwarapan, S., 1994. Deformation and Metamorphism of the Sukhothai Fold Belt, Northern Thailand. Ph.D. thesis. University of Tasmania, Hobart, Australia.

Singharajwarapan, S., 1998. Provenance and tectonic setting of deposition of metagreywackes in the Nan River Suture, northern Thailand. *Programme and Abstracts of the Ninth Regional Conference on Geology, Mineral and Energy Resources of Southeast Asia*, 44.

Singharajwarapan, S., and Berry, R. F., 1993. Structural analysis of the accretionary complex in Sirikit Dam area, Uttaradit, Northern Thailand. *Journal of Southeast Asian Earth Sciences*, 8, 233 – 245.

Singharajwarapan, S., and Berry, R. F., 2000. Tectonic Implications of the Nan Suture Zone and Its Relationship to the Sukhothai Fold Belt, Northern Thailand. *Journal of Asian Earth Sciences*, 18, 663–673.

Sone, M. and Metcalfe, I. 2008. Parallel Tethyan sutures in mainland Southeast Asia: new insights for Palaeotethys closure and implications for the Indosinian orogeny. *Comptes Rendus Geoscience*, 340, 166 – 179.

Thanasuthipitak, T. , 1978, Geology of the Uttaradit area and its implications on tectonic history of Thailand, In Nutalaya, P. (eds.), *Proceedings of the 3rd Regional Conference on Geology and Mineral Resources of Southeast Asia*: Bangkok, Thailand, Asian Institute of Technology, 187 – 197.

Ueno, K. and Charoentitirat, T. 2011. Carboniferous and Permian. In: Ridd, M. F., Barber, A. J. and Crow, M. J. (eds) *The Geology of Thailand*. Geological Society, London, 71 – 136.

Ueno, K., and Hisada, K. I., 2001. The Nan-Uttaradit-Sa Kaeo Suture as a Main Paleo – Tethyan Suture in Thailand: Is It Real? *Gondwana Research*, 4, 804 – 806.

Proceedings of the Second International Symposium on Geoscience Resources and Environments of Asian Terranes (GREAT 2018)
19 - 23 November 2018 Bangkok, Thailand

Facies analysis and paleoenvironmental interpretation of Tha Manao Limestone (Middle Ordovician) in Sri Sawat district, Kanchanaburi province

Thitikan Junrattanamanee [1*], Nitipon Noipow [2] and Anisong Chitnarin [1]

1 School of Geotechnology, Suranaree University of Technology, 111 University Avenue, Suranaree subdistrict, Mueang district, Nakhon Ratchasima province, 30000, Thailand
2 Disaster Management and Public Hazard Mitigation Program, Faculty of Science and Technology, Valaya Alongkorn Rajabhat University under the Royal Patronage, Pathum Thani 13180, Thailand
*Corresponding author: t_junrattanamanee@hotmail.co.th

Abstract

The Ordovician carbonate succession exposed on the East side of Srinagarind reservoir in Kanchanaburi province, western Thailand was investigated and rock samples were collected in order to study stratigraphy and define the depositional environment. Nautiloid fossils were found along the studied section giving the age of Middle Ordovician (Darriwilian). Examined specimens are mostly wackestone, packstone and the rests are mudstone and grainstone containing peloids, intraclasts, and bioclasts. From 127 thin sections, eleven microfacies (MF) types can be classified and contributed in six depositional environments including peritidal, lagoon, carbonate shoal, open marine, mid ramp, and outer ramp. The studied succession is divided into three sequences: Lower sequence representing the outer ramp to inner ramp environment; Middle sequence representing mid ramp to inner ramp environments; Upper sequence evidencing the outer ramp to inner ramp.

Key words: Microfacies, Tha Manao Limestone, Sibumasu Terrane, Middle Ordovician

1. Introduction

Ordovician rocks are distributed in western part of Sibumasu terrane (Figure 1A) and consist of carbonate sequences that are poorly known because they have been rarely investigated. In the West of Thailand, the Ordovician rocks are exposed extensively, and the successions are broadly similar to the South of Thailand (Hagen and Kemper, 1976). Bunopas (1981) investigated an area closed to Kanchanaburi city and Sri Sawat district where he reported a sequence of argillaceous limestone with cephalopods and he introduced the Tha Manao Limestone Formation. These

limestones contain nautiloids (*Armenoceras* sp., *Ormoceras langkawiense*) which indicate Middle Ordovician in age and gastropods, pelecypods and crinoids were also found.

The age of the Tha Manao exposed in the North of Kanchanaburi city is assigned by receptaculitalean *(?Fisherites* sp.) as Early-Middle Ordovician (Ibexian-Whiterockian or Dapingian-Darriwilian age) (Kruse, 1989). However, details of stratigraphy and paleoenvironment of this formation are rarely known. This research is aimed to investigate carbonate strata of the Tha Manao Formation which exposed on the East side of Sri Nakharind reservoir in order to understand its environment of deposition.

2. Location and Geological setting

Thailand comprises two continental blocks including Indochina block and Sibumasu block (Figure 1B). The palaeomagnetic, lithostratigraphic and paleontological data have been used to support plate tectonic theory of South East Asia which is now proved that both blocks were parts of northern Gondwana during the Early Paleozoic, then broke up and drifted paleo-ocean, before they subducted and merged during Late Paleozoic-Mesozoic Era (e.g., Metcalfe, 1988; 1998). Ordovician rocks are exposed only in western geological province of the country (Sibumasu block) which covers northern, western, eastern and southern regions (Bunopas, 1983; Wongwanich et al., 1983). In general, the Ordovician rocks are composed mainly of limestones, less clastic rock and the ages were indicated by nautiloids, trilobites and conodonts (e.g., Stait and Burrett, 1982; 1984; 1987; Fortey, 1997; Fortey and Cocks 1998; Agematsu et al., 2006; 2007). A Complete sequence of Ordovician carbonate rocks was studied by Wongwanich (1990) in Satun province, southern Thailand. He found the rock composed of limestones, dolomites and shale deposited on a homoclinal ramp where environments varied from tidal flat, reef, lagoon, local build up barrier reefs and deeper water carbonates. The whole sequence ranged from Lower Ordovician (Upper Tremadoc) to upper Ordovician (Ashgill).

Geology of the area closed to Sri Nakharind reservoir was investigated and mapped by many works e.g., Koch (1973), Bunopas (1976, 1981), and Meesook (2015). Geomorphologically, the area shows dominant monoclinal features of the Ordovician limestone overlying the Cambrian sandstones to the north. The mountainous areas of the Ordovician limestone are confined to the eastern and southern sides of the area and the Silurian-Devonian rocks are represented by low-level mountain ranges to the west and east.

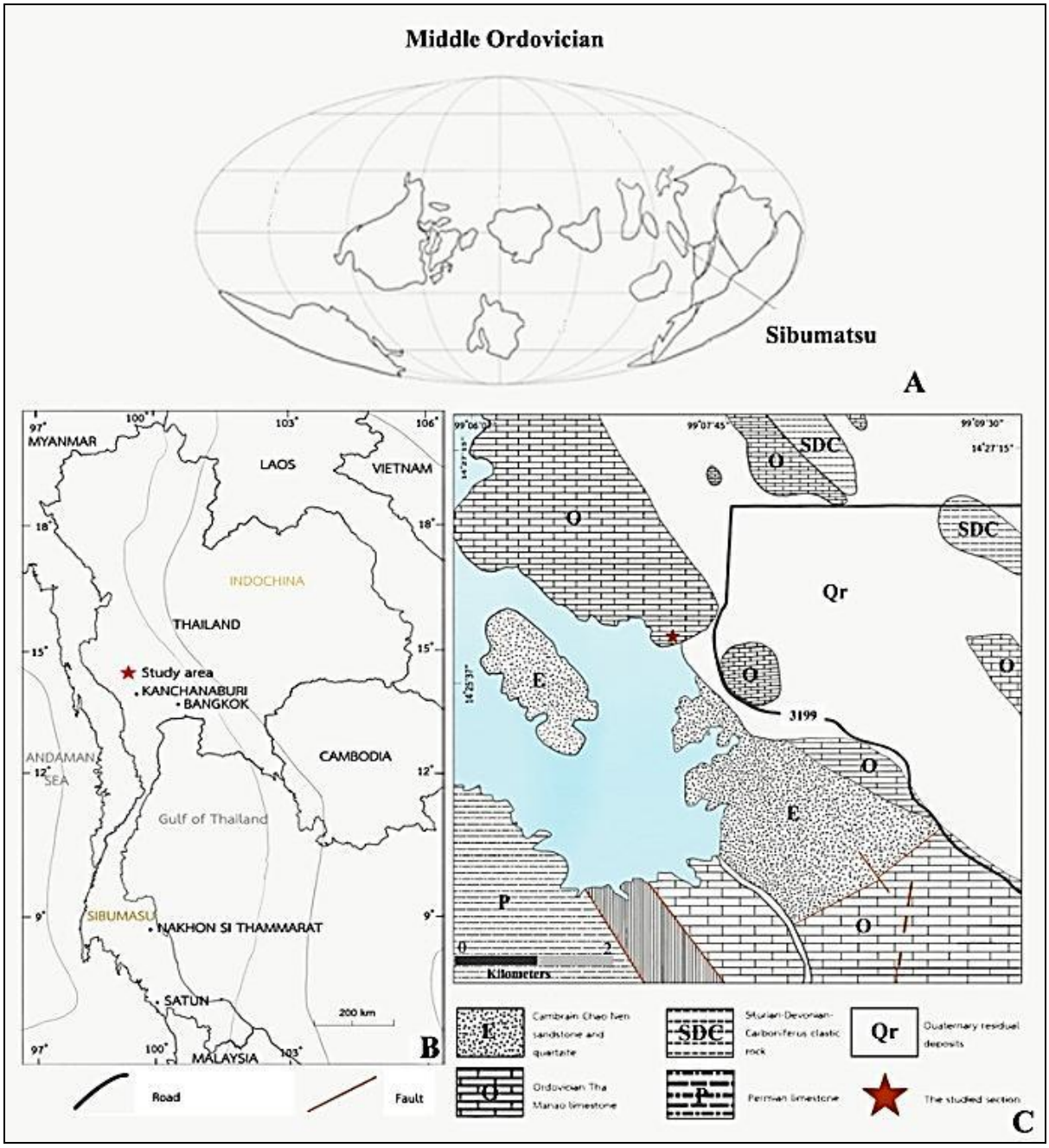

Figure 1. Maps of the studied area. (A) Palaeogeographic map of Middle Ordovician time showing location of Sibumasu terrane (modified from Agematsu et al., 2008) (B) Location map of the studied section at Ban Tha Kradan, Si Sawat district, Kanchanaburi province (modified from Wongwanich et al., 1983 and Ridd, 2011). (C) Geologic map of the Khuean Srinagarinda Quadrangle (4837 IV, UTM 47 P), Kanchanaburi province, western Thailand (modified after Khaowiset et al., 2011 and Meesook 2015). The red star indicates the studied section.

The studied section (Wat Mong Krathae section) is located on the East side of Sri Nakharind reservoir about 76 km NW of Kanchanaburi city (Figure 1C) at approximately longitude 99 ° 07.581 ' E, Latitude 14 ° 25.924 ' N). From a total 157-meters thick section (Figure 2A), 26 samples were collected. The sequence of stylolitic greenish grey to dark grey limestone showing thin-to-thick beds is exposed continuously with bedding trend N60W dipping 30NE and predominantly of wackestone to packstone, less of mudstone and grainstone. (Figure 2B and 2C).

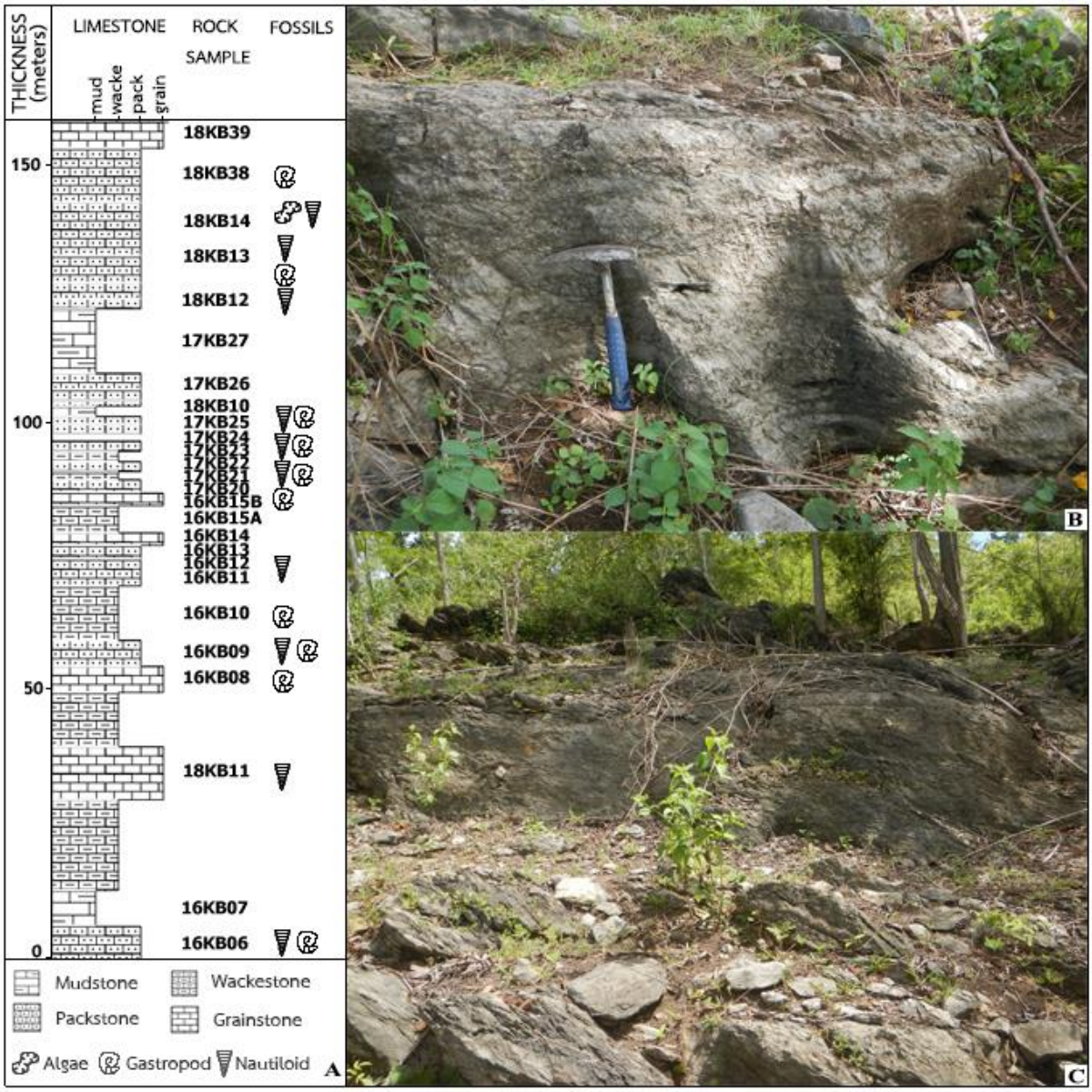

Figure 2. Lithologic column and photographs of the Wat Mong Kratae section (A) lithologic log of the studied sections (B-C) photograph of the studied section showing limestone outcrop.

Macrofossils are also found in many beds along the sequence. Nautiloids *Armenoceras chediforme* (Kobayashi, 1958), gastropods *Teiichispirina* sp. and Receptaculitalean *?Fisherites* sp. are found. These fossils known from other places and indicate Middle Ordovician age (Dapingian-Darriwilian).

3. Methodology

Twenty rock samples were collected and brought to the laboratory. Rock slabs and 127 thin sections were prepared (Hill, R. 1999; Grundmann, G. and Scholzand, H. 2015; Green, O. 2001). Polished thin sections are studied under stereomicroscope and polarized-light microscope to determine the microfacies. Flügel (2004) described the constituents for the microfacies analyses which consist of the grain type, matrix type, fossils in thin section and depositional texture. The facies classification by Dunham (1962) is used in this study.

4. Microfacies analysis

Lithological and microscopic analysis led to the result of eleven microfacies types of the middle Ordovician in Tha Manao Limestone Formation (Table 1) in Ban Tha Kradan area on the basis of texture/fabrics, main constituents, sedimentary structure and fossil contents. Facies association of these microfacies can be interpreted to six depositional facies belts including outer ramps, mid ramps, open-marine, shoals, lagoon and peritidal facies associations. These microfacies can be described the distribution from deep to shallow environment.

4.1 Outer ramp facies

Two microfacies identified in this environment are composed of algal-intraclast-peloidal packstone and peloid calcisiltite. This facies comprises mainly of peloids, intraclasts, algae and shell fragment.

4.1.1. MF1, Algal-intraclast-peloidal packstone (Figure 3A, 3B)

Facies description: This facies conspicuously includes micrite matrix, grain supported allochems. The allochems are both skeletal and non-skeletal grains. Bioclast components include mollusk shell fragments, algal fragments, crinoid fragments, trilobite fragments and carbonate grains consists of intraclasts (including micritic intraclast, sandy micritic intraclast and small intraclast, peloids) and some microbially skeletal grain. Their grain sizes range from calcirudite to calcarenite.

Depositional environment: The presences of abundant micrite and completed skeletal grains indicate the low energy depositional environment and the mud peloids are generally found in outer ramps.

Table 1. Characteristics and depositional setting of the lithofacies of the studied section.

FACIES	LITHOLOGY	COMPONENTS	FACIES BELTS
MF1 Algal-intraclast-peloidal packstone	Gray, stylolitic shell limestone	-55%-70% of Intraclast (include micritic intraclast, sandy micritic intraclast and small intraclast) and peloid. -up to 7% of skeletal grain (mollusk shell fragments, algal, crinoid, trilobite and bryozoans	Outer ramp
MF2 Peloidal calcisiltite	Dark gray to grayish brown, argillaceous limestone	-up to 7% of carbonate grains (mainly peloid) -less than 3% of micro-sized bioclasts	Outer ramp
MF3 Coarse packstone with microbially coated grains	Grayish black to brownish gray, coarse limestone	-20%-60% of intraclast, microbially coated skeletal grain, and some peloid. -10%-50% of bioclast (commonly shell, bivalve, gastropod , algae, crinoid, bryozoan)	Mid ramp
MF4 Fine packstone with intraclast	Light gray, medium to thick bed shell limestone	-15%-45% of carbonate grain (mainly intraclast, peloids, cortoids, and some microbially coated skeletal grain) -15%-35% of fragmented bioclast (bivalve, gastropods, cephalopods, crinoids and algae)	Mid ramp
MF5 Bio-intraclast packstone	Light gray to gray, medium to thick bed limestone	-50%- 60% of carbonate grains including intraclasts, oncoid, some peloids -up to 10% of shell	Mid ramp

FACIES	LITHOLOGY	COMPONENTS	FACIES BELTS
MF6 Intraclast-peloidal wackestone with microbially coated grains	Grayish black, medium argillaceous limestone	-30%-50% of intraclast, peloid and microbially coated grains -less than 10% of skeletal grains (abundant microbially coated shell fragment grains, algae and bivalve)	Mid ramp
MF7 Rounded clast grainstone	Light gray to brownish gray, dense shell limestone	-30%-60% of rounded carbonate grains (peloid, cortoid and some intraclast) -up to 40% of worm skeletal grain (algae, bryozoan, shell fragment)	Carbonate shoal
MF8 Abundant shell packstone	Brownish gray to gray, abundant brachiopod limestone	-15%-40% of peloid -30%-45% of shell (include brachiopod, gastropod and cephalopod)	Carbonate shoal
MF9 Molluscan-peloidal packstone	Brownish gray to light gray, medium to thin bed shell limestone	-20%-25% of peloid, oncoid and intraclast -10%-40% of skeletal grains (shell, molluscan, bryozoan, crinoid and algae)	Open marine
MF10 Molluscan packstone	Brownish gray to moderate olive brown, gastropod limestone	-up to 50% of carbonate grains including peloid and intraclast -10%-40% of bioclast (commonly mollusk and gastropod)	Lagoon
MF11 Fine-grained peloidal grainstone	Grayish brown to grayish yellow, medium bed limestone	-approximated 10% of peloid and some small intraclast	Peritidal

4.1.2. MF2, Peloidal calcisiltite (Figure 3C, 3D)

Facies description: This facies contains a fine-grained matrix which is composed of detrital silt-size calcite particle called calcisiltite. The allochems are rare both bioclast and carbonate grains. Bioclasts are found as micro-sized bioclasts and carbonate grain consists commonly of mud peloids. Depositional environment: The presences of calcisiltite and micro-bioclastic grain indicate the abrasion in storm-influenced ramp parts and transportation to deeper water ramps parts. The mud peloids normally occur in outer ramps.

4.2 Mid ramp facies

Four microfacies are associated in mid – ramp and they are chiefly of peloids, intraclasts, algae, crinoids, gastropods, shell fragments. This facies mainly includes coarse packstone with microbially coated grains, fine packstone with intraclast, bio-intraclast packstone and intraclast-peloidal wackestone with microbially coated grains.

4.2.1. MF3, Coarse packstone with microbially coated grains (Figure 3E, 3F)

Facies description: This microfacies consists of algae, shell, crinoid, bivalve, bryozoan, and gastropod which bioclasts are complete grains and some carbonate grains including intraclasts, microbially coated skeletal grains and some peloid are found. Texturally, lime mud matrix and grain supported allochems are predominantly observed. Grain size is mainly calcirudite.

Depositional environment: This facies represented by the packstone texture indicates moderate wave energy. The limestone contains whole-body fossil and fossil fragments such as shells, bivalves, bryozoans, algae and gastropods. This facies association shows the deposition in the mid-ramp between fair weather wave base and storm weather wave base. A mixture of different grain is common in mid-ramp settings and steepened ramps.

4.2.2. MF4, Fine packstone with intraclast (Figure 3G, 3H)

Facies description: This facies is chiefly composed of intraclast, peloids, skeletal grains, cortoids, and some microbially coated grains. This facies is composed of lime mud matrix, grain supported allochems. Sediments are abundant fragments of bivalves, gastropods, cephalopods, crinoids and algae. Grain size is chiefly calcarenite.

Depositional environment: This facies contains whole-body fossil and fossil fragments Packstone texture indicates moderate wave energy and the association represents the deposition in the mid-ramp between fair weather wave base and storm weather wave base. Mixture of allochems is found in mid-ramp settings and steepened ramps.

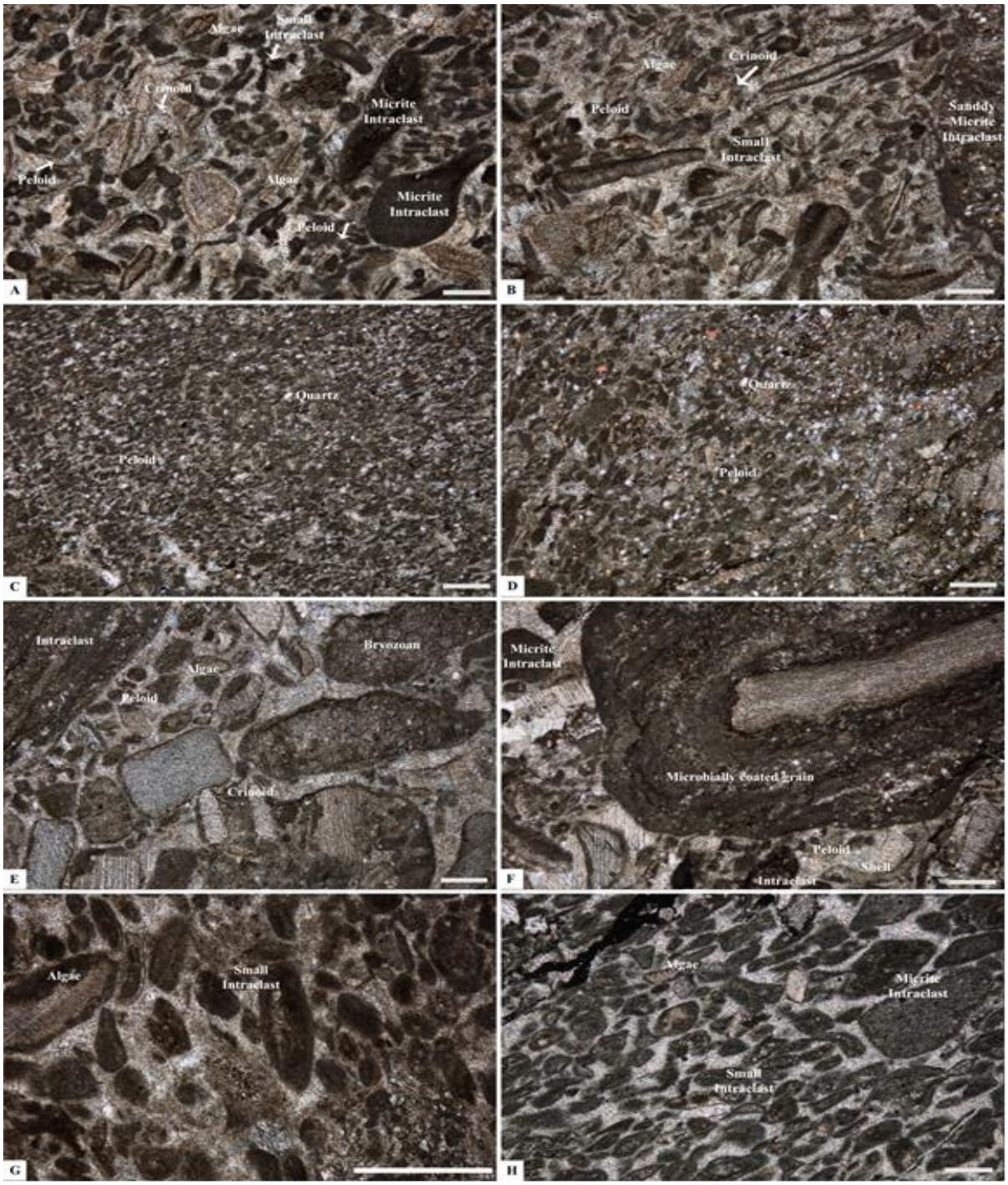

Figure 3. Microfacies of outer ramp facies. (A-B) MF1, Algal-intraclast-peloidal packstone (16KB01; 16 = 2016 (year of investigation), KB = Kanchanaburi, 01 = sample number). All materials are stored at Laboratory of Geotechnology, Suranaree University of Technology, Nakhon Ratchasima, Thailand. (C-D) MF2, Peloidal calcisiltite. Microfacies of mid ramp facies (16KB07, 17KB27; 17 = 2017). (E-F) MF3, Coarse packstone with microbially coated grains (16KB09, 16KB11, 18KB38; 18 = 2018). (G-H) MF4, Fine packstone with intraclast (17KB23, 17KB25). Scale = 0.5 mm

4.2.3. MF5, Bio-intraclast packstone (Figure 4A, 4B)

Facies description: This facies represents grain supported allochems, micrite matrix. The allochems are almost carbonate grains including intraclasts, some microbially coated grain, and some peloids. The bioclasts are composed mainly of shells. Their grain size ranges from calcirudite to calcarenite.

Depositional environment: This facies is mainly composed of shells which are major constituents of storm and current induced skeletal shoals in mid-ramp setting. The presence of packstone is normality of mid ramp setting.

4.2.4. MF6, Intraclast-peloidal wackestone with microbially coated grains (Figure 4C, 4D)

Facies description: This facies is composed mainly of micrite or lime mud matrix texture and matrix supported allochems. The main characteristic carbonate grains of this facies are mainly intraclast, peloid and microbially coated grain. The skeletal grains consist of abundant microbially coated shell fragment grains, algae, bivalve, which bioclasts are normally various in size, commonly fragmentary and broken bioclasts.

Depositional environment: The presence of abundant allomicrite indicates the low wave energy or quiet water deposition to moderate wave energy. The presence of mixture of different grains and incomplete grains can be a normality of mid ramp setting.

4.3 Carbonate shoal facies

Two microfacies associated in this environment are mainly composed of algae, shell, gastropod, crinoid, cephalopod, peloid, cortoid and some microbially coated grain. This facies represented by two microfacies includes rounded clast grainstone and abundant shell packstone.

4.3.1. MF7, Rounded clast grainstone (Figure 4E, 4F)

Facies description: The predominant grain type is rounded peloid and worm skeletal grains. Bioclasts such as algae, bryozoan, shell fragment and non-skeletal grain consisting of peloid, cortoid and some intraclast can be seen. Grains are calcirudite to calcarenite sizes, well sorting and well rounded. Textures are dominated grainstone.

Depositional environment: Grainstone texture and sparry calcite cement indicate that the microfacies deposited in high-energy areas located above or below the fair weather wave base and grain characteristic are affected. They are commonly originated in carbonate shoal depositional belt.

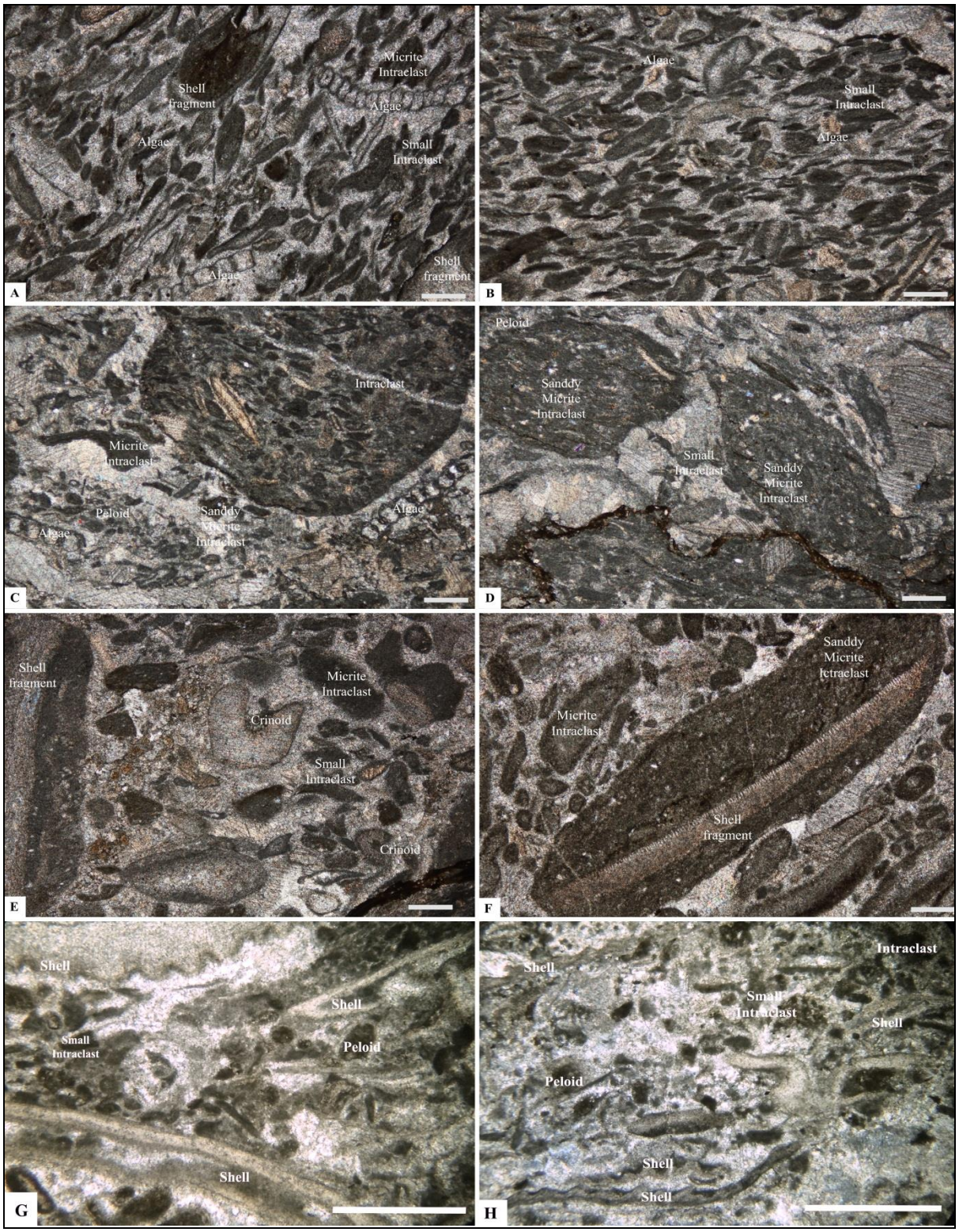

Figure 4. Microfacies of mid ramp facies. (A-B) MF5, Bio-intraclast packstone (16KB12, 16KB14, 17KB21, 17KB22) and (C-D) MF10, Intraclast-peloidal wackestone with microbially coated grains (17KB20). Microfacies of Carbonate shoals facies. (G-H) MF6, Rounded clast grainstone (16KB08, 16KB13, 16KB15A, 18KB11) and (E-F) MF8, Abundant shell packstone (18KB12, 18KB13). Scale bars = 0.5 mm.

4.3.2. MF8, Abundant shell packstone (Figure 4G, 4H)

Facies description: The main characteristic of this microfacies is mainly peloid and skeletal grain. Abundant shell such as shell, gastropod and cephalopod can be seen. Texturally, lime mud matrix, grain supported allochems are predominantly observed.

Depositional environment: The presences of abundant micrite and skeletal grain are abundant and completely shell fragments indicate the microfacies are deposited in moderate to high wave energy, which is considered as a shoal facies.

4.4 Open marine facies

One microfacies is identified in this environment and composed of molluscan-peloidal packstone. This facies is composed mainly of peloid, intraclast and microbially coated grain.

4.4.1. MF9, Molluscan-peloidal packstone (Figure 5A, 5B)

Facies description: This microfacies is mainly composed of peloid, microbially coated grain and intraclast. Skeletal grains such as shell, molluscan, bryozoan, crinoid and algae present in this facies. Texture is dominantly micrite matrix and grain supported allochems.

Depositional environment: The occurrences of abundant micrite and fecal pellets are common in the inner ramps. The feature of this facies indicates moderate to high energy shallow water.

4.5 Lagoon facies

One microfacies is identified in this environment. It is mainly composed of peloid, cortoid and molluscan. This facies includes molluscan packstone.

4.5.1 MF10, Molluscan packstone (Figure 5C, 5D)

Facies description: This facies dominantly includes allomicrite matrix or mud matrix and grain supported texture. The allochems are both skeletal grains and non-skeletal grains including bioclastic component namely mollusk shell fragments and carbonate grains consisting of finely peloid, some intraclast and microbially coated grain.

Depositional environment: The presences of abundant allomicrite and completed skeletal grain are commonly well preserved indicated the low wave energy depositional environment and the fecal peloids are commonly found in inner ramps.

4.6 Peritidal facies

One microfacies is identified in this environment and mainly composed of fine-grained peloidal grainstone. This facies consists of finely peloid, small intraclast and rarely skeletal grain.

4.6.1. MF11, Fine-grained peloidal grainstone (Figure 5E, 5F)

Facies description: The microfacies contains 30 percent of the lime mud. Bioclasts are very rare and carbonate grains are occasionally found as peloid and small intraclast. Grain orientation can be observed.

Depositional environment: The presence of allomicrite characterizes the poorly sorted matrix with very fine peloids within a matrix indicating the inner ramps. Fossils are not found in this facies.

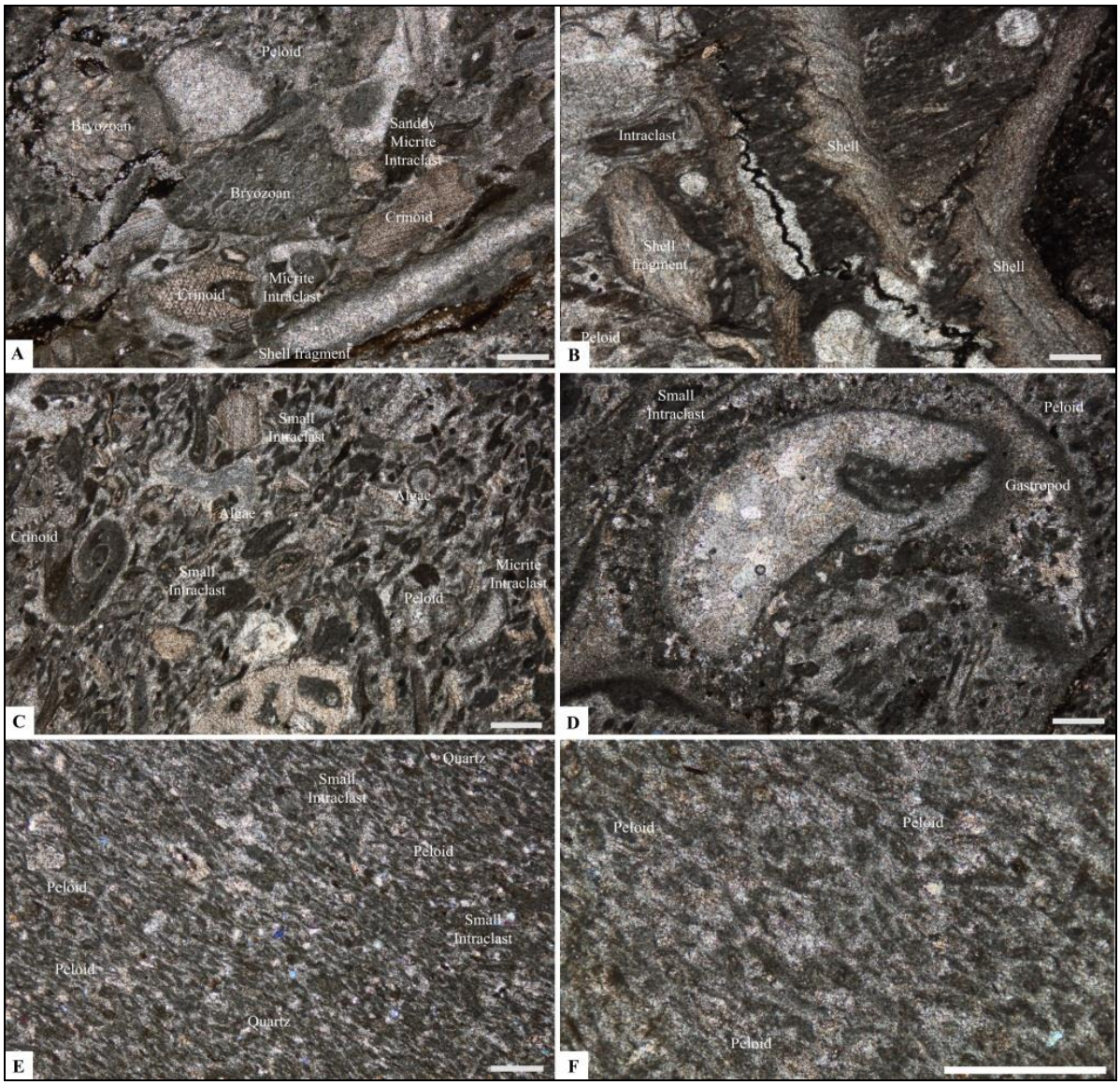

Figure 5. Microfacies of Lagoon facies (A-B) MF9, Molluscan peloidal packstone (17KB24, 17KB26). Microfacies of open marine facies. (C-D) MF10, Molluscan packstone (16KB15B, 18KB14). (E-F) MF11, Fine-grained peloidal grainstone (18KB39). Scale bars = 0.5 mm.

5. Depositional models

According to the environmental interpretation on the basis of the detailed microfacies analysis and the studied succession in Ban Tha Kradan area, Sri Sawat district, Kanchanaburi province, the depositional models were reconstructed to understand the concepts of the studied facies deposition. The microfacies (MF) were analyzed and can be divided into six types of facies zones including peritidal inner ramp, lagoon, carbonate shoal, open marine, mid ramp, outer ramp facies associations. These environments of deposition are interpreted as subtidal offshore open marine environment. The environmental conditions and depositional characteristics of each facies belts are summarized in Figure 6.

6. Discussion

The detailed facies stratigraphic column for the Wat Mong Krathae section is shown in Figure 2. The carbonate succession in the Tha Manao Limestone formation is chiefly thin to thick bedded stylolitic limestone which composed of greenish gray to dark gray, dominant wackestone to packstone and less of grainstone and mudstone. According to vertical facies distribution showing many upward-shallowing sequences, three upward-shallowing sequences are briefly recognized (Figure 6). Lower sequence was developed on the outer ramp to inner ramp environments. Middle sequence represents a shallowing process from mid ramp to inner ramp environment. Upper sequence was deposited from outer ramp to inner ramp. The depositional environment which interpreted from the detailed microfacies analysis and investigation and lithostratigraphy of the studied section are quite similar to upper part of Thong Pha Phum section (Bunopas, 1981; 1992; Agematsu, 2003; Agematsu et al., 2008; 2009; Hagen and Kemper, 1976) and can be correlated to Thung Wa section in Satun in southern Thailand and Langkawi in Malaysia (Wongwanich et al., 1990; Bunopas, 1981; 1993; Agematsu et al., 2008). Macrofossils recorded in Tha Manao Limestone Formation are also found in this sequence. Nautiloid *Armenoceras chediforme* (Kobayashi, 1958), *Ormoceras langkawiense* (Niko and Sone, 2015), gastropod *Teiichispirina* sp. (Yochelson and Jones, 1968) and receptaculitalean *? Fisherites* sp. (Kruse, 1989) were found and indicate Middle Ordovician (Dapingian – Darriwilian age). These fossils can be correlated to Setul Formation of the Langkawi Island (Malaysia), peninsular Thailand (Yochelson and Jones 1968), and central Burma (Rietschel and Nitecki, 1984).

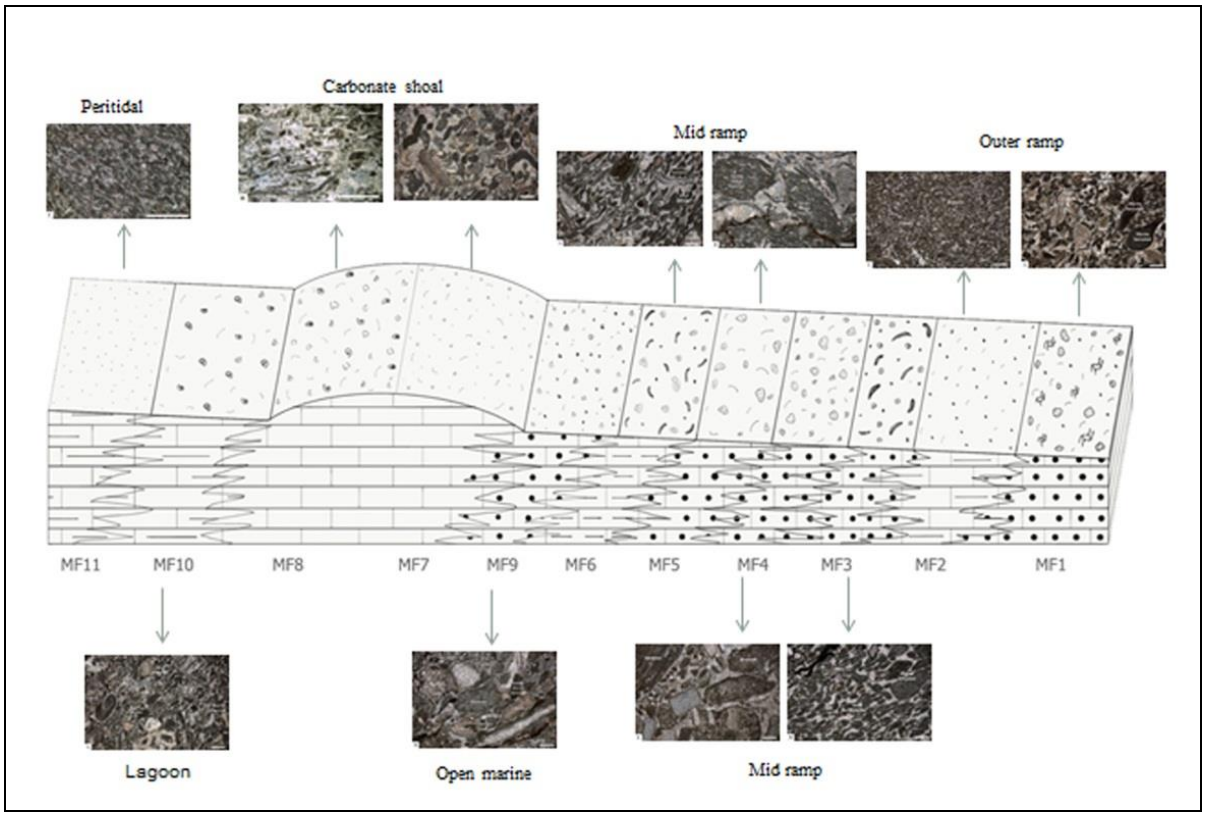

Figure 6 Depositional model of carbonate ramp system proposed for the Tha Manao Limestone Formation in the study area.

7. Conclusion

Ordovician limestone deposited on a carbonate ramp in the East side of Srinagarind reservoir in Kanchanaburi province. The microfacies analysis can be divided into eleven facies types and six depositional facies belts comprising outer ramp, mid ramp, open marine, shoal, lagoon, and peritidal inner ramp were recognized in this studied section. Algal-intraclast-peloidal packstone (MF1), peloidal calcisiltite (MF2) are categorized into outer ramp facies, coarse packstone with microbially coated grains (MF3), fine packstone with intraclast (MF4), bio-intraclast packstone (MF5) and intraclast-peloidal wackestone with microbially coated grains (MF6) belong to mid ramp facies, rounded clast grainstone (MF7), abundant shell packstone (MF8) are classified into the carbonate shoal facies, molluscan-peloidal packstone (MF9) is referred to open marine, molluscan packstone (MF10) is categorized in the lagoon depositional belt, fine-grained peloidal grainstone (MF11) is classified in the peritidal facies. The successions are divided into 3 sequences from bottom to top respectively; 1) Lower sequence (0-55 meters), the sequence is dominated by intraclast and peloid-rich pack-grainstone

facies which represents the outer ramp to inner ramp environment; 2) Middle sequence (55-110 meters), the sequence represents mid ramp to inner ramp environments from the evidence of larger and mixed grains; 3) Upper sequence (110-157 meters), in this sequence shows abundant shell and mollusk, which were normally deposited in the outer ramp to the inner ramp.

8. Acknowledgements

This project was supported by Suranaree University of Technology (SUT). The authors are grateful to Dr. Stephen Kershaw for comments and suggestions on a previous version of this paper.

9. Reference

Agematsu, S, 2003. Ordovician conodonts from the Thong Pha Phum and Satun areas in Thailand. Doctoral Program in Earth Erolution Seience, University of Tsukaba.

Agematsu, S., Sashida, K., Salyapongse, S. and Sardsud, A. 2006. Ordovician conodonts from the Thong Pha Phum area, western Thailand. *Journal of Asian Earth Sciences*, 26, 1, 49-60.

Agematsu, S., Sashida, K., Salyapongse, S. and Sardsud, A. 2007. Ordovician Conodonts from the satun area, southern Peninsular Thailand. *Journal of Paleontology*, 81, 1, 19-37.

Agematsu, S., Sashida, K. and Ibrahim, A.B. 2008. Biostratigraphy and Paleobiogeography of Middle and Late Ordovician Conodonts from the Langkawi Islands, Northwestern Peninsular Malaysia. *Journal of Paleontology*, 82, 5, 957-973.

Agematsu, S, and Sashida, K. 2009. Ordovician sea-level change and Paleogeography of the Sibumasu Terrane Based on the Conodont Biostatigraphy. *Paleontological Research,* 13, 4, 327-336.

Bunopas, S. 1976. Stratigraphic succession in Thailand - A preliminary summary. *Journal of the Geological Society of Thailand*, 2(1-2), 31-58.

Bunopas, S. 1981. Paleogeographic history of western Thailand and adjacent parts of Southeast Asia-A plate tectonic interpretation. Doctoral dissertation, Victoria University of Wellington.

Bunopas, S. 1983. Palaeozoic succession in Thailand. In *proceedings of the Workshop on stratigraphic Correlation of Thailand and Malaysia,* Haad Yai, Thailand, 1, 39-76.

Dunham, R.J. 1962. Classification of carbonate rocks according to depositional texture. In: Ham, W.E. (Ed.). Classification of

carbonate rocks. *The American Association of Petroleum Geologists*, 1, 108-121.

Flügel, E. 2004. Microfacies of Carbonate Rocks Analysis, Interpretation and Application, 1st Edition, *Springer Dordrecht Heidelberg*, London, New York.

Fortey, R.A. 1997. Late Ordovician trilobites from southern Thailand. *Palaeontology*, 40, 2, 397–449.

Fortey, R.A. and Cocks, L.R.M. 1998. Biogeography and palaeogeography of the Sibumasu terrane in the Ordovician: a review In: R. Hall and J.D. Holloway (eds.), *Biogeography and Geological Evolution of Southeast Asia*, 43–57.

Green, O.R. 2001. A Manual of Practical Laboratory and Field Techniques in Palaeobiology. Dordrecht, Boston, Kluwer Academic.

Grundmann, G & Scholz, H. 2015. Preparation methods in Mineralogy & Geology: The Preparation of thin sections, polished sections, acetate foil prints, preparation for elutriation analysis, and staining tests for the optical and electron microscopy. Engineering Geology Technische Universität München, 1-27.

Hagen, D., and Kemper, E. 1976. Geology of the Thong Pha Phum area (Kanchanaburi province, western Thailand). *Geologisches Jahrbuch*, 21, 53-91.

Hill, R. 1999. Making thin sections by hand. Mid - America Paleontology Society. Digest, [Online]. Available: *http://www.lpl.arizona.edu/~rhill/fossil/sections.html*

Khaowiset, K., Leewongcharoen, S., Charoenmit, J., Yathakum, W. and Chaikam, A. 2011. Geological map of Khuean Srinagarindra Quadrangle (4837 IV), scale 1:50,000. *Bureau of Geological Survey, Department of Mineral Resources*.

Kobayashi, Y. 1958. Some Ordovician fossils from the Thailand- Malayan Borderland. *Japanese Journal of Geology and Geography*, 29, 223-231.

Koch, K.E. 1973. Geology of the Region Sri Sawat-Thong Pha Phum-Sangkhlaburi (Kanchanaburi province, Thailand). In B. K., Tan (Ed.), *Proceedings of the Regional Conference on the Geology of SE Asia*, 1, 177-185.

Kruse, P.D. 1989. A Thai Ordovician receptaculitalean. *Alcheringa: An Australasian Journal of Palaeontology*, 13. 2:141-144

Meesook, A. 2015. Lithostratigraphy and marine faunal assemblages of the Cambrain-Ordovician Thung Song group in, Ordovician-Silurian-Devonian-Carboniferous,Ordovician-Silurian-Devonian-Carboniferous sequence in

Phet Fa, Mong Kra Thae, Wat Tha Kra Dan Phu Phlu area, Ban Tha Kradan area, Si Saw Wat District, Kanchanaburi Province, Western Thailand. In Technical report No BFP 2/2013, of *Bureau of Geological SurveyFossil Protection, Department of Mineral Resources*. .

Metcalfe, I. 1988. Origin and assembly of Southeast Asian continental terranes. In: Audley-Charles, M. G. & Hallam, A. (eds) *Gondwana and Tethys. Geological Society, London,* Special Publications, 37, 101–118.

Metcalfe, I. 1998. Palaeozoic and Mesozoic geological evolution of the SE Asian region: multidisciplinary constraints and implications for biogeography. In: Hall, R. & Holloway, J. D. (eds) *Biogeography and Geological Evolution of SE Asia*. Backhuys Publishers, Amsterdam, the Netherlands, 25–41.

Niko, S. and Sone, M. 2015. Gondwanan Nautiloid Cephalopods feom the Ordovician of Myanmar. *Paleontological Research*, 288-293.

Ridd, M.F. 2011. Lower palaeozoic. In Ridd, M. F., Barber, A. J., and Crow, M. J. (eds.) *The Geology of Thailand: The Geological Society London*, 33-51.

Rietschel, S. and Nitecki, M.H. 1984. Ordovician receptaculitid algae from Burma. *Palaeontology*, 27, 415-420.

Stait, B. and Burrett, C. F. 1982. Wutinoceras (Nautiloidea) from the Setul Limestone (Ordovician) of Malaysia. *Alcheringa*, 6, 193-196.

Stait, B.A., and Burrett, C.F. 1984. Ordovician nautiloids from central and southern Thailand. *Geological magazine*, 121, 115-124.

Stait, B., Wyatt, D. and Burrett, C. F. 1987. Ordovician nautiloid faunas of Langkawi Islands, Malaysia and Tarutao Island, Thailand. *Neues Jahrbuch für Geologie und Paläontologie, Abhandlungen*, 174, 373-391.

Wongwanich, T., Wyatt, D., Stait, B. and Burrett, C. 1983. The Ordovician system in Southern Thailand and Northern Malaysia. In *proceedings of the Workshop on stratigraphic Correlation of Thailand and Malaysia*, Haad Yai, Thailand, 77-95.

Wongwanich, T. 1990. Lithostratigraphy, sedimentology and diagenesis of the Ordovician carbonates, southern Thailand. PhD thesis, University of Tasmania.

Yochelson. E. L and Jones. C. R 1968. Teiichispira, a New Early Ordovician Gastropod Genus. *Geological Survey Professional* 613-B, 1-27.

บริษัทเอสซีจี ซิเมนต์ จำกัด

Morphology of Earth Surface and Advanced Geohazards in Southeast Asia Research Unit (MESA RU), Department of Geology, Faculty of Science, Chulalongkorn University

Basin Analysis and Structural Evolution Special Task Force for Activating Research (BASE STAR), Department of Geology, Faculty of Science, Chulalongkorn University

TURNING TARGETS INTO PERFORMANCE

As part of our global petroleum exploration and production, PTTEP strives for a balance that creates long-term value for business, environment and society in order to become a leading Asian E&P company driven by competitive performance, advanced technology and green practices. We are committed to conducting business under proper ethical practices, and good governance in tandem with outstanding environment and social performance which underpin our license to grow in a sustainable way.

www.pttep.com

Passion to Explore for a Sustainable Future

PTTEP